

**KINETICS AND MECHANISMS OF THE ELECTRON
TRANSFER REACTIONS OF DIAQUOTETRAKIS (2, 2'-
BIPYRIDINE)- μ -OXODIRUTHENIUM(III) IONS AND
SOME REDUCTANTS IN AQUEOUS MEDIUM**

BY

YAHAYA MOHAMMED

**DEPARTMENT OF CHEMISTRY
FACULTY OF SCIENCE
AHMADU BELLO UNIVERSITY
ZARIA**

OCTOBER, 2015

**KINETICS AND MECHANISMS OF THE ELECTRON
TRANSFER REACTIONS OF DIAQUOTETRAKIS (2, 2'-
BIPYRIDINE)- μ -OXODIRUTHENIUM(III) IONS AND
SOME REDUCTANTS IN AQUEOUS MEDIUM**

BY

YAHAYA MOHAMMED

B.Sc. (University of Jos, 1994), M.Sc (A.B.U Zaria, 2009)

(Ph.D/SCIE/2881/2010-2011)

**A THESIS SUBMITTED TO THE SCHOOL OF
POSTGRADUATE STUDIES, AHMADU BELLO
UNIVERSITY ZARIA, IN PARTIAL FULFILLMENT FOR
THE AWARD OF Ph.D. INORGANIC CHEMISTRY**

**DEPARTMENT OF CHEMISTRY
AHMADU BELLO UNIVERSITY
ZARIA**

OCTOBER, 2015

Declaration

I declare that the work in this thesis entitled 'KINETICS AND MECHANISMS OF THE ELECTRON TRANSFER REACTIONS OF DIAQUOTETRAKIS (2, 2'-BIPYRIDINE) - μ - OXODIRUTHENIUM(III) IONS AND SOME REDUCTANTS IN AQUEOUS MEDIUM' has been carried out by me in the Department of Chemistry, Ahmadu Bello University, Zaria. The information derived from the literature has been duly acknowledged in the text and a list of references provided. No part of this thesis was previously presented for another degree or diploma at this or any other institution.

Yahaya MOHAMMED

Signature

Date

Certification

This thesis entitled 'KINETICS AND MECHANISMS OF THE ELECTRON TRANSFER REACTIONS OF DIAQUOTETRAKIS (2, 2'- BIPYRIDINE) - μ - OXODIRUTHENIUM (III) IONS AND SOME REDUCTANTS IN AQUEOUS MEDIUM' by Yahaya MOHAMMED meets the regulations governing the award of the degree of Doctor of Philosophy of the Ahmadu Bello University, and is approved for its contribution to knowledge and literary presentation.

Dr. S.O Idris

Chairman, Supervisory Committee

Signature

Date

Prof. J.F. Iyun

Member, Supervisory Committee

Signature

Date

Dr. A.D. Onu

Member, Supervisory Committee

Signature Date

Prof. V.O Ajibola

Head of Department

Signature

Date

Prof. K. Bala

Dean, School of Postgraduate Studies

Signature Date

Acknowledgements

All Praises are due to Allah, the Lord of the Worlds. He kept me alive and healthy. He provided me with the peace of mind and the wherewithal to carry out this work with as little stress as possible. In His wisdom, He made it possible for me to be supervised by wonderful people. Also, in His wisdom, He gave me a family that is very considerate and understanding. All Glory is due to Him, The Lord of the Day of Judgement!

To my Supervisor, Dr. S.O. Idris who is not only a supervisor to me but a father, brother, mentor; role model all in one, your reward from Allah would surely come to pass. You have been wonderful! Prof. J.F Iyun, of blessed memory, you had been great, humane, detribalised and a source of inspiration for all of us that came across you. May you continue to rest in peace. Dr. A.D Onu, you have been wonderful and of great assistance as you supervised this study. May God continue to bless you.

To my wives, Maimuna and Fatima, you have been a great asset to me as I toiled to get this work done - You gave me peace, comfort and encouragement. Remain blessed! To my children, Yusuf, Maryam, Lubna, Auwal and Safwan, I acknowledge your cooperation throughout the duration of this work. May you live long!

Prof. M.O Aremu, words cannot describe my appreciation to you for your concern, encouragement and support – both moral and financial. May God continue to ease your ways! Dr. Mercy Mbursa of Newcastle Hospital, UK, my gratitude goes to you for footing the bills for the purchase of some of the reagents directly from the manufacturers. God bless you! Dr. Ibrahim Khalil Adam, I thank you for your role in the procurement of some of the reagents. Mr. Bernard Ashika'a of the Department of Chemistry, Nasarawa State University Laboratory, I am grateful for your technical support. God bless!

Abstract

The kinetics and mechanisms of the electron transfer reactions of diaquotetrakis (2, 2'-bipyridine)- μ -oxodiruthenium(III) ions (hereafter denoted as Ru_2O^{4+} or $[(\text{H}_2\text{O})_2\text{Ru}_2\text{O}]^{4+}$) and thiourea (TU), *N*-methylthiourea (MTU), *N*-allylthiourea (ATU), *N,N'*-dimethylthiourea (DMTU) (collectively denoted by TSH), thiosulphate ions ($\text{S}_2\text{O}_3^{2-}$), dithionite ions ($\text{S}_2\text{O}_4^{2-}$), hypophosphorous acid (H_3PO_2), methanol (CH_3OH), ethanol ($\text{C}_2\text{H}_5\text{OH}$) and propanol ($\text{C}_3\text{H}_7\text{OH}$) (collectively denoted as ROH) were studied in aqueous perchloric acid (HClO_4) medium (except for $\text{S}_2\text{O}_4^{2-}$ and the alcohols) at $I = 0.5 \text{ mol dm}^{-3}$ and $T = (31.0 \pm 1) \text{ }^\circ\text{C}$. The stoichiometry was found to be 1:2 (Ru_2O^{4+} /reductant) in the TSH and $\text{S}_2\text{O}_3^{2-}$ systems but 1:1 in the $\text{S}_2\text{O}_4^{2-}$, H_3PO_2 and ROH systems. The rate of reaction is first order in oxidants and reductants for all the systems. Addition of acid has inverse effect on the rates of reaction for the TSH system, but direct dependence for the $\text{S}_2\text{O}_3^{2-}$ system. The overall rate equation for the TSH reaction can be given as :

$$-\frac{d}{dt} [\text{Ru}_2\text{O}^{4+}] = (a + b[\text{H}^+]^{-1})[\text{Ru}_2\text{O}^{4+}][\text{Reductant}] \quad .$$

while that for $\text{S}_2\text{O}_3^{2-}$ reaction can be given as:

$$-\frac{d}{dt} [\text{Ru}_2\text{O}^{4+}] = (a + b[\text{H}^+])[\text{Ru}_2\text{O}^{4+}][\text{S}_2\text{O}_3^{2-}]$$

Varying the ionic strength (I) and dielectric constant (D) of the reaction medium had no effect on rates of reaction for the TSH, $\text{S}_2\text{O}_4^{2-}$, H_3PO_2 and ROH reactions, while for the $\text{S}_2\text{O}_3^{2-}$ reaction, increase in I led to a decrease in rate while decrease in D led to increase in rate of reaction. Added ions had no effect on the TSH and H_3PO_2 reactions but led to

catalysis and/ or inhibition in $S_2O_3^{2-}$, $S_2O_4^{2-}$ and ROH systems. Free radicals were identified in the TSH, H_3PO_2 and ROH reactions only. Spectroscopic information and the results of the Michaelis – Menten plots suggest the lack of formation of intermediate complex prior to electron transfer for all the systems. For all the reactions, $[(H_2O)_2(bipy)_2Ru]^{2+}$ was found to be the product of Ru_2O^{4+} reduction. For the TSH reaction, disulphides was found to be the oxidation product of TSH while, for H_3PO_2 reaction, test for phosphorous acid (H_3PO_3) presence was positive and for the ROH system, test for aldehydes was also positive. The order of reactivity for the TSH system is $ATU > DMTU > MTU > TU$, while the order of reactivity for the sulphur oxyanions' reactions is $S_2O_4^{2-} > S_2O_3^{2-}$ and that for the ROH reactions is $CH_3OH > C_2H_5OH > C_3H_7OH$. Based on the Michaelis–Menten plots and the interactions with added ions, all the reactions are proposed to have proceeded through the outer–sphere electron transfer mechanism. Plausible mechanisms for all the reactions have been proposed.

Table of Contents

	Page
Title Page	ii
Declaration	iii
Certification	iv
Acknowledgements	v
Abstract	vi
Table of Contents	viii
List of Tables	xiv
List of Figures	xv
List of Abbreviations	xxi
CHAPTER ONE	
INTRODUCTION	1
1.1 Electron Transfer Reactions	1
1.2 Types of Electron Transfer Reactions	2
1.2.1 Homonuclear or self-exchange electron transfer reactions	2
1.2.2 Heteronuclear or cross-electron transfer reactions	2
1.3 Mechanisms of Electron Transfer	3
1.3.1 The innersphere mechanism	4
1.3.2 The outersphere mechanism	5
1.3.3 Proton couple electron transfer process	6
1.3.4 Solvated electron theory	6
1.4 Diagnosis of Redox Reaction Mechanism	7
1.4.1 Comparison of the rate of electron transfer and the rate of substitution (k_{redox} versus k_{subs})	7
1.4.2 Identification of binuclear intermediate	8
1.4.3 Product analysis	8

1.4.4 Use of ambidentate ligands	9
1.4.5 Effect of added ions	10
1.4.6 Reactivity pattern	11
1.4.7 Activation Parameters	11
1.5 Effect of Pressure on Electron Transfer	12
1.6 Rate Monitoring Techniques	12
1.6.1 Conventional methods	13
1.6.2 Fast reaction techniques	13
1.7 Justification of the Study	15
1.8 Aims and Objectives of the Study	18
CHAPTER TWO	
LITERATURE REVIEW	20
2.1 Ruthenium Chemistry	20
2.1.1 Properties of ruthenium polypyridyl complexes	20
2.1.2 Electron transfer in ruthenium complexes	22
2.1.3 Photosynthesis and water oxidation catalysis	24
2.1.4 Homogenous water oxidation by ruthenium complexes	25
2.1.5 Heterogeneous water oxidation catalysis by ruthenium complexes	29
2.2 Thiourea and Its Derivatives	30
2.2.1 Electron transfer reactions of thiourea and its derivatives	31
2.3 Electron Transfer Reaction of $S_2O_3^{2-}$	36
2.4 Electron Transfer Reactions of $S_2O_4^{2-}$	37
2.5 Electron Transfer Reactions of H_3PO_2	39
2.6 Electron Transfer Reactions of ROH	42

CHAPTER THREE

MATERIALS AND METHODS	44
3.1 Materials and Reagents	44
3.1.1 Diaquotetrakis (2, 2'- bipyridine)- μ -oxo-diruthenium(III) perchlorate	44
3.1.2 Thiourea solution	45
3.1.3 <i>N</i> -methylthiourea solution	45
3.1.4 <i>N,N'</i> - dimethylthiourea solution	45
3.1.5 <i>N</i> - allylthiourea solution	45
3.1.6 Sodium thiosulphate solution	45
3.1.7 Sodium dithionite solution	46
3.1.8 Hypophosphorous acid solution	46
3.1.9 Sodium perchlorate solution	46
3.1.10 Magnesium chloride solution	46
3.1.11 Ammonium chloride solution	47
3.1.12 Sodium acetate solution	47
3.1.13 Sodium formate solution	47
3.1.14 Sodium nitrate solution	47
3.1.15 Perchloric acid solution	47
3.1.16 Methanol	48
3.1.17 Ethanol	48
3.1.18 Propan-1-ol	48
3.2 Methods	49
3.2.1 Stoichiometric studies	49
3.2.2 Kinetic measurements	50
3.2.3 Effect of changes in hydrogen ion concentration	51

3.2.4	Effect of changes in ionic strength	51
3.2.5	Effect of changes in dielectric constant of reaction medium	52
3.2.6	Effect of added ions	52
3.2.7	Test for free radicals	52
3.2.8	Test for Intermediate complex formation	53
3.2.9	Product analysis	53

CHAPTER FOUR

RESULTS		55
4.1	Stability of Ru_2O^{4+}	55
4.2	Stoichiometric Studies	55
4.3	Determination of Pseudo – First Order and Second Order Rate Constants and Order of Reaction	61
4.3.1	Ru_2O^{4+} reaction with thiourea and its derivatives (TU, MTU, ATU and DMTU)	61
4.3.2	Reaction of Ru_2O^{4+} with $\text{S}_2\text{O}_3^{2-}$ and $\text{S}_2\text{O}_4^{2-}$	72
4.3.3	Reaction of Ru_2O^{4+} with H_3PO_2	83
4.3.4	Reaction of Ru_2O^{4+} with ROH	90
4.4	Effect of Changes in Hydrogen Ion Concentration, $[\text{H}^+]$	98.
4.4.1	Reaction of Ru_2O^{4+} with TU, MTU, ATU and DMTU	98
4.4.2	Reaction of Ru_2O^{4+} with $\text{S}_2\text{O}_3^{2-}$	106
4.4.3	Reaction of Ru_2O^{4+} with H_3PO_2	109
4.5	Effect of Changes in Ionic Strength of Reaction Medium	109
4.5.1	Reaction of Ru_2O^{4+} with thiourea and its derivatives	109
4.5.2	Reaction of Ru_2O^{4+} with $\text{S}_2\text{O}_3^{2-}$	109
4.5.3	Reaction of Ru_2O^{4+} with $\text{S}_2\text{O}_4^{2-}$	110

4.5.4	Reaction of Ru_2O^{4+} with H_3PO_2 and ROH	110
4.6	Effect of Changes in Dielectric Constant of Reaction Medium	110
4.6.1	Reaction of Ru_2O^{4+} with TU, MTU, ATU and DMTU	110
4.6.2	Reaction of Ru_2O^{4+} with $\text{S}_2\text{O}_3^{2-}$	112
4.6.3	Reaction of Ru_2O^{4+} with $\text{S}_2\text{O}_4^{2-}$, H_3PO_2 and ROH	119
4.7	Effect of Added Ions	119
4.7.1	Reaction of Ru_2O^{4+} with TU, MTU, ATU and DMTU	119
4.7.2	Reaction of Ru_2O^{4+} with $\text{S}_2\text{O}_3^{2-}$	119
4.7.3	Reaction of Ru_2O^{4+} with $\text{S}_2\text{O}_4^{2-}$	134
4.7.4	Reaction of Ru_2O^{4+} with H_3PO_2	145
4.7.5	Reaction of Ru_2O^{4+} with the ROH	145
4.8	Tests for the Formation of Intermediate Complex	157
4.8.1	Spectroscopic test	157
4.8.2	Michaelis – Menten plots	157
4.9	Free Radicals Test	168
4.10	Product Analysis	168
4.9.1	Reaction of Ru_2O^{4+} with TU, MTU, ATU and DMTU	168
4.9.2	Reaction of Ru_2O^{4+} with H_3PO_2	168
4.9.3	Reaction of Ru_2O^{4+} with ROH	169
CHAPTER FIVE		
DISCUSSION		170
5.1	Ru_2O^{4+} Reaction with TU, MTU, ATU and DMTU	170
5.2	Ru_2O^{4+} Reaction with $\text{S}_2\text{O}_3^{2-}$	180
5.3	Ru_2O^{4+} Reaction with $\text{S}_2\text{O}_4^{2-}$	186

5.4	Ru₂O⁴⁺ Reaction with H₃PO₂	189
5.5	Ru₂O⁴⁺ Reaction with ROH	198
5.6	Comparison of the Redox Reactions of Ru₂O⁴⁺ and the Various Reductants under Study	198
 CHAPTER SIX		
	SUMMARY, CONCLUSION AND RECOMMENDATIONS	200
6.1	Summary	200
6.2	Conclusion	201
6.3	Recommendation	201
	REFERENCES	202
	APPENDIX	221

List of Tables

2.1 Comparison of the catalytic activity (k_{O_2}) of various ruthenium complexes in water oxidation	27
4.1 Pseudo – first order and second order rate constants for the reaction of $[(H_2O)_2Ru_2O]^{4+}$ and TU	73
4.2 Pseudo – first order and second order rate constants for the reaction of $[(H_2O)_2Ru_2O]^{4+}$ and MTU	74
4.3 Pseudo – first order and second order rate constant for the reaction of $[(H_2O)_2Ru_2O]^{4+}$ and ATU	75
4.4 Pseudo – first order and second order rate constants for the reaction of $[(H_2O)_2Ru_2O]^{4+}$ and DMTU	76
4.5 Pseudo – first order and second order rate constants for the reaction of $[(H_2O)_2Ru_2O]^{4+}$ and $S_2O_3^{2-}$	81
4.6 Pseudo – first order and second order rate constants for the reaction of $[(H_2O)_2Ru_2O]^{4+}$ and $S_2O_4^{2-}$	82
4.7 Pseudo – first order and second order rate constants for the reaction of $[(H_2O)_2Ru_2O]^{4+}$ and H_3PO_2	89
4.8 Pseudo – first order and second order rate constants for the reaction of $[(H_2O)_2Ru_2O]^{4+}$ and CH_3OH	95
4.9 Pseudo – first order and second order rate constants for the reaction of $[(H_2O)_2Ru_2O]^{4+}$ and C_2H_5OH	96
4.10 Pseudo – first order and second order rate constants for the reaction of $[(H_2O)_2Ru_2O]^{4+}$ and C_3H_7OH	97
4.11 Effect of changes in the dielectric constant for the reaction of $[(H_2O)_2Ru_2O]^{4+}$ and TU	113
4.12 Effect of changes in the dielectric constant for the reaction of $[(H_2O)_2Ru_2O]^{4+}$ and MTU	114
4.13 Effect of changes in the dielectric constant for the reaction of $[(H_2O)_2Ru_2O]^{4+}$ and ATU	115
4.14 Effect of changes in the dielectric constant for the reaction of $[(H_2O)_2Ru_2O]^{4+}$ and DMTU	116
4.15 Effect of changes in the dielectric constant for the reaction of $[(H_2O)_2Ru_2O]^{4+}$ and $S_2O_3^{2-}$	117

4.16 Effect of changes in the dielectric constant for the reaction of $[(\text{H}_2\text{O})_2\text{Ru}_2\text{O}]^{4+}$ and $\text{S}_2\text{O}_4^{2-}$	120
4.17 Effect of changes in the dielectric constant for the reaction of $[(\text{H}_2\text{O})_2\text{Ru}_2\text{O}]^{4+}$ and H_3PO_2	121
4.18 Effect of changes in the dielectric constant for the reaction of $[(\text{H}_2\text{O})_2\text{Ru}_2\text{O}]^{4+}$ and CH_3OH	122
4.19 Effect of changes in the dielectric constant for the reaction of $[(\text{H}_2\text{O})_2\text{Ru}_2\text{O}]^{4+}$ and $\text{C}_2\text{H}_5\text{OH}$	123
4.20 Effect of changes in the dielectric constant for the reaction of $[(\text{H}_2\text{O})_2\text{Ru}_2\text{O}]^{4+}$ and $\text{C}_3\text{H}_7\text{OH}$	124
4.21 Effect of added anions to reaction medium for the reaction of $[(\text{H}_2\text{O})_2\text{Ru}_2\text{O}]^{4+}$ and TU	125
4.22 Effect of added anions to reaction medium for the reaction of $[(\text{H}_2\text{O})_2\text{Ru}_2\text{O}]^{4+}$ and MTU	126
4.23 Effect of added cation (Mg^{2+}) to reaction medium for the reaction of $[(\text{H}_2\text{O})_2\text{Ru}_2\text{O}]^{4+}$ and MTU	127
4.24 Effect of added anions to reaction medium for the reaction of $[(\text{H}_2\text{O})_2\text{Ru}_2\text{O}]^{4+}$ and ATU	128
4.25 Effect of added cation (Mg^{2+}) to reaction medium for the reaction of $[(\text{H}_2\text{O})_2\text{Ru}_2\text{O}]^{4+}$ and ATU	129
4.26 Effect of added anions to reaction medium for the reaction of $[(\text{H}_2\text{O})_2\text{Ru}_2\text{O}]^{4+}$ and DMTU	130
4.27 Effect of added cations to reaction medium for the reaction of $[(\text{H}_2\text{O})_2\text{Ru}_2\text{O}]^{4+}$ and DMTU	131
4.28 Effect of added cations to reaction medium for the reaction of $[(\text{H}_2\text{O})_2\text{Ru}_2\text{O}]^{4+}$ and $\text{S}_2\text{O}_3^{2-}$	132
4.29 Effect of added anions to reaction medium for the reaction of $[(\text{H}_2\text{O})_2\text{Ru}_2\text{O}]^{4+}$ and $\text{S}_2\text{O}_3^{2-}$	133
4.30 Effect of added anions to reaction medium for the reaction of $[(\text{H}_2\text{O})_2\text{Ru}_2\text{O}]^{4+}$ and $\text{S}_2\text{O}_4^{2-}$	139
4.31 Effect of added cations to reaction medium for the reaction of $[(\text{H}_2\text{O})_2\text{Ru}_2\text{O}]^{4+}$ and $\text{S}_2\text{O}_4^{2-}$	140
4.32 Effect of added anions to reaction medium for the reaction of $[(\text{H}_2\text{O})_2\text{Ru}_2\text{O}]^{4+}$ and H_3PO_2	146

4.33	Effect of added cations to reaction medium for the reaction of $[(\text{H}_2\text{O})_2\text{Ru}_2\text{O}]^{4+}$ and H_3PO_2	147
4.34	Effect of added cations to reaction medium for the reaction of $[(\text{H}_2\text{O})_2\text{Ru}_2\text{O}]^{4+}$ and CH_3OH	148
4.35	Effect of added cations to reaction medium for the reaction of $[(\text{H}_2\text{O})_2\text{Ru}_2\text{O}]^{4+}$ and $\text{C}_2\text{H}_5\text{OH}$	149
4.36	Effect of added anions to reaction medium for the reaction of $[(\text{H}_2\text{O})_2\text{Ru}_2\text{O}]^{4+}$ and $\text{C}_3\text{H}_7\text{OH}$	150
5.1	A Summary of the stoichiometries of similar systems studied elsewhere	171

List of Figures

4.1 Plot of absorbance versus mole ratio of the reaction of $[(\text{H}_2\text{O})_2\text{Ru}_2\text{O}]^{4+}$ and TU	57
4.2 Plot of absorbance versus mole ratio for the reaction of $[(\text{H}_2\text{O})_2\text{Ru}_2\text{O}]^{4+}$ and MTU	58
4.3 Plot of absorbance versus mole ratio for the reaction of $[(\text{H}_2\text{O})_2\text{Ru}_2\text{O}]^{4+}$ and ATU	59
4.4 Plot of absorbance versus mole ratio for the reaction of $[(\text{H}_2\text{O})_2\text{Ru}_2\text{O}]^{4+}$ and DMTU	60
4.5 Plot of absorbance versus mole ratio for the reaction of $[(\text{H}_2\text{O})_2\text{Ru}_2\text{O}]^{4+}$ and $\text{S}_2\text{O}_3^{2-}$	62
4.6 Plot of absorbance versus mole ratio for the reaction of $[(\text{H}_2\text{O})_2\text{Ru}_2\text{O}]^{4+}$ and dithionite $\text{S}_2\text{O}_4^{2-}$	63
4.7 Plot of absorbance versus mole ratio for the reaction of $[(\text{H}_2\text{O})_2\text{Ru}_2\text{O}]^{4+}$ and H_3PO_2	64
4.8 Plot of absorbance versus mole ratio for the reaction of $[(\text{H}_2\text{O})_2\text{Ru}_2\text{O}]^{4+}$ and CH_3OH	65
4.9 Plot of absorbance versus mole ratio for the reaction of $[(\text{H}_2\text{O})_2\text{Ru}_2\text{O}]^{4+}$ and $\text{C}_2\text{H}_5\text{OH}$	66
4.10 Plot of absorbance versus mole ratio for the reaction of $[(\text{H}_2\text{O})_2\text{Ru}_2\text{O}]^{4+}$ and $\text{C}_3\text{H}_7\text{OH}$	67
4.11 Typical Pseudo- first order plot for the reaction of $[(\text{H}_2\text{O})_2\text{Ru}_2\text{O}]^{4+}$ and TU	68
4.12 Typical Pseudo- first order plot for the reaction of $[(\text{H}_2\text{O})_2\text{Ru}_2\text{O}]^{4+}$ and MTU	69
4.13 Typical Pseudo- first order plot for the reaction of $[(\text{H}_2\text{O})_2\text{Ru}_2\text{O}]^{4+}$ and ATU	70
4.14 Typical pseudo - first order plot for the reaction of $[(\text{H}_2\text{O})_2\text{Ru}_2\text{O}]^{4+}$ and DMTU	71
4.15 Plot of $\log k_{\text{obs}}$ against $\log [\text{TU}]$ for the reaction of $[(\text{H}_2\text{O})_2\text{Ru}_2\text{O}]^{4+}$ and TU	77
4.16 Plot of $\log k_{\text{obs}}$ against $\log [\text{MTU}]$ for the reaction of $[(\text{H}_2\text{O})_2\text{Ru}_2\text{O}]^{4+}$ and MTU	78

4.17 Plot of $\log k_{\text{obs}}$ against $\log [\text{ATU}]$ for the reaction of $[(\text{H}_2\text{O})_2\text{Ru}_2\text{O}]^{4+}$ and ATU	79
4.18 Plot of $\log k_{\text{obs}}$ against $\log [\text{DMTU}]$ for the reaction of $[(\text{H}_2\text{O})_2\text{Ru}_2\text{O}]^{4+}$ and DMTU	80
4.19 Typical Pseudo- first order plot for the reaction of $[(\text{H}_2\text{O})_2\text{Ru}_2\text{O}]^{4+}$ and $\text{S}_2\text{O}_3^{2-}$	84
4.20 Typical Pseudo- first order plot for the reaction of $[(\text{H}_2\text{O})_2\text{Ru}_2\text{O}]^{4+}$ and $\text{S}_2\text{O}_4^{2-}$	85
4.21 Plot of $\log k_{\text{obs}}$ against $\log [\text{S}_2\text{O}_3^{2-}]$ for the reaction of $[(\text{H}_2\text{O})_2\text{Ru}_2\text{O}]^{4+}$ and $\text{S}_2\text{O}_3^{2-}$	86
4.22 Plot of $\log k_{\text{obs}}$ against $\log [\text{S}_2\text{O}_4^{2-}]$ for the reaction of $[(\text{H}_2\text{O})_2\text{Ru}_2\text{O}]^{4+}$ and $\text{S}_2\text{O}_4^{2-}$	87
4.23 Typical Pseudo- first order plot for the reaction of $[(\text{H}_2\text{O})_2\text{Ru}_2\text{O}]^{4+}$ and H_3PO_2	88
4.24 Plot of $\log k_{\text{obs}}$ against $\log [\text{H}_3\text{PO}_2]$ for the reaction of $[(\text{H}_2\text{O})_2\text{Ru}_2\text{O}]^{4+}$ and H_3PO_2	91
4.25 Typical Pseudo- first order plot for the reaction of $[(\text{H}_2\text{O})_2\text{Ru}_2\text{O}]^{4+}$ and CH_3OH	92
4.26 Typical Pseudo- first order plot for the reaction of $[(\text{H}_2\text{O})_2\text{Ru}_2\text{O}]^{4+}$ and $\text{C}_2\text{H}_5\text{OH}$	93
4.27 Typical Pseudo- first order plot for the reaction of $[(\text{H}_2\text{O})_2\text{Ru}_2\text{O}]^{4+}$ and $\text{C}_3\text{H}_7\text{OH}$	94
4.28 Plot of $\log k_{\text{obs}}$ against $\log [\text{CH}_3\text{OH}]$ for the reaction of $[(\text{H}_2\text{O})_2\text{Ru}_2\text{O}]^{4+}$ and CH_3OH	99
4.29 Plot of $\log k_{\text{obs}}$ against $\log [\text{C}_2\text{H}_5\text{OH}]$ for the reaction of $[(\text{H}_2\text{O})_2\text{Ru}_2\text{O}]^{4+}$ and $\text{C}_2\text{H}_5\text{OH}$	100
4.30 Plot of $\log k_{\text{obs}}$ against $\log [\text{C}_3\text{H}_7\text{OH}]$ for the reaction of $[(\text{H}_2\text{O})_2\text{Ru}_2\text{O}]^{4+}$ and $\text{C}_3\text{H}_7\text{OH}$	101
4.31 Plot of $k_2(\text{H}^+)$ against $[\text{H}^+]$ for the reaction of $[(\text{H}_2\text{O})_2\text{Ru}_2\text{O}]^{4+}$ and TU	102
4.32 Plot of $k_2(\text{H}^+)$ against $[\text{H}^+]$ for the reaction of $[(\text{H}_2\text{O})_2\text{Ru}_2\text{O}]^{4+}$ and MTU	103
4.33 Plot of $k_2[\text{H}^+]$ against $[\text{H}^+]$ for the reaction of $[(\text{H}_2\text{O})_2\text{Ru}_2\text{O}]^{4+}$ and ATU	104

4.34 Plot of $k_2(\text{H}^+)$ against $[\text{H}^+]$ for the reaction of $[(\text{H}_2\text{O})_2\text{Ru}_2\text{O}^{4+}]$ and DMTU	105
4.35 Plot of $k_2(\text{H}^+)$ against $[\text{H}^+]$ for the reaction of $[(\text{H}_2\text{O})_2\text{Ru}_2\text{O}]^{4+}$ and $\text{S}_2\text{O}_3^{2-}$	107
4.36 Plot of $\log k_{\text{obs}}$ against $\log [\text{H}^+]$ for the reaction of $[(\text{H}_2\text{O})_2\text{Ru}_2\text{O}^{4+}]$ and $\text{S}_2\text{O}_3^{2-}$	108
4.37 Plot of $\log k_2$ versus \sqrt{I} for the reaction of $[(\text{H}_2\text{O})_2\text{Ru}_2\text{O}^{4+}]$ and $\text{S}_2\text{O}_3^{2-}$	111
4.38 Plot of $\log k_2$ against $1/D$ for the reaction of $[(\text{H}_2\text{O})_2\text{Ru}_2\text{O}]^{4+}$ and $\text{S}_2\text{O}_3^{2-}$	118
4.39 Plot of $k_2(\text{Mg}^{2+})$ versus $[\text{Mg}^{2+}]$ for the reaction of $[(\text{H}_2\text{O})_2\text{Ru}_2\text{O}]^{4+}$ and $\text{S}_2\text{O}_3^{2-}$	135
4.40 Plot of $k_2(\text{NH}_4^+)$ versus $[\text{NH}_4^+]$ for the reaction of $[(\text{H}_2\text{O})_2\text{Ru}_2\text{O}]^{4+}$ and $\text{S}_2\text{O}_3^{2-}$	136
4.41 Plot of $k_2(\text{CH}_3\text{COO}^-)$ versus $[\text{CH}_3\text{COO}^-]$ for the reaction of $[(\text{H}_2\text{O})_2\text{Ru}_2\text{O}]^{4+}$ and $\text{S}_2\text{O}_3^{2-}$	137
4.42 Plot of $k_2(\text{NO}_3^-)$ versus $[\text{NO}_3^-]$ for the reaction of $[(\text{H}_2\text{O})_2\text{Ru}_2\text{O}]^{4+}$ and $\text{S}_2\text{O}_3^{2-}$	138
4.43 Plot of $k_2(\text{CH}_3\text{COO}^-)$ versus $[\text{CH}_3\text{COO}^-]$ for the reaction of $[(\text{H}_2\text{O})_2\text{Ru}_2\text{O}]^{4+}$ and $\text{S}_2\text{O}_4^{2-}$	141
4.44 Plot of $k_2(\text{HCOO}^-)$ versus $[\text{HCOO}^-]$ for the reaction of $[(\text{H}_2\text{O})_2\text{Ru}_2\text{O}]^{4+}$ and $\text{S}_2\text{O}_4^{2-}$	142
4.45 Plot of $k_2(\text{NH}_4^+)$ versus $[\text{NH}_4^+]$ for the reaction of $[(\text{H}_2\text{O})_2\text{Ru}_2\text{O}]^{4+}$ and $\text{S}_2\text{O}_4^{2-}$	143
4.46 Plot of $k_2(\text{Mg}^{2+})$ versus $[\text{Mg}^{2+}]$ for the reaction of $[(\text{H}_2\text{O})_2\text{Ru}_2\text{O}]^{4+}$ and $\text{S}_2\text{O}_4^{2-}$	144
4.47 Plot of $k_2(\text{NH}_4^+)$ versus $[\text{NH}_4^+]$ for the reaction of $[(\text{H}_2\text{O})_2\text{Ru}_2\text{O}]^{4+}$ and CH_3OH	151
4.48 Plot of $k_2(\text{Mg}^{2+})$ versus $[\text{Mg}^{2+}]$ for the reaction of $[(\text{H}_2\text{O})_2\text{Ru}_2\text{O}]^{4+}$ and CH_3OH	152
4.49 Plot of $k_2(\text{NH}_4^+)$ versus $[\text{NH}_4^+]$ for the reaction of $[(\text{H}_2\text{O})_2\text{Ru}_2\text{O}]^{4+}$ and $\text{C}_2\text{H}_5\text{OH}$	153
4.50 Plot of $k_2(\text{Mg}^{2+})$ versus $[\text{Mg}^{2+}]$ for the reaction of $[(\text{H}_2\text{O})_2\text{Ru}_2\text{O}]^{4+}$ and $\text{C}_2\text{H}_5\text{OH}$	154

4.51	Plot of $k_2(\text{CH}_3\text{COO}^-)$ versus $[\text{CH}_3\text{COO}^-]$ for the reaction of $[(\text{H}_2\text{O})_2\text{Ru}_2\text{O}]^{4+}$ and $\text{C}_3\text{H}_7\text{OH}$	155
4.52	Plot of $k_2(\text{HCOO}^-)$ versus $[\text{HCOO}^-]$ for the reaction of $[(\text{H}_2\text{O})_2\text{Ru}_2\text{O}]^{4+}$ and $\text{C}_3\text{H}_7\text{OH}$	156
4.53	Plot of $1/k_{\text{obs}}$ versus $1/[\text{TU}]$ for the reaction of $[(\text{H}_2\text{O})_2\text{Ru}_2\text{O}]^{4+}$ and thiourea TU	158
4.54	Plot of $1/k_{\text{obs}}$ versus $1/[\text{MTU}]$ for the reaction of $[(\text{H}_2\text{O})_2\text{Ru}_2\text{O}]^{4+}$ and MTU	159
4.55	Plot of $1/k_{\text{obs}}$ versus $1/[\text{ATU}]$ for the reaction of $[(\text{H}_2\text{O})_2\text{Ru}_2\text{O}]^{4+}$ and ATU	160
4.56	Plot of $1/k_{\text{obs}}$ versus $1/[\text{DMTU}]$ for the reaction of $[(\text{H}_2\text{O})_2\text{Ru}_2\text{O}]^{4+}$ and DMTU	161
4.57	Plot of $1/k_{\text{obs}}$ versus $1/[\text{S}_2\text{O}_3^{2-}]$ for the reaction of $[(\text{H}_2\text{O})_2\text{Ru}_2\text{O}]^{4+}$ and $\text{S}_2\text{O}_3^{2-}$	162
4.58	Plot of $1/k_{\text{obs}}$ versus $1/[\text{S}_2\text{O}_4^{2-}]$ for the reaction of $[(\text{H}_2\text{O})_2\text{Ru}_2\text{O}]^{4+}$ and $\text{S}_2\text{O}_4^{2-}$	163
4.59	Plot of $1/k_{\text{obs}}$ versus $1/[\text{H}_3\text{PO}_2]$ for the reaction of $[(\text{H}_2\text{O})_2\text{Ru}_2\text{O}]^{4+}$ and H_3PO_2	164
4.60	Plot of $1/k_{\text{obs}}$ versus $1/[\text{CH}_3\text{OH}]$ for the reaction of $[(\text{H}_2\text{O})_2\text{Ru}_2\text{O}]^{4+}$ and methanol CH_3OH	165
4.61	Plot of $1/k_{\text{obs}}$ versus $1/[\text{C}_2\text{H}_5\text{OH}]$ for the reaction of $[(\text{H}_2\text{O})_2\text{Ru}_2\text{O}]^{4+}$ and $\text{C}_2\text{H}_5\text{OH}$	166
4.62	Plot of $1/k_{\text{obs}}$ versus $1/[\text{C}_3\text{H}_7\text{OH}]$ for the reaction of $[(\text{H}_2\text{O})_2\text{Ru}_2\text{O}]^{4+}$ and $\text{C}_3\text{H}_7\text{OH}$	167

Abbreviations

A_t	=	Absorbance at time 't'
A_∞	=	Absorbance at infinity
ATP	=	Adenosine triphosphate
ATU	=	<i>N</i> - allylthiourea
Bipy, bpy	=	Bipyridyl
B.D.H	=	British Drug House
cyt	=	cytochrome
DMF	=	Dimethyl formamide
DMTU	=	<i>N,N'</i> - dimethylthiourea
D_{op}	=	optical dielectric constant
D_s	=	static dielectric constant
E°	=	Redox potential
e^-	=	Electron
EDTA	=	Ethylenediammine tetraacetic acid
E_{mad}	=	Madelung energy
e.s.r	=	electron spin resonance
ET	=	Electron transfer
E.P.R	=	Electron paramagnetic Rresonance
ϵ	=	molar extinction coefficient
IR	=	Infra red
k_{cal}	=	calculated rate constant
k_{deact}	=	rate constant for deactivation
k_{obs}	=	observed rate constant
k_2	=	second order rate constant

k_{redox}	=	Rate constant of oxidation – reduction process (electron transfer)
k_{subs}	=	Rate constant for substitution
K	=	Equilibrium constant
MMCT	=	Metal to metal charge transfer
MTU	=	<i>N</i> - methylthiourea
Obs	=	observed
PCET	=	Proton coupled electron transfer
phen	=	1, 10 - phenanthroline
PT	=	Proton Transfer
tpy	=	terpyridiyl
TU	=	Thiourea
UV	=	Ultra violet
λ_{max}	=	wavelength of maximum absorption

CHAPTER ONE

INTRODUCTION

1.1 Electron Transfer Reactions

A fundamental understanding of electron transfer (ET) reactions is vital to the inorganic chemist in the context of energy transduction, corrosion processes, metallurgy, redox processes in environmental chemistry, metalloenzymes and metalloproteins involved in ET (Adman, 1979; Bennet, 1972). ET reactions of transition metal complexes are accompanied by a change in the oxidation state of the metal atom and the overall charge on the complex ion.

Since the late 1940s, ET reactions' has grown greatly in biochemical processes. This development, as well as its relation to the study of other kinds of chemical reactions, represents a very interesting history in which many unanswered puzzles have been pieced together.

ET reactions play very important roles in many biological processes including collagen synthesis, steroid metabolism, the immune response, drug activation, neurotransmitter metabolism, nitrogen fixation, respiration and photosynthesis (Prince and George, 1990). The latter two processes are fundamentally significant as they provide most of the energy that is required for the maintenance of life. The extraction of energy from organic compounds, carried out by several catabolic pathways (e.g. the citric acid cycle) involves the oxidation of these compounds to CO_2 and H_2O with the concomitant production of water-soluble reductants (Simonsen and Tollin, 1980). These reductants

donate electrons to components of the mitochondrial electron-transfer chain, resulting in the reduction of oxygen to water.

1.2 Types of Electron Transfer Reactions

1.2.1 Homonuclear or self-exchange electron transfer reactions

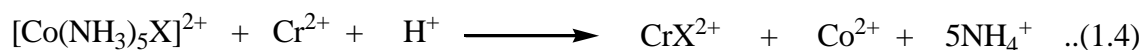
Transfer of electrons can occur between two identical metal ion centres existing in different oxidation states, in what is usually referred to as homonuclear or self-exchange electron transfer reactions. For such reactions, the reactant and product ion concentrations are the same and hence the overall free energy of the reaction is approximately zero with the possibility of very small differences in the free energies of the reactant and products existing as a result of mixing. Isotopic labelling techniques have been employed to monitor the rate of such electron exchange reactions when they are slow. For fast exchange reactions, however, the nuclear magnetic resonance spectroscopic technique is employed (Meyer and Taube, 1987; Wilkins, 1974). Examples of self-exchange reactions are depicted in Equations 1.1 – 1.3.



1.2.2 Heteronuclear or cross electron transfer reactions

Here, different metal ion centres are involved in electron transfer reaction. The difference in the concentrations of the reactants and the products observed in such reactions implies that there must be a net change in the free energy of the reaction, i.e. $\Delta G^{\circ} \neq 0$. It has been found that for most reactions, $\Delta G^{\circ} < 0$. However, in some reactions

$\Delta G^{\circ} > 0$ and the driving force for such reactions is provided by the necessity to maintain the equilibrium concentration of certain intermediate species in one or more of the reaction steps (Ramaraj *et al.*, 1986a, 1986b). Examples of such electron transfer reactions in which $\Delta G^{\circ} < 0$ are represented by Equations 1.4 – 1.6,



Heteronuclear electron transfer reactions can be either complementary, in which the oxidant and the reductant undergo equal changes in oxidation state. Equations (1.4) to (1.6) above are examples of complementary reactions. On the other hand, non-complementary reactions are those in which there are unequal changes in oxidation states by the oxidant and the reactant. Examples of non-complementary reactions are given in Equations (1.7 – 1.9).



1.3 Mechanisms of Electron Transfer

In order to state the mechanism of electron transfer, after knowing that a particular electron transfer is a self-exchange reaction (homonuclear) or a cross-reaction (heteronuclear), complementary or non-complementary, certain very important considerations have to be made:

- (1) Comparison of the rate of electron transfer with the rate of substitution into the inner coordination sphere of the reactant ions.
- (2) The possibility of identifying or inferring the closeness of approach of reactant metal centres in the activated complex prior to electron transfer.
- (3) Is the reaction thermodynamically feasible? If not, what drives the reaction?
- (4) How many electrons are transferred at a time? (if more than one electron is transferred).
- (5) What dictates the interpretation of the acid and base catalysis in some of these reactions? Do the structures of the reactants, transition state products form a basis for rationalisation?
- (6) Are the large variations of rates which usually accompany the variation of reactant ions indicative of the effect of the variation of electronic structure of reactant ions on the rate and mode of electron transfer?

The fundamental classification scheme for the stoichiometric mechanism of redox reactions was established in the 1950s by the Nobel Prize winner in Chemistry of 1983, Henry Taube (Taube, 1959). Taube delineated the innersphere mechanism against the outersphere mechanism for electron transfer reactions.

1.3.1 The innersphere mechanism

Taube in the 1950s recognised that many oxidation–reduction reactions occur by a ligand–bridging mechanism in which substitution of the coordination shell of one of the metal ions occurs. An intermediate or a bridged binuclear complex is therefore formed in which a ligand forms a bridge between one metal ion and the other metal prior to electron transfer. Electron transfer processes occurring through this bridging ligand are

classified as innersphere electron transfer reactions (Lagford, 1979). The bridging ligand is usually, but not always, transferred from one reactant to the other.

1.3.2 The outersphere mechanism

Since electrons are capable of passing through barriers such as ligands via quantum mechanical process of tunnelling, some electron transfers could proceed without any change in the coordination spheres of either reactant. Consider the reactions in Equations 1.10 and 1.11.



Reactions, such as in Equations (1.10) and (1.11), during which the ligands remain coordinated in the primary spheres of the respective central atoms (i.e. no ligand exchange or substitution occurs), are classified as outersphere electron transfer reactions (Taube *et al.*, 1953). The coordination shells of the two reactants remain essentially intact before and after the electron transfer (Larsen and Wahl, 1965). When either or both the oxidant and the reductant are inert to substitution during the time sufficient for electron transfer to take place, outersphere electron transfer is most likely to take place. The activated complex that results during the electron transfer process is designated ‘the outersphere activated complex’.

Outersphere reactions between complexes of different metals are usually very fast: for these reactions are accompanied by a decrease in standard free energy.

1.3.3 Proton couple electron transfer process

In this model, a proton and electron are transferred simultaneously during redox reaction. The study of this model has received a great deal of attention and consideration in the past two decades by researchers (Ghosh *et al.*, 1994; Lohdip and Iyun, 1998 and 2003; Ukoha and Iyun, 2002; Babatunde and Iyun, 2004; Lohdip and Ogara, 2004; Lohdip and Shamle, 2004). The importance of this coupling between movement of proton, which may be a proton transfer (PT) reaction, and electron transfer (ET) is a well elaborated theme in the study of a number of biological assemblies (Babcock *et al.*, 1989; Wikstrom, 1989; Morgan and Wikstrom, 1991). The coupling of PT and ET is referred to as proton coupled electron transfer (PCET) reaction (Turro *et al.*, 1992). Coupling between proton motion and electron transfer is a fundamental mechanism for energy conversion in biological and chemical systems. The translocation of protons across biological membranes in the proteins involved in photosynthesis (Babcock *et al.*, 1989; Okamura and Feher, 1992) and respiration (Wikstrom, 1989; Babcock and Wikstrom, 1992; Malmstrom, 1993) is based on PCET.

1.3.4 Solvated electron theory

A solvated electron is a free electron in solution. Solvated electrons are widely occurring and represent a more diffuse charge distribution than do electrons in molecules. The solvated electron theory presents a mechanism of electron transfer that occurs in non-aqueous media like NH_3 and halides (Ayoko, 1981). The basic assumption of this theory is that there is ejection of an electron by the reducing agent into the solvent which solvates the electron and holds it until an oxidising agent picks it up.

1.4 Diagnosis of Redox Reaction Mechanisms

Assigning outersphere or innersphere to redox reactions can be adequately done by considering some criteria.

1.4.1 Comparison of the rate of electron transfer and the rate of substitution (k_{redox} versus k_{subs})

Comparison of the rate of electron transfer versus the rate of substitution into the inner coordination shell of the more labile of the reactants can be used to assign mechanism of the redox reaction since in the innersphere mechanism, substitution into the inner coordination shell of one of the reactant ion precedes electron transfer.

When the rate of electron transfer (rate of redox process) is much greater than the rate of substitution i.e. when $k_{\text{redox}} \gg \gg k_{\text{subs}}$, the outer-sphere mechanism of electron transfer is implicated (Rossenheim *et al.*, 1974), while if $k_{\text{redox}} \ll \ll k_{\text{subs}}$, the innersphere mechanism is said to be operating. However, if $k_{\text{redox}} = k_{\text{subs}}$, both the innersphere and the outersphere mechanisms are simultaneously in operation (Endicott and Taube, 1964). In the electron transfer reaction between $\text{Fe}(\text{phen})_3^{2+}$ and $^*\text{Fe}(\text{phen})_3^{3+}$ (Larsen and Wahl, 1965) given in Equation (1.12), the rate constants for the substitution of phen



for $^*\text{Fe}(\text{phen})_3^{2+}$ and $\text{Fe}(\text{phen})_3^{3+}$ are $7.5 \times 10^{-5} \text{ s}^{-1}$ and $5.01 \times 10^{-5} \text{ s}^{-1}$, respectively, while the rate constant for electron exchange is $10^5 \text{ dm}^3 \text{ mol}^{-1} \text{ s}^{-1}$. Since in this reaction $k_{\text{red}} \gg k_{\text{sub}}$, it has been explained in favour of outersphere. This was also observed for

the electron exchange reaction between $\text{Fe}(\text{CN})_6^{4-}$ and $\text{Fe}(\text{CN})_6^{3-}$ (Campion *et al.*, 1967; Deck and Wahl, 1954).

1.4.2 Identification of binuclear intermediate

Innersphere mechanism is said to be in operation if there is an evidence of the presence of a binuclear complex either as a transient or stable intermediate along a pathway between reactants and products (Haim, 1983). In the reduction process involving $\text{Fe}(\text{OH}_2)_6^{2+}$ (Haim and Sutin, 1966) and $\text{V}(\text{OH}_2)_6^{2+}$ (Espenson, 1967; Price and Taube, 1968), detection of transient intermediates from ligand transfer processes was possible by the use of rapid flow techniques. In the course of the reaction between VO^{2+} and Cr^{2+} , an intermediate, VOCr^{4+} was characterized (Espenson, 1965). The possibility of identifying binuclear intermediates in the inner–sphere mechanism occurs when reduced oxidant and the oxidised reductant are relatively inert to substitution. Initial investigations suggest that most of the intermediates formed are successor complexes. For example, halide-bridged successor complexes have been found in the reactions of IrCl_6^{2-} with $\text{Co}(\text{CN})_5^{2-}$ (Grossman and Haim, 1970) and IrBr_6^{2-} and $\text{Cr}(\text{OH}_2)_6^{2+}$ or $\text{Co}(\text{CN})_5^{2-}$ (Melvin and Haim, 1977) and the rate of decomposition of the intermediate is slower than the rate of electron transfer. In situations where the binuclear intermediate is transient in nature, their presence can only be confirmed indirectly from kinetics data or from empirical rate law.

1.4.3 Product analysis

In the innersphere mechanism where there is the formation of a bridging ligand, transfer of the latter from one metal ion to another provides an empirical proof that the

innersphere mechanism is in operation. Taube and co-workers (Taube *et al.*, 1953) have shown that reaction (Equation 1.13) occurs.



where X = Halide, SO_4^{2-} , NCS^- , N_3^- , PO_4^{3-} , $\text{P}_2\text{O}_7^{2-}$, CH_3COO^- , $\text{CH}_3\text{C}_7\text{CO}_2^-$, succinate, maleate and oxalate.

Also, the same researchers reported that in the redox reaction involving $\text{Co}(\text{NH}_3)_5\text{Cl}^{2+}$ and Cr^{2+} , the CrCl^{2+} product identified has been associated with the binuclear intermediate $(\text{NH}_3)_5\text{Co}-\text{Cl}-\text{Cr}^{4+}$ proffering evidence in favour of innersphere mechanism (Taube *et al.*, 1953).

1.4.4 Use of ambidentate ligands

The difference in the rate of electron transfer observed with symmetrical and unsymmetrical bridging ligands such as azide, thiocyanate, and isothiocyanate provide a basis for making a distinction between the innersphere and the outersphere mechanisms.

If there is no difference between the ratio of the rate constant for the reduction of the azide complex to that of the reduction of the thiocyanate complex, ($k_{\text{N}}/ k_{\text{NCS}}$) or for isothiocyanate and thiocyanate complex ($k_{\text{SCN}}/ k_{\text{NCS}}$), then the outer sphere mechanism is suspected to be operating. This scenario is observed in the outer-sphere reduction of $[\text{Co}(\text{NH}_3)_5\text{NCS}]^{2+}$ and $[\text{Co}(\text{NH}_3)_5\text{N}_3]^{2+}$ by $[\text{Cr}(\text{bpy})_3]^{2+}$, $[\text{Ru}(\text{NH}_3)_6]^{2+}$, $[\text{Ru}(\text{en})_3]^{2+}$ and $[\text{Ru}(\text{NH}_3)_5\text{OH}_2]^{2+}$, in which there is no discrimination between NCS^- and N_3^- (Haim, 1983). However, if the ratios of the rate constants are dissimilar, then

the innersphere mechanism is suspected (Caldin *et al.*, 1964; Espenson, 1965; Sutin, 1966).

1.4.5 Effect of added ions

The rates of redox reactions are reported to be markedly affected by added ions for a variety of reactions known to occur by the outersphere mechanism. The effects of added ions on the rates of reactions occurring through the innersphere pathway are not so glaring. Thus, observation of the dependence of rate of redox reaction on added cation or anion has been used to distinguish between the two pathways (Lohdip *et al.*, 1998; Ukoha and Iyun, 2001 and 2002; Ukoha and Ibrahim, 2004). However, addition of Cl^- can lead to serious complication in the interpretation of observed rates and kinetics (Thakuria and Gupta, 1975; Adegite *et al.*, 1977). It should be noted that outersphere electron transfer reactions are, theoretically, easier to determine than innersphere reactions because in the latter bond breaking and bond forming steps are pronounced. In the outersphere reaction, the redox nuclei must be sufficiently close to enhance electronic interaction which results in the delocalisation of exchanging electrons. Consequently, reactions proceeding by outersphere mechanism can be catalysed by added ions which shorten the distance to which electron can be transferred (Meyer and Taube, 1987). Added cations affect the electron transfer reaction involving two positive nuclei by the cation repelling away the oxidant, thus reducing the degree of repulsion between the redox centres. This enhances the electron transfer reaction. Also, added anions enhance the electron transfer reaction by the anion coordinating between the redox centres by electrostatic attraction. However, when two oppositely charged ions are involved, added ions could retard the rate of electron transfer because coordination to any of the reactants could reduce the degree of attraction between the redox centres.

This, expectedly, would increase the distance between the redox partners thereby slowing down the electron transfer process (Ukoha, 1999).

1.4.6 Reactivity pattern

Reactivity patterns can successfully be used to assign mechanisms to redox reactions, some of which include:

(1) Reactivity pattern with a wide range of reactants

Comparing the rates of reactions when similar complexes like $\text{Co}(\text{NH}_3)_5\text{X}^{2+}$ (where $\text{X} = \text{Cl}^-$, F^- , Br^- or NO_3^-) are reacted with a particular reductant gives an idea into which of the mechanisms is operating. Since the outersphere mechanism does not depend on the identity of the bridging ligands, it means that the outersphere mechanism is implicated when the rates of the reactions are similar. Conversely, when the rates of reactions are different, the innersphere is suspected since the rates of the reactions in the inner-sphere mechanism depend on the nature of the bridging group (Sykes, 1967; Shea and Haim, 1973)

(2) Relative rates of reactions of hydroxyl and aquo complexes

Since the hydroxyl group (OH^-) is a better bridging ligand than water (H_2O), it follows that hydroxo complexes are expected to react faster via the innersphere mechanism. Therefore, where $k_{\text{OH}} \ll k_{\text{H}_2\text{O}}$, the outer - sphere mechanism is said to be operating while the converse applies when $k_{\text{OH}} \gg k_{\text{H}_2\text{O}}$ (Endicott and Taube, 1964).

1.4.7 Activation parameters

There seems to be no strong correlation between activation parameters ΔH^\ddagger , ΔG^\ddagger and ΔS^\ddagger and the type of mechanism operating in a particular redox process. However, the

signs or the magnitudes of the activation parameters could give a clue as to which mechanism is inherent in a reaction. Formation of precursor complex as in innersphere mechanism is indicated by a negative ΔH^\ddagger (Wilkins, 1974). However, despite the difference in mechanisms for the reaction of Cr^{2+} and V^{2+} with Ru^{3+} complexes, the ΔS^\ddagger are almost the same. Measurements of the volume of activation (ΔV^\ddagger) for the reduction of various complexes has been applied as diagnostic tool in reaction kinetics (Hubbard *et al.*, 1991).

1.5 Effect of Pressure on Electron Transfer

The value of mechanistic information that emerges from kinetic measurements over a series of elevated pressures for solution reactions in inorganic chemistry has been realised for some time (Stranks, 1974). However, many inorganic reactions are too fast to follow using conventional instrumentation. The momentum regarding investigation at high pressures *vis-à-vis* organic reactions was delayed somewhat until adaptation of rapid reaction techniques for operation at high pressures had been achieved, mostly in the period from 1975 to 1985 (Kotowski and van Eldik, 1989; van Eldik *et al.*, 1989; van Eldik and Merbach, 1992). Studies on the effect of pressure on electron transfer reactions can assist the elucidation of the intimate reaction mechanisms of such processes.

1.6 Rate Monitoring Techniques

A variety of experimental techniques have been developed and used to investigate redox reactions (Sykes, 1966, 1967; Rosseinsky, 1972; Wilkins, 1974). The range of techniques used depends on how fast the reactions go. Many authors have extensively

reviewed the techniques (Stranks, 1960; Caldin, 1974; Wilkins, 1974), which are summarized below:

1.6.1 Conventional methods

The conventional methods involve the measurement, as a function of time, the concentration of one or more of the reactants or products or any physical property like absorbance which is directly related to the concentration. Conventional methods, which are used to monitor slow redox reactions with half – lives approximately 30 seconds, include photometric, spectrometric, polarometric and radiometric techniques. Other physical properties that are directly related to concentration are conductivity, pressure changes, changes in volume, refractive index, optical activity etc.

1.6.2 Fast reaction techniques

These techniques are used to monitor fast reactions with half – lives of about a millisecond. These techniques are in turn classified into (a) flow, (b) relaxation and (c) resonance methods.

(a) Flow Method

This technique involves the mixing of separate solutions of two reactants inside a mixing device. Different flow techniques exist, depending on the treatment the reaction mixture is subjected to (Caldin *et al.*, 1964). The commonest flow methods used are:

(i) Continuous Flow Method

Here, the reaction mixture flows continuously along an observation tube while conventional monitoring is made either at different points along the observation tube with the flow maintained at constant rate or at a fixed

point on the tube with varied flow rate. In either case, a series of values for the extent of reaction is obtained at different times. These values constitute the kinetic data required.

(ii) Stopped – Flow Method

In this method, the solutions are mixed together in a mixing device and as the mixed solutions flow along the tube, it is abruptly stopped so that the solution comes to rest within a few milliseconds. The rate of the flow along the observation tube is such that when the solution is stopped, a segment within 1 cm of mixing device has been mixed for only 1–2 milliseconds. Any reaction taking place in this segment of solution is then monitored and the signal relayed to an oscilloscope.

(iii) Quenched – Flow Method

In this method, the reaction solution is quenched after a pre – determined time and the quenched solution is analysed by any conventional method.

(b) Relaxation Method

Very fast reversible reactions with half – lives ($t_{1/2}$) as short as 10^{-9} seconds are measured using the relaxation methods (Eigen and De Maeyer, 1963). Any equilibrium attained during the reaction is perturbed by sudden variation of a physical parameter such as temperature, pressure, or electric field intensity and the time taken to readjust to a new equilibrium is monitored, which is then related to the rate constants of the forward and reverse reactions. The dependence of a particular equilibrium on a chosen external physical parameter largely determines the method of perturbation used for such equilibrium and hence these

methods are referred to as ‘temperature–jump’, ‘pressure–jump’ or ‘electric field–jump’.

(c) Resonance Methods

Burlamacchi *et al.* (1967) reported the use of both nuclear magnetic resonance (N.M.R) and electron spin resonance (E.S.R) in the study of rates of reactions. In the N.M.R. technique, the resonance absorption line is related to the life-time of the nucleus in a given state, while in E.S.R it is related to the life-time of paramagnetic species in a given energy state. Line broadening is always the result of any reduction of life-time of these states by a chemical interaction. By adding an increasing amount of a reagent, measurement of the corresponding increase in width of the line due to the second reagent can be made. H_{nmr} line broadening, for example, has been used to measure the rate of exchange of several mono- and bidentate nitrogen and oxygen donor ligands coordinated to Mn^{II} , Fe^{II} , Co^{II} , Ni^{II} and Cu^{II} (Caldin *et al.*, 1964).

1.7 Justification of the Study

Transition metal systems in which metal ions are linked by a bridging ligand can differ significantly with regard to the nature and/ or extent of metal – metal interactions. For nonorganometallic first row transition metal ions’ systems like Fe–O–Fe, relatively weak metal – metal interactions are commonly found. The nature and extent of the interactions have been studied extensively using magnetic techniques (Weaver *et al.*, 1975). Although interactions do exist, the component ions usually have chemical and electronic properties similar to the properties expected for isolated monomeric complexes. The same strong modification in properties can also occur in ligand-bridged complexes if the metal-metal interaction across the bridging ligand is sufficiently

strong. Griffiths (1970) reported that oxo – bridged complexes of the first row transition element series, like Fe–O–Fe, exhibit only weak metal-metal interactions, but the interactions seem to be much stronger for the second and third rows, consecutively. Compared to the Ru and Os system in which the extent of metal-metal interaction between Ru(III) ions and Os(III) ions is sufficient to change appreciably the chemical and electronic properties of the dimeric ions, the metal – metal interactions between the Fe(III) ions is apparently insufficient to change the properties of the dimeric ions to an appreciable extent. This is probably because of a greater d-orbital radial extension for Ru(III) and Os(III) when compared to Fe(III) (Weaver *et al.*, 1975). Consequently, the Ru(III) and Os(III) have been grouped in Class II of Robin and Day (1967) classification, while the Fe–O–Fe system has been classified in Class III of the Robin and Day Scheme. An example of a Ru–O–Ru system is the *blue dimer*, $[(\text{H}_2\text{O}(\text{bipy})_2\text{Ru}-\text{O}-\text{Ru}(\text{bipy})_2\text{H}_2\text{O})]^{4+}$ or diaquotetrakis (2,2'- bipyridine)- μ -oxodiruthenium(III) ions. This dimer has generated a lot of interest due to its versatility, including its ability to mimic photosynthesis. The catalytic oxidation of water and chloride with the *blue dimer* was reported by the Meyers research team (Gersten *et al.*, 1982; Gilbert *et al.*, 1985). Consequent upon Meyers and his co-researchers report on the catalytic activity of the dimer, many studies have been carried out on the mechanism of this catalysis with Ce^{IV} and Co^{III} as oxidants (Nagoshi *et al.*, 1999; Binstead *et al.*, 2000; Yamada *et al.*, 2001; Meyer and Huynh, 2003). The versatility of the *blue dimer* cuts across its potential use in diverse areas such as photosensitisers for photochemical conversion of solar energy (Meyer, 1990; Balzani *et al.*, 1996; Kalyanasundaram and Gratzel, 1998; Juris *et al.*, 1998; Hammerstrom *et al.*, 2000 and Islam *et al.*, 2003), molecular electronic devices (Barigelletti and Flamigni, 2000; El-Ghayoury *et al.*, 2000; Mishra *et al.*, 2003 and Newkome *et al.*, 2004).

The oxo-bridged ruthenium dimer has been synthesised, characterised and a lot of kinetic data have been documented as regards its redox behaviour (Weaver *et al.*, 1975; Iyun *et al.* 1992a, 1992b, 1992c, 1992d, 1995a, 1995b, 1996). It has been reported that in oxo-bridged systems having the Ru–O–Ru moiety, chemically significant interactions exist between the Ru atoms through the bridging ligand (Meyer, and Huynh, 2003). Such compounds manifest unusual physical and chemical properties. This is possibly as a result of the strong Ru–O–Ru interaction which makes the separate Ru³⁺ ions lose their identity since the valence levels which largely determine these properties are molecular orbitals delocalised over the Ru–O–Ru linkage.

The use of thiourea and its derivatives, thiosulphates ions, dithionite ions (all oxyanions of sulphur), hypophosphorous acid (phosphorous oxyacid) and the alcohols as reductants of choice in this work is based on the role they play both in chemical and biochemical systems. Thiourea and its derivatives have been used as effective scavenger of reactive oxygen intermediates (Fox, 1984). Due to their reducing properties, they have been used in the textile industry (Arifoglu *et al.*, 1992), as corrosion inhibitors (Ayres, 1970) and in industrial equipment such as boilers which develop scales due to corrosion. Besides these, several thiourea derivatives have various agricultural uses as fungicides, herbicides and rodenticides and industrial uses which include applications in rubber industries as accelerators, and in photography as fixing agents and to remove stains from negatives. Gaining an insight into the redox pattern of this important class of reductants would be of immense value to knowledge, thus including them as reductants in this study. Thiosulphates and dithionites are oxyanions of sulphur which are good reducing agents. The reducing property of the thiosulphate ions has made it gain wide application in photographic processing as a fixer and also used in gold extraction. By

this study, we hope to promote the knowledge of the redox behaviour of these sulphur oxyanions. The peculiar reduction property of hypophosphorous acid as reported by Carroll and Thomas (1966), involving the active H_3PO_2 species obtained by acid induced activation of the inactive H_3PO_2 through a reversible tautomeric shift has made hypophosphorous acid attractive to us for this study. Various possibilities exist in the oxidation of alcohols. These possibilities include mechanisms that involve hydride ion transfer to the oxidant prior to the rate determining decomposition of the intermediate to products (Lee and Spitzer, 1975; Sengupta *et al.*, 1986; Lee and Congson, 1990; Nimbalkar and Chavan, 1998; Saraswat *et al.*, 2003; Dharmaraja *et al.*, 2008; Kothari and Banerji, 2011; Dhage *et al.*, 2013 and Bijudas, 2014), attack of ClO_2^- on an $\alpha - \text{H}$ in ethanol in the oxidation of ethanol by ClO_4^- (Gaswick and Krueger, 1969) and initial equilibrium formation of chromate ester followed by a rate determining decomposition to products (Yusuf *et al.*, 2004). The above highlights have stirred up our interest in investigating the kinetics and mechanisms of oxidation of methanol, ethanol and propanol by the oxo-bridged ruthenium dimer. Understanding the mechanisms of these reactions may assist in the improvement of breadth analysis for detecting the level of alcohol in the system. It is our hope that redox kinetics and mechanistic studies involving alcohols like earlier ones (Iyun and Ukoha, 1999; Yusuf *et al.*, 2004) will assist in further understanding of these complex but seemingly simple reactions.

1.8 Aim and Objectives of the Study

The aim of the research is to generate kinetic data which would give an insight into the mechanisms of the electron transfer reactions of diaquotetrakis (2,2'- bipyridine) - μ - oxodiruthenium (III) ions and some reductants. The findings would contribute to knowledge of the redox behaviour of this versatile μ -oxo-bridged ruthenium complex

and μ -oxo-bridged systems, in general. The objectives to achieve the aim of the study include the following:

- i. To synthesise and characterize the diaquotetrakis(2,2'-bipyridine)- μ -oxodiruthenium(III) complex ions.
- ii. To determine the stoichiometries of the reactions.
- iii. To determine the pseudo-first order and second order rate constants of the reactions.
- iv. To determine the order of reactions' with respect to each of the reductants.
- v. To determine the effects of changing the hydrogen ion concentration on the rates of the reactions that took place in acid medium.
- vi. To determine the effects of changes of ionic strength and dielectric constant of reaction medium on the rates of the reactions.
- vii. To determine the effect of added ions to the reaction medium on the rates of reactions.
- viii. To determine the participation of free radicals in the various reactions.
- ix. To determine the formation of intermediate complexes in the course of the reactions.

CHAPTER TWO

LITERATURE REVIEW

2.1 Ruthenium Chemistry

Studies on ruthenium chemistry have, in the recent past, been receiving considerable attention (Weaver *et al.*, 1975; Iyun and Adegite, 1990 and Iyun *et al.*, 1992a, 1992b, 1992c, 1992d, 1995a, 1995b, 1996) The transition metal offers a wide range of oxidation states, a property which makes it very accessible chemically and electrochemically (from oxidation states -2 in $[\text{Ru}(\text{CO})_4]^{2-}$ to +8 in RuO_4). This important observation makes ruthenium complexes very active as far as redox reactions are concerned. This redox activity makes their applications as redox reagents in different chemical reactions of much current interest. Interest in ruthenium complexes as targets of study is attributed to many factors including the kinetic stability of ruthenium in several oxidation states, the often reversible nature of its redox couples and the relative ease with which mixed – ligand complexes can be prepared by controllable stepwise methods (Weaver *et al.*, 1975)

Applications of ruthenium complexes in many fields of chemistry are numerous. Observations can be made on the clear correlations between the properties of the ruthenium complexes and the nature of the ligands bonded to the central ion. For example, ruthenium sulphoxide complexes are very useful in catalysis (Kagan and Roman, 1992) and chemotherapy (Alessio *et al.*, 2004).

2.1.1 Properties of ruthenium polypyridyl complexes

Ruthenium complexes with polypyridyl ligands have received much attention owing to their interesting spectroscopic, photophysical, photochemical and electrochemical

properties, which are responsible for their potential uses in diverse areas such as photosensitizers for photochemical conversion of solar energy (Kalyanasundaram, 1982; Juris *et al.*, 1988; Meyer, 1989, 1990; Balzani *et al.*, 1996; Kalyanasundaram and Gratzel, 1998; Hammerstrom *et al.*, 2000; Islam *et al.*, 2003), molecular electronic devices (El-Ghayoury *et al.*, 2000; Barigelletti and Flamigni, 2000; Mishra *et al.*, 2003; Newkome *et al.*, 2004). Ruthenium bipyridyl complexes have been used as efficient sensitizers for photochemical cells based on non-porous films of TiO₂ (Tennakone *et al.*, 1998). These polypyridyl complexes have been used as photoactive DNA cleavage agents for therapeutic purposes (Chao *et al.*, 2002; Holze *et al.*, 2002; Ossipov *et al.*, 2002; Jiang *et al.*, 2003). They are also known to perform a variety of inorganic and organic transformations. Their synthetic versatility, high catalytic performance under relatively mild reaction conditions and high selectivity make these complexes particularly well suited for their use in organic and inorganic transformations.

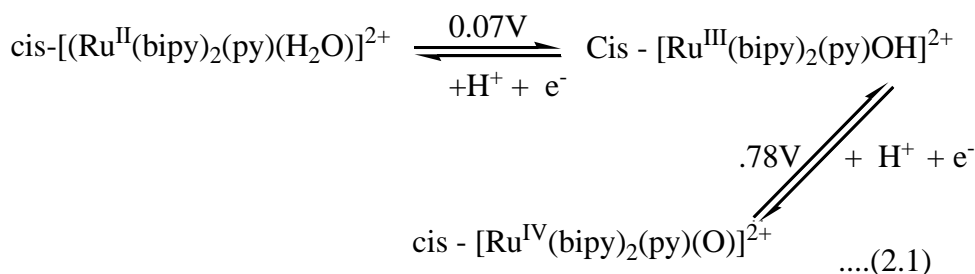
Polypyridyl complexes of ruthenium with aqua ligands are used extensively for the oxidation of organic substrates and multiple oxidative pathways have been detected including atom transfer, C-H insertion and proton coupled electron transfer (Lebeau and Meyer, 1999; Catalano *et al.*, 2000; Rodriguez *et al.*, 2001; Geneste and Moinet, 2004). The suitability of ruthenium polypyridyl aqua complexes in the design of redox catalysts has been documented for a variety of reasons. Firstly, these compounds are useful catalysts in redox reactions since one or more oxidation states are frequently available, thus enabling multiple electron transfers to occur. Also, their inertness to substitution allows for chemically reversible electron transfer uncomplicated by ligand exchange. This, therefore, makes these ruthenium complexes retain their integrity in solution and are relatively easy to study. Finally, the oxo-aqua ligands provide for rapid

proton transfer concomitant with electron transfer, permitting the accessibility of reversal oxidation states via gain or loss of protons.

2.1.2 Electron transfer in ruthenium complexes

Ruthenium (II)–polypyridyl complexes of similar size but with variable reduction potential undergo efficient photoinduced electron transfer reactions with phenolate ions in aqueous medium. All these reactions are exergonic and are in accordance with the Marcus theory of electron transfer. At high negative ΔG° , Marcus inverted region is observed in this bimolecular photoinduced charge separation reaction (Thanasekaran, *et al.*, 1997).

A typical example for electron transfer reactions of ruthenium complexes with an aqua ligand is shown in equation (2.1)



at $I = 0.1 \text{ mol dm}^{-3}$ and $\text{pH} = 7$

Stabilisation of Ru^{IV} in the aqua – containing coordination environment is indicated by equation (2.1). The cause of this is the proton loss and electronic stabilisation of the higher oxidation state by oxoformation, which causes the near overlap of Ru (IV/ III) and Ru(III/ II) couples (Che and Yam, 1992). Thermodynamically, Ru^{IV} is nearly as good acting as a two–electron oxidant as a one – electron oxidant at $\text{pH} = 7$. This fact is

very important implications in catalysis since the two – electron pathways with concomitant formation of the two–electron oxidised product are the most favourable energetically. An additional advantage is that two–electron pathways avoid high energy one–electron intermediates which have often indiscriminate chemistries that can lead to a lack of selectivity (Keene, 1999 and Meyer, 1984). The oxo group is also mechanistically important since it provides an O transfer pathway and initial lead–in site for attack on a substrate or an acceptor site for transferred hydrogen in hydrogen transfer. Ruthenium oxo and hydroxo species, generated through the reaction of low–valent ruthenium complexes and various oxidants, are used extensively for the oxidation of organic substrates. These complexes are versatile oxidants which are able to provide a variety of redox products which are illustrated, with examples, in Equations 2.2 – 2.9

Outersphere electron transfer:



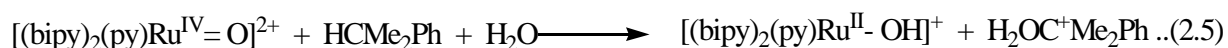
Proton–coupled electron transfer



Hydride transfer:



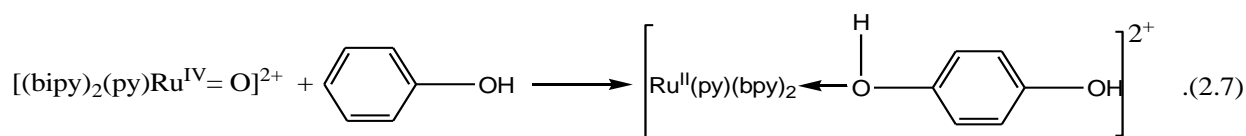
Hydride transfer and nucleophilic addition:



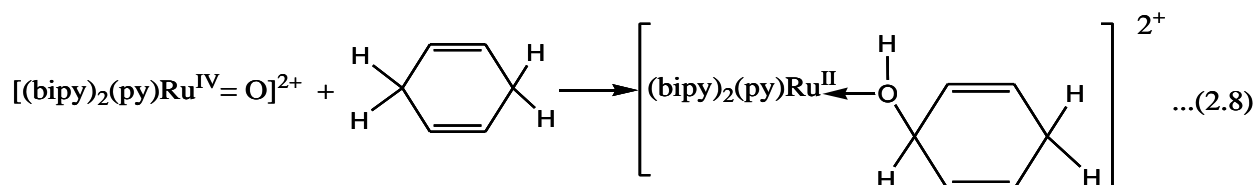
Oxygen – atom transfer:



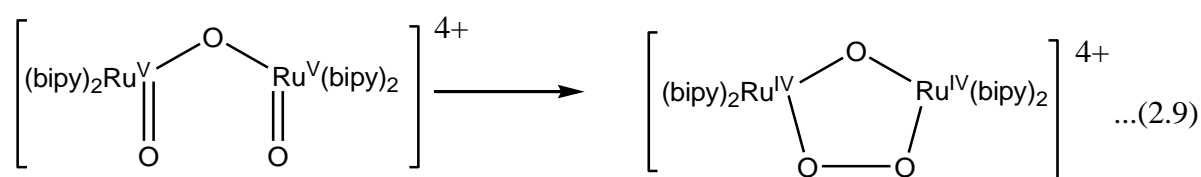
Electrophilic ring attack



C – H Insertion



Oxidative coupling:



Special attention has been paid to Ru-oxo complexes as catalysts for water oxidation to oxygen. As can be seen in Equation 2.10, the mechanism demands the evolution of O₂ and the loss of 4e⁻ and 4H⁺ with the formation of an O–O bond.



One possible approach to the design of a water oxidation catalyst is a dimeric structure with two Ru-oxo groups in close proximity, a good example of which is the *blue dimer* reported by Meyer *et al* in 1982 (Gilbert *et al.*, 1985, Meyer, 1989 and Gersten *et al.*, 1982), which is the first reported ruthenium catalyst able to oxidise water to molecular oxygen.

2.1.3 Photosynthesis and water oxidation catalysis

The demand for energy in today's society is on the increase. This increase is being taken care of by the use of fossil fuels. However, fossil fuels, not being renewable, will definitely be used up in a no distant future. The fossil fuel is not, therefore, a long-term

solution for the increasing need for energy. Exploitation of other sources of energy would, definitely, allow us use fossil fuels in a more sustainable way to produce common products such as detergents, synthetic fibres, plastics, paints, food additives, pesticides etc. The negative effects of the use of fossil fuels on the environment is another reason why the use of fossil fuels should be avoided. There is, therefore, a pressing need to find alternative, renewable and environment friendly energy sources. The amount of solar energy that reaches the Earth's surface in one hour is equal to the amount of fossil fuels that is consumed globally in one year (Freemantle, 1998). If this enormous energy could be used to produce a clean and renewable energy source, the advantages would be obvious. In photosynthesis, green plants convert solar energy into chemical energy that they need for their survival. The driving force in artificial photosynthesis is the idea of constructing an artificial device capable of converting sunlight into electricity or some kind of fuel, by mimicking the process responsible for the energy conversion in photosynthesis. Since these devices would not generate any harmful byproducts, they are attractive from the environmental point of view. During the last four decades, a lot of effort has been devoted to the construction of an artificial system that mimics the natural way of converting solar energy to chemical energy. By using knowledge obtained from the natural system, several model systems have been constructed and studied.

2.1.4 Homogenous water oxidation by ruthenium complexes

The catalytic oxidation of water and chloride with a binuclear ruthenium complex known as the *blue dimer* $[(bpy)_2(H_2O)RuORu(H_2O)(bpy)_2]^{4+}$ was reported by the Meyer's group in 1982 (Gersten *et al.*, 1982; Gilbert *et al.*, 1985). Oxidative degradation and water-ion ligand exchange of the catalyst, however, limits its activity to

10-25 turnovers. Since then, the *blue dimer* and related compounds have been extensively studied in order to elucidate their mechanism of water oxidation and increase their efficiency and stability (Rotzinger *et al.*, 1987; Nazeeruddin *et al.*, 1988; Petach and Elliot, 1992)

The catalytic activity of a number of mono-, di- and trinuclear ammine complexes have been reported (Ramaraj *et al.*, 1986a, 1986b, 1987, 1991). Water oxidation catalysis by these complexes was investigated in homogenous aqueous solution to evaluate the influence of structure on their catalytic activity and mechanism (Nagoshi *et al.*, 2000; Yagi *et al.*, 1996, 1997, 1999a, 1999b, 2000a, 2000b, Yagi and Kaneko, 2001). Catalytic activities of various ruthenium complexes are summarized in Table 2.1.

Consequent upon Meyers *et al* report of the catalytic activity of the *blue dimer*, many studies have been carried out on the mechanism of this catalysis with Ce^{IV} and Co^{III} as oxidants (Nagoshi *et al.*, 1999; Binstead *et al.*, 2000; Meyer and Huynh, 2003; Yamada *et al.* 2001, 2004;). Literature has shown that, so far, only the species with oxidation state $\text{Ru}^{\text{III}}(\mu\text{-O})\text{Ru}^{\text{III}}$ and $\text{Ru}^{\text{III}}(\mu\text{-O})\text{Ru}^{\text{IV}}$ have been characterised by X-ray crystallography (Schoonover *et al.*, 1996). While the higher oxidation state species $\text{Ru}^{\text{IV}}(\mu\text{-O})\text{Ru}^{\text{IV}}$, $\text{Ru}^{\text{IV}}(\mu\text{-O})\text{Ru}^{\text{V}}$ and $\text{Ru}^{\text{V}}(\mu\text{-O})\text{Ru}^{\text{V}}$ have been characterized by uv-vis resonance Raman and EPR spectroscopy (Schoonover *et al.*, 1996, Lei and Hurst, 1994a, 1994b, Hurst, 2005). It has been observed generally that a species with a $\text{O}=\text{Ru}^{\text{V}}(\mu\text{-O})\text{Ru}^{\text{V}}=\text{O}$ core is generated before the key O-O bond formation. The ruthenium terminal oxo bond ($\text{Ru}^{\text{V}}=\text{O}$) was characterized in solution by a resonance Raman band shift from 818 to 780 cm^{-1} upon ^{18}O -isotope labelling (Yamada *et al.*,

Table 2.1: Comparison of the Catalytic Activity (k_{O_2}) of Various Ruthenium Complexes in Water Oxidation

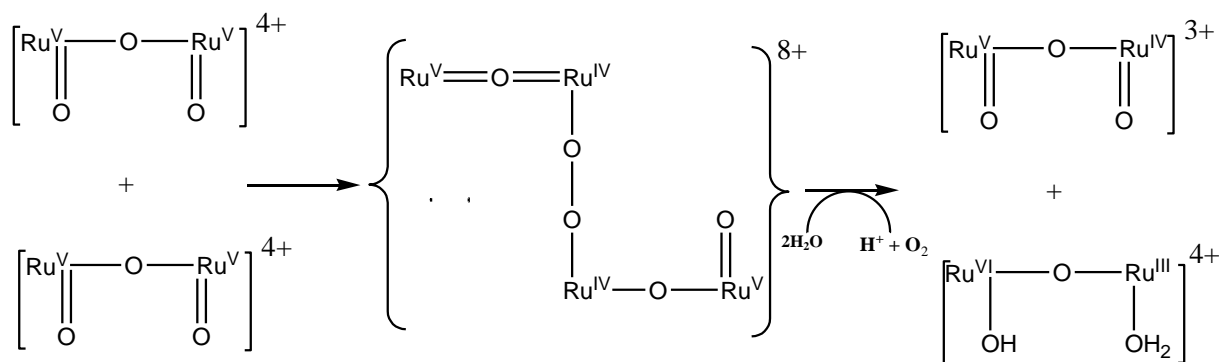
	$k_{O_2} / 10^{-3} \text{ s}^{-1}$	
	Homogenous System	Heterogenous system
$[(\text{NH}_3)_5\text{Ru}^{\text{III}}(\mu\text{-O})\text{Ru}^{\text{IV}}(\text{NH}_3)_4(\mu\text{-O})\text{Ru}^{\text{III}}(\text{NH}_3)_5]^{6+}$ (a)	51	45
$[(\text{bpy})_2(\text{H}_2\text{O})\text{Ru}^{\text{III}}(\mu\text{-O})\text{Ru}^{\text{III}}(\text{H}_2\text{O})(\text{bpy})_2]^{4+}$ (b)	4.2	2.4
$[(\text{NH}_3)_5\text{Ru}^{\text{III}}(\mu\text{-O})\text{Ru}^{\text{III}}(\text{NH}_3)_5]^{4+}$ (c)	13	13
$[(\text{NH}_3)_3\text{Ru}^{\text{III}}(\mu\text{-Cl})_3\text{Ru}^{\text{II}}(\text{NH}_3)_3]^{2+}$ (d)	56	63
$[\text{Ru}^{\text{III}}(\text{NH}_3)_6]^{3+}$ (e)	0.014	0.035
$[\text{Ru}^{\text{III}}(\text{NH}_3)_5\text{Cl}]^{2+}$ (f)	0.31	2.7
<i>cis</i> - $[\text{Ru}^{\text{III}}(\text{NH}_3)_4\text{Cl}_2]^{+}$ (g)	2	14
$[\text{Ru}^{\text{III}}(\text{en})_3]^{3+}$ (h)	0.17	0.085

(a)(Yagi *et al.*, 1996); (b)(Nagoshi *et al.*, 1999); (c)(Nagoshi *et al.*, 2000); (d)(Yagi *et al.*, 1999a); (e)(Yagi *et al.*, 1999b); (f)(Yagi *et al.*, 1997); (g)(Yagi *et al.*, 2000); (h)(Yagi *et al.*, 1999b)

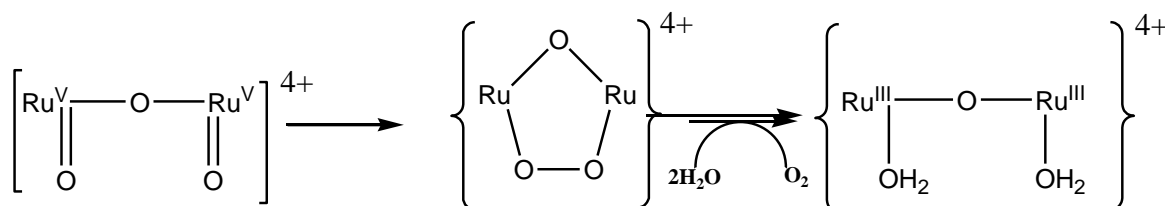
2001). This intermediate was also isolated as a ClO_4^- salt under cold and strong acidic conditions although handling of this compound is difficult owing to its instability (Schoonover *et al.*, 1996).

^{18}O -labelled $\text{Ru}^{\text{III}}(\mu\text{-O})\text{Ru}^{\text{IV}}$ was prepared by Geselowitz and Meyer and oxidised in $^{18}\text{OH}_2$ and 0.1M $\text{CF}_3\text{SO}_3\text{H}$ with Ce^{IV} (Geselowitz and Meyer, 1990). The product distribution $^{36}\text{O}_2$. $^{34}\text{O}_2$. $^{32}\text{O}_2$. was found to be 13.64.23. There is a qualitative consistency of these results with a bimolecular mechanism. After considering these data and stopped flow kinetic measurements, Meyer and co-workers proposed a bimolecular reaction (Scheme 1a) in which the key O-O bond forming step involves the coupling of two $\text{O}=\text{Ru}^{\text{V}}(\mu\text{-O})\text{Ru}^{\text{V}}=\text{O}$ species, giving O_2 , $\text{Ru}^{\text{V}}(\mu\text{-O})\text{Ru}^{\text{V}}$ as a result (Nagoshi *et al.*, 1999; Binstead *et al.*, 2000). They also mentioned the possibility that multiple pathways for water oxidation may contribute to the overall mechanism; the bimolecular mechanism, an intramolecular mechanism (Scheme 1b) and direct water attack on an oxo group are all reasonable pathways that could operate.

Hurst and co-workers carried out similar ^{18}O -labeling/ MS experiments using Co^{III} and Ce^{IV} as oxidants in $\text{CF}_3\text{SO}_3\text{H}$ aqueous solutions (Hurst *et al.*, 1992; Yamada *et al.*, 2004). In these experiments, they obtained only trace amounts of $^{36}\text{O}_2$ in contrast with the aforementioned results by Geselowitz and Meyer, who obtained significant relative yields of $^{36}\text{O}_2$. Considering these results as well as the measured temperature and deuterium solvent isotope dependencies of the O_2 evolution rate, Hurst *et al.* (1992) recently proposed a mechanism involving two reaction pathways, both of which involve nucleophilic addition of water to the ruthenium complex.



Scheme 1a : Bimolecular Pathway



Scheme 1b : Intramolecular Pathway

Mechanism for O - O bond formation proposed by T.J. Meyer and co - workers.

Scheme adopted from Binstead, 2000

Such addition can be either direct to $\text{Ru}^{\text{V}}\text{=O}$ forming Ru-O-OH or can involve the oxidised form of bpy as intermediate (Yamada *et al.*, 2004).

2.1.5 Heterogeneous water oxidation catalysis by ruthenium complexes

Water oxidation catalysis by ruthenium ammine complexes in a Nafion membrane has been demonstrated using Ce^{IV} as oxidant (Yagi *et al.*, 1999; Nagoshi, 2000; Yagi *et al.*, 2000a, 2000b). The complexes can work as active water catalysts in the membrane as well as in solution. Significantly, bimolecular decomposition of the catalysts, which has been found to deactivate them, was remarkably suppressed by incorporating them into the membrane, leading to high activities at high concentrations. One of this ammine complexes, $[(\text{NH}_3)_3\text{Ru}^{\text{III}}(\mu\text{-Cl})_3\text{Ru}^{\text{II}}(\text{NH}_3)_3]^{2+}$ constitutes the most active molecule based

water oxidation catalyst studied to date. From kinetic analysis based on the competitive reactions of water oxidation and bimolecular decomposition of the catalyst, the first-order rate constants for O₂ evolution in a Nafion membrane and in solution were determined as $6.3 \times 10^{-2} \text{ s}^{-1}$ and 5.6 s^{-1} , respectively (Yagi *et al.*, 1999). The similar value of these constants shows that incorporation of the complex into the membrane does not cause a significant loss of its intrinsic activity. On the contrary, the second-order rate constant for deactivation by molecular decomposition ($8.4 \text{ dm}^3 \text{ mol}^{-1} \text{ s}^{-1}$) in the membrane is lower than that ($1.4 \text{ dm}^3 \text{ mol}^{-1} \text{ s}^{-1}$) in solution by 17 times. In this system, the cationic complex is electrostatically attached to anionic sulphonate groups on the Nafion chain, so that there is a strong restriction for the complex to diffuse in the membrane. The bimolecular decomposition would be suppressed by such restrictions of the diffusion, resulting in the lower k_{deact} value of the heterogeneous system.

2.2 Thiourea and Its Derivatives

Reaction of thiourea with hydrogen peroxide under certain conditions produces a powerful reductive bleaching agent, which is routinely used in the textile industry (Arifoglu *et al.*, 1992). Thiourea and its derivatives are used as corrosion inhibitors in industrial equipment such as boilers, which develop scales due to corrosion (Ayres, 1970). The slow build-up of the corrosion products over a period adversely affects the performance of the boilers. Solution of thiourea in dilute hydrochloric acid is used as a complexing agent for removing scales from boilers. In addition, several thiourea derivatives have been used in agriculture as fungicides, herbicides and rodenticides (Sahu *et al.*, 2011) and in other areas, which include rubber industries as accelerators and in photography as fixing agents and to remove stains from negatives. Thiourea is also used as a spectrophotometric reagent for the determination of several metals (Snell,

1978) and its presence in urine was reported to be a non – specific indicator of cancer (Sahu *et al.*, 2011). It is found to be toxic owing to its influence on the metabolism of carbohydrates (Shubha and Puttaswamy, 2009) and has been tagged as carcinogenic (Simoyi, 1986), necessitating greatest care when working with it to prevent direct exposure to humans.

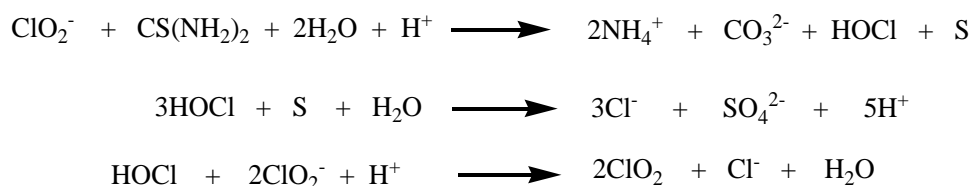
Thiourea and 1,3-dimethyl-2-thiourea (DMTU) are effective scavengers of reactive oxygen intermediates (Fox, 1984). DMTU is reported to be capable of preventing ROI – induced lung injury in *vitro* and *in vivo* (Fox, 1984). Dong *et al.* (2000) have investigated the antioxidant activities of a series of novel phenethyl-5-bromo-pyridyl thioureas (PEPT) with potent anti-HIV activity.

2.2.1 Electron transfer reactions of thiourea and its derivatives

Thiourea, which is the simplest and one of the most reactive sulphur compounds, and its derivatives can be oxidised by a wide variety of oxidising agents (Hoffman and Edwards, 1977; El - Wassimy *et al.*, 1983; Simoyi and Epstein, 1987; Vaidya *et al.*, 1991; Rabai *et al.*, 1993). The reaction pathways and final products of the oxidation reaction depend on the reagents used and condition of the reaction mixtures (Sahu, *et al.*, 2011). The oxidation products may be urea, disulphide, and in some cases, it may undergo either oxidative cyclisation or degradation.

Oxidation of thiourea by iodate (Rabai and Beck, 1985), chlorite (Alamgir and Epstein, 1985), and bromate (Chigwada *et al.*, 2007) has been found to give complex kinetic behaviour. With iodate, the reaction displays oligo-oscillation, in which the concentration of iodide goes through several maxima in a single reaction (Rabai and

Beck, 1985). Simoyi and Epstein (1987) have used chlorine dioxide at low pH in excess of thiourea to generate sulphur and cyanamide. With excess of chlorine dioxide, formamidine sulphanic acid was obtained. When $\text{pH} > 3$, sulphate was detected as a by-product. In a closed system, the reaction between chlorite and thiourea showed a long induction period followed by a rapid production of ClO_2 (Simoyi, 1986). The long induction period was explained by invoking a two-step process in which the thiourea reduced the chlorite to HOCl, followed by the reaction between HOCl and chlorite to give ClO_2 (Scheme 2)



Scheme 2: Reaction Between Chlorite and Thiourea

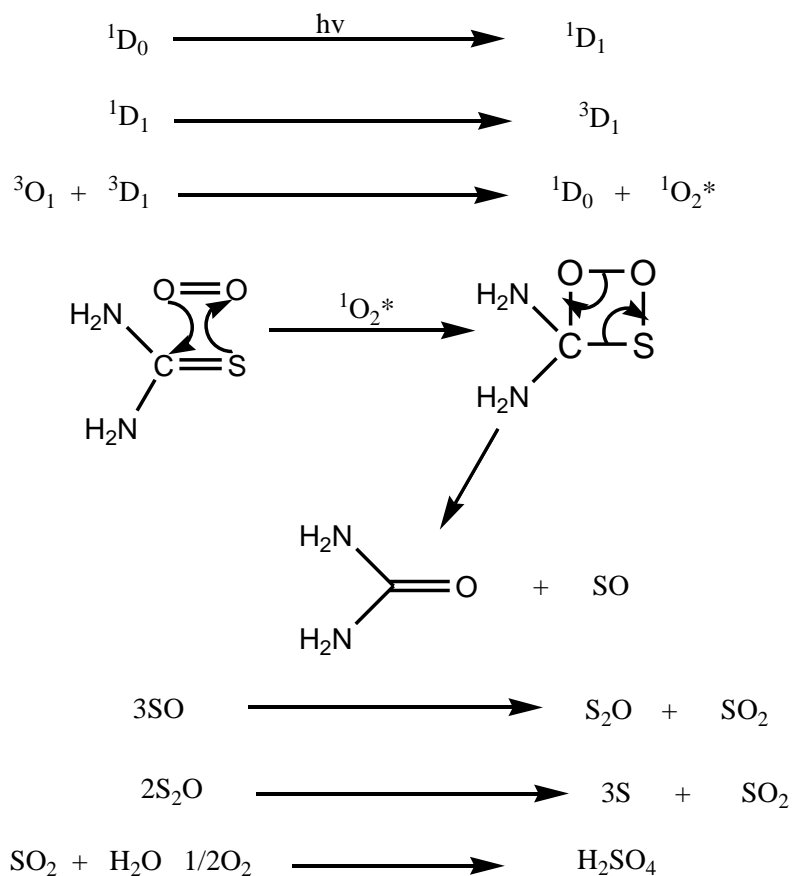
The reaction between thiourea and excess bromate in acidic medium also proceeded by a long induction period involving a slow evolution of bromine (Simoyi, 1986) as shown in Equation 2.11. The long induction period might be resulted from a two-step process, in which thiourea reduced bromate to bromide followed by the reaction of bromide with bromate to give bromine.



Vaidya *et al.* (1991) reported the dye-sensitized photo-oxidation of thiourea to corresponding urea (Scheme 3). However, under acidic conditions, with excess of sodium peroxysulphate or hydrogen peroxide, the oxidation of thiourea led to the formation of NH_4^+ , sulphur, SO_4^{2-} , and CO_2 (Simoyi, 1986). But in excess thiourea, the

formamidine disulphide was formed at low pH, and thiourea dioxide was produced under neutral conditions (Arifoglu *et al.*, 1992).

The conversion of thioureas into ureas has attracted the interest of chemists for a very long time (Corsaro, 1998). Toxic thiourea conversion to biologically benign urea can be made possible by the use of biological as well as chemical oxidants including dioxygen (Miller *et al.*, 1988).



Scheme 3 : Dye-sensitized Photo-oxidation of Thiourea to Urea

1,3-Dimethylthiourea has a protective effect by inactivating reactive oxygen species through desulphurisation (Sprong *et al.*, 1997; Matsumoto *et al.*, 2000; de Agazio and Zacchini, 2001). The kinetics and mechanism of oxidation of thiourea to corresponding

urea have been investigated by various researchers using different reagents. Simoyi and Epstein(1987), in the kinetic studies of oxidation of thiourea in bromine water ($\text{Br}_2/\text{H}_2\text{O}$) in the pH range 1.5 – 4, reported that the reaction occurs in two steps: an initial fast step in which 1 mole of bromine was consumed by 1 mole of thiourea, followed by a slower step in which the rest of the bromine is consumed. Within the pH range 2 – 4, thiourea is oxidised by bromine water to urea (Equation 2.12). However, at a lower pH, thiourea is converted to ammonium sulphate (Equation 2.13). Earlier workers on thiourea reported that the C=S double bond is extremely polar (Simoyi and Epstein, 1987) due to the mismatch in size between the carbon and sulphur



atoms resulting in an incomplete π – bond overlap. Thus, a permanent negative dipole resides on the sulphur atom, making it vulnerable to electrophilic attack. Oxidation of thiourea by bromate in acidic medium was found to proceed via oxygen additions on sulphur, subsequently forming $\text{HOSC}(\text{NH})\text{NH}_2$, $\text{HO}_2\text{SC}(\text{NH})\text{NH}_2$, $\text{HO}_3\text{SC}(\text{NH})\text{NH}_2$, and SO_4^{2-} (Simoyi *et al.*, 1994). Thomas *et al.* (1998) reported the reduction of Cr(VI) to Cr(III) by thiourea in Cr(VI)–thiourea–polyacrylamide gel polymer system. Oxidation of the sulphur atom in a molecule of thiourea by chromium(VI) proceeds via a two – step reaction. In the first step, the sulphur atom in thiourea is oxidised from its oxidation state of -2 to -1, converting thiourea to a disulphide and chromium(VI) to chromium(III). In the second step, the sulphur atoms in the disulphide are oxidised from -1 to +6 oxidation state, converting the disulphide to sulphate and chromium(VI) to chromium(III).

Other than the ureas, formamidine disulphide is also obtained from the oxidation of the thioureas by various oxidants. Zalko and Kratochvil (1968) have reported the oxidation of a series of thiourea to corresponding disulphides by copper (II) in acetonitrile (Dong *et al.*, 2000). An outersphere oxidant, IrCl_6^{2-} , was reported to oxidise thiourea to formamidine disulphide (Henry *et al.*, 1979). Other thioureas such as *N,N'*-dimethylthiourea also gave corresponding disulphide derivatives as the oxidised products (Sahu *et al.*, 2011). Hexacyanoferrate(III) was used to oxidise thiourea and *N*-substituted thioureas under acidic conditions to yield formamidine disulphide (Rabai and Beck, 1985). The reaction proceeds through an outersphere mechanism.

After oral administration to human and animals, thiourea, an antioxidant, is almost completely absorbed and is excreted largely unchanged through the kidneys. However, some metabolic oxidations can take place by biological oxidants. Thyroid gland peroxidase oxidises thiourea in the presence of iodine or iodide and hydrogen peroxide to form formamidine disulphide which, being unstable decomposes at $\text{pH} > 3.0$ to form cyanamide, elemental sulphur and thiourea. It has been reported that, *in vitro* and *in vivo*, both cyanamide and thiourea are inhibitors of thyroid peroxidase (Davidson *et al.*, 1979). In liver microsomes, it has been shown that flavin-containing monooxygenase catalyses the S-oxygenation of thiourea to the reactive electrophilic formamidine sulphenic acid and formamidine sulphinic acid. Thiourea is also oxidised in the rat liver (Shubha and Puttaswamy, 2009). In the presence of glutathione, formamidinesulphenic acid is rapidly reduced.

Under comparable experimental conditions, the rate of oxidation of thiourea increases in the order; *N*-allylthiourea > *N*-phenylthiourea > *N*-methylthiourea > thiourea > *N*-tolylthiourea (Sahu *et al.*, 2011).

2.3 Electron Transfer Reaction of $S_2O_3^{2-}$

The oxidation reactions of thiosulphate ions have been examined by using a variety of oxidants such as hexacyanoferrate(III) (Howelett and Wedzicha, 1970), chromate (Balden and Niac, 1970), octacyanotungstate(V) (Dennis *et al.*, 1985), ferrate (Johnson and Read, 1996), peroxymonosulphate (Johnson and Balahura, 1998) and copper ions (Byerley *et al.*, 1973). Many important analytical procedures utilise these reactions (Nickless, 1968). The usual products are sulphates as in the reaction of thiosulphates and chlorite ions (Nagypal and Epstein, 2004) or tetrathionates as in the reaction of thiosulphates and copper ions (Byerly *et al.*, 1973) or chromate (Balden and Niac, 1970). A few studies involve the activation of thiosulphates by coordination to metal ion (Byerly *et al.*, 1973, Nickless, 1968). For example, the oxidation of $S_2O_3^{2-}$ by molecular oxygen is known to be slow (Nickless, 1968) but in the presence of a copper(II) amine complex, the reaction rates are dramatically increased. It was postulated that coordination of $S_2O_3^{2-}$ to the metal centre catalysed the redox reaction with O_2 . Ferrate rapidly oxidises sulphur-containing compounds presumably by formation of an Fe–O–S intermediate (Johnson and Read, 1996). This intermediate undergoes a two-electron intramolecular electron transfer to form Fe(VI) with transfer of an oxygen to the sulphur centre. Also, Johnson and Read (1996) reported that when the reductant is in excess, ferrate rapidly oxidises thiosulphates to sulphite and the rate law is first order in both reactants. In the oxidation of thiosulphates by copper ions in aqueous ammonia solution, Byerley *et al.* (1973) reported that the copper(II) ions

oxidise thiosulphate ions initially to tetrathionate ions; the latter then undergo a subsequent disproportionation reaction to yield trithionate and thiosulphate ions. The detailed kinetics of the reaction suggest a mechanism which involves substitution of thiosulphate ion into the co-ordination sphere of a triamminecopper(II) complex in the rate-determining step. A one-equivalent electron transfer from the thiosulphate to the copper(II) ion, occurring in the intermediate triamminecopper(II)–thiosulphate complex, gives rise to copper(I) and $S_2O_3^{2-}$ ions, the latter dimerizing to tetrathionate ions. However, in the oxidation of thiosulphate ions by hexachloroiridate(IV) ion Goyal *et al* (1995) documented that the reaction is first-order with respect to $[S_2O_3^{2-}]$ whereas k_{obs} , the pseudo-first-order rate constant ($[IrCl_6^{2-}] \lllll [S_2O_3^{2-}]$), increased with increasing pH. The dependence of k_{obs} on $[H^+]$ indicated that both $HS_2O_3^-$ and $S_2O_3^{2-}$ are involved in the reduction which can only be explained on the basis of an asymmetrical structure for thiosulphuric acid. The reactivity of the $S_2O_3^{2-}$ ion is almost 10^4 times greater than that of the $HS_2O_3^-$ ion (Goyal *et al.*, 1995).

2.4 Electron Transfer Reactions of $S_2O_4^{2-}$

Dithionite is a strong two-electron reducing agent, the property that makes it very suitable for use as a bleaching agent, for chemicals manufacture (Hamza *et al.*, 2012) and as a biochemical reductant (Mayhew, 1978; Davies and Lawther, 1989). The use of dithionite as a general reducing agent in biochemistry include scavenging of oxygen from solutions and maintenance of anaerobiosis and the preparation of the reduced forms of enzymes and electron transfer proteins (Hintz and Peterson, 1980). Reduction-oxidation reactions involving $S_2O_4^{2-}$ with flavodoxin (Mayhew and Massey, 1973), neutrophil cytochrome (Aviram and Sharabani, 1986) and some haemopoetins mainly occurred by a mechanism consistent with the participation of the sulphonyl free radical,

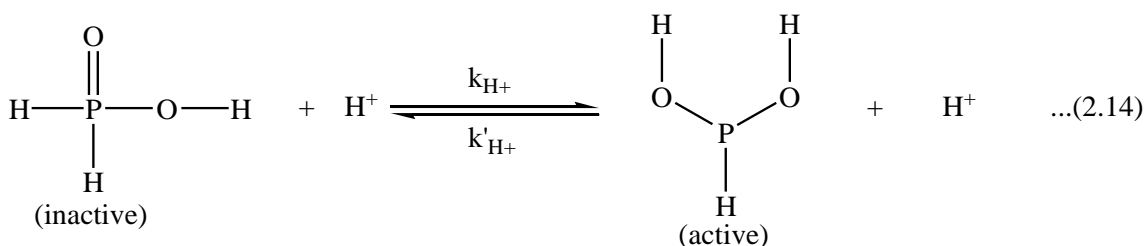
$S^*O_2^-$. Dithionite oxidation has been used to measure oxygen transfer parameters (Camacho *et al.*, 1997) and is studied only at high pH values because of its rapid hydrolysis below the pH of about 10 (Read *et al.*, 2001).

In the study of the oxidation of dithionite by ferrate ions, Read *et al.*, (2001) observed that kinetics for the dithionite oxidation involved two-term rate law, one being first order with respect to [hydrogen ion], [dithionite ion] and [ferrate ion] (where acid is used) and the other being first order in only the dithionite and ferrate ion concentrations. The mechanism has a rate-determining step involving reaction between the protonated ferrate and the oxysulphur ions, when the reaction is carried out in the presence of acid, and between unprotonated ferrate and dithionite ions (where reaction proceeds in absence of acid). However, in the reduction of hexachloroplatinate(IV) by dithionite examined spectrophotometrically in sodium–acetic acid buffer medium, the reaction was reported to be first order in both Pt(IV) species and dithionite (Pal and Gupta, 2012). In the report, H^+ has inhibiting effect on the rate of reaction in the pH range 3.68 – 4.80. The rate of reaction was found to increase with increase in I and D, suggesting a mechanism involving an initial transition state between two like charged ions, which then decomposes to give SO_3^- through the intermediate formation of free radicals, while the study of the kinetics of reactions of cobalamin and cobinamide with dithionite by UV–visible and stopped–flow spectroscopy revealed that the reaction led to the transfer of one electron by dithionite. The reactive species of dithionite oxidation was reported to be $S_2O_4^{2-}$ and SO_2^- (Dereven'kov *et al.*, 2013).

2.5 Electron Transfer Reactions of H₃PO₂

A monobasic acid, hypophosphorous acid, H₃PO₂, also called phosphinic acid is one of the seven oxyacids of phosphorus, the others being phosphorous acid (H₃PO₃), phenylphosphonic acid (C₆H₅H₂PO₂), orthophosphoric acid (H₃PO₄), metaphosphoric acid (HPO₃), hypophosphoric acid (H₄P₂O₆), and pyrophosphoric acid (H₄P₂O₇) (Mehrotra, 2013). It has phosphorus in an oxidation state of +1 and is a powerful reducing agent (Greenwood and Earnshaw, 1997). Hypophosphorous acid has been found to be a better reducing agent than phosphorous acid (Ben – Zvi, 1967).

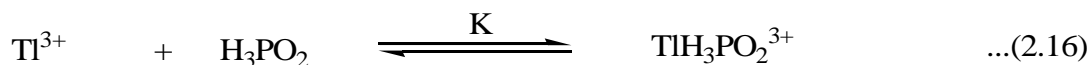
The acid is mainly used in electro less plating and in pharmaceutical industry. Its other uses are in the treatment of water, in preventing discoloration of polymers and in preserving meat (Mehrotra, 2013). Innersphere 1:1 complex formation is thought to precede the act of electron transfer in a number of hypophosphorous oxidations with metal ion oxidants (Caroll and Thomas, 1966; Mishra and Gupta, 1967; Gupta and Gupta, 1970; Sengupta *et al.*, 1973; Indrayan *et al.*, 1981). Reactions of iron(VII) with a variety of phosphorus centres are proposed to occur via the formation of an oxygen-bridged intermediate followed by a two–electron transfer. Most of electron transfer reactions of hypophosphorous acid proceed by mechanisms involving two tautomeric forms of hypophosphorous acid in aqueous solution. Reversible tautomeric shift catalysed by acid between the predominant inactive species of H₃PO₂ and the active form is represented by Equation 2.14 which is followed by reaction of the active form with the oxidant (Equation 2.15).





The reactions with various oxidizing agents show the same $k_2(\text{H}^+)$, which is the catalytic coefficient for the tautomeric shift for strong acids. The reality of the tautomeric shift in Equation 2.14 as the primary step in the reaction has been verified by experiments on the isotopic exchange rates between tritiated and deuterated water and H_3PO_2 .

The reaction of Tl^{3+} with H_3PO_2 solution, for instance, proceeds through the formation of an intermediate. The intermediate can produce the products through three alternatives (Jordan and Catherino, 1963). In the first alternative Equation 2.16 is followed by the rate limiting reaction involving a single-step two-electron transfer to H_2O .

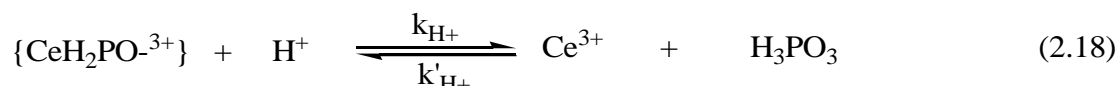


In the second alternative, Equation 2.16 is followed by the rate-limiting H^- transfer from H_3PO_2 to Tl^{3+} to produce $\text{H}_2\text{P}^+\text{O}_2$ which reacted rapidly with H_2O to give H_3PO_3 . In the third alternative, Equation 2.16 is followed by its possible rate determining disintegration to Tl^{2+} and $\text{H}_2\text{P}^*\text{O}_2$ because Tl^{2+} has been postulated in several reactions (Warnqvist and Dodson, 1971). The $\text{H}_2\text{P}^*\text{O}_2$ is rapidly oxidised by Tl^{2+} in presence of H_2O . All the three possibilities lead to common rate law (Mehrotra, 2013).

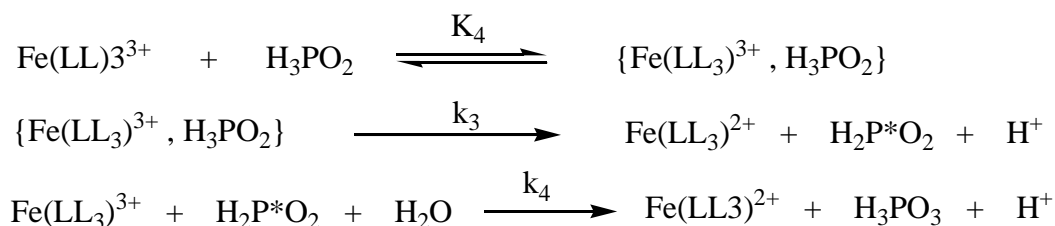
In perchloric acid, the oxidation of H_3PO_2 by Ce^{4+} proceeds through the complexes formed by the two reactants' species, and acceleration of the rate with acid. The mechanism of the reaction involved the formation of a complex in Equation 2.17.



The complex containing the active form rapidly decomposes to the products as in Equation 2.18.



For the reaction of H_3PO_2 and cobalt ion such as $[\text{CoW}_{12}\text{O}_{40}]^{5-}$ in HCl , a reversible rate-determining reaction led to the formation of the hypophosphorous acid radical ($\text{H}_2\text{P}^*\text{O}_2$), which rapidly reacted with the $[\text{CoW}_{12}\text{O}_{40}]^{5-}$ in the presence of H_2O to form H_3PO_3 . The probability of the formation of $\text{H}_3\text{P}^+\text{O}_2$ from the reaction of $\text{H}_2\text{P}^*\text{O}_2$ with $[\text{CoW}_{12}\text{O}_{40}]^{5-}$ was not excluded from the reaction that was independent of H^+ (Ayoko, 1990). While in the oxidation of H_3PO_2 with vanadium ions, $\text{V}(\text{OH})^{3+}$ as the reactive species in H_2SO_4 was reported by Sengupta *et al* (1970). Here, H_3PO_2 was oxidised in its reactive form to the free radical, $\text{H}_2\text{P}^*\text{O}_2$, which subsequently refracted with another V^{V} molecule in the presence of H_2O to form H_3PO_3 . In the oxidation of H_3PO_2 by FeLL_3^{3+} ($\text{L} = 1,10$ phenanthroline or 2,2'bipyridine) in HClO_4 , an outersphere complex was formed which decomposed to a free radical in the rate determining step (Sengupta and De, 1975, Yusuf *et al.*, 2004) according to Scheme (4).



Scheme 4 : Oxidation of Hypophosphorous Acid by $\text{Fe}(\text{LL}_3)^{3+}$

2.6 Electron Transfer Reactions of ROH

Oxidation of alcohols by Cr(VI) is regarded as a two-step reaction with the initial equilibrium formation of chromate ester followed by the decomposition of the latter to products in the rate-determining step (Iyun and Shehu, 2004). The three possible modes of hydrogen transfer proposed for the ester decomposition mechanism include cyclic H-transfer with concerted bond making and breaking, cyclic H-transfer without the formation of free radical intermediates and cyclic H-transfer with the formation of free radical intermediate (Edwards, 1954; Gaswic and Krueger, 1969; Iyun and Shehu, 2004). Mechanisms involving hydride ion transfer have also been implicated in the oxidation of nine aliphatic alcohols by quinolinium bromochromate in dimethylsulphoxide (Saraswat *et al.*, 2003), nine alcohols by pyridinium hydrobromide perbromide in aqueous acetic acid (Mathur *et al.*, 1993), some alcohols by periodate (Rao *et al.*, 1989).

The kinetics of the oxidation of methanol, ethanol, *n*-propanol, *n*-butanol, isopropanol and benzyl alcohols by periodate in the presence of rhodium(III) chloride in basic medium revealed the formation of a complex between Rh(III) and alcohol followed by its disproportionation in the rate-determining step (Rao *et al.*, 1989). The reactivity of the alcohols was found to follow the order: benzyl alcohols > methanol > ethanol > *n*-propanol > *n*-butanol > isopropanol. Increase in chain length and branching at the α -carbon decreased the rate, probably due to increase in electron density at this carbon, which renders it difficult to part with the hydrogen. This is suggesting cleavage of an α -CH proton from an acid (Jerry, 1977). The oxidation of nine aliphatic primary alcohols by quinolinium bromochromate in dimethylsulphoxide, identification of a substantial primary kinetic isotopic effect confirms the cleavage of an α -CH in the rate-

determining step (Saraswat *et al.*, 2003). In the oxidation of fifteen alcohols (methanol, 2-chloroethanol, 2-methoxyethanol, ethanol, 1-chloropropan-2-ol, 1-propanol, 1-butanol, 1-pentanol, 2-methylpropan-1-ol, 1-methoxypropan-1-ol, 2-propanol, 2-butanol, 2-pentanol, 3-methylbutan-1-ol and 2-hexanol) by butyltriphenylphosphoniumdichromate, it is observed that the rate of oxidation shows excellent correlation with the polar and steric substituent constants (Kothari *et al.*, 2005). Also, in the oxidation of nine primary alcohols by pyridinium bromochromate (Aparna *et al.*, 1995) and in the oxidation of nine primary alcohols by pyridinium hydrobromide perbromide in aqueous acetic acid (Mathur *et al.*, 1993), reactivity of the alcohols was susceptible to both polar and steric effects.

CHAPTER THREE

MATERIALS AND METHODS

3.1. Materials and Reagents

3.1.1 Diaquotetrakis(2,2'- bipyridine)- μ -oxo-diruthenium(III) perchlorate

The oxo-bridged ruthenium binuclear complex, diaquotetrakis(2, 2'-bipyridine)- μ -oxo-diruthenium(III) perchlorate, $[(bipy)_2(H_2O)RuORu(H_2O)(bipy)_2](ClO_4)_4$ was prepared according to literature (Weaver *et al.*, 1975)

The complex *cis*-Dichlorobis(2,2'- bipyridine)ruthenium(II) (purchased from Sigma-Aldrich) (2.00 g, 4.13 mmol) was suspended in water (80 ml) containing silver nitrate (1.76g, 10.36 mmol, 2.51 equiv) and the mixture heated to reflux for 8 h, cooled to room temperature and centrifuged. The supernatant liquid was then filtered by suction onto a fine frit. In this way, silver chloride and silver metal were removed. The filtrate was heated on a steam bath and treated with a saturated solution of sodium perchlorate until precipitation began to occur. The precipitate was then subjected to slow cooling to 0°C to obtain the desired material which was collected by suction filtration and washed with a small amount of cold water and dried in air. Recrystallization of the salt was achieved from hot water containing small amounts of NaClO₄, giving rise to a dark microcrystalline solid and a deep green solution in water or acetonitrile. The yield was 1.24 g or 47.1% (literature, 56%). Stability of complex in water and in the presence of acid and added ions agreed to literature (Iyun *et al.*, 1992d). The complex had a λ_{max} of 660 nm (Appendix I), and a molar extinction coefficient, $\epsilon = 21,167 \text{ dm}^3 \text{ mol}^{-1} \text{ cm}^{-1}$ (literature: $\epsilon = 25,000 \text{ dm}^3 \text{ mol}^{-1} \text{ cm}^{-1}$) (Weaver *et al.*, 1975). The substance was stored in amber coloured bottle in a dark cupboard.

$3.0 \times 10^{-4} \text{ mol dm}^{-3}$ standard solution of the ruthenium dimer was prepared by dissolving $3.83 \times 10^{-2} \text{ g}$ of the synthesised complex in a 100 cm^3 volumetric flask and made up to the mark.

3.1.2 Thiourea (NH_2CSNH_2) solution

A 0.5 mol dm^{-3} stock solution of thiourea was prepared by dissolving 3.806g of thiourea (Sigma–Aldrich) in a 100 cm^3 volumetric flask and made up to the mark.

3.1.3 *N*-methylthiourea ($\text{CH}_3\text{HNCSNH}_2$) solution

A 0.5 mol dm^{-3} stock solution of *N*–methyl thiourea was prepared by dissolving 4.50g of *N*-methylthiourea (Sigma–Aldrich) in a 100 cm^3 volumetric flask and made up to the mark.

3.1.4 *N, N'*-Dimethylthiourea ($\text{CH}_3\text{HNCSNHCH}_3$) solution

A 0.5 mol dm^{-3} stock solution of *N, N'*-Dimethyl thiourea was prepared by dissolving 5.20g of *N, N'*-dimethylthiourea ((Sigma–Aldrich)) in a 100 cm^3 volumetric flask and made up to the mark.

3.1.5 *N*-allylthiourea ($\text{CH}_2=\text{CHCH}_2\text{HNSNH}_2$) solution

A 0.5 mol dm^{-3} stock solution of *N*–allylthiourea was prepared by dissolving 5.81g of *N*–allylthiourea (Sigma-Aldrich) in a 100 cm^3 volumetric flask and making up to the mark.

3.1.6 Sodium thiosulphate ($\text{Na}_2\text{S}_2\text{O}_3$) solution

A 2.0 mol dm^{-3} stock solution of $\text{Na}_2\text{S}_2\text{O}_3$ was prepared by dissolving 31.6g of $\text{Na}_2\text{S}_2\text{O}_3$ (May and Baker, Analar grade, 99%) in distilled water in a 100 cm^3 volumetric

flask and made up to the mark.. Its accurate concentration was determined by iodometric titration using starch as indicator.

3.1.7 Sodium dithionite ($\text{Na}_2\text{S}_2\text{O}_4$) solution

A 2.0 mol dm^{-3} stock solution of $\text{Na}_2\text{S}_2\text{O}_4$ was prepared by dissolving 31.6g of $\text{Na}_2\text{S}_2\text{O}_4$ (Sigma-Aldrich, Analar grade, 85%) in distilled water in a 100cm^3 volumetric flask and making up to the mark. Its accurate concentration was determined by iodometric titration using starch as indicator.

3.1.8 Hypophosphorous acid (H_3PO_2) solution

Stock solution of hypophosphorous acid was prepared by diluting a concentrated solution of the acid (Sigma – Aldrich, 50% Analar grade) to about 4.0 mol dm^{-3} . The solution was standardized volumetrically against NaOH. A 0.5 mol dm^{-3} solution of the acid was prepared by serial dilution.

3.1.9 Sodium perchlorate (NaClO_4) solution

24.5g of NaClO_4 (May and Baker, Analytical grade, $\geq 98.0\%$) were dissolved in distilled water in a 100 cm^3 volumetric flask and volume made up to the mark to prepare 2.0 mol dm^{-3} stock solution of the salt.. The solutions were standardized gravimetrically.

3.1.10 Magnesium chloride (MgCl_2) solution

A 2.0 mol dm^{-3} stock solution of MgCl_2 was prepared by dissolving 19.0g of MgCl_2 (Sigma- Aldrich, Analar grade 98%) in distilled water in a 100 cm^3 volumetric flask and

volume made to the mark in a 100cm³ volumetric flask. The solutions obtained were standardized gravimetrically.

3.1.11 Ammonium chloride (NH₄Cl) solution

NH₄Cl stock solutions of 2.0 mol dm⁻³ concentration were prepared by dissolving 10.7g of NH₄Cl (BDH, Analar grade 99.5%) in a 100cm³ volumetric flask and the volume made up to the mark. The solutions were standardized gravimetrically.

3.1.12 Sodium acetate (CH₃COONa) solution

Stock solutions of CH₃COONa (May and Baker, 99.8%) of concentration 2.0 mol dm⁻³ were prepared by dissolving 16.4g of the salt in distilled water in 100 ml volumetric flasks and the volumes made up to the mark. Accurate concentrations of the salt solutions were determined gravimetrically.

3.1.13 Sodium formate (HCOONa) solution

A 2.0 mol dm⁻³ stock solution of HCOONa was prepared by dissolving 13.6g of HCOONa (May and Baker, 99.5%) in 100 cm³ volumetric flasks with distilled and the volumes made to the mark. The solutions were standardized gravimetrically.

3.1.14 Sodium nitrate (NaNO₃) solution

Stock solutions of NaNO₃ of concentration 2.0 mol dm⁻³ were prepared by dissolving 17.0g of NaNO₃ (BDH, Analar 98%) in distilled water in 100 cm³ volumetric flasks and the volumes made up to the mark. The solutions obtained were standardized gravimetrically.

3.1.15 Perchloric acid (HClO₄) solution

Stock solution of 5.0 mol dm⁻³ perchloric acid was prepared by diluting concentrated solution of HClO₄ (Sigma–Aldrich, Analar grade, 60%) in standard flask. The solution was standardized volumetrically using sodium tetraborate decahydrate (borax) as primary standard and methyl red as indicator (Vogel, 1978).

3.1.16 Methanol (CH₃OH)

Standard solution of methanol was prepared by diluting accurately measured volumes of methanol (BDH, Analar grade, 97%) with doubly distilled water by taking into consideration the specific gravity of the alcohol. Lower concentrations were obtained by serial dilution.

3.1.17 Ethanol (C₂H₅OH)

Standard solution of ethanol was prepared by diluting accurately measured volumes of ethanol (BDH, Analar grade, 99.5%) with doubly distilled water by taking into consideration the specific gravity of the alcohol. Lower concentrations were obtained by serial dilution.

3.1.18 Propan–1–ol (C₃H₇OH)

Standard solution of propan–1–ol was prepared by diluting accurately measured volumes of propanol (BDH, Analar grade, 99.5%) with doubly distilled water by taking into consideration the specific gravity of the alcohol. Lower concentrations were obtained by serial dilution.

3.2 Methods

3.2.1 Stoichiometric study

The stoichiometry of each system was determined by spectrophotometric titration using the mole ratio method (Iyun and Adegite, 1990, Vaidya *et al.*, 1991, Iyun *et al.*, 1992a, 1992b, 1992c, 1992d, 1995a, 1995b, 1996, Ukoha, 1999, Ukoha and Iyun, 2001, 2002, Ukoha and Ibrahim, 2004) The concentration of the oxo-bridged ruthenium complex was kept constant while that of the reductants was varied between the mole ratio 1:0.25 to 1:4 ([reductant]/ [oxidant]) as follows:

For thiourea (TU) as reductant: $[\text{Ru}_2\text{O}^{4+}] = 6.0 \times 10^{-5} \text{ mol dm}^{-3}$, $[\text{TU}] = (1.5 - 24.0) \times 10^{-5} \text{ mol dm}^{-3}$, $[\text{H}^+] = 5.0 \times 10^{-2} \text{ mol dm}^{-3}$ and $\text{I} = 0.5 \text{ mol dm}^{-3}(\text{NaClO}_4)$.

For *N*-methylthiourea (MTU) as reductant: $[\text{Ru}_2\text{O}^{4+}] = 6.5 \times 10^{-5} \text{ mol dm}^{-3}$, $[\text{TU}] = (1.63 - 26.0) \times 10^{-5} \text{ mol dm}^{-3}$, $[\text{H}^+] = 5.0 \times 10^{-2} \text{ mol dm}^{-3}$, $\text{I} = 0.5 \text{ mol dm}^{-3}(\text{NaClO}_4)$.

For *N*-allylthiourea (ATU) as reductant: $[\text{Ru}_2\text{O}^{4+}] = 5.75 \times 10^{-5} \text{ mol dm}^{-3}$, $[\text{TU}] = (1.44 - 23.0) \times 10^{-5} \text{ mol dm}^{-3}$, $[\text{H}^+] = 5.0 \times 10^{-2} \text{ mol dm}^{-3}$, $\text{I} = 0.5 \text{ mol dm}^{-3}(\text{NaClO}_4)$.

For *N,N'*-dimethylthiourea (DMTU) as reductant: $[\text{Ru}_2\text{O}^{4+}] = 6.0 \times 10^{-5} \text{ mol dm}^{-3}$, $[\text{TU}] = (1.5 - 24.0) \times 10^{-5} \text{ mol dm}^{-3}$, $[\text{H}^+] = 5.0 \times 10^{-2} \text{ mol dm}^{-3}$, $\text{I} = 0.5 \text{ mol dm}^{-3}(\text{NaClO}_4)$.

For $\text{S}_2\text{O}_3^{2-}$ as reductant: $[\text{Ru}_2\text{O}^{4+}] = 6.5 \times 10^{-5} \text{ mol dm}^{-3}$, $[\text{S}_2\text{O}_3^{2-}] = (1.63 - 26.0) \times 10^{-5} \text{ mol dm}^{-3}$, $[\text{H}^+] = 5.0 \times 10^{-2} \text{ mol dm}^{-3}$, $\text{I} = 0.5 \text{ mol dm}^{-3}(\text{NaClO}_4)$.

For $\text{S}_2\text{O}_4^{2-}$ as reductant: $[\text{Ru}_2\text{O}^{4+}] = 5.75 \times 10^{-5} \text{ mol dm}^{-3}$, $[\text{S}_2\text{O}_3^{2-}] = (1.44 - 23.0) \times 10^{-5} \text{ mol dm}^{-3}$, $[\text{H}^+] = 5.0 \times 10^{-2} \text{ mol dm}^{-3}$, $I = 0.5 \text{ mol dm}^{-3}$ (NaClO_4).

For H_3PO_2 as reductant: $[\text{Ru}_2\text{O}^{4+}] = 6.0 \times 10^{-5} \text{ mol dm}^{-3}$, $[\text{H}_3\text{PO}_2] = (1.5 - 24.0) \times 10^{-5} \text{ mol dm}^{-3}$, $[\text{H}^+] = 5.0 \times 10^{-2} \text{ mol dm}^{-3}$, $I = 0.5 \text{ mol dm}^{-3}$ (NaClO_4). For CH_3OH as reductant: $[\text{Ru}_2\text{O}^{4+}] = 5.5 \times 10^{-5} \text{ mol dm}^{-3}$, $[\text{CH}_3\text{OH}] = (1.4 - 22.0) \times 10^{-5} \text{ mol dm}^{-3}$, $I = 0.5 \text{ mol dm}^{-3}$ (NaClO_4).

For $\text{C}_2\text{H}_5\text{OH}$ as reductant: $[\text{Ru}_2\text{O}^{4+}] = 6.0 \times 10^{-5} \text{ mol dm}^{-3}$, $[\text{C}_2\text{H}_5\text{OH}] = (1.5 - 24.0) \times 10^{-5} \text{ mol dm}^{-3}$, $I = 0.5 \text{ mol dm}^{-3}$ (NaClO_4).

For $\text{C}_3\text{H}_7\text{OH}$ as reductant: $[\text{Ru}_2\text{O}^{4+}] = 6.0 \times 10^{-5} \text{ mol dm}^{-3}$, $[\text{C}_3\text{H}_7\text{OH}] = (1.5 - 24.0) \times 10^{-5} \text{ mol dm}^{-3}$, $I = 0.5 \text{ mol dm}^{-3}$ (NaClO_4).

The reactions were allowed to go to completion and the absorbances of the completely reacted mixtures (A_∞) were monitored at 660 nm (the λ_{max} of Ru_2O^{4+}) using Seward Biomedical Digital Colorimeter. The absorbances obtained were plotted against the mole ratios of the reactants. Points of sharp breaks in these plots gave the stoichiometries of the reactions.

3.2.2 Kinetic measurements

The rates of reactions of the Ru_2O^{4+} with the reductants were studied by monitoring the decrease in absorbance of the dimer at its λ_{max} (660 nm) using Seward Biomedical Digital Colorimeter. All kinetic measurements were carried out under pseudo-first order conditions with respective reductant concentrations in excess of the oxidant

concentration at stated temperature. Ionic strength as well as $[H^+]$ were maintained constant for each system unless otherwise stated (Iyun and Adegite, 1990, Vaidya *et al.*, 1991, Iyun *et al.*, 1992a, 1992b, 1992c, 1992d, 1995a, 1995b, 1996, Ukoha, 1999, Ukoha and Iyun, 2001, 2002, Ukoha and Ibrahim, 2004)

The pseudo – first order plots of $\log (A_t - A_\infty)$ against time were made and the slopes of the plots gave the pseudo – first order rate constants, k_{obs} . The second order rate constants, k_2 , were determined from k_{obs} as $k_{obs}/ [\text{reductant}]$. (Iyun and Adegite, 1990, Vaidya *et al.*, 1991, Iyun *et al.*, 1992a, 1992b, 1992c, 1992d, 1995a, 1995b, 1996, Ukoha, 1999, Ukoha and Iyun, 2001, 2002, Ukoha and Ibrahim, 2004)

3.2.3 Effect of change in hydrogen ion concentration on rate of reaction

The effect of changes in the hydrogen ion concentration on the reaction rate was investigated by keeping the concentrations of the dimer and the reductants constant while that of the hydrogen ion concentration was varied. Ionic strength, I , was maintained constant at the stated temperature at 0.50 mol dm^{-3} [salt] and reaction was carried out at. Order of reaction with respect to acid concentration was obtained as the slope of the plot of $\log k_{obs}$ against $\log [H^+]$. Variation of acid-dependent second order rate constant, $k_2(H^+)$ with $[H^+]$ was obtained by plotting $k_2(H^+)$ against $[H^+]$ (Iyun and Adegite, 1990, Vaidya *et al.*, 1991, Iyun *et al.*, 1992a, 1992b, 1992c, 1992d, 1995a, 1995b, 1996, Ukoha, 1999, Ukoha and Iyun, 2001, 2002, Ukoha and Ibrahim, 2004).

3.2.4 Effect of change in ionic strength of reaction medium on rate of reaction

The ionic strength of the reaction mixture was varied while maintaining the concentrations of the dimer, reductant and hydrogen ion constant at stated reaction

temperature. Relationship of reaction rate with changes in the ionic strength was determined by plotting $\log k_2$ against \sqrt{I} (Iyun and Adegite, 1990, Vaidya *et al.*, 1991, Iyun *et al.*, 1992a, 1992b, 1992c, 1992d, 1995a, 1995b, 1996, Ukoha, 1999, Ukoha and Iyun, 2001, 2002, Ukoha and Ibrahim, 2004).

3.2.5 Effect of change in dielectric constant of reaction medium on rate of reaction

Effect of change in dielectric constant of the reaction medium on the reaction rate was investigated by adding various amounts of acetone to the reaction mixture. The concentrations of the dimer, reductant and hydrogen ion as well as the ionic strength were maintained constant. The relationship between the second order rate constant and the dielectric constant, D was obtained from the plot of $\log k_2$ against $1/D$ (Zaidi, 1991).

3.2.6 Effect of addition of ions to reaction medium on rate of reaction

The effect of added ions on the reaction rate was observed by the addition of various amounts of ions (Mg^+ , NH_4^+ , NO_3^- , CH_3COO^- , $HCOO^-$) while maintaining the dimer, reductant and hydrogen ion concentrations constant. The ionic strength and temperature were maintained constant, also. (Iyun and Adegite, 1990, Vaidya *et al.*, 1991, Iyun *et al.*, 1992a, 1992b, 1992c, 1992d, 1995a, 1995b, 1996, Ukoha, 1999, Ukoha and Iyun, 2001, 2002, Ukoha and Ibrahim, 2004).

3.2.10 Test for participation of free radicals in the course of reaction

Test for free radicals was carried out by adding 2 g of acrylamide to a partially oxidised reaction mixture containing various concentrations of oxidant, reductant and hydrogen ion for each system. A large excess of methanol was added to the reaction mixture. Control experiment was carried out by adding acrylamide to solutions of oxidant and

reductant separately at the same conditions of $[H^+]$, I and temperature. Any polymerisation as indicated by gel formation suggested the presence of free radicals in the reaction mixture. (Iyun and Adegite, 1990, Vaidya *et al.*, 1991, Iyun *et al.*, 1992a, 1992b, 1992c, 1992d, 1995a, 1995b, 1996, Ukoha, 1999, Ukoha and Iyun, 2001, 2002, Ukoha and Ibrahim, 2004).

3.2.11 Test for formation of intermediate complex prior to electron transfer

Test for the presence of stable, detectable intermediate complexes formed in the course of the reaction was carried out by recording the electronic spectra of partially reacted reaction mixtures at various time intervals depending on the speed of the reaction. Similar runs were made for reactants separately in each case. A shift in, or consistent, λ_{max} and/ or enhancement of peak as the reaction progressed is determined. Furthermore, identification or non-identification of intercepts in the Michaelis–Menten plots of $1/k_{obs}$ versus $1/[reductant]$ would give an idea of the presence or absence of intermediate complex formation. (Iyun and Adegite, 1990, Vaidya *et al.*, 1991, Iyun *et al.*, 1992a, 1992b, 1992c, 1992d, 1995a, 1995b, 1996, Ukoha, 1999, Ukoha and Iyun, 2001, 2002, Ukoha and Ibrahim, 2004)

3.2.9 Product analysis

Where possible, completely reacted solutions were analysed for the type of products that will be formed. For the reactions where thioureas were used as reductants, test for the presence of disulphide formed was carried out according to literature (McAuley and Gomwalk, 1968, 1969). The thiourea was reacted with a little excess of the oxidant in acid medium and ionic strength of reaction. At the completion of the reaction, the mixture was extracted six times with diethyl ether. The combined ether extracts were

washed and dried with anhydrous Na_2SO_4 and left overnight to dry. Appearance of crystals suggested that the products of reaction included disulphide. Where alcohols were used as reductants, the presence or absence of aldehydes is tested as follows: to 1 cm^3 of Fehling's solution A, Fehling's solution B was added until precipitation occurs. More of the Fehling's Solution B was added until the precipitation just disappears. A small quantity of the product was added and boiled. A brick-red colouration indicated the presence of aldehydes in the products. The product of the oxidation of hypophosphorous acid, phosphorous acid, was confirmed by the addition of saturated sodium molybdate solution to the reaction mixture; the absence of any precipitate of ammonium phosphomolybdate indicated the absence of phosphate ion and thus the presence of phosphorous acid was confirmed (Yusuf *et al.*, 2004).

CHAPTER FOUR

RESULTS

4.1 Stability of Ru_2O^{4+}

Monitoring the absorbance of an aqueous solution of Ru_2O^{4+} after one week showed no change in the absorbance. Also, the stability of the complex in dilute acids was investigated by adding varying concentrations of inorganic acids such HClO_4 , HCl , H_2SO_4 and HNO_3 to an aqueous solution of Ru_2O^{4+} . It was observed that the absorbance of the complex at its λ_{max} (660nm) remained constant for several days in dilute solutions of the acids and also in the presence of anions (CH_3COO^- , HCOO^- , NO_3^- and ClO_4^-).

Since the oxo-bridged ruthenium complex has the possibility of decomposing if stored in the presence of light for a long period, the complex was stored in an amber-coloured bottle in the dark.

4.2 Stoichiometric Studies

Results of stoichiometric studies for the reduction of Ru_2O^{4+} by thiourea (TU) and its derivatives i.e. *N*-methylthiourea (MTU), *N*-allylthiourea (ATU), *N,N*-dimethylthiourea (DMTU) show that two moles of each of the reductants was consumed by one mole of Ru_2O^{4+} . The titration curves of each of the systems was determined and are presented in Figures 4.1 to 4.4.

Based on the above findings, the stoichiometric equations for the four systems can be represented by Equations 4.1 – 4.4.

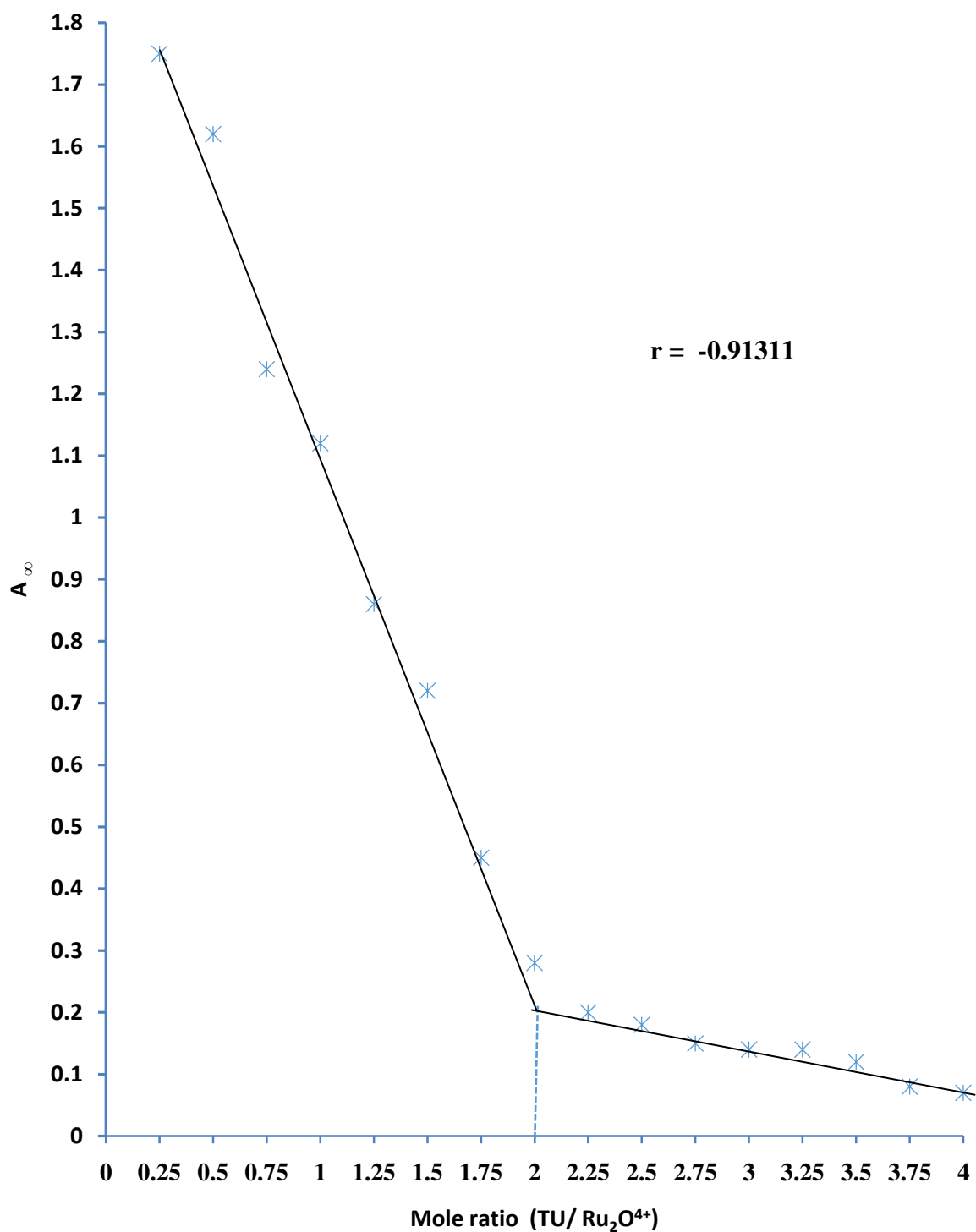


Fig 4.1: Plot of Absorbance versus Mole Ratio for the Reaction of $[(\text{H}_2\text{O})_2\text{Ru}_2\text{O}]^{4+}$ and Thiourea (TU) $[(\text{H}_2\text{O})_2\text{Ru}_2\text{O}^{4+}] = 6.0 \times 10^{-5} \text{ mol dm}^{-3}$, $[\text{TU}] = (1.5 - 24.0) \times 10^{-3} \text{ mol dm}^{-3}$, $[\text{H}^+] = 5.0 \times 10^{-2} \text{ mol dm}^{-3}$, $I = 0.5 \text{ mol dm}^{-3}$ and $\lambda_{\text{max}} = 660 \text{ nm}$

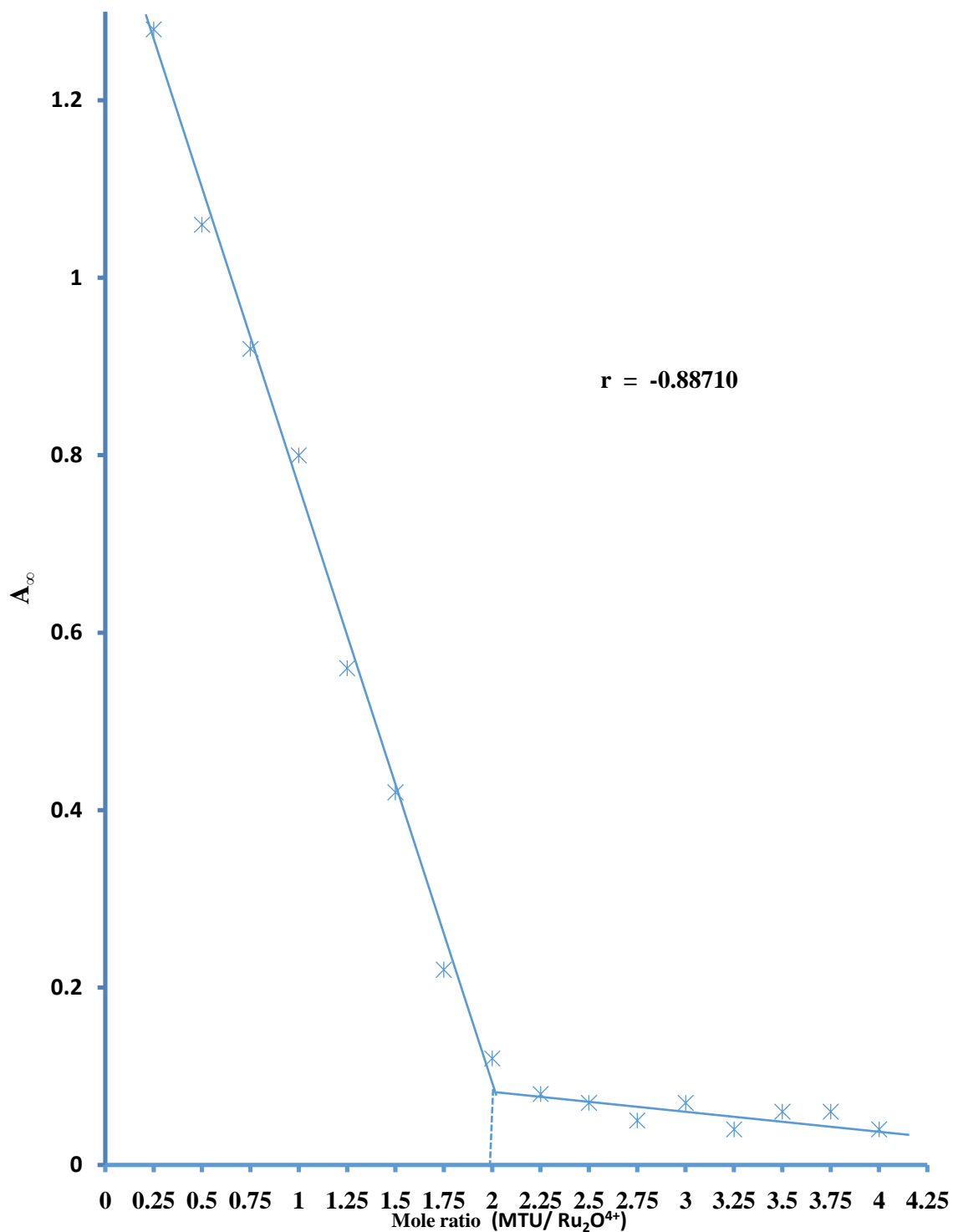


Figure 4.2: Plot of Absorbance versus Mole Ratio for the Reaction of $[(\text{H}_2\text{O})_2\text{Ru}_2\text{O}]^{4+}$ and *N*-methylthiourea (MTU) at $[(\text{H}_2\text{O})_2\text{Ru}_2\text{O}^{4+}] = 6.5 \times 10^{-5} \text{ mol dm}^{-3}$, $[\text{MTU}] = (1.63 - 26.0) \times 10^{-5} \text{ mol dm}^{-3}$, $[\text{H}^+] = 5.0 \times 10^{-2} \text{ mol dm}^{-3}$, $I = 0.5 \text{ mol dm}^{-3}$ and $\lambda_{\text{max}} = 660 \text{ nm}$

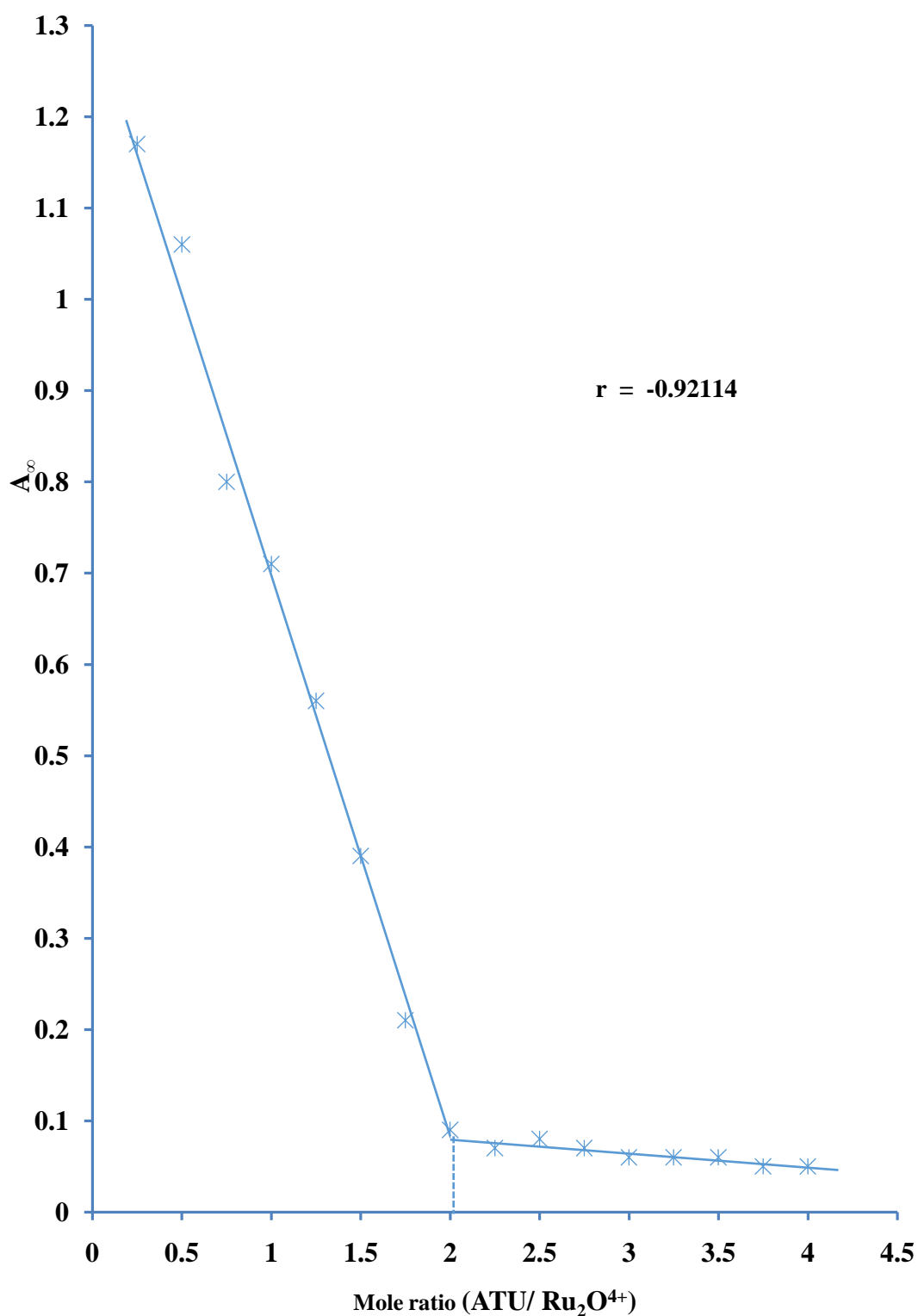


Figure 4.3: Plot of Absorbance versus Mole Ratio for the Reaction of $[(\text{H}_2\text{O})_2\text{Ru}_2\text{O}]^{4+}$ and *N*-allyl thiourea (ATU) at $[(\text{H}_2\text{O})_2\text{Ru}_2\text{O}^{4+}] = 5.75 \times 10^{-5} \text{ mol dm}^{-3}$, $[\text{ATU}] = (1.44 - 23.0) \times 10^{-5} \text{ mol dm}^{-3}$, $[\text{H}^+] = 5.0 \times 10^{-2} \text{ mol dm}^{-3}$, $I = 0.5 \text{ mol dm}^{-3}$ and $\lambda_{\text{max}} = 660 \text{ nm}$

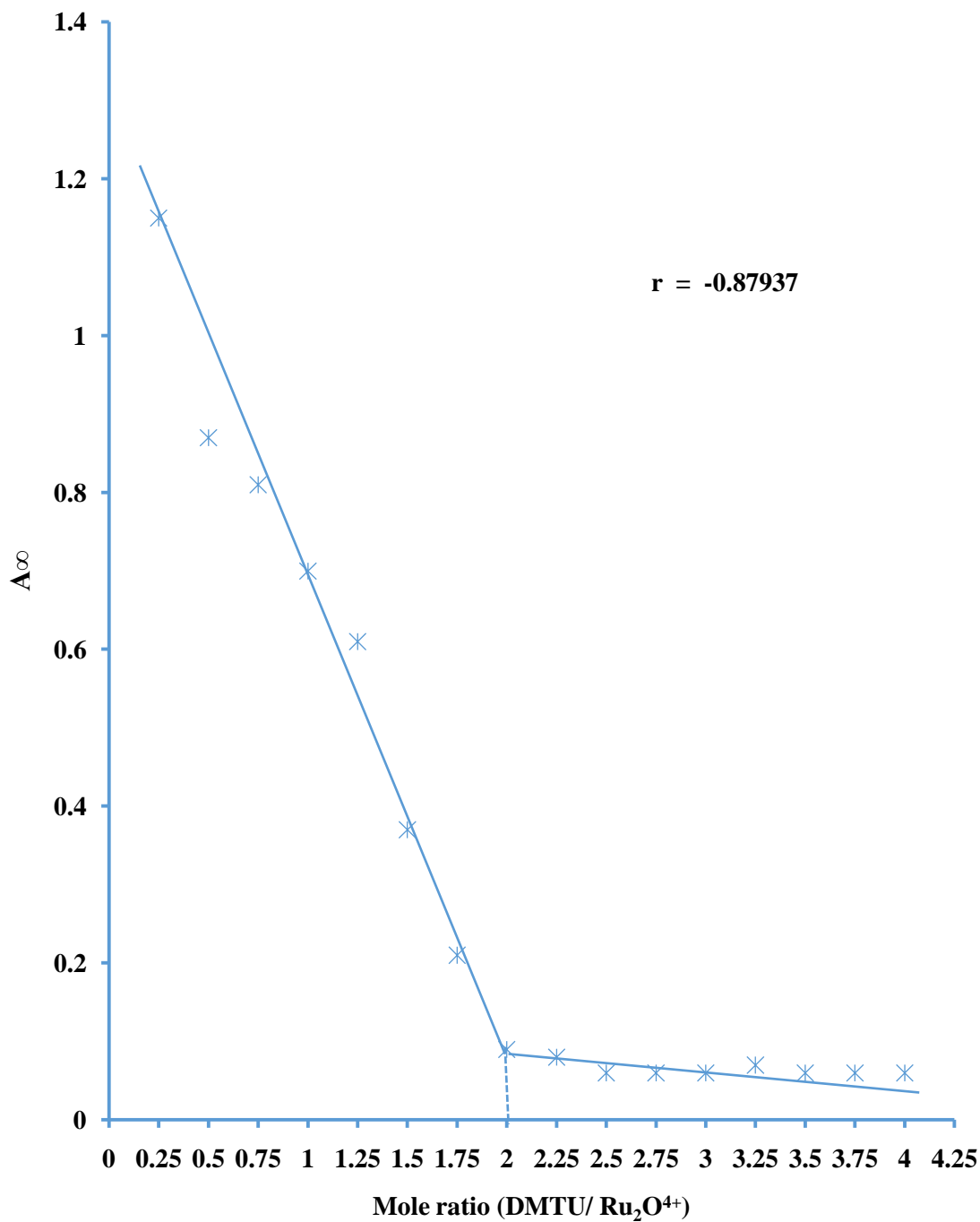
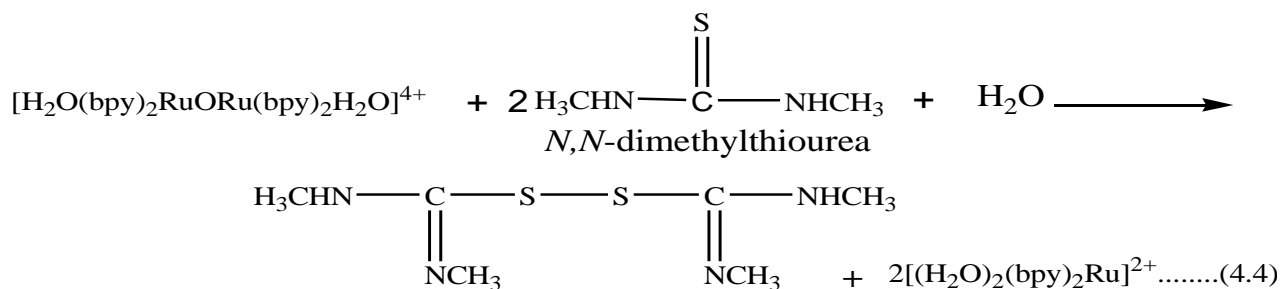
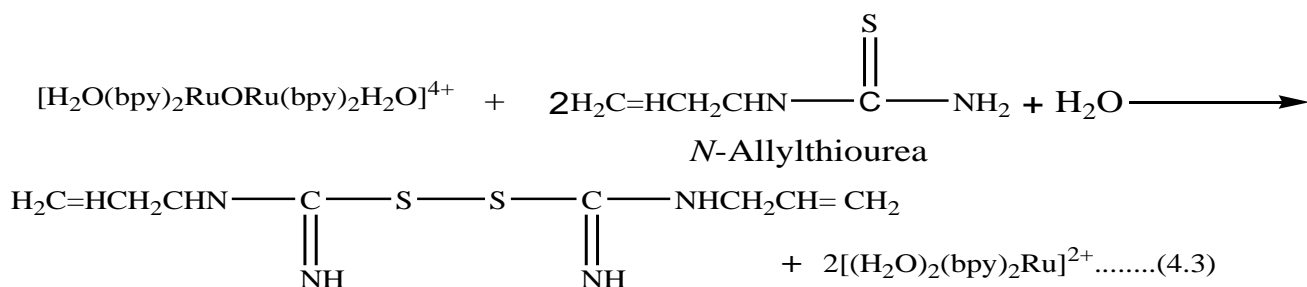
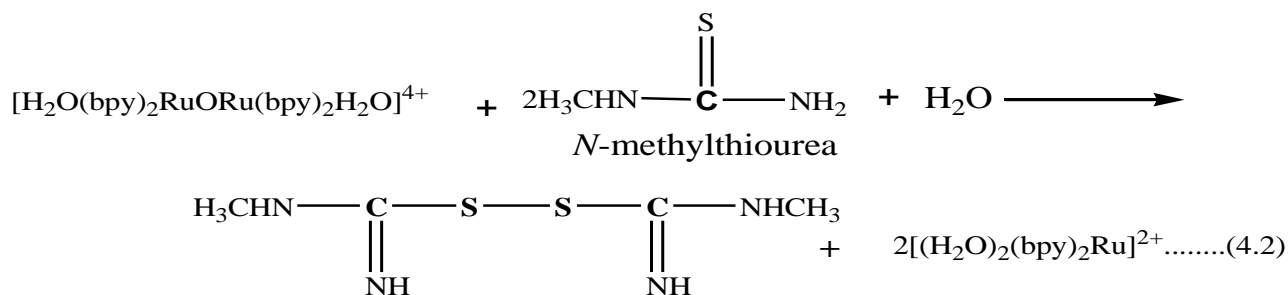
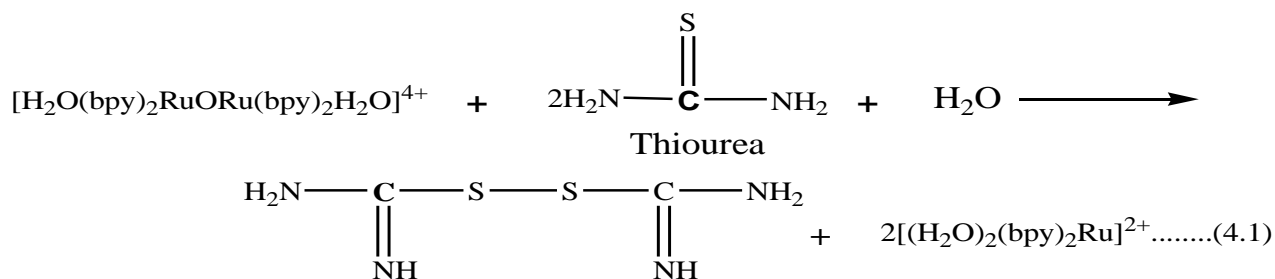


Figure 4.4: Plot of Absorbance versus Mole Ratio for the Reaction of $[(\text{H}_2\text{O})_2\text{Ru}_2\text{O}]^{4+}$ and N, N' -dimethylthiourea (DMTU) at $[(\text{H}_2\text{O})_2\text{Ru}_2\text{O}^{4+}] = 6.0 \times 10^{-5} \text{ mol dm}^{-3}$, $[\text{DMTU}] = (1.5 - 24.0) \times 10^{-5} \text{ mol dm}^{-3}$, $[\text{H}^+] = 5.0 \times 10^{-2} \text{ mol dm}^{-3}$, $I = 0.5 \text{ mol dm}^{-3}$ and $\lambda_{\text{max}} = 660 \text{ nm}$



Results of the stoichiometric studies for the reaction of the oxo – bridged ruthenium dimer with $\text{S}_2\text{O}_3^{2-}$, $\text{S}_2\text{O}_4^{2-}$, H_3PO_2 , CH_3OH , $\text{C}_2\text{H}_5\text{OH}$ and $\text{C}_3\text{H}_7\text{OH}$ are presented in Figures 4.5 – 4.10. The stoichiometric equations of these reactions considering the mole ratios are:

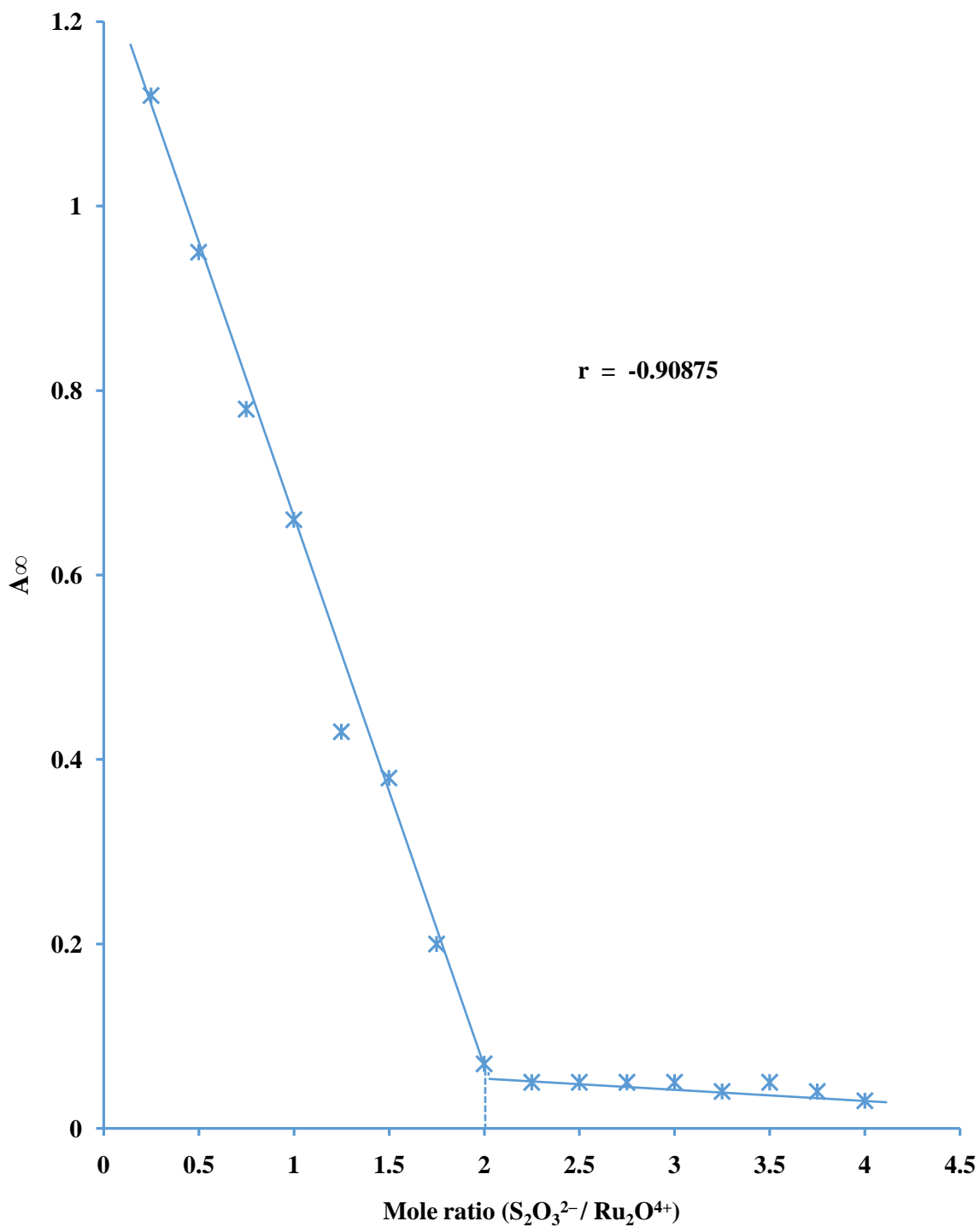


Figure 4.5 : Plot of Absorbance versus Mole Ratio for the Reaction of $[(\text{H}_2\text{O})_2\text{Ru}_2\text{O}]^{4+}$ and $\text{S}_2\text{O}_3^{2-}$ at $[(\text{H}_2\text{O})_2\text{Ru}_2\text{O}^{4+}] = 6.5 \times 10^{-5} \text{ mol dm}^{-3}$, $[\text{S}_2\text{O}_3^{2-}] = (1.63 - 26.0) \times 10^{-5} \text{ mol dm}^{-3}$, $[\text{H}^+] = 5.0 \times 10^{-2} \text{ mol dm}^{-3}$, $I = 0.5 \text{ mol dm}^{-3}$ and $\lambda_{\text{max}} = 660 \text{ nm}$

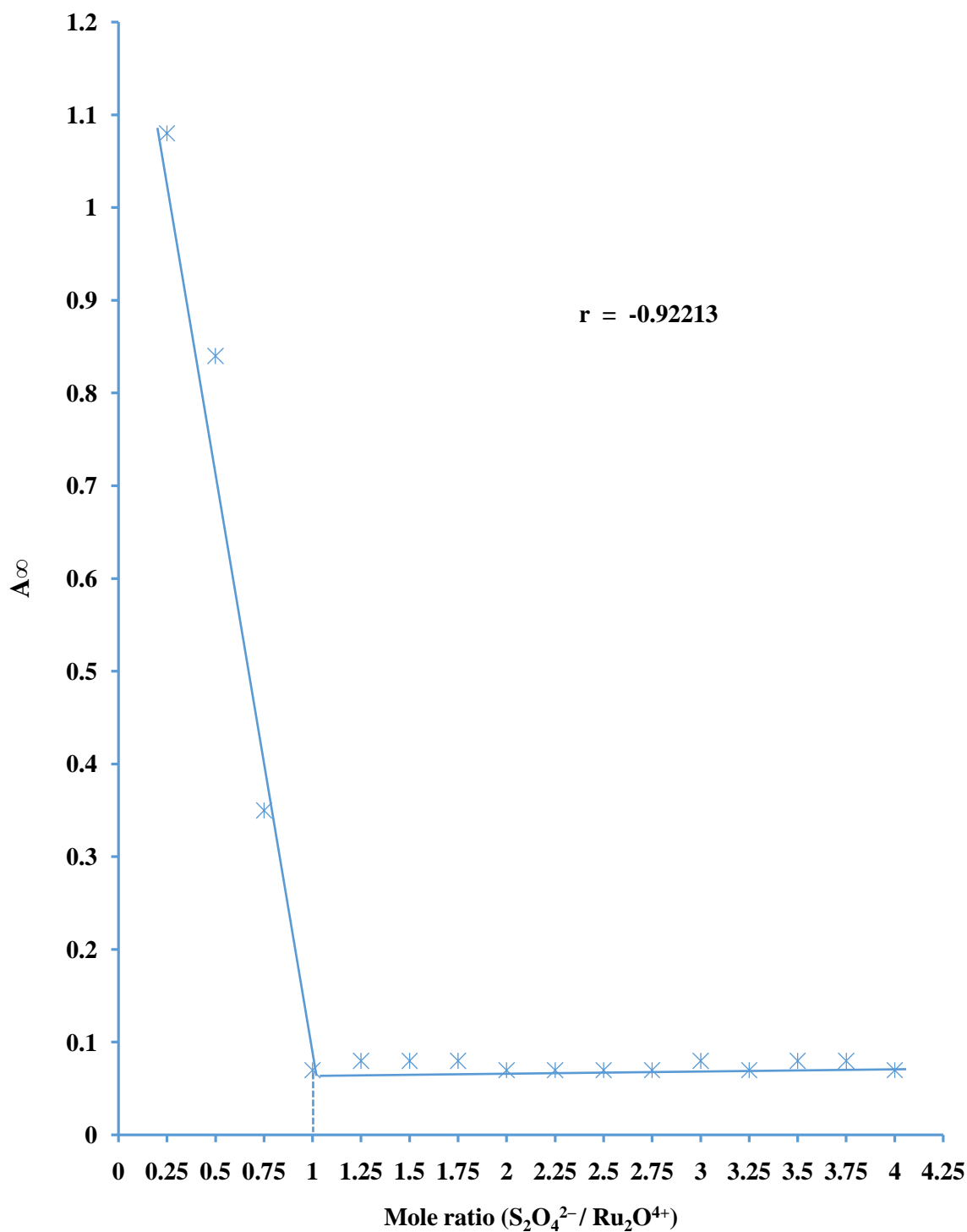


Figure 4.6 : Plot of Absorbance versus Mole ratio for the Reaction of $[(\text{H}_2\text{O})_2\text{Ru}_2\text{O}]^{4+}$ and $\text{S}_2\text{O}_4^{2-}$ at $[(\text{H}_2\text{O})_2\text{Ru}_2\text{O}^{4+}] = 5.75 \times 10^{-5} \text{ mol dm}^{-3}$, $[\text{S}_2\text{O}_4^{2-}] = (1.44 - 23.0) \times 10^{-5} \text{ mol dm}^{-3}$, $I = 0.5 \text{ mol dm}^{-3}$ and $\lambda_{\text{max}} = 660 \text{ nm}$

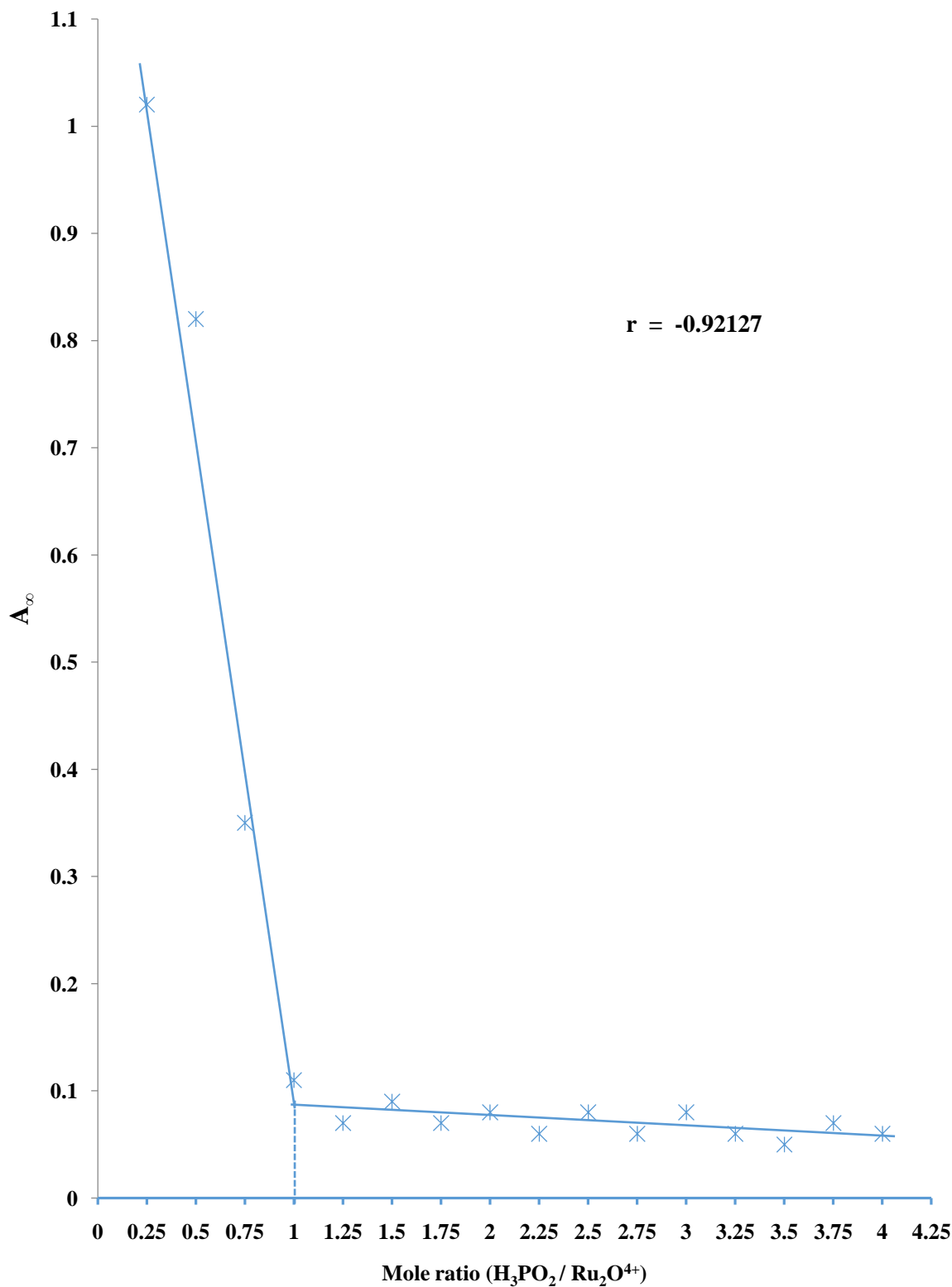


Figure 4.7: Plot of Absorbance versus Mole Ratio for the Reaction of $[(\text{H}_2\text{O})_2\text{Ru}_2\text{O}]^{4+}$ and H_3PO_2 at $[(\text{H}_2\text{O})_2\text{Ru}_2\text{O}^{4+}] = 6.0 \times 10^{-5} \text{ mol dm}^{-3}$, $[\text{H}_3\text{PO}_2] = (1.5 - 24.0) \times 10^{-5} \text{ mol dm}^{-3}$, $[\text{H}^+] = 5.0 \times 10^{-2} \text{ mol dm}^{-3}$, $I = 0.5 \text{ mol dm}^{-3}$ and $\lambda_{\text{max}} = 660 \text{ nm}$

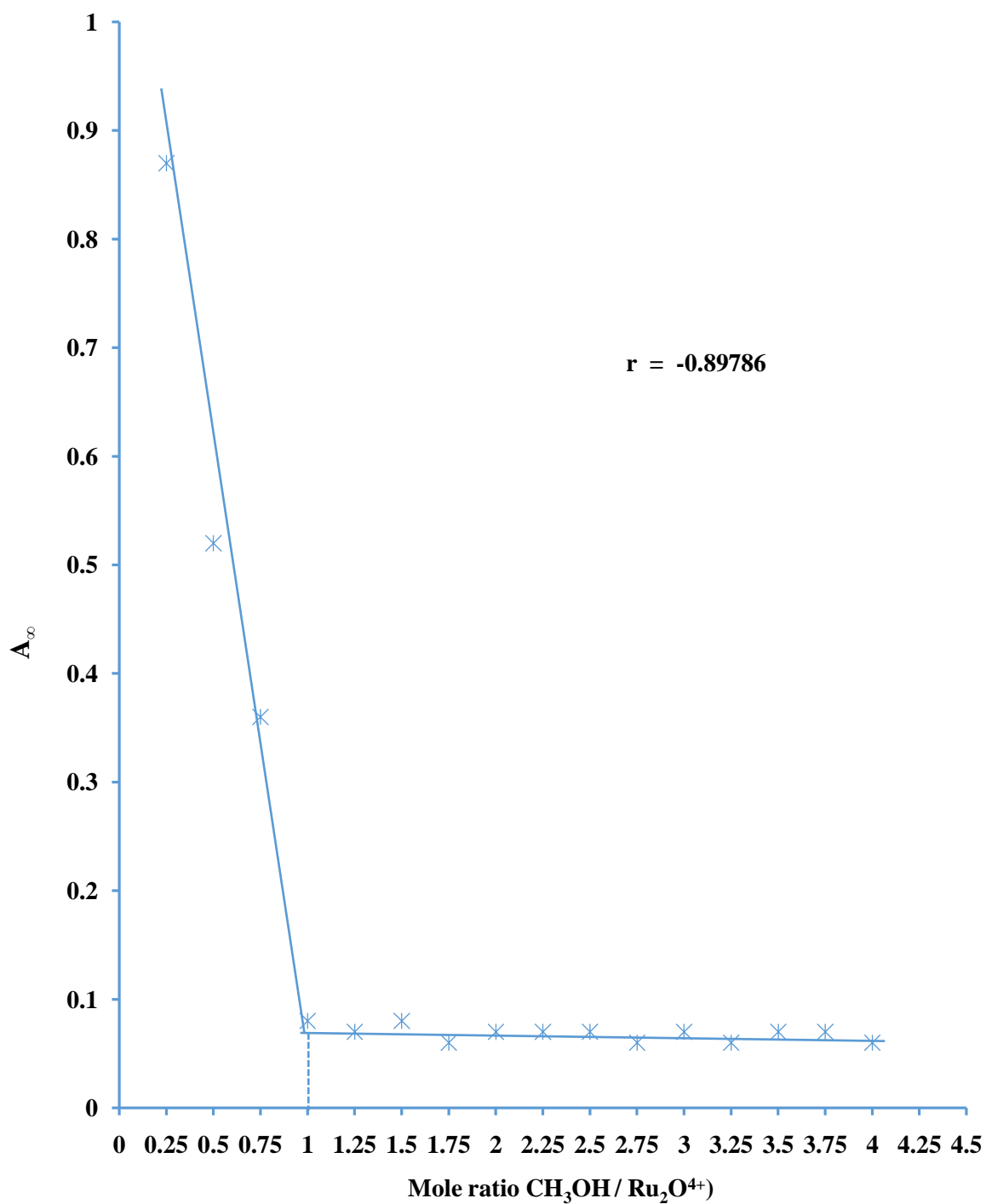


Figure 4.8: Plot of Absorbance versus Mole ratio for the Reaction of $[(\text{H}_2\text{O})_2\text{Ru}_2\text{O}]^{4+}$ and CH_3OH at $(\text{H}_2\text{O})_2\text{Ru}_2\text{O}^{4+} = 5.5 \times 10^{-5} \text{ mol dm}^{-3}$, $[\text{CH}_3\text{OH}] = (1.4 - 22.0) \times 10^{-5} \text{ mol dm}^{-3}$, $I = 0.5 \text{ mol dm}^{-3}$ and $\lambda_{\text{max}} = 660 \text{ nm}$

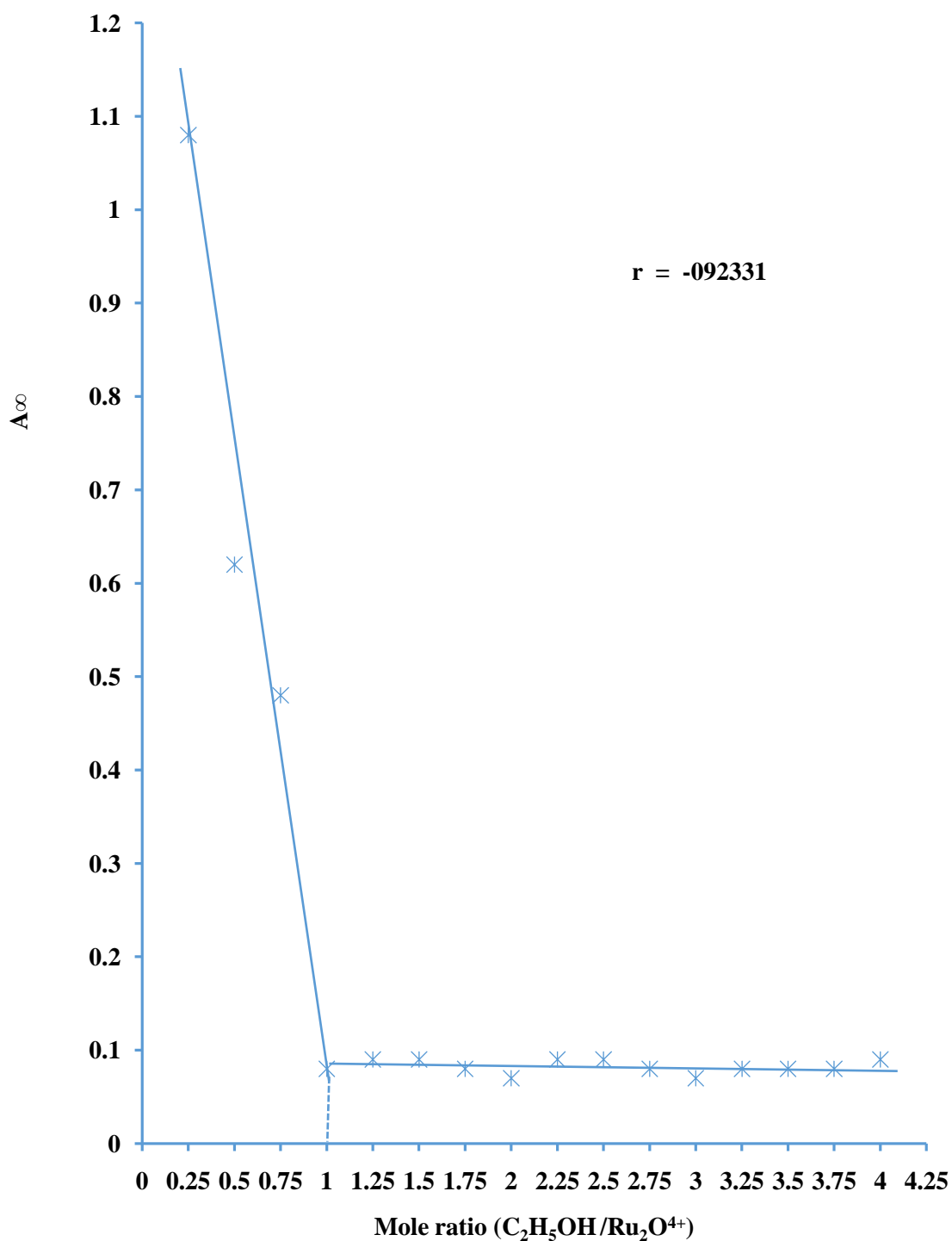


Figure 4.9: Plot of absorbance versus mole ratio for the reaction of $[(\text{H}_2\text{O})_2\text{Ru}_2\text{O}]^{4+}$ and $\text{C}_2\text{H}_5\text{OH}$ at $[(\text{H}_2\text{O})_2\text{Ru}_2\text{O}^{4+}] = 6.5 \times 10^{-5} \text{ mol dm}^{-3}$, $[\text{C}_2\text{H}_5\text{OH}] = (1.63 - 26.0) \times 10^{-5} \text{ mol dm}^{-3}$, $I = 0.5 \text{ mol dm}^{-3}$ and $\lambda_{\text{max}} = 660 \text{ nm}$

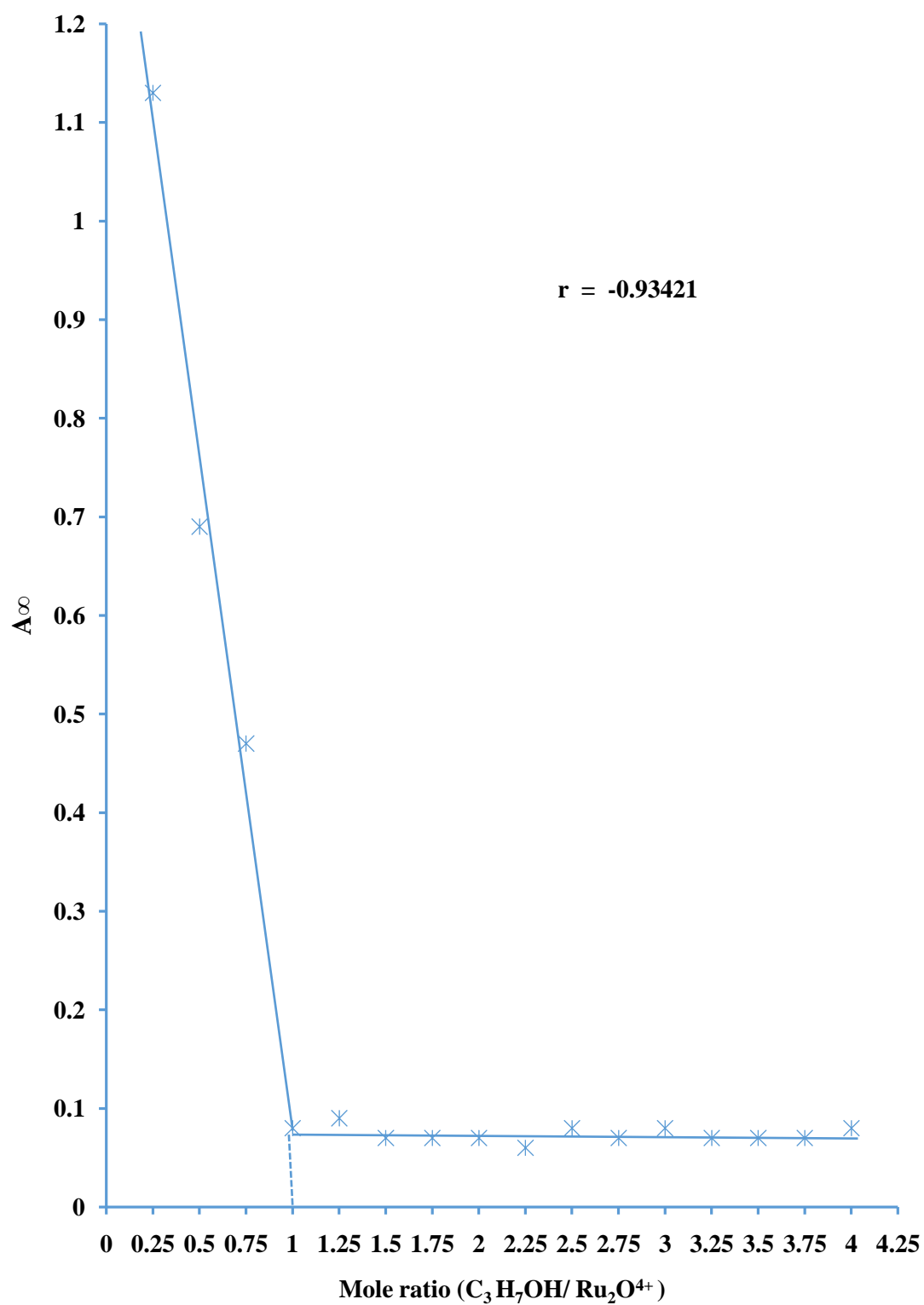
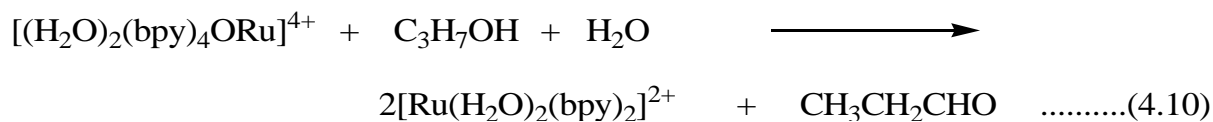
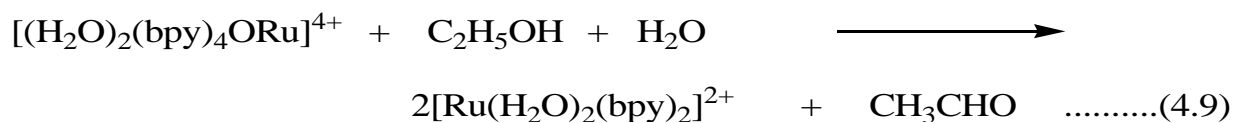
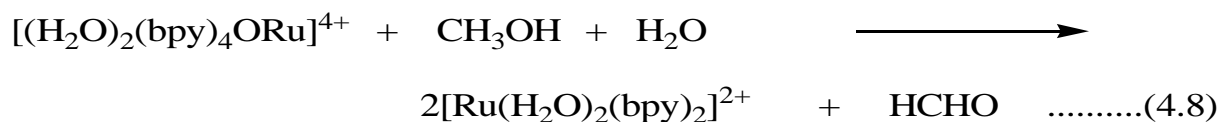
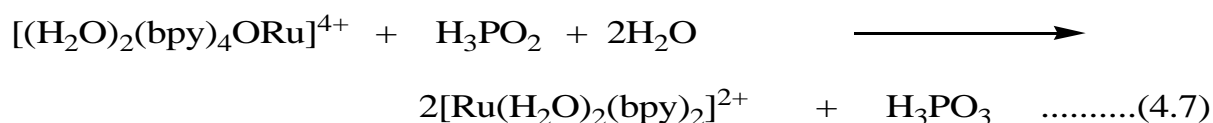
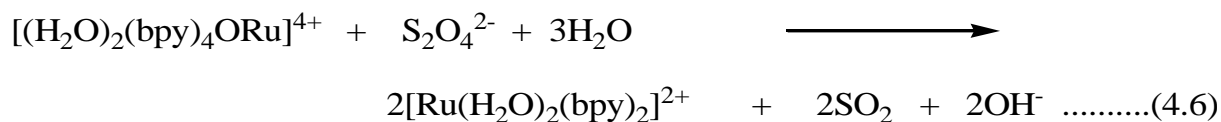
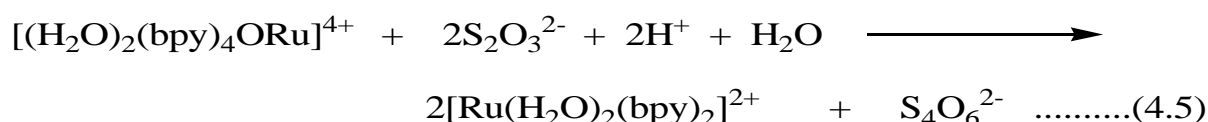


Figure 4.10: Plot of Absorbance versus Mole Ratio for the Reaction of $[(\text{H}_2\text{O})_2\text{Ru}_2\text{O}^{4+}]$ and $\text{C}_3\text{H}_7\text{OH}$ at $[(\text{H}_2\text{O})_2\text{Ru}_2\text{O}^{4+}] = 6.0 \times 10^{-5} \text{ mol dm}^{-3}$, $[\text{C}_3\text{H}_7\text{OH}] = (1.50 - 24.0) \times 10^{-5} \text{ mol dm}^{-3}$; $I = 0.5 \text{ mol dm}^{-3}$ and $\lambda_{\text{max}} = 660 \text{ nm}$



4.3 Determination of Pseudo-first Order and Second Order Rate Constants and Order of Reaction

4.3.1 Ru_2O^{4+} reaction with thiourea and thiourea derivatives (*N*-methylthiourea, *N,N'*-dimethylthiourea and *N*-allylthiourea)

Pseudo-first order plots of $\log (A_t - A_\infty)$ versus time (where A_t and A_∞ are absorbances at time 't' and at infinity, respectively) were linear to more than 90% extent of reaction.

This seems to suggest a first order dependence of rate on $[\text{Ru}_2\text{O}^{4+}]$ for all the systems.

Typical pseudo – first order plots for the reactions of the oxo- bridged ruthenium dimer and the thioureas are presented as Figures 4.11-4.14.

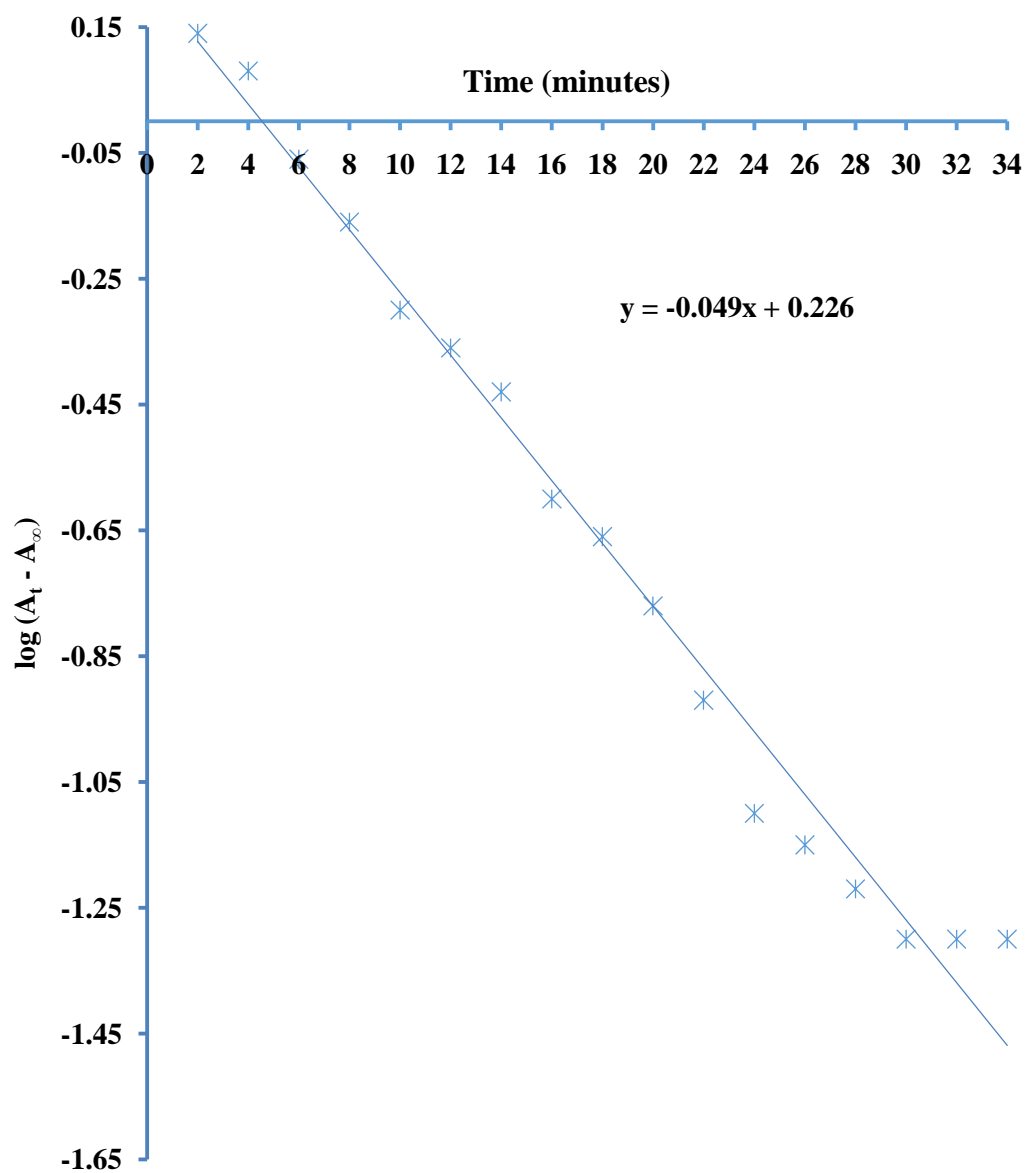


Fig 4.11: Typical Pseudo-First Order Plot for the Reaction of $[(\text{H}_2\text{O})_2\text{Ru}_2\text{O}]^{4+}$ and Thiourea (TU) at $[(\text{H}_2\text{O})_2\text{Ru}_2\text{O}]^{4+} = 6.0 \times 10^{-5} \text{ mol dm}^{-3}$, $[\text{TU}] = 7.7 \times 10^{-3} \text{ mol dm}^{-3}$, $[\text{H}^+] = 5.0 \times 10^{-2} \text{ mol dm}^{-3}$, $I = 0.5 \text{ mol dm}^{-3}$, $T = 32 \text{ } ^\circ\text{C}$ and $\lambda_{\text{max}} = 660 \text{ nm}$

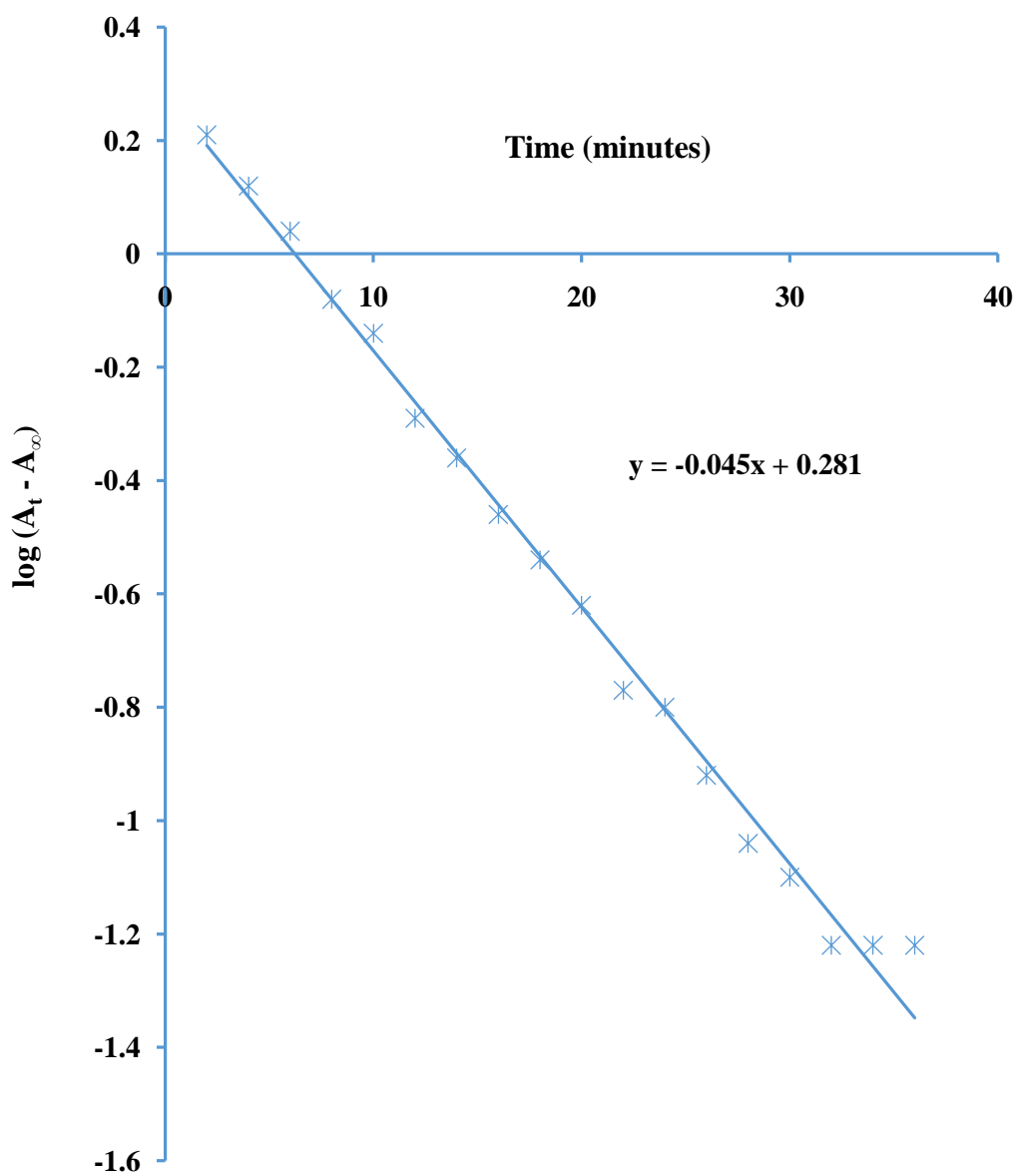


Figure 4.12: Typical Pseudo-first Order Plot for the Reaction of $[(\text{H}_2\text{O})_2\text{Ru}_2\text{O}]^{4+}$ and *N*-methylthiourea MTU) at $[(\text{H}_2\text{O})_2\text{Ru}_2\text{O}^{4+}] = 6.5 \times 10^{-5} \text{ mol dm}^{-3}$, $[\text{MTU}] = 2.6 \times 10^{-2} \text{ mol dm}^{-3}$, $[\text{H}^+] = 5.0 \times 10^{-2} \text{ mol dm}^{-2}$, $I = 0.5 \text{ mol dm}^{-3}$, $T = 31 \pm 1 \text{ }^\circ\text{C}$ and $\lambda_{\text{max}} = 660 \text{ nm}$

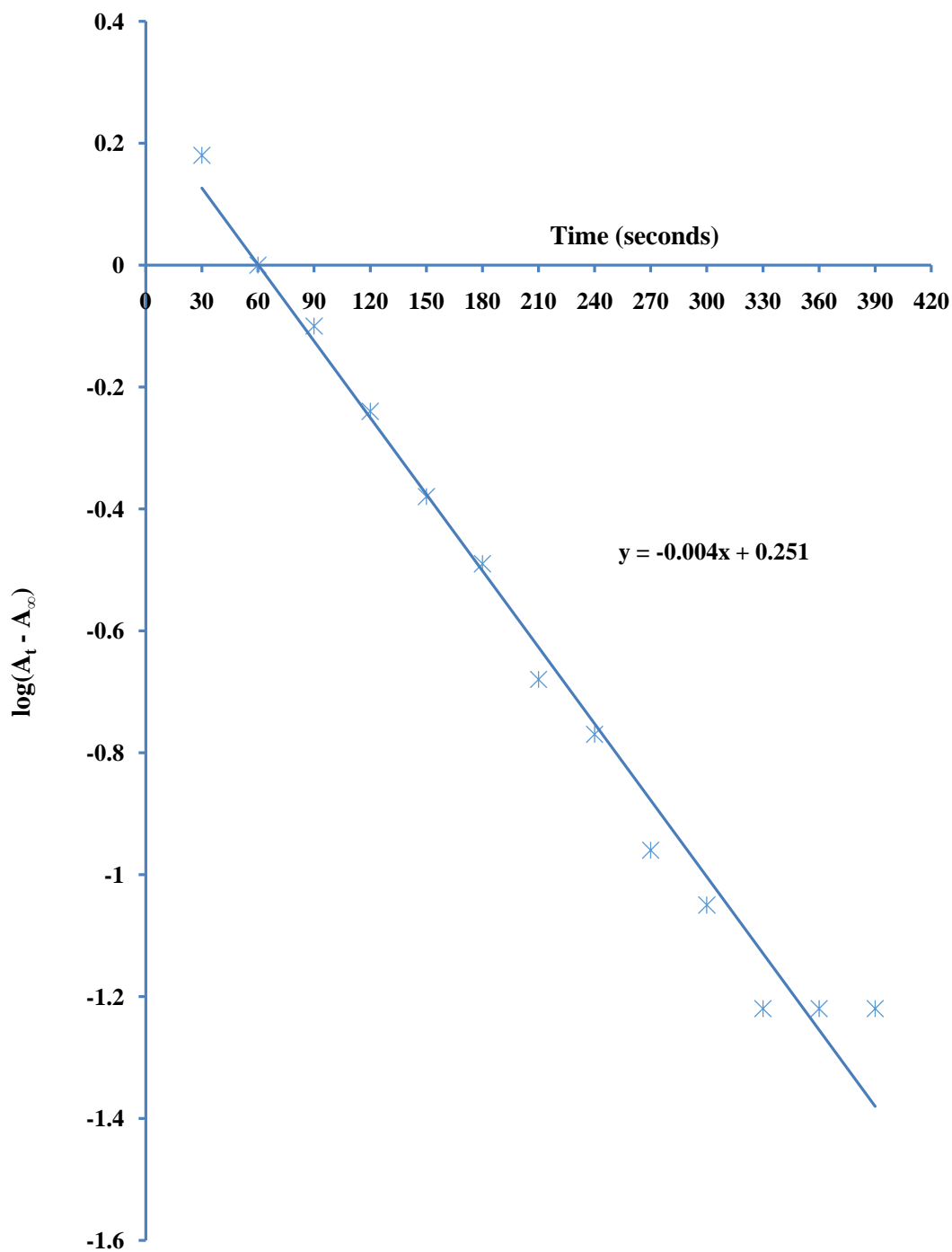


Figure 4.13: Typical Pseudo-first Order Plot for the Reaction of $[(\text{H}_2\text{O})_2\text{Ru}_2\text{O}]^{4+}$ and *N*-allylthiourea (ATU) at $[(\text{H}_2\text{O})_2\text{Ru}_2\text{O}^{4+}] = 5.75 \times 10^{-5} \text{ mol dm}^{-3}$, $[\text{ATU}] = 2.3 \times 10^{-2} \text{ mol dm}^{-3}$, $[\text{H}^+] = 5.0 \times 10^{-2} \text{ mol dm}^{-2}$; $I = 0.5 \text{ mol dm}^{-3}$, $T = 31 \pm 1 \text{ }^\circ\text{C}$ and $\lambda_{\text{max}} = 660 \text{ nm}$

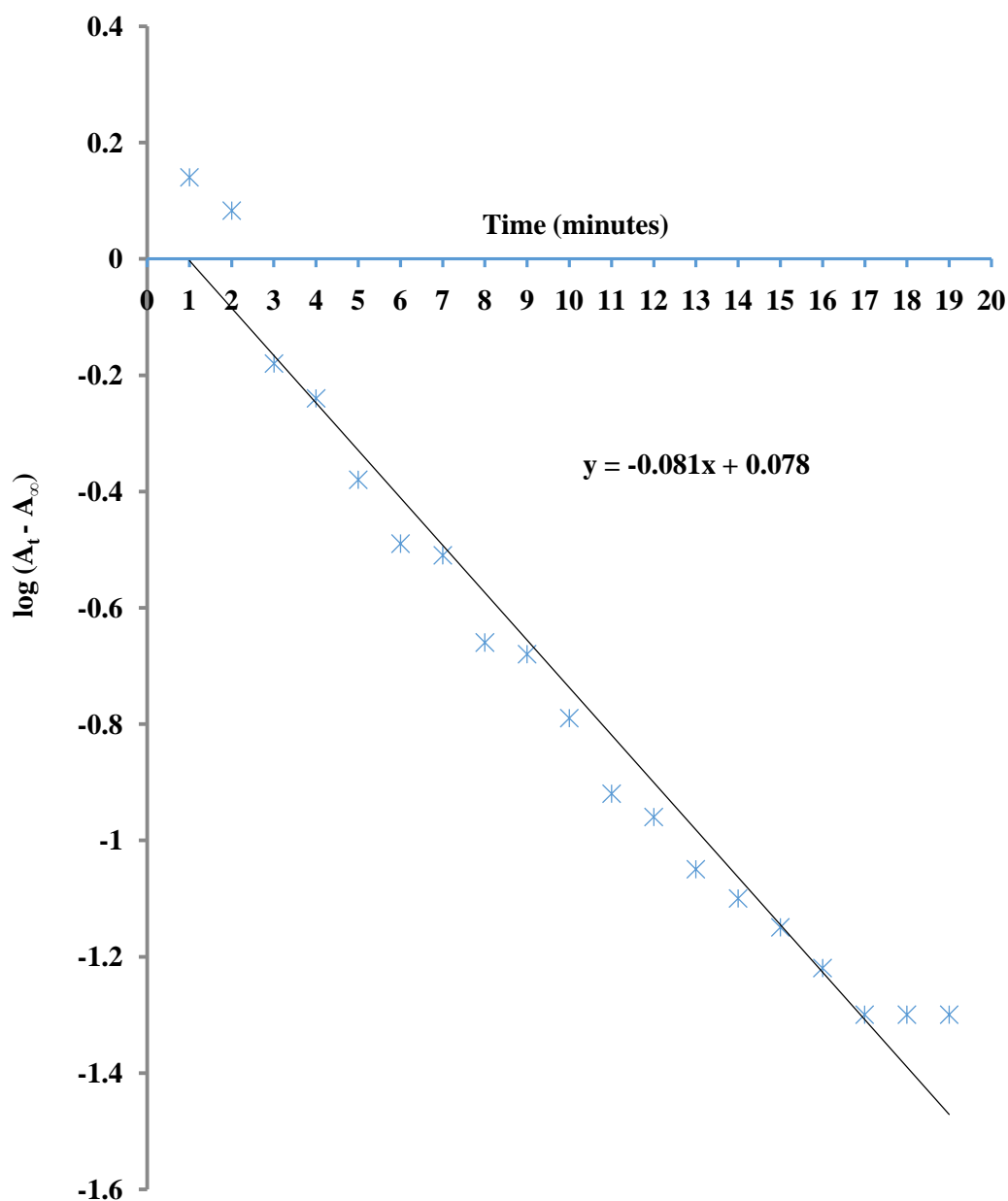


Figure 4.14: Typical Pseudo-first Order Plot for the Reaction of $[(\text{H}_2\text{O})_2\text{Ru}_2\text{O}]^{4+}$ and *N, N'*-dimethylthiourea (DMTU) at $[(\text{H}_2\text{O})_2\text{Ru}_2\text{O}^{4+}] = 7.0 \times 10^{-5} \text{ mol dm}^{-3}$, $[\text{DMTU}] = 3.5 \times 10^{-2} \text{ mol dm}^{-3}$, $[\text{H}^+] = 5.0 \times 10^{-2} \text{ mol dm}^{-2}$, $I = 0.5 \text{ mol dm}^{-3}$, $T = 31 \text{ } ^\circ\text{C}$ and $\lambda_{\text{max}} = 660 \text{ nm}$

The slopes of the plots gave the pseudo-first order rate constants, k_{obs} . The values of k_{obs} for each of the systems are presented in Tables 4.1 – 4.4. The second order rate constants, k_2 , were determined as the ratio of k_{obs} to [reductants], and were found to be fairly constant (Tables 4.1 – 4.4). The second order rate constants for the four systems were found to be $(7.39 \pm 0.05) \times 10^{-3}$ (Ru_2O^{4+} / TU); $(3.14 \pm 0.05) \times 10^{-2}$ (Ru_2O^{4+} / MTU); $(20.22 \pm 0.01) \times 10^{-2}$ (Ru_2O^{4+} / ATU); and $(8.12 \pm .04) \times 10^{-2}$ (Ru_2O^{4+} / DMTU) $\text{dm}^3 \text{mol}^{-1} \text{s}^{-1}$, respectively. Order of reaction with respect to [TU], [MTU], [ATU] and [DMTU] as obtained from the slopes of the plots of $\log k_{\text{obs}}$ versus \log [reductant] at constant $[\text{H}^+]$ and constant ionic strength were found to be 1.00 (TU), 0.99 (MTU), 1.06 (ATU) and 0.97 (DMTU), indicating first order dependence of the rates of reaction on [TU], [MTU], [ATU] and [DMTU] (Figures 4.15 – 4.18) .

The rate law at constant $[\text{H}^+]$ for the reaction of Ru_2O^{4+} and the thioureas can be represented as Equation 4.11.:

$$-\frac{d}{dt} [\text{Ru}_2\text{O}^{4+}] = k_2[\text{Ru}_2\text{O}^{4+}][\text{Reductant}] \quad \dots \quad (4.11)$$

where the reductants are thiourea (TU), *N*-methylthiourea (MTU), *N*-allylthiourea (ATU) and *N,N*-dimethylthiourea (DMTU). The values of the second order rate constants, k_2 , in $\text{dm}^3 \text{mol}^{-1} \text{s}^{-1}$ are the same as the ones reported in Tables 4.1 – 4.4.

4.3.2 : Ru_2O^{4+} reaction with $\text{S}_2\text{O}_3^{2-}$ and $\text{S}_2\text{O}_4^{2-}$

Pseudo-first order plots of $\log (A_t - A_\infty)$ versus time were linear for over 90% extent of reaction. This suggests that the reaction is first order with respect to $[\text{Ru}_2\text{O}^{4+}]$ for the two systems under discussion. The slopes of the pseudo-first order plots gave the pseudo-first order rate constants, k_{obs} , and are reported in Tables 4.5 and 4.6.

Table 4.1: Pseudo-first Order and Second Order Rate Constants for the Reaction of $[(\text{H}_2\text{O})_2\text{Ru}_2\text{O}]^{4+}$ and Thiourea (TU) at $[(\text{H}_2\text{O})_2\text{Ru}_2\text{O}^{4+}] = 6.0 \times 10^{-5} \text{ mol dm}^{-3}$, $I = 0.5 \text{ mol dm}^{-3}$ (NaClO_4), $T = 31 \pm 1^\circ\text{C}$ and $\lambda_{\text{max}} = 660 \text{ nm}$

$10^2 [\text{TU}], \text{ mol dm}^{-3}$	$10^3 [\text{H}^+], \text{ mol dm}^{-3}$	$I, \text{ mol dm}^{-3}$	$10^4 k_{\text{obs}}, \text{ s}^{-1}$	$10^3 k_2, \text{ dm}^3 \text{ mol}^{-1} \text{ s}^{-1}$
4.80	5.0	0.5	3.57	7.43
7.20	5.0	0.5	5.23	7.27
9.60	5.0	0.5	7.15	7.45
12.00	5.0	0.5	8.83	7.36
14.40	5.0	0.5	10.72	7.44
16.80	5.0	0.5	12.40	7.38
21.60	5.0	0.5	16.03	7.42
12.00	1.0	0.5	13.45	11.21
12.00	2.0	0.5	12.04	10.03
12.00	3.0	0.5	11.11	9.26
12.00	4.0	0.5	10.33	8.61
12.00	5.0	0.5	8.80	7.33
12.00	6.0	0.5	8.15	6.79
12.00	10.0	0.5	4.10	3.41
12.00	5.0	0.1	8.86	7.38
12.00	5.0	0.3	8.90	7.42
12.00	5.0	0.5	8.88	7.40
12.00	5.0	0.7	8.82	7.35
12.00	5.0	0.9	8.86	7.38

Table 4.2: Pseudo-first Order and Second Order Rate Constants for the Reaction of $[(\text{H}_2\text{O})_2\text{Ru}_2\text{O}]^{4+}$ and *N*-methylthiourea (MTU) at $[(\text{H}_2\text{O})_2\text{Ru}_2\text{O}^{4+}] = 6.5 \times 10^{-5} \text{ mol dm}^{-3}$, $I = 0.5 \text{ mol dm}^{-3}$ (NaClO_4), $T = 31 \pm 1^\circ\text{C}$ and $\lambda_{\text{max}} = 660 \text{ nm}$

$10^2 [\text{MTU}], \text{ mol dm}^{-3}$	$10^3 [\text{H}^+], \text{ mol dm}^{-3}$	$I, \text{ mol dm}^{-3}$	$10^4 k_{\text{obs}}, \text{ s}^{-1}$	$10^3 k_2, \text{ dm}^3 \text{ mol}^{-1} \text{ s}^{-1}$
1.30	5.0	0.5	4.12	3.17
1.95	5.0	0.5	6.22	3.19
2.60	5.0	0.5	7.92	3.04
3.90	5.0	0.5	12.35	3.17
5.20	5.0	0.5	16.67	3.20
6.50	5.0	0.5	19.94	3.07
7.80	5.0	0.5	24.54	3.14
5.20	2.0	0.5	19.76	3.80
5.20	3.0	0.5	18.20	3.50
5.20	4.0	0.5	17.42	3.35
5.20	5.0	0.5	16.38	3.15
5.20	7.0	0.5	14.04	2.70
5.20	10.0	0.5	11.40	2.20
5.20	20.0	0.5	5.20	0.10
5.20	5.0	0.1	16.28	3.13
5.20	5.0	0.2	16.02	3.08
5.20	5.0	0.5	16.41	3.16
5.20	5.0	0.6	16.33	3.14
5.20	5.0	0.9	16.17	3.11

Table 4.3: Pseudo-first Order and Second Order Rate Constants for the Reaction of $[(\text{H}_2\text{O})_2\text{Ru}_2\text{O}]^{4+}$ and *N*-allylthiourea (ATU) at $[(\text{H}_2\text{O})_2\text{Ru}_2\text{O}^{4+}] = 5.75 \times 10^{-5} \text{ mol dm}^{-3}$, $I = 0.5 \text{ mol dm}^{-3}$ (NaClO_4), $T = 31 \pm 1^\circ\text{C}$ and $\lambda_{\text{max}} = 660 \text{ nm}$

$10^2 [\text{ATU}], \text{ mol dm}^{-3}$	$10^3 [\text{H}^+], \text{ mol dm}^{-3}$	$I, \text{ mol dm}^{-3}$	$10^3 k_{\text{obs}}, \text{ s}^{-1}$	$k_2, \text{ dm}^3 \text{ mol}^{-1} \text{ s}^{-1}$
1.15	5.0	0.5	2.19	0.19
1.73	5.0	0.5	3.58	0.21
2.30	5.0	0.5	4.60	0.20
3.45	5.0	0.5	6.18	0.18
4.60	5.0	0.5	10.46	0.23
5.75	5.0	0.5	12.04	0.21
3.45	1.0	0.5	8.97	0.26
3.45	3.0	0.5	7.56	0.22
3.45	5.0	0.5	6.55	0.19
3.45	7.0	0.5	5.19	0.15
3.45	10.0	0.5	3.81	0.11
3.45	14.0	0.5	1.05	0.03
3.45	5.0	0.1	6.21	0.18
3.45	5.0	0.2	7.56	0.22
3.45	5.0	0.5	7.01	0.20
3.45	5.0	0.6	6.54	0.19
3.45	5.0	0.7	6.21	0.18
3.45	5.0	0.9	7.31	0.21

Table 4.4: Pseudo-first Order and Second Order Rate Constants for the Reaction of $[(\text{H}_2\text{O})_2\text{Ru}_2\text{O}]^{4+}$ and N,N' -dimethylthiourea (DMTU) at $[(\text{H}_2\text{O})_2\text{Ru}_2\text{O}^{4+}] = 7.0 \times 10^{-5} \text{ mol dm}^{-3}$, $I = 0.5 \text{ mol dm}^{-3}$ (NaClO_4), $T = 31.5 \pm 1^\circ\text{C}$ and $\lambda_{\text{max}} = 660 \text{ nm}$

$10^2 [\text{DMTU}],$ mol dm^{-3}	$10^3 [\text{H}^+],$ mol dm^{-3}	$I,$ mol dm^{-3}	$10^3 k_{\text{obs}}, \text{ s}^{-1}$	$10^2 k_2, \text{ dm}^3 \text{ mol}^{-1} \text{ s}^{-1}$
1.40	5.0	0.5	1.14	8.16
2.10	5.0	0.5	1.71	8.14
3.50	5.0	0.5	2.86	8.16
5.60	5.0	0.5	4.57	8.14
6.30	5.0	0.5	5.03	7.98
7.00	5.0	0.5	5.69	8.13
8.40	5.0	0.5	6.82	8.12
5.60	2.0	0.5	5.49	9.80
5.60	3.0	0.5	4.93	8.80
5.60	5.0	0.5	4.54	8.11
5.60	7.0	0.5	4.14	7.39
5.60	10.0	0.5	3.04	5.43
5.60	20.0	0.5	0.74	1.32
5.60	5.0	0.1	4.55	8.13
5.60	5.0	0.2	4.54	8.11
5.60	5.0	0.5	4.47	7.99
5.60	5.0	0.6	4.56	8.14
5.60	5.0	0.7	4.55	8.13
5.60	5.0	0.9	4.55	8.13

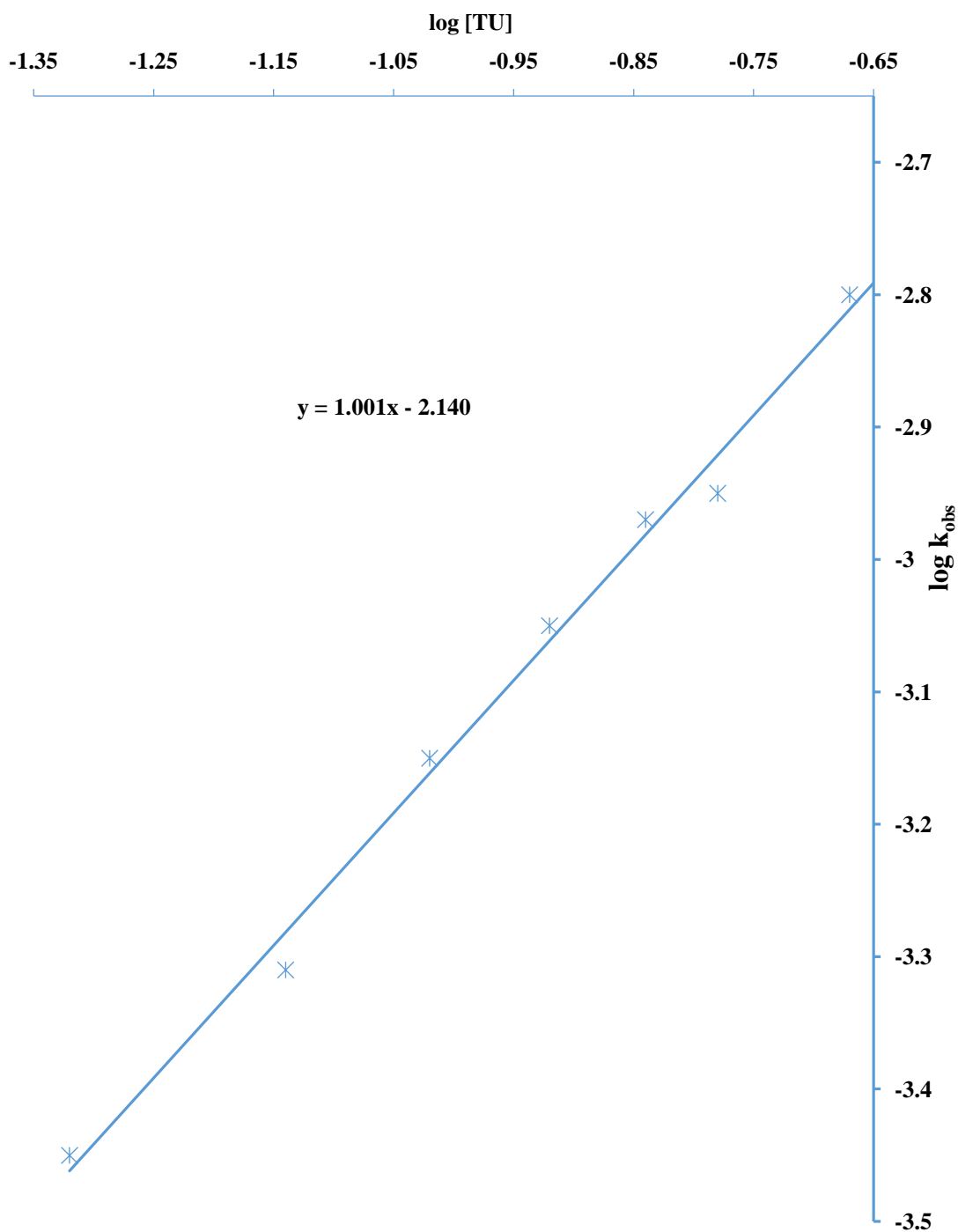


Figure 4.15: Plot of $\log k_{\text{obs}}$ against $\log [\text{TU}]$ for the Reaction of $[(\text{H}_2\text{O})_2\text{Ru}_2\text{O}]^{4+}$ and Thiourea (TU) at $[(\text{H}_2\text{O})_2\text{Ru}_2\text{O}^{4+}] = 6.0 \times 10^{-5} \text{ mol dm}^{-3}$, $[\text{TU}] = (4.8 - 21.60) \times 10^{-2} \text{ mol dm}^{-3}$, $[\text{H}^+] = 5.0 \times 10^{-2} \text{ mol dm}^{-3}$, $I = 0.5 \text{ mol dm}^{-3}$, $T = 31 \text{ } ^\circ\text{C}$ and $\lambda_{\text{max}} = 660 \text{ nm}$

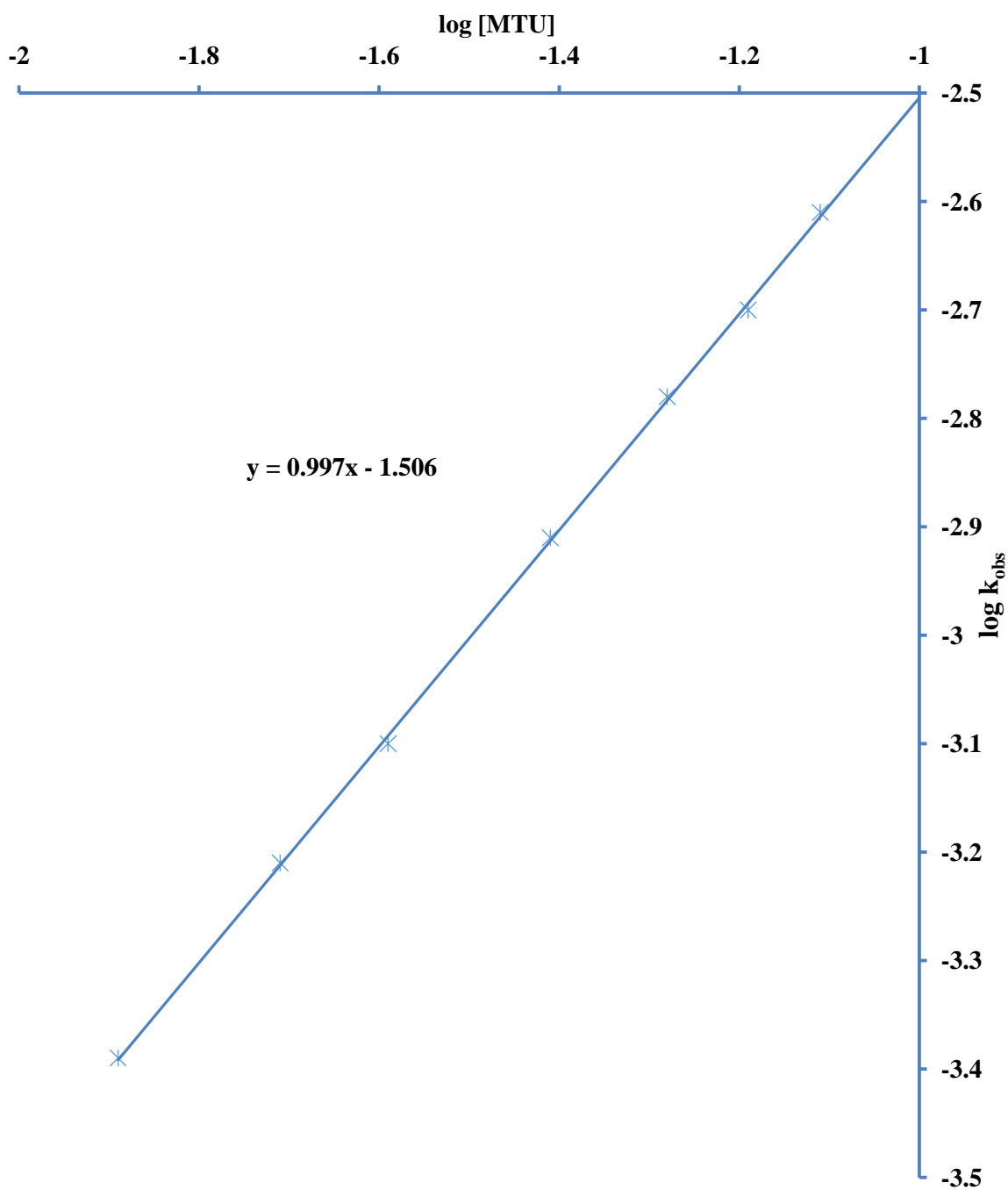


Figure 4.16: Plot of $\log k_{\text{obs}}$ against $\log [\text{MTU}]$ for the Reaction of $[(\text{H}_2\text{O})_2\text{Ru}_2\text{O}]^{4+}$ and *N*-methylthiourea (MTU) at $[(\text{H}_2\text{O})_2\text{Ru}_2\text{O}^{4+}] = 6.0 \times 10^{-5} \text{ mol dm}^{-3}$, $[\text{MTU}] = (1.3 - 7.8) \times 10^{-2} \text{ mol dm}^{-3}$, $[\text{H}^+] = 5.0 \times 10^{-2} \text{ mol dm}^{-3}$; $I = 0.5 \text{ mol dm}^{-3}$, $T = 31 \text{ } ^\circ\text{C}$ and $\lambda_{\text{max}} = 660 \text{ nm}$

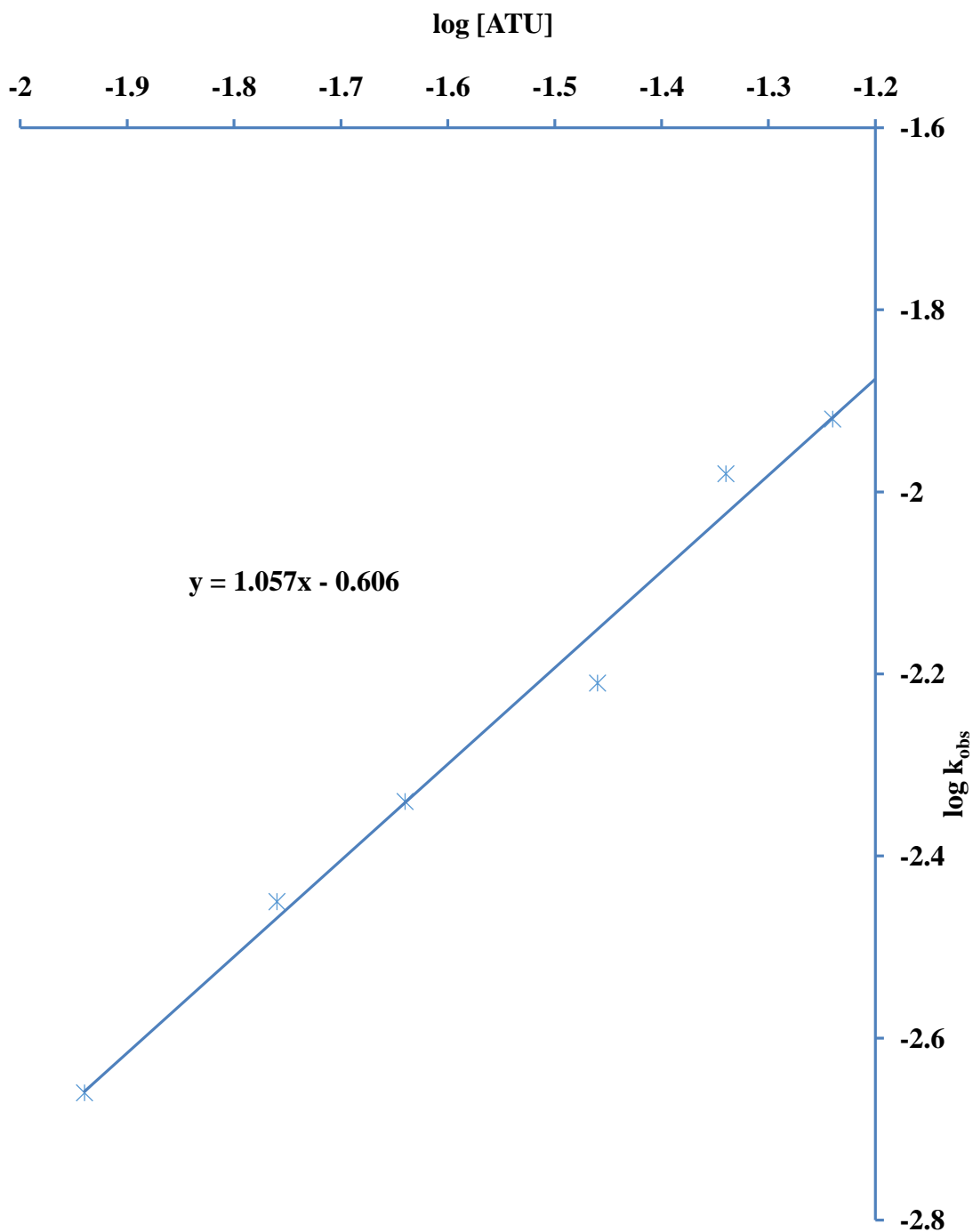


Figure 4.17: Plot of $\log k_{\text{obs}}$ against $\log [\text{ATU}]$ for the Reaction of $[(\text{H}_2\text{O})_2\text{Ru}_2\text{O}]^{4+}$ and *N*-allylthiourea (ATU) at $[(\text{H}_2\text{O})_2\text{Ru}_2\text{O}^{4+}] = 5.75 \times 10^{-5} \text{ mol dm}^{-3}$, $[\text{ATU}] = (1.15 - 5.75) \times 10^{-2} \text{ mol dm}^{-3}$, $[\text{H}^+] = 5.0 \times 10^{-2} \text{ mol dm}^{-3}$, $I = 0.5 \text{ mol dm}^{-3}$, $T = 31 \pm 1 \text{ C}$ and $\lambda_{\text{max}} = 660 \text{ nm}$

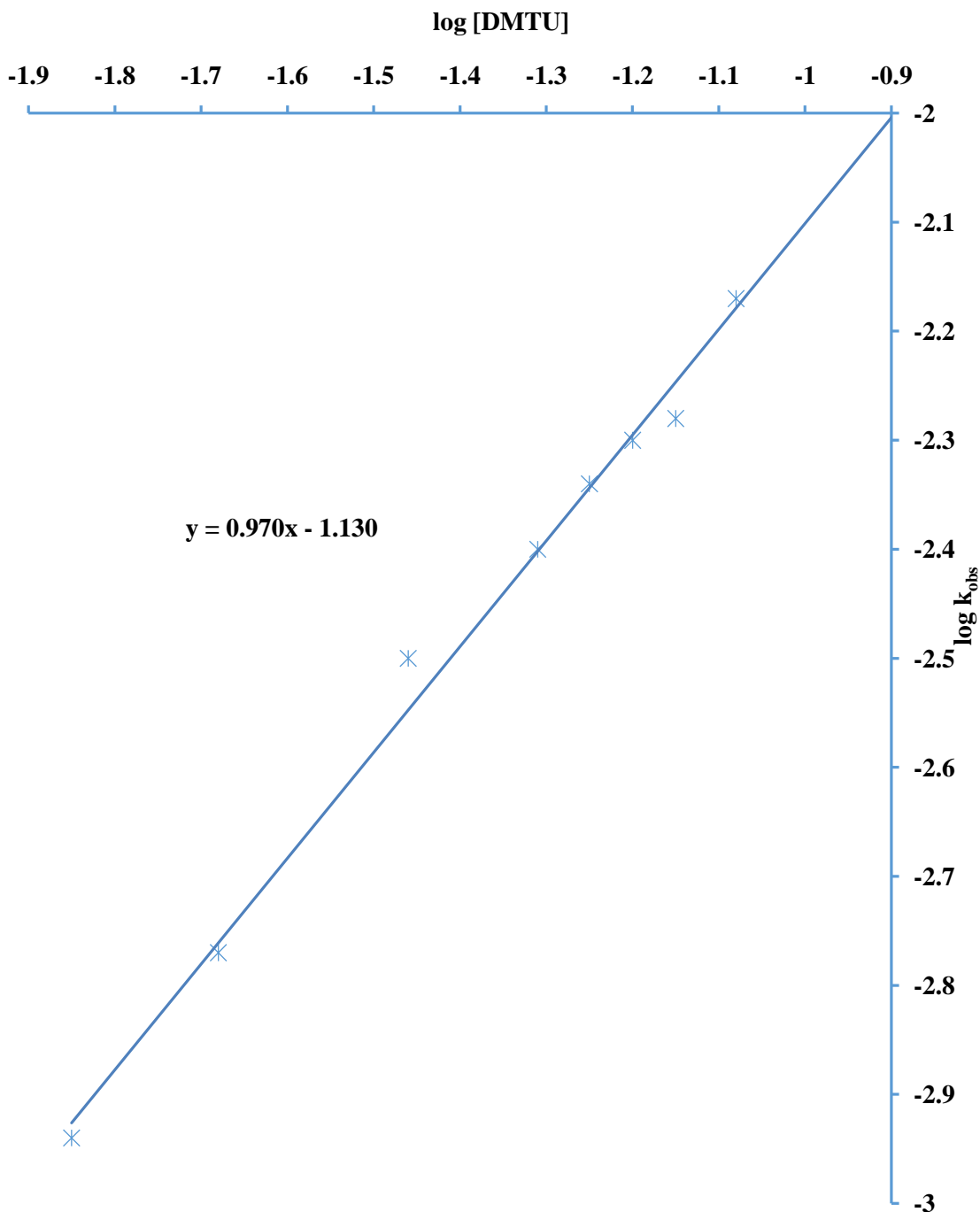


Figure 4.18: Plot of $\log k_{\text{obs}}$ against $\log [\text{DMTU}]$ for the Reaction of $[(\text{H}_2\text{O})_2\text{Ru}_2\text{O}]^{4+}$ and *N,N'*-dimethylthiourea (DMTU) at $[(\text{H}_2\text{O})_2\text{Ru}_2\text{O}^{4+}] = 7.0 \times 10^{-5} \text{ mol dm}^{-3}$, $[\text{DMTU}] = (1.4 - 8.4) \times 10^{-2} \text{ mol dm}^{-3}$, $[\text{H}^+] = 5.0 \times 10^{-2} \text{ mol dm}^{-3}$, $I = 0.5 \text{ mol dm}^{-3}$, $T = 31 \pm 1 \text{ C}$ and $\lambda_{\text{max}} = 660 \text{ nm}$

Table 4.5: Pseudo-first Order and Second Order Rate Constants for the Reaction of $[(\text{H}_2\text{O})_2\text{Ru}_2\text{O}]^{4+}$ and $\text{S}_2\text{O}_3^{2-}$ at $[(\text{H}_2\text{O})_2\text{Ru}_2\text{O}^{4+}] = 6.5 \times 10^{-5} \text{ mol dm}^{-3}$, $I = 0.5 \text{ mol dm}^{-3}$ (NaClO_4), $T = 31 \pm 1^\circ\text{C}$ and $\lambda_{\text{max}} = 660 \text{ nm}$

$10^2[\text{S}_2\text{O}_3^{2-}]$, mol dm^{-3}	$10^3 [\text{H}^+]$, mol dm^{-3}	I , mol dm^{-3}	$10^3 k_{\text{obs}}$, s^{-1}	$10^2 k_2$, $\text{dm}^3 \text{ mol}^{-1} \text{ s}^{-1}$
3.25	5.0	0.5	1.23	3.78
6.50	5.0	0.5	2.44	3.75
13.00	5.0	0.5	4.89	3.76
19.50	5.0	0.5	7.30	3.74
32.50	5.0	0.5	12.20	3.75
45.50	5.0	0.5	16.97	3.73
13.00	2.0	0.5	2.39	1.84
13.00	4.0	0.5	3.93	3.02
13.00	5.0	0.5	4.88	3.75
13.00	7.0	0.5	6.86	5.28
13.00	10.0	0.5	9.83	7.56
13.00	15.0	0.5	14.10	10.85
13.00	20.0	0.5	20.36	15.66
13.00	5.0	0.2	23.83	18.33
13.00	5.0	0.3	14.87	11.44
1300	5.0	0.5	4.91	3.78
13.00	5.0	0.7	2.45	1.88
13.00	5.0	0.9	0.94	0.72

Table 4.6: Pseudo-first Order and Second Order Rate Constants for the Reaction of $[(\text{H}_2\text{O})_2\text{Ru}_2\text{O}]^{4+}$ and $(\text{S}_2\text{O}_4^{2-})$ at $[(\text{H}_2\text{O})_2\text{Ru}_2\text{O}^{4+}] = 5.75 \times 10^{-5} \text{ mol dm}^{-3}$, $I = 0.5 \text{ mol dm}^{-3}$ (NaClO_4), $T = 31 \pm 1^\circ\text{C}$ and $\lambda_{\text{max}} = 660 \text{ nm}$

$10^2 [\text{S}_2\text{O}_4^{2-}]$, mol dm^{-3}	I , mol dm^{-3}	$10^3 k_{\text{obs}}$, s^{-1}	$10^2 k_2$, $\text{dm}^3 \text{ mol}^{-1} \text{ s}^{-1}$
1.44	0.5	1.59	11.03
2.01	0.5	2.21	10.99
2.88	0.5	2.94	11.02
4.31	0.5	4.73	10.97
5.75	0.5	6.34	11.02
8.36	0.5	9.10	10.89
11.50	0.5	12.59	10.95
14.38	0.5	15.88	11.04
4.31	0.2	4.72	10.95
4.31	0.3	4.76	11.04
4.31	0.4	4.74	11.00
4.31	0.5	4.75	11.02
4.31	0.6	4.73	10.97
4.31	0.8	4.71	10.93
4.31	0.9	4.74	11.00
4.31	1.1	4.71	10.93

Typical plots are depicted in Figures (4.19 – 4.20). The ratios of k_{obs} to $[\text{S}_2\text{O}_3^{2-}]$ and $[\text{S}_2\text{O}_4^{2-}]$, respectively, gave the second order rate constants, k_2 , in $\text{dm}^3 \text{mol}^{-1} \text{s}^{-1}$. The values of k_2 are fairly constant and are presented in Tables 4.5 and 4.6, whose averages are $(3.75 \pm .01) \times 10^{-3}$ and $(10.99 \pm .04) \times 10^{-2} \text{ dm}^3 \text{mol}^{-1} \text{s}^{-1}$ for $\text{Ru}_2\text{O}^{4+}/\text{S}_2\text{O}_3^{2-}$ and $\text{Ru}_2\text{O}^{4+}/\text{S}_2\text{O}_4^{2-}$ systems, respectively. The order of reaction with respect to $[\text{S}_2\text{O}_3^{2-}]$ and $[\text{S}_2\text{O}_4^{2-}]$, as obtained from the slopes of the plots of $\log k_{\text{obs}}$ versus $\log [\text{reductant}]$ at constant $[\text{H}^+]$ (for the $\text{Ru}_2\text{O}^{4+}/\text{S}_2\text{O}_3^{2-}$ system) and ionic strength (Figures 4.21 and 4.22) were found to be 1.02 for ($\text{Ru}_2\text{O}^{4+}/\text{S}_2\text{O}_3^{2-}$) system and 1.04 for ($\text{Ru}_2\text{O}^{4+}/\text{S}_2\text{O}_4^{2-}$) system. The rate law at constant $[\text{H}^+]$ for the reaction of Ru_2O^{4+} and the reductants ($\text{S}_2\text{O}_3^{2-}$ and $\text{S}_2\text{O}_4^{2-}$) can be represented as Equation 4.12.

$$-\frac{d}{dt} [\text{Ru}_2\text{O}^{4+}] = k_2[\text{Ru}_2\text{O}^{4+}][\text{Reductant}] \quad \dots \quad (4.12)$$

where reductants, here, are $\text{S}_2\text{O}_3^{2-}$ and $\text{S}_2\text{O}_4^{2-}$ and k_2 values are presented on Tables 4.5 and 4.6.

4.3.3 Ru_2O^{4+} reaction with H_3PO_2

Pseudo-first order plots of $\log (A_t - A_\infty)$ versus time were linear for greater than 90% of extent of reaction. This suggests a first order dependence of rate of reaction on $[\text{Ru}_2\text{O}^{4+}]$ for the $\text{Ru}_2\text{O}^{4+}/\text{H}_3\text{PO}_2$ system. A typical pseudo-first order plot is presented on Figure 4.23. The slopes of the plots gave the pseudo-first order rate constants, k_{obs} for each run. The second order rate constants determined from $k_{\text{obs}}/[\text{H}_3\text{PO}_2]$ were found to be nearly constant. The pseudo-first and second order rate constants are presented on Table 4.7. The second order rate constants, k_2 , for this system, as obtained from $k_{\text{obs}}/[\text{H}_3\text{PO}_2]$, are also presented in Table 4.7. The average was found to be $(7.12 \pm 0.01) \times 10^{-3} \text{ dm}^3 \text{mol}^{-1} \text{s}^{-1}$.

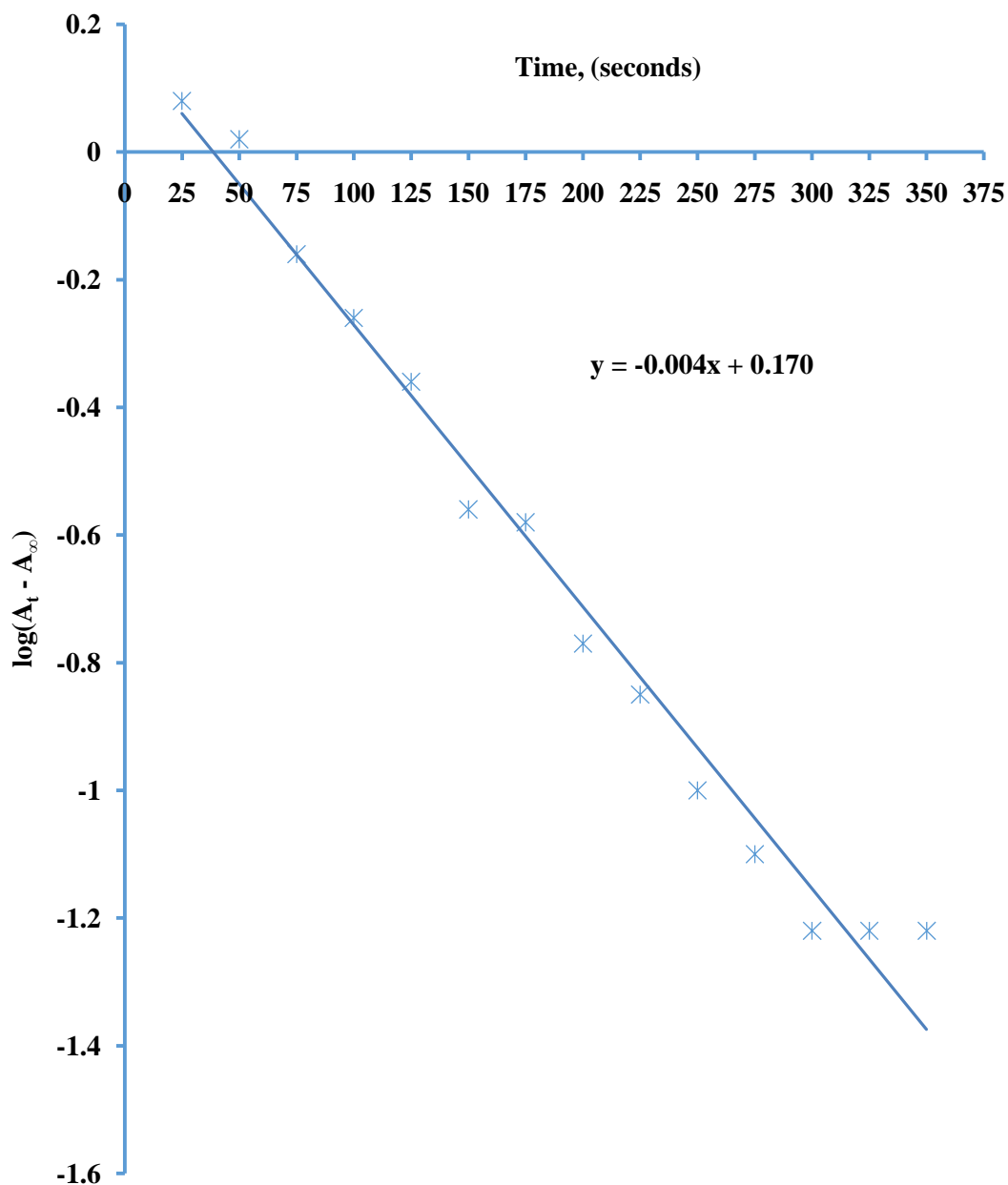


Figure 4.19: Typical Pseudo-first Order Plot for the Reaction of $[(\text{H}_2\text{O})_2\text{Ru}_2\text{O}]^{4+}$ and $\text{S}_2\text{O}_3^{2-}$ at $[(\text{H}_2\text{O})_2\text{Ru}_2\text{O}^{4+}] = 6.5 \times 10^{-5} \text{ mol dm}^{-3}$, $[\text{S}_2\text{O}_3^{2-}] = 1.3 \times 10^{-2} \text{ mol dm}^{-3}$, $[\text{H}^+] = 5.0 \times 10^{-2} \text{ mol dm}^{-2}$, $I = 0.5 \text{ mol dm}^{-3}$, $T = 31 \text{ } ^\circ\text{C}$ and $\lambda_{\text{max}} = 660 \text{ nm}$

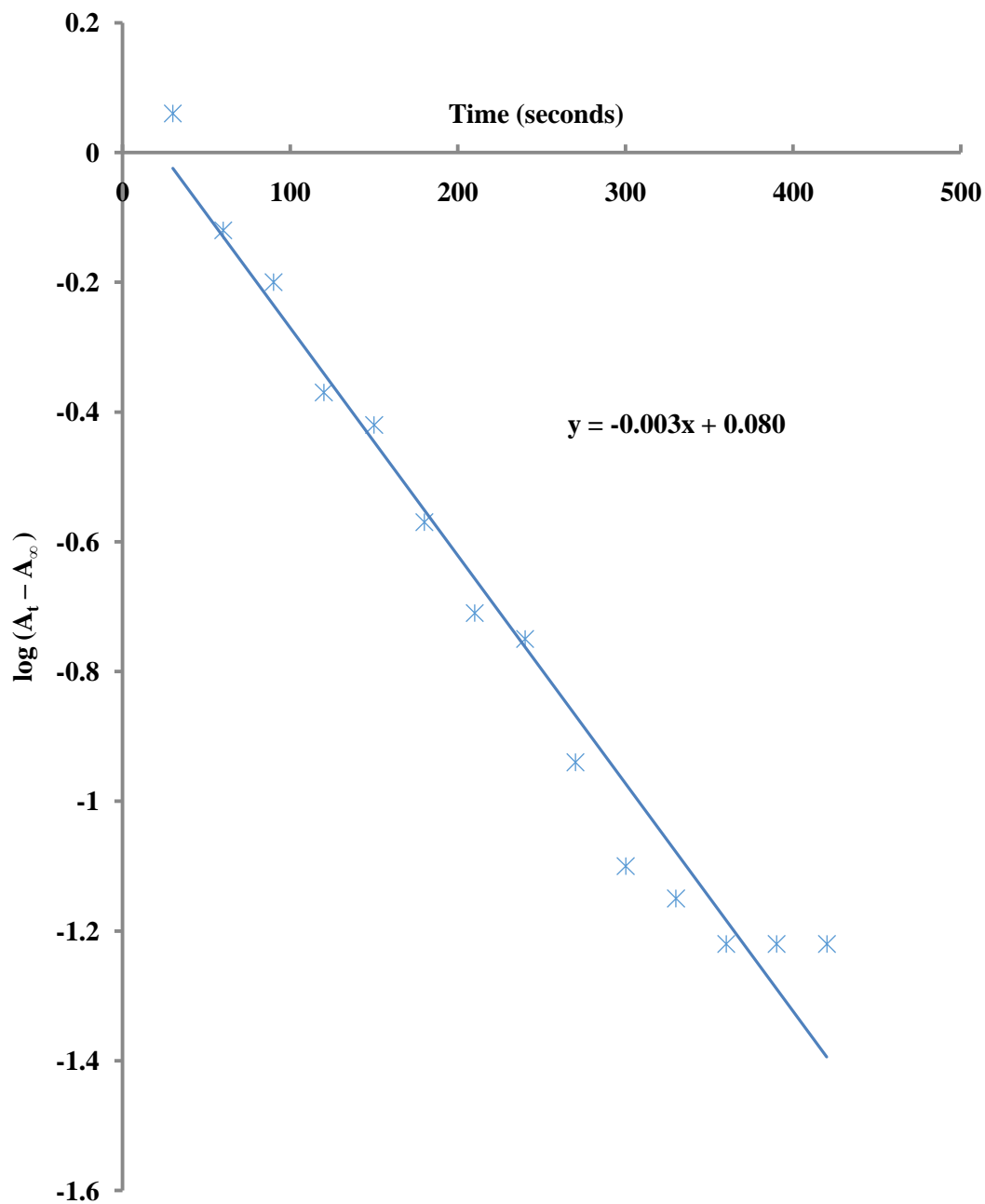


Figure 4.20: Typical Pseudo-first Order Plot for the Reaction of $[(\text{H}_2\text{O})_2\text{Ru}_2\text{O}^{4+}]$ and $\text{S}_2\text{O}_4^{2-}$ at $[(\text{H}_2\text{O})_2\text{Ru}_2\text{O}^{4+}] = 5.75 \times 10^{-5} \text{ mol dm}^{-3}$, $[\text{S}_2\text{O}_4^{2-}] = 4.31 \times 10^{-2} \text{ mol dm}^{-3}$, $I = 0.5 \text{ mol dm}^{-3}$, $T = 31 \pm 1 \text{ C}$ and $\lambda_{\text{max}} = 660 \text{ nm}$

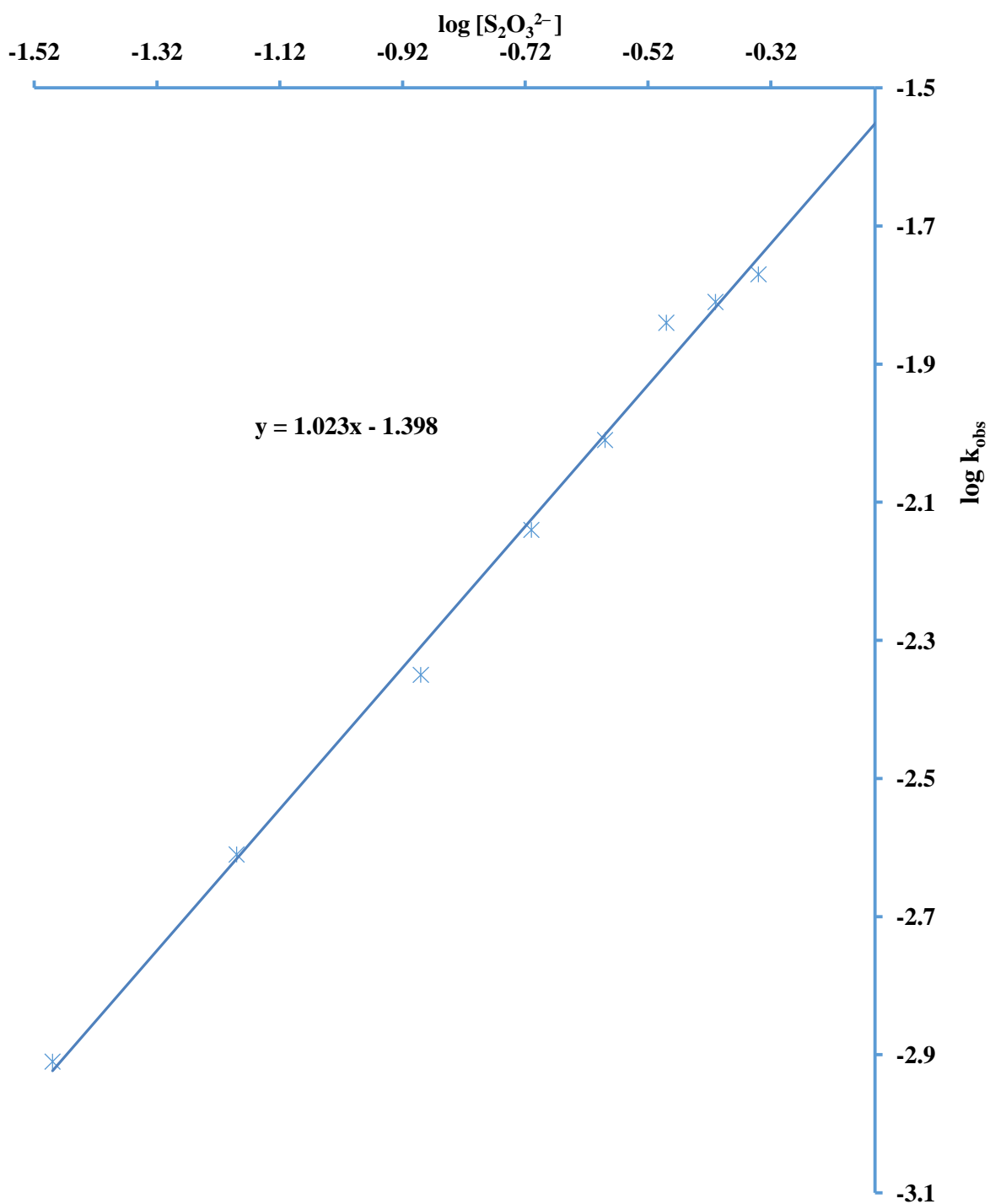


Figure 4.21: Plot of $\log k_{\text{obs}}$ against $\log [S_2O_3^{2-}]$ for the Reaction of $[(H_2O)_2Ru_2O]^{4+}$ and $S_2O_3^{2-}$ at $[(H_2O)_2Ru_2O^{4+}] = 6.5 \times 10^{-5} \text{ mol dm}^{-3}$, $[S_2O_3^{2-}] = (3.25 - 45.50) \times 10^{-3} \text{ mol dm}^{-3}$, $[H^+] = 5.0 \times 10^{-2} \text{ mol dm}^{-3}$, $I = 0.5 \text{ mol dm}^{-3}$, $T = 31 \pm 1 \text{ C}$ and $\lambda_{\text{max}} = 660 \text{ nm}$

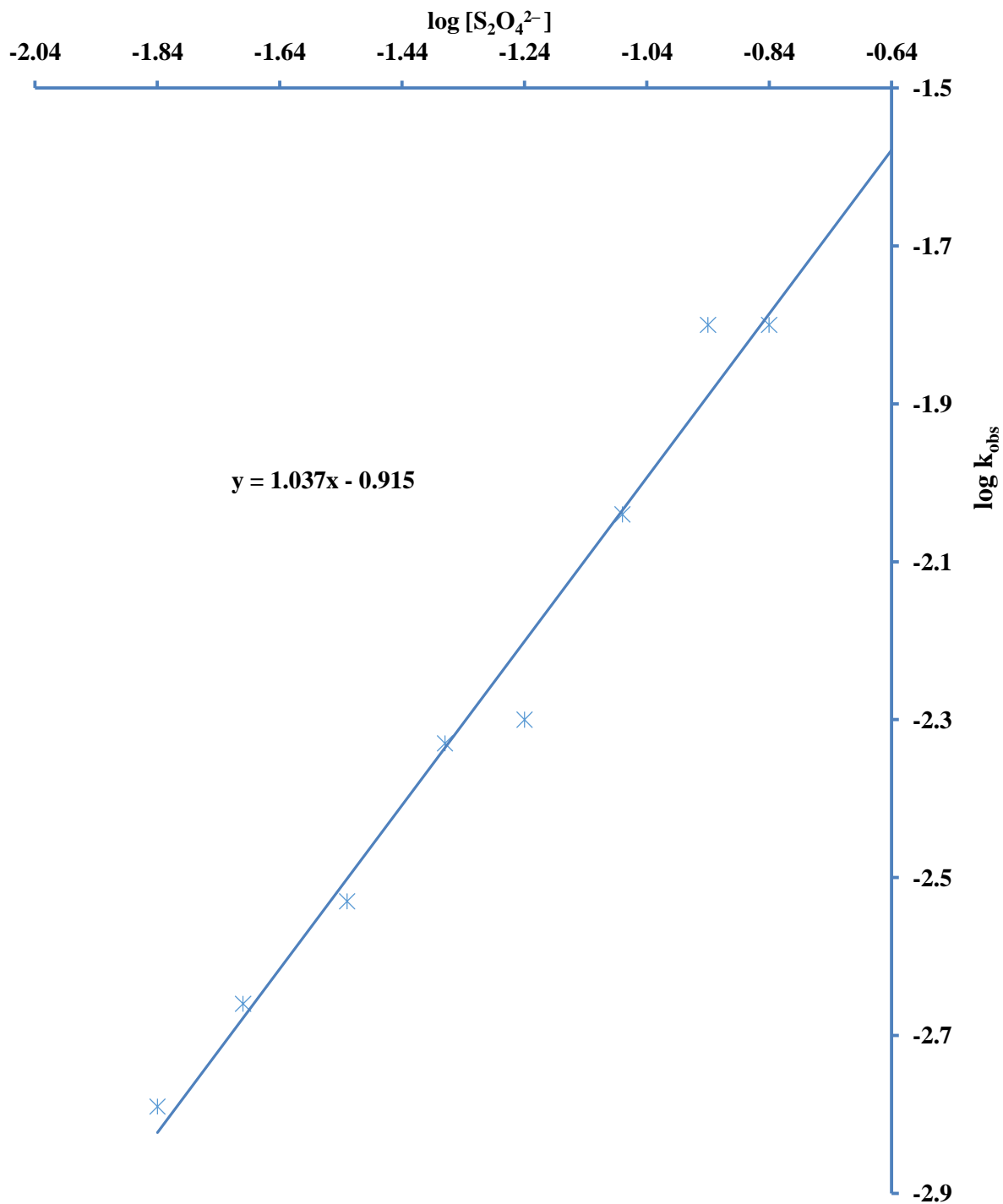


Figure 4.22: Plot of $\log k_{obs}$ against $\log [S_2O_4^{2-}]$ for the Reaction of $[(H_2O)_2Ru_2O]^{4+}$ and $S_2O_4^{2-}$ at $[(H_2O)_2Ru_2O^{4+}] = 5.75 \times 10^{-5} \text{ mol dm}^{-3}$, $[S_2O_4^{2-}] = (1.44 - 14.38) \times 10^{-2} \text{ mol dm}^{-3}$, $I = 0.5 \text{ mol dm}^{-3}$, $T = 31 \pm 1 \text{ C}$ and $\lambda_{max} = 660 \text{ nm}$

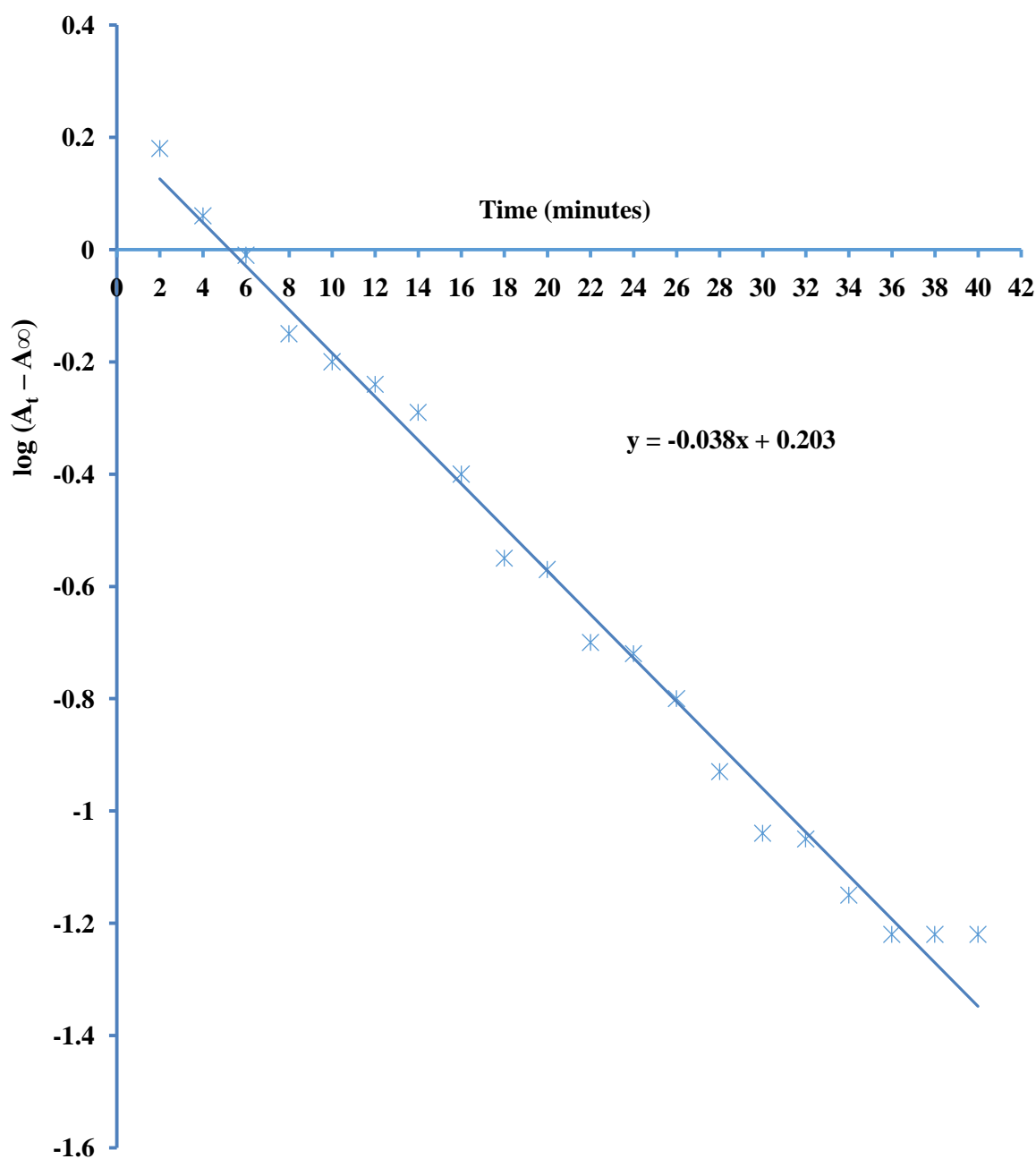


Figure 4.23: Typical Pseudo-first Order Plot for the Reaction of $[(\text{H}_2\text{O})_2\text{Ru}_2\text{O}]^{4+}$ and H_3PO_2 at $[(\text{H}_2\text{O})_2\text{Ru}_2\text{O}^{4+}] = 6.0 \times 10^{-5} \text{ mol dm}^{-3}$, $[\text{H}_3\text{PO}_2] = 9.6 \times 10^{-2} \text{ mol dm}^{-3}$, $[\text{H}^+] = 5.0 \times 10^{-2} \text{ mol dm}^{-2}$, $I = 0.5 \text{ mol dm}^{-3}$, $T = 31 \text{ } ^\circ\text{C}$ and $\lambda_{\text{max}} = 660 \text{ nm}$

Table 4.7: Pseudo-first Order and Second Order Rate Constants for the Reaction of $[(\text{H}_2\text{O})_2\text{Ru}_2\text{O}]^{4+}$ and H_3PO_2 at $[(\text{H}_2\text{O})_2\text{Ru}_2\text{O}^{4+}] = 6.0 \times 10^{-5} \text{ mol dm}^{-3}$, $I = 0.5 \text{ mol dm}^{-3}$ (NaClO_4), $T = 31 \pm 1^\circ\text{C}$ and $\lambda_{\text{max}} = 660 \text{ nm}$

$10^2 [\text{H}_3\text{PO}_2]$, mol dm^{-3}	$10^3 [\text{H}^+]$, mol dm^{-3}	I , mol dm^{-3}	$10^4 k_{\text{obs}}$, s^{-1}	$10^3 k_2$, $\text{dm}^3 \text{ mol}^{-1} \text{ s}^{-1}$
6.00	5.0	0.5	4.28	7.14
7.20	5.0	0.5	5.12	7.11
9.60	5.0	0.5	6.84	7.12
10.80	5.0	0.5	7.70	7.13
12.00	5.0	0.5	8.56	7.13
16.80	5.0	0.5	11.93	7.10
20.00	5.0	0.5	14.23	7.12
12.00	2.0	0.5	6.85	7.14
12.00	3.0	0.5	6.82	7.10
12.00	5.0	0.5	6.84	7.13
12.00	7.5	0.5	6.82	7.10
12.00	15.0	0.5	6.83	7.12
12.00	20.0	0.5	6.82	7.10
12.00	5.0	0.2	6.80	7.08
12.00	5.0	0.3	6.83	7.12
12.00	5.0	0.5	6.82	7.10
12.00	5.0	0.7	6.83	7.13
12.00	5.0	0.9	6.84	7.13
12.00	5.0	1.0	6.83	7.13

Order of reaction with respect to $[\text{H}_3\text{PO}_2]$, as obtained from the slope of the plot $\log k_{\text{obs}}$ versus $\log [\text{H}_3\text{PO}_2]$ at constant $[\text{H}^+]$ and ionic strength (Figure 4.24) was found to be 0.98, indicating a first order dependence of the reaction on $[\text{H}_3\text{PO}_2]$. The rate law, at constant $[\text{H}^+]$, for the reaction of Ru_2O^{4+} and H_3PO_2 can be presented as Equation 4.13.

$$-\frac{d}{dt} [\text{Ru}_2\text{O}^{4+}] = k_2[\text{Ru}_2\text{O}^{4+}][\text{H}_3\text{PO}_2] \quad \dots \quad (4.13)$$

4.3.4 Ru_2O^{4+} reaction with alcohols (CH_3OH , $\text{C}_2\text{H}_5\text{OH}$ and $\text{C}_3\text{H}_7\text{OH}$)

Pseudo-first order plots of $\log (A_t - A_\infty)$ versus time were linear to more than 90% of reaction for the $\text{Ru}_2\text{O}^{4+}/\text{CH}_3\text{OH}$, $\text{Ru}_2\text{O}^{4+}/\text{C}_2\text{H}_5\text{OH}$ and $\text{Ru}_2\text{O}^{4+}/\text{C}_3\text{H}_7\text{OH}$ systems. This indicated a first order dependence of rate on $[\text{Ru}_2\text{O}^{4+}]$ for all the systems. Typical pseudo-first order plots are presented on Figures 4.25 – 4.27. The pseudo-first order rate constants, k_{obs} , are obtained as the slopes of the pseudo-first order plots. The second order rate constants, k_2 , are obtained as $k_{\text{obs}}/[\text{alcohol}]$ for each run and for each system. The pseudo-first order and second order rate constants are presented on Tables 4.8 – 4.10. The second order rate constants, k_2 , were fairly constant for each system and their averages found to be $(12.01 \pm .03) \times 10^{-3} \text{ dm}^3 \text{ mol}^{-1} \text{ s}^{-1}$ for $\text{Ru}_2\text{O}^{4+}/\text{CH}_3\text{OH}$ system; $(8.79 \pm .02) \times 10^{-3} \text{ dm}^3 \text{ mol}^{-1} \text{ s}^{-1}$ for $\text{Ru}_2\text{O}^{4+}/\text{C}_2\text{H}_5\text{OH}$ system and $(3.51 \pm .02) \times 10^{-3} \text{ dm}^3 \text{ mol}^{-1} \text{ s}^{-1}$ for $\text{Ru}_2\text{O}^{4+}/\text{C}_3\text{H}_7\text{OH}$ system.

Order of reaction with respect to the reductants' concentrations, as obtained from the slopes of the plots of $\log k_{\text{obs}}$ versus $\log [\text{alcohol}]$ in the absence of acid and at constant ionic strength were found to be 1.06 for the $\text{Ru}_2\text{O}^{4+}/\text{CH}_3\text{OH}$ system; 1.03 for the

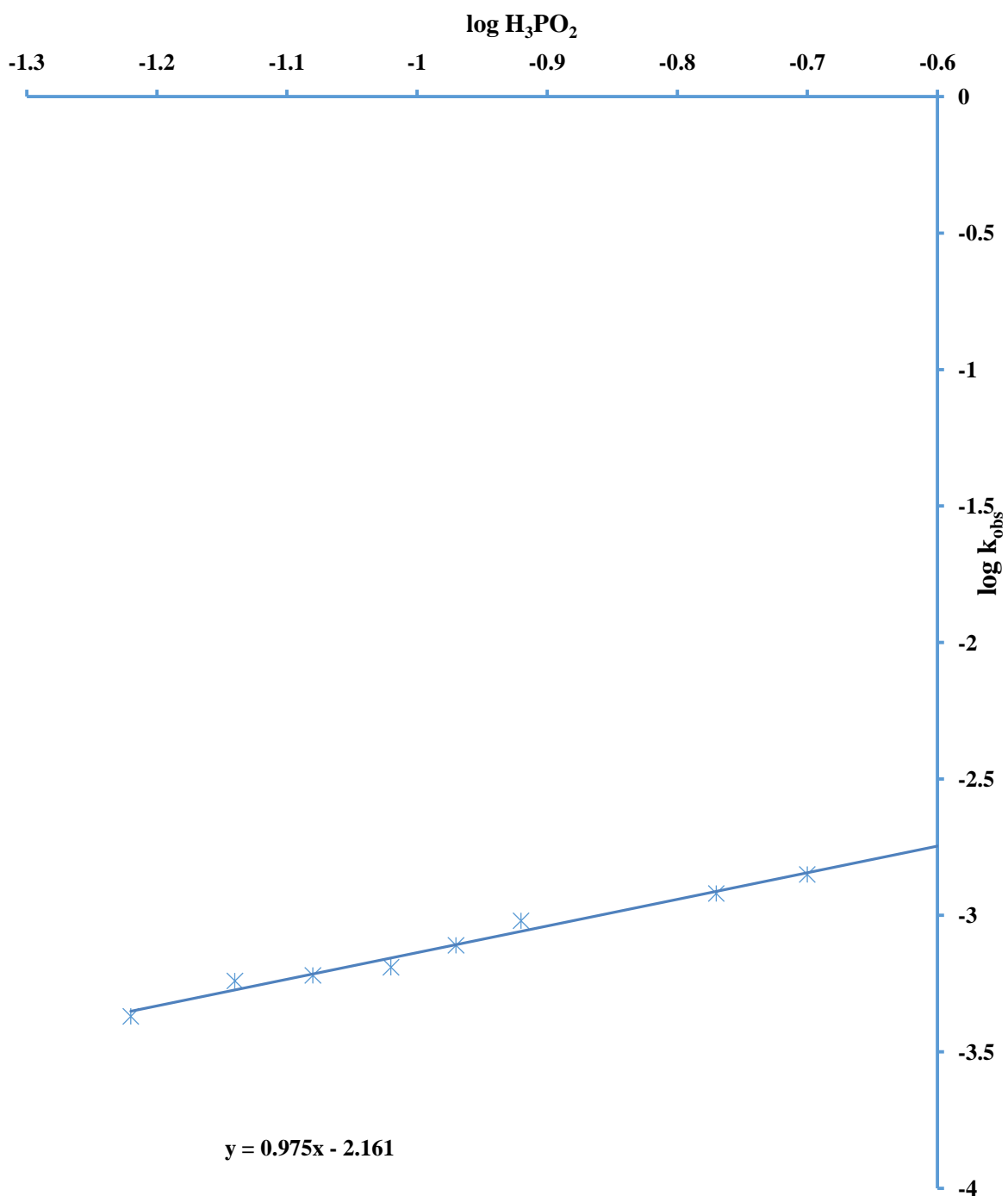


Fig 4.24: Plot of $\log k_{\text{obs}}$ against $\log [\text{H}_3\text{PO}_2]$ for the Reaction of $(\text{H}_2\text{O})_2\text{Ru}_2\text{O}^{4+}$ and H_3PO_2 at $[(\text{H}_2\text{O})_2\text{Ru}_2\text{O}^{4+}] = 6.0 \times 10^{-5} \text{ mol dm}^{-3}$, $[\text{H}_3\text{PO}_2] = (6.0 - 20.0) \times 10^{-2} \text{ mol dm}^{-3}$, $[\text{H}^+] = 5.0 \times 10^{-2} \text{ mol dm}^{-3}$, $I = 0.5 \text{ mol dm}^{-3}$, $T = 31 \text{ } ^\circ\text{C}$ and $\lambda_{\text{max}} = 660 \text{ nm}$

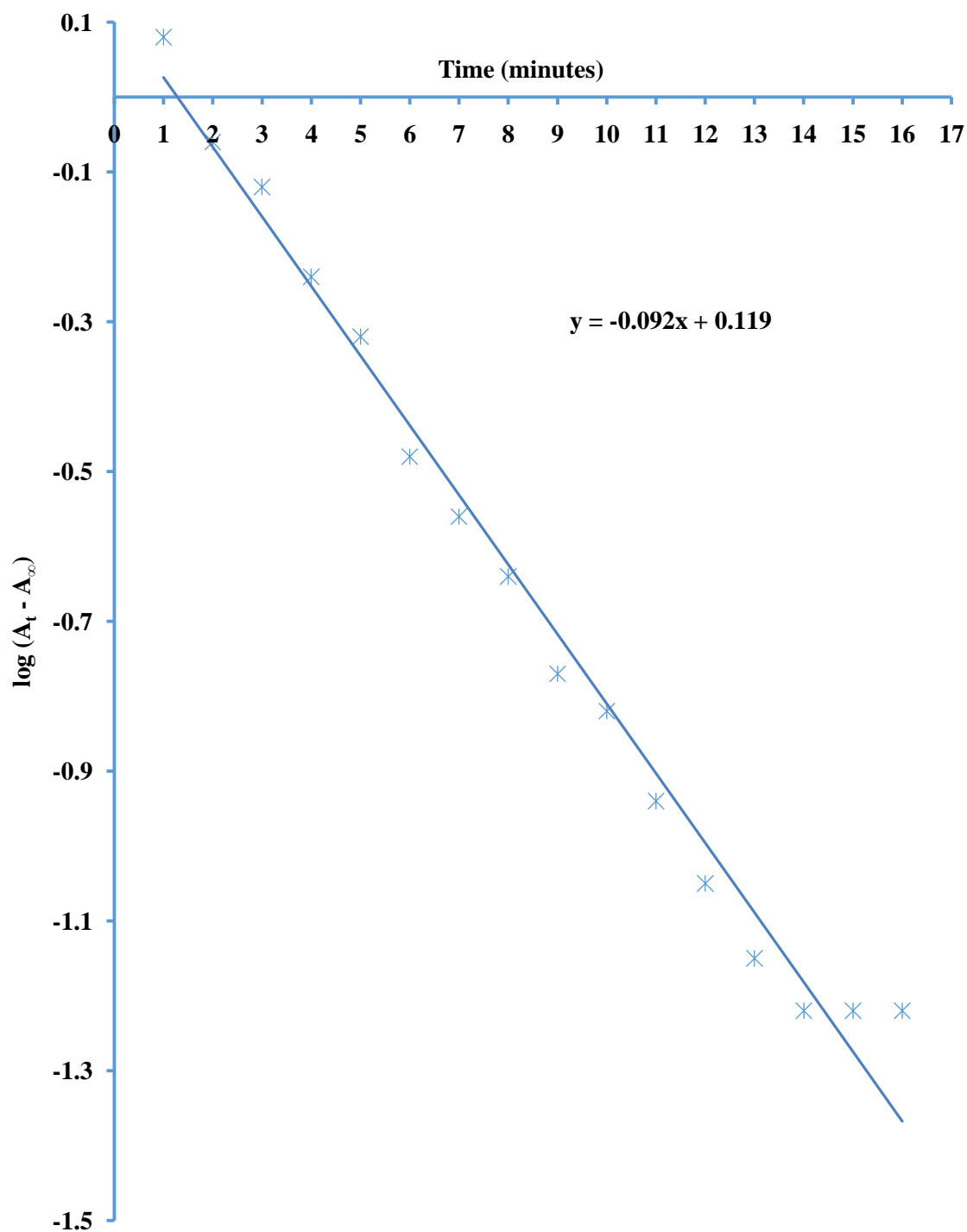


Figure 4.25: Typical Pseudo-first Order Plot for the Reaction of $[(\text{H}_2\text{O})_2\text{Ru}_2\text{O}]^{4+}$ and CH_3OH at $[(\text{H}_2\text{O})_2\text{Ru}_2\text{O}^{4+}] = 5.5 \times 10^{-5} \text{ mol dm}^{-3}$, $[\text{CH}_3\text{OH}] = 13.75 \times 10^{-2} \text{ mol dm}^{-3}$, $I = 0.5 \text{ mol dm}^{-3}$, $T = 31 \pm 1 \text{ }^\circ\text{C}$ and $\lambda_{\text{max}} = 660 \text{ nm}$

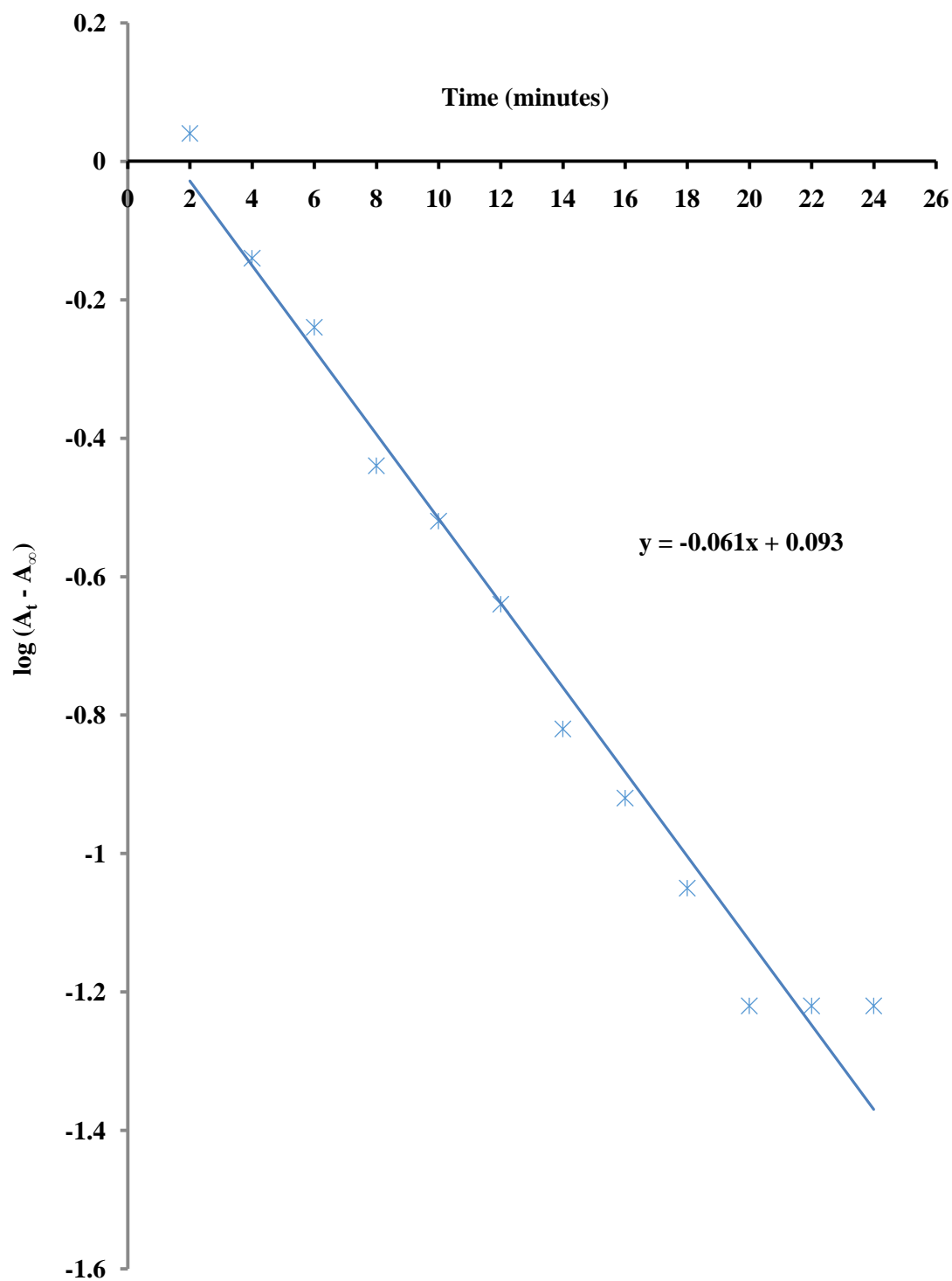


Figure 4.26: Typical Pseudo-first Order Plot for the Reaction of
 $[(\text{H}_2\text{O})_2\text{Ru}_2\text{O}]^{4+}$ and $\text{C}_2\text{H}_5\text{OH}$ at $[(\text{H}_2\text{O})_2\text{Ru}_2\text{O}^{4+}] = 6.5 \times 10^{-5}$
 mol dm^{-3} , $[\text{C}_2\text{H}_5\text{OH}] = 13.0 \times 10^{-2} \text{ mol dm}^{-3}$, $I = 0.5 \text{ mol dm}^{-3}$,
 $T = 31 \text{ } ^\circ\text{C}$ and $\lambda_{\text{max}} = 660 \text{ nm}$

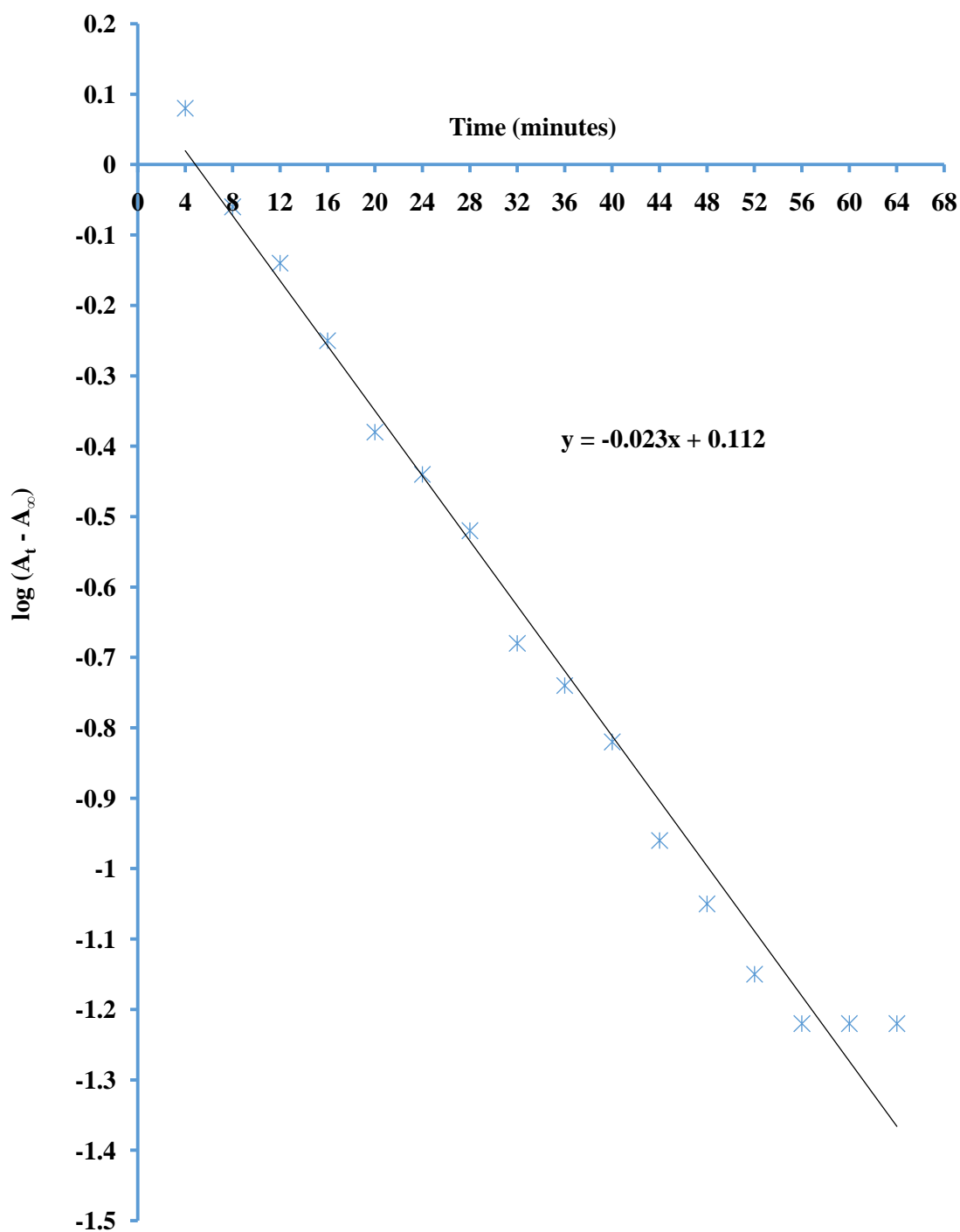


Figure 4.27: Typical Pseudo-first Order Plot for the Reaction of
 $[(\text{H}_2\text{O})_2\text{Ru}_2\text{O}]^{4+}$ and $\text{C}_3\text{H}_7\text{OH}$ at $[(\text{H}_2\text{O})_2\text{Ru}_2\text{O}^{4+}] = 6.0 \times 10^{-5}$
 mol dm^{-3} , $[\text{C}_3\text{H}_7\text{OH}] = 12.0 \times 10^{-2} \text{ mol dm}^{-3}$, $I = 0.5 \text{ mol dm}^{-3}$, T
 $= 31 \text{ } ^\circ\text{C}$ and $\lambda_{\text{max}} = 660 \text{ nm}$

Table 4.8: Pseudo-first Order and Second Order Rate Constants for the Reaction of $[(\text{H}_2\text{O})_2\text{Ru}_2\text{O}]^{4+}$ and CH_3OH at $[(\text{H}_2\text{O})_2\text{Ru}_2\text{O}^{4+}] = 5.50 \times 10^{-5} \text{ mol dm}^{-3}$, $I = 0.5 \text{ mol dm}^{-3}$ (NaClO_4), $T = 31 \pm 1^\circ\text{C}$ and $\lambda_{\text{max}} = 660 \text{ nm}$

$10^2 [\text{CH}_3\text{OH}]$, mol dm^{-3}	I , mol dm^{-3}	$10^4 k_{\text{obs}}$, s^{-1}	$10^3 k_2$, $\text{dm}^3 \text{mol}^{-1} \text{s}^{-1}$
5.50	0.5	6.60	12.01
8.25	0.5	9.87	11.96
11.00	0.5	13.19	11.99
13.75	0.5	16.55	12.04
16.50	0.5	19.85	12.03
19.25	0.5	23.08	11.99
22.00	0.5	26.41	12.00
24.75	0.5	29.82	12.05
16.50	0.1	19.77	11.98
16.50	0.2	19.86	11.04
16.50	0.3	19.85	12.03
16.50	0.4	19.82	12.01
16.50	0.5	19.87	12.04
16.50	0.6	19.82	12.00
16.50	0.7	19.77	11.98
16.50	0.8	19.87	12.04
16.50	0.9	19.83	12.02

Table 4.9: Pseudo-first Order and Second Order Rate Constants for the Reaction of $[(\text{H}_2\text{O})_2\text{Ru}_2\text{O}]^{4+}$ and $\text{C}_2\text{H}_5\text{OH}$ at $[(\text{H}_2\text{O})_2\text{Ru}_2\text{O}^{4+}] = 5.75 \times 10^{-5} \text{ mol dm}^{-3}$, $I = 0.5 \text{ mol dm}^{-3}$ (NaClO_4), $T = 31 \pm 1^\circ\text{C}$ and $\lambda_{\text{max}} = 660 \text{ nm}$

$10^2 [\text{C}_2\text{H}_5\text{OH}]$, mol dm^{-3}	I , mol dm^{-3}	$10^4 k_{\text{obs}}$, s^{-1}	$10^3 k_2$, $\text{dm}^3 \text{ mol}^{-1} \text{ s}^{-1}$
1.44	0.5	1.59	11.03
2.01	0.5	2.21	10.99
2.88	0.5	2.94	11.02
4.31	0.5	4.73	10.97
5.75	0.5	6.34	11.02
8.36	0.5	9.10	10.89
11.50	0.5	12.59	10.95
14.38	0.5	15.88	11.04
4.31	0.2	4.72	10.95
4.31	0.3	4.76	11.04
4.31	0.4	4.74	11.00
4.31	0.5	4.75	11.02
4.31	0.6	4.73	10.97
4.31	0.8	4.71	10.93
4.31	0.9	4.74	11.00
4.31	1.1	4.71	10.93

**Table 4.10 : Pseudo-first Order and Second Order Rate Constants for the
Reaction of $[(\text{H}_2\text{O})_2\text{Ru}_2\text{O}]^{4+}$ and $\text{C}_3\text{H}_7\text{OH}$ at $[(\text{H}_2\text{O})_2\text{Ru}_2\text{O}^{4+}] = 6.0 \times 10^{-5}$
 mol dm^{-3} , $I = 0.5 \text{ mol dm}^{-3}$ (NaClO_4), $T = 31 \pm 1^\circ\text{C}$ and $\lambda_{\text{max}} = 660 \text{ nm}$**

$10^2 [\text{C}_3\text{H}_7\text{OH}]$, mol dm^{-3}	I , mol dm^{-3}	$10^4 k_{\text{obs}}$, s^{-1}	$10^3 k_2$, $\text{dm}^3 \text{ mol}^{-1} \text{ s}^{-1}$
3.00	0.5	1.05	3.50
6.00	0.5	2.12	3.53
9.00	0.5	2.94	3.50
12.00	0.5	4.15	3.48
15.00	0.5	5.23	3.49
18.00	0.5	6.34	3.52
21.00	0.5	7.39	3.52
24.00	0.5	8.47	3.53
12.00	0.1	4.19	3.49
12.00	0.2	4.24	3.53
12.00	0.3	4.18	3.48
12.00	0.4	4.25	3.54
12.00	0.5	4.21	3.51
12.00	0.6	4.24	3.53
12.00	0.7	4.20	3.50
12.00	0.8	4.22	3.52
12.00	1.1	4.19	3.41

$\text{Ru}_2\text{O}^{4+}/\text{C}_2\text{H}_5\text{OH}$ system and 1.01 for the $\text{Ru}_2\text{O}^{4+}/\text{C}_3\text{H}_7\text{OH}$ system (Figures 4.28 – 4.30). These results suggest first order dependence with respect to [alcohol] for all the three systems. From the results obtained, the overall order of reaction for each of the reactions is second order. The rate equation for the reaction of Ru_2O^{4+} and the alcohols can be represented as Equation 4.14.

$$-\frac{d}{dt} [\text{Ru}_2\text{O}^{4+}] = k_2[\text{Ru}_2\text{O}^{4+}][\text{ROH}] \quad \dots \quad (4.14)$$

Where R = CH_3 , C_2H_5 and C_3H_7 and k_2 for the various dimer/ alcohol systems are as presented earlier in the report.

4.4 Effect of Changes in Hydrogen Ion Concentration, $[\text{H}^+]$, on Rates of Reaction

4.4.1: Ru_2O^{4+} reaction with thiourea and thiourea derivatives (*N*-methyl thiourea, *N,N'*-dimethylthiourea and *N*-allyl thiourea)

Within the hydrogen ion concentration $[\text{H}^+]$ range, $1.0 \times 10^{-2} \leq [\text{H}^+] \leq 10.0 \times 10^{-2} \text{ mol dm}^{-3}$, kinetic runs were carried out at constant ionic strength, while keeping oxidant and reductant concentrations constant. Inverse acid dependence was observed for this reaction at $I = 0.5 \text{ mol dm}^{-3}$ (NaClO_4), and $T = 31 \pm 1^\circ\text{C}$. The pseudo-first order and second order rate constants at increasing $[\text{H}^+]$, but constant $[\text{Ru}_2\text{O}^{4+}]$, [Reductant], I and T are presented in Tables 4.1 – 4.4. The plots of the hydrogen ion-dependent second order rate constants, $k_2(\text{H}^+)$ versus $[\text{H}^+]$ were linear with intercept for all the four systems under study (Figures 4.31 – 4.34). The dependence of rate constants on $[\text{H}^+]$ can be represented by Equation (4.15).

$$k_2[\text{H}^+] = a + b[\text{H}^+]^{-1} \quad \dots\dots\dots 4.15$$

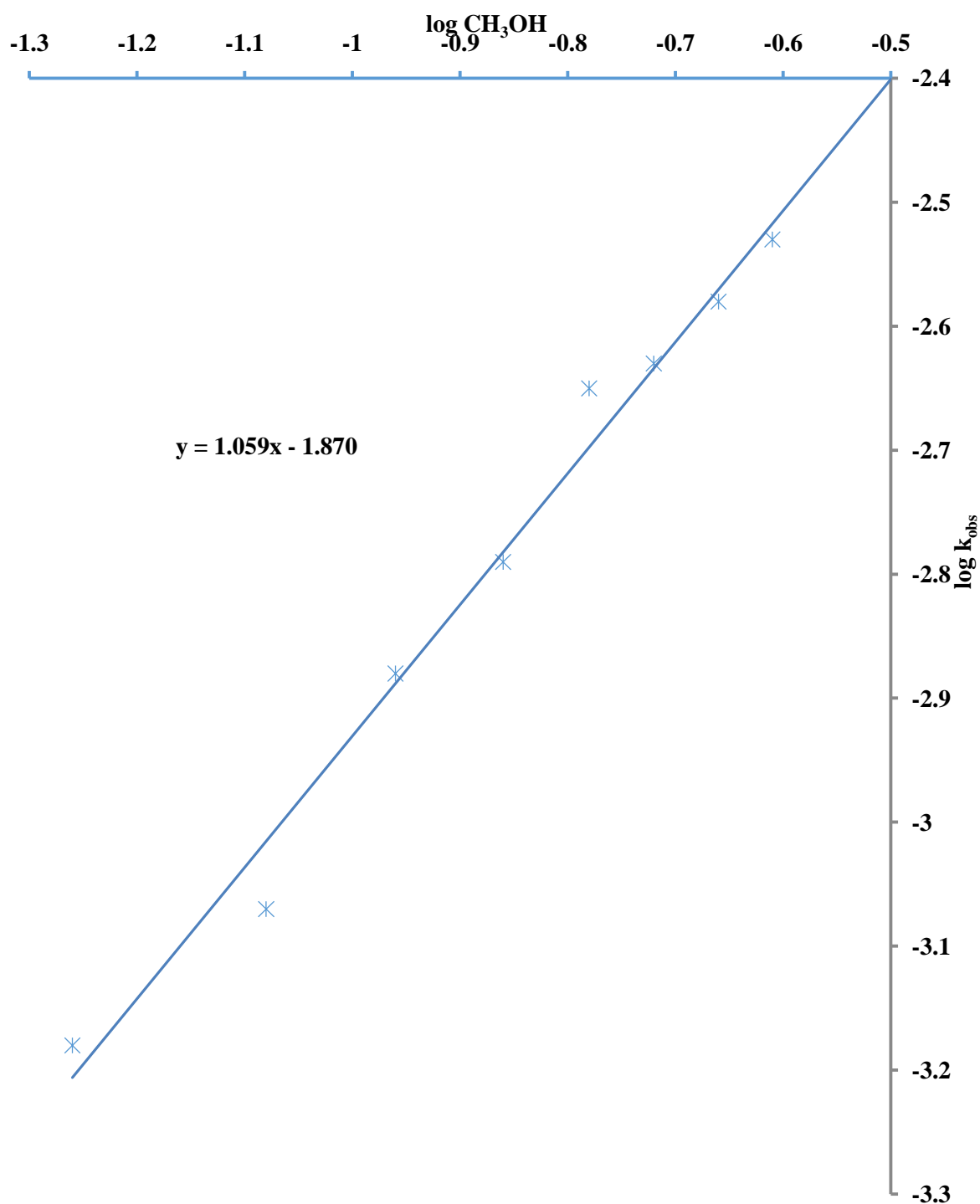


Figure 4.28: Plot of $\log k_{\text{obs}}$ against $\log [\text{CH}_3\text{OH}]$ for the Reaction of $[(\text{H}_2\text{O})_2\text{Ru}_2\text{O}]^{4+}$ and CH_3OH at $[(\text{H}_2\text{O})_2\text{Ru}_2\text{O}^{4+}] = 5.5 \times 10^{-5} \text{ mol dm}^{-3}$, $[\text{CH}_3\text{OH}] = (5.5 - 24.8) \times 10^{-2} \text{ mol dm}^{-3}$, $I = 0.5 \text{ mol dm}^{-3}$, $T = 31 \pm 1 \text{ C}$ and $\lambda_{\text{max}} = 660 \text{ nm}$

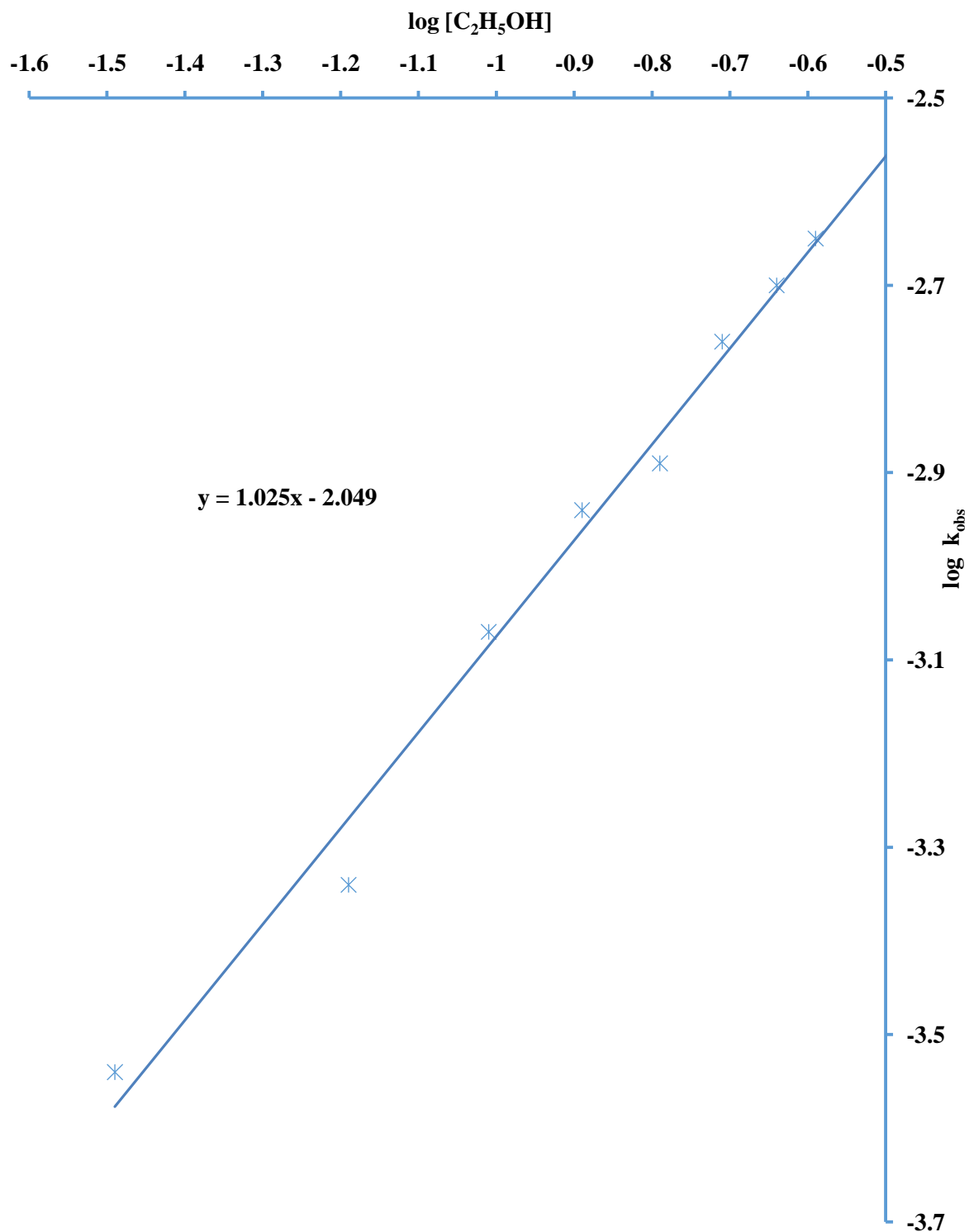


Fig 4.29: Plot of $\log k_{obs}$ against $\log [C_2H_5OH]$ for the Reaction of $[(H_2O)_2Ru_2O]^{4+}$ and C_2H_5OH at $[(H_2O)_2Ru_2O^{4+}] = 6.0 \times 10^{-5} \text{ mol dm}^{-3}$, $[C_2H_5OH] = (6.5 - 26.0) \times 10^{-2} \text{ mol dm}^{-3}$, $I = 0.5 \text{ mol dm}^{-3}$, $T = 31 \pm 1 \text{ C}$ and $\lambda_{max} = 660 \text{ nm}$

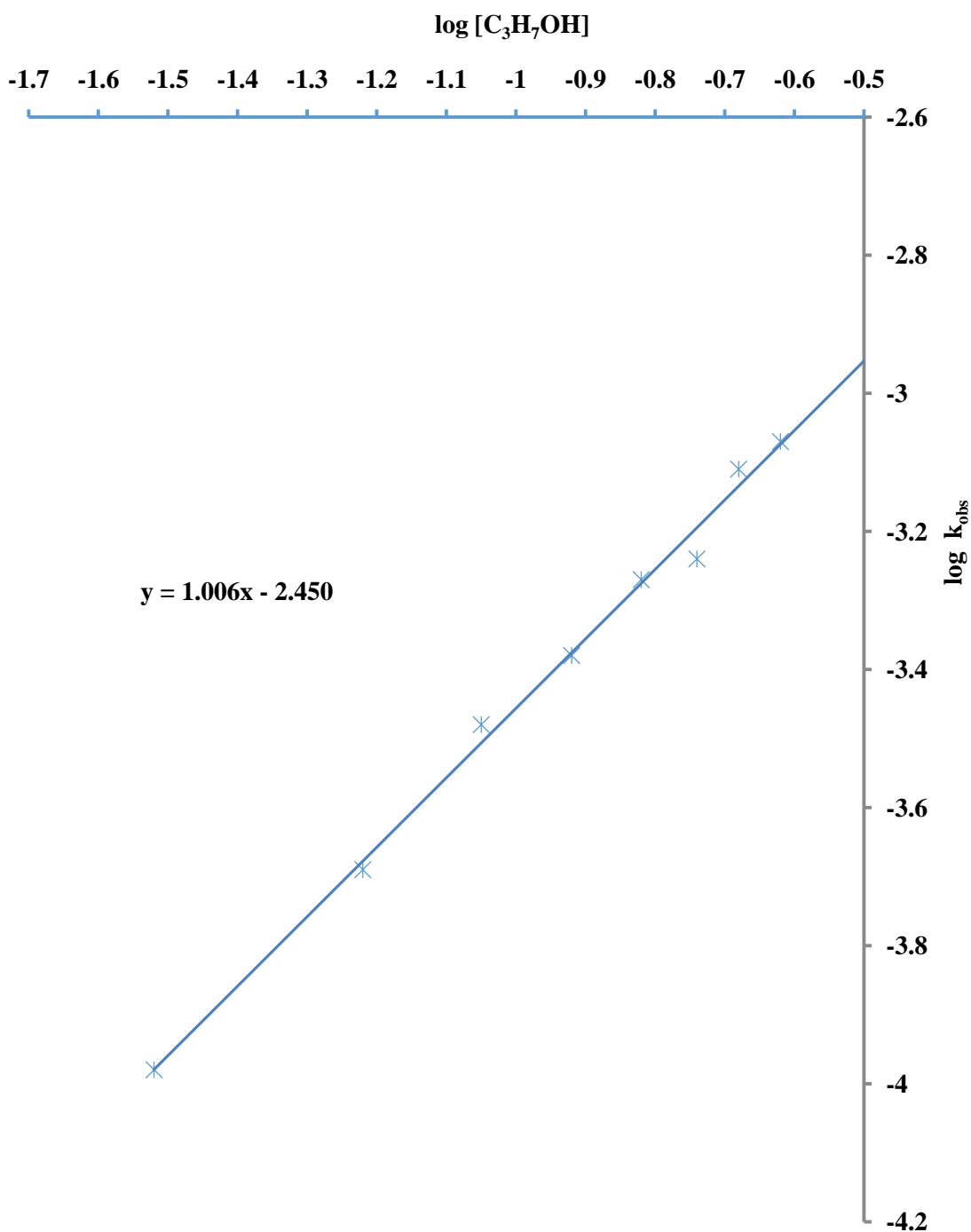


Fig 4.30: Plot of $\log k_{obs}$ against $\log [C_3H_7OH]$ for the Reaction of $[(H_2O)_2Ru_2O]^{4+}$ and C_3H_7OH at $[(H_2O)_2Ru_2O^{4+}] = 6.0 \times 10^{-5} \text{ mol dm}^{-3}$, $[C_3H_7OH] = (3.0 - 24.0) \times 10^{-2} \text{ mol dm}^{-3}$, $I = 0.5 \text{ mol dm}^{-3}$, $T = 31 \pm 1 \text{ C}$ and $\lambda_{max} = 660 \text{ nm}$

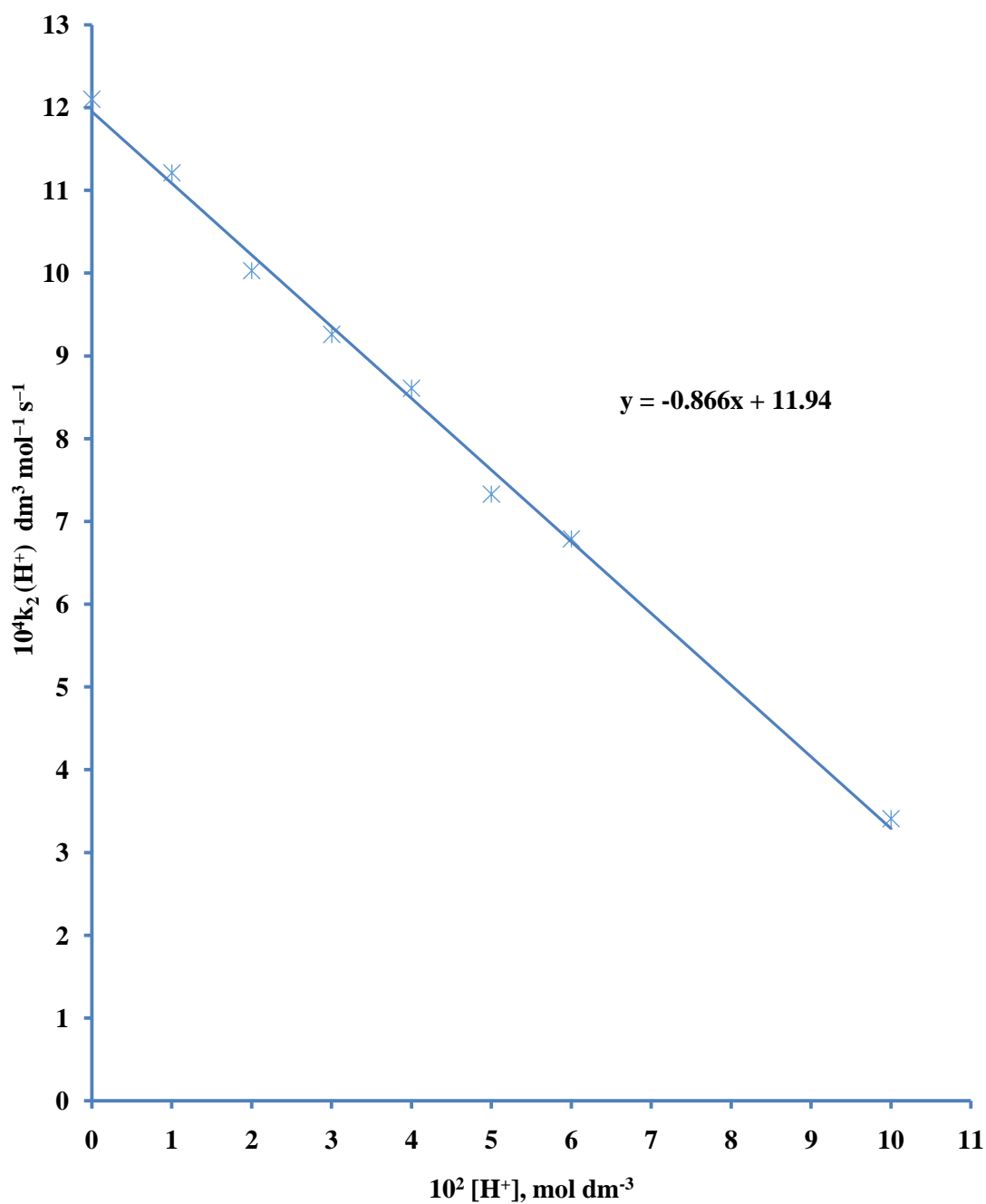


Fig 4.31: Plot of $k_2(H^+)$ against $[H^+]$ for the Reaction of $[(H_2O)_2Ru_2O]^{4+}$ and Thiourea (TU) at $[(H_2O)_2Ru_2O^{4+}] = 6.0 \times 10^{-5} \text{ mol dm}^{-3}$, $[TU] = 12.0 \times 10^{-2} \text{ mol dm}^{-3}$, $[H^+] = (1.0 - 10.0) \times 10^{-2} \text{ mol dm}^{-3}$, $I = 0.5 \text{ mol dm}^{-3}$, $T = 31 \text{ } ^\circ\text{C}$ and $\lambda_{\text{max}} = 660 \text{ nm}$

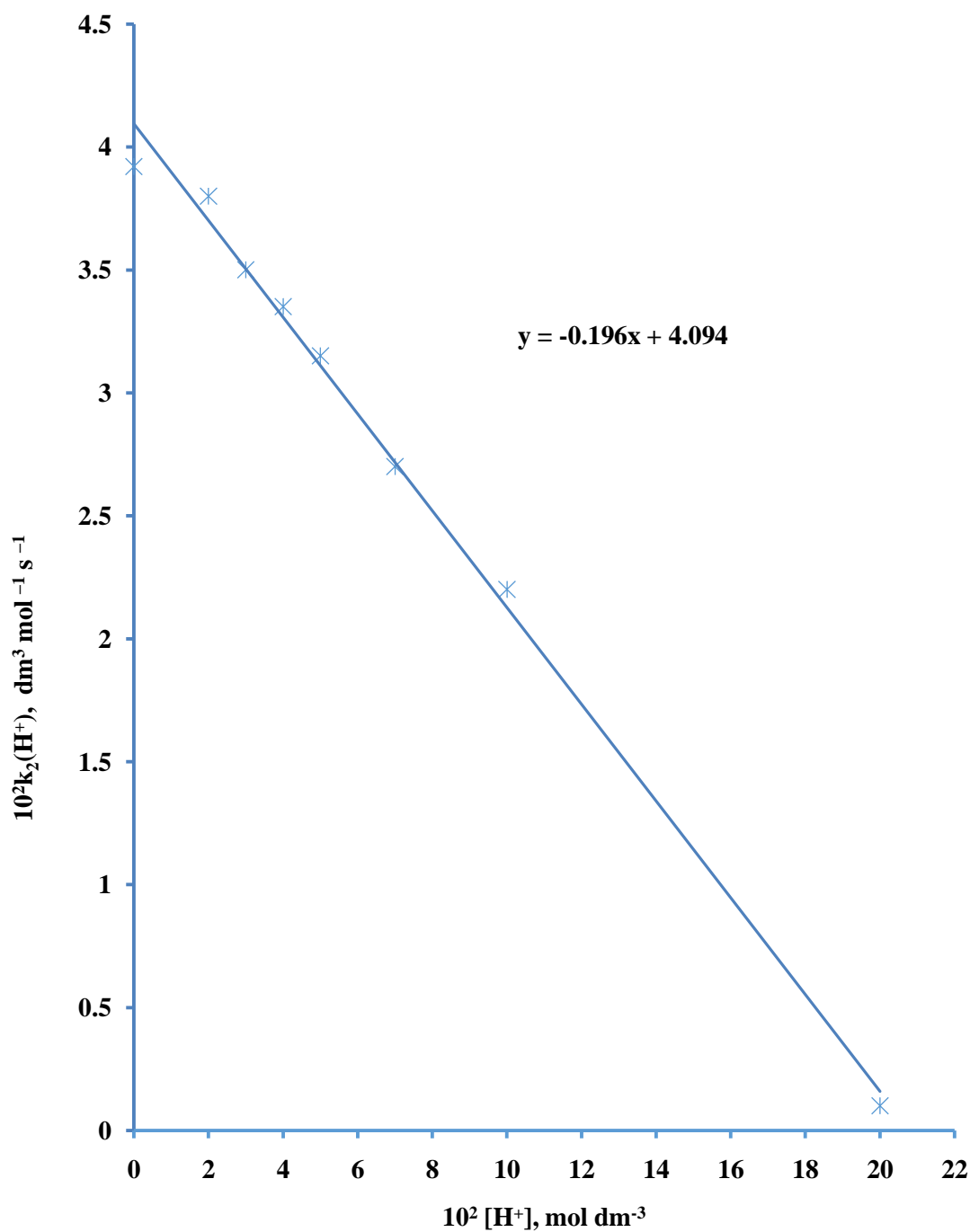


Figure 4.32: Plot of $k_2(H^+)$ against $[H^+]$ for the Reaction of $[(H_2O)_2Ru_2O]^{4+}$ and *N*-methylthiourea (MTU) at $[(H_2O)_2Ru_2O^{4+}] = 6.5 \times 10^{-5} \text{ mol dm}^{-3}$, $[MTU] = 5.2 \times 10^{-2} \text{ mol dm}^{-3}$, $[H^+] = (2.0 - 20.0) \times 10^{-2} \text{ mol dm}^{-3}$, $I = 0.5 \text{ mol dm}^{-3}$, $T = 31 \pm 1 \text{ } ^\circ\text{C}$ and $\lambda_{\text{max}} = 660 \text{ nm}$

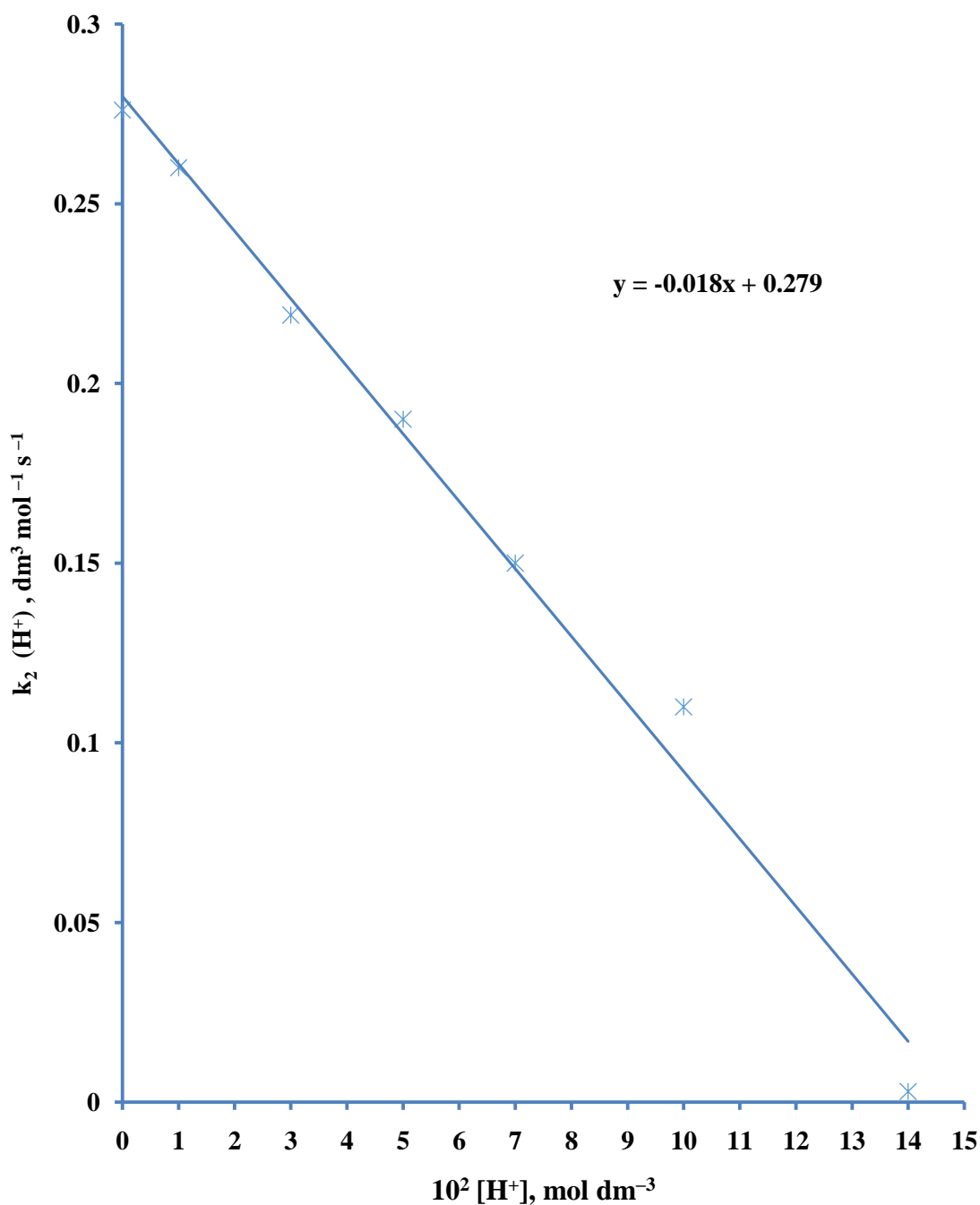


Figure 4.33: Plot of $k_2[\text{H}^+]$ against $[\text{H}^+]$ for the Reaction of $[(\text{H}_2\text{O})_2\text{Ru}_2\text{O}]^{4+}$ and *N*-Allylthiourea (ATU) at $[(\text{H}_2\text{O})_2\text{Ru}_2\text{O}^{4+}] = 5.75 \times 10^{-5} \text{ mol dm}^{-3}$, $[\text{ATU}] = 3.45 \times 10^{-2} \text{ mol dm}^{-3}$, $[\text{H}^+] = (1.0 - 14.0) \times 10^{-2} \text{ mol dm}^{-3}$, $I = 0.5 \text{ mol dm}^{-3}$, $T = 31 \pm 1 \text{ }^\circ\text{C}$ and $\lambda_{\text{max}} = 660 \text{ nm}$

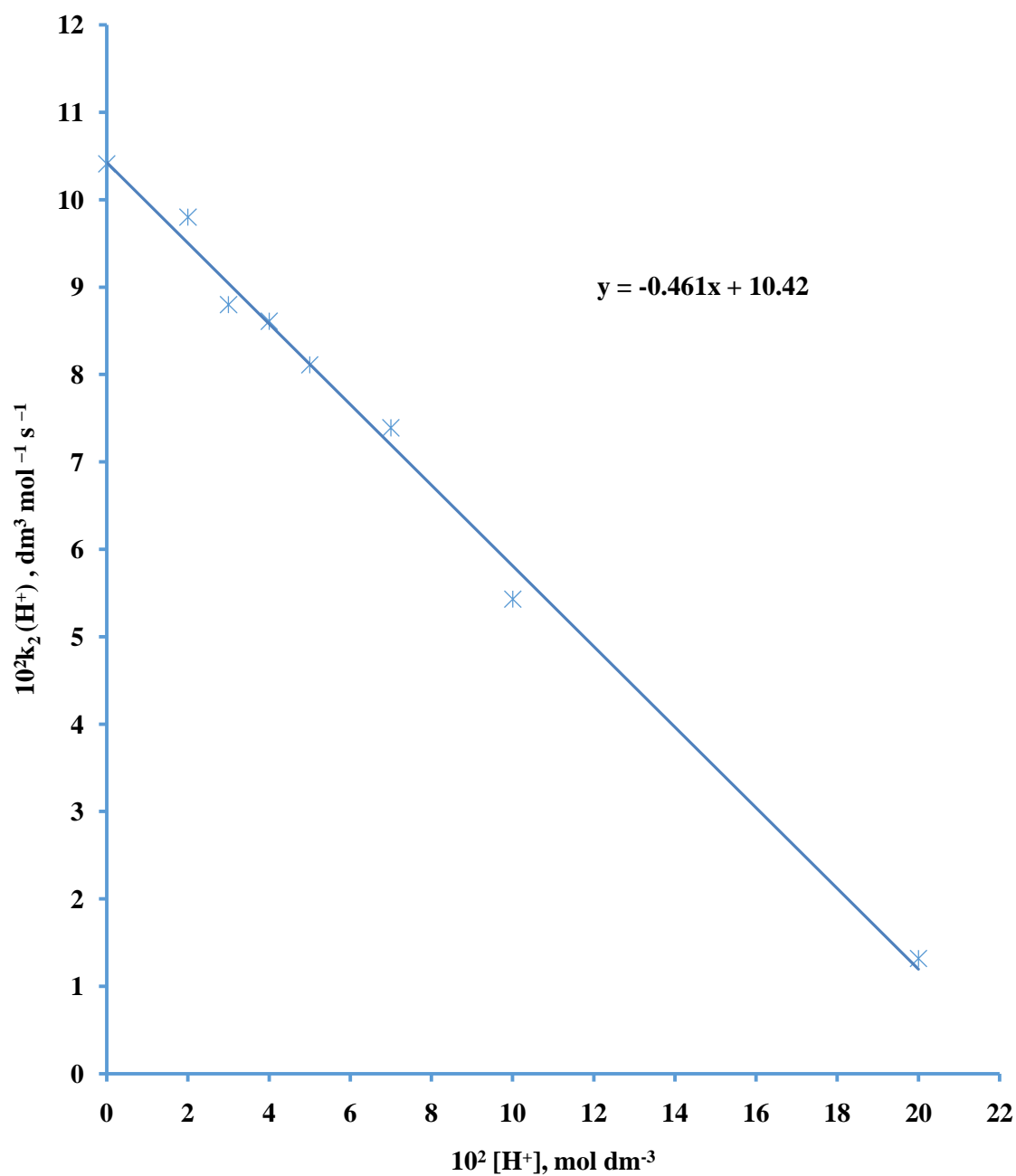


Fig 4.34: Plot of $k_2(H^+)$ against $[H^+]$ for the Reaction of $[(H_2O)_2Ru_2O]^{4+}$ and *N,N'*-dimethylthiourea (DMTU) at $[(H_2O)_2Ru_2O^{4+}] = 7.0 \times 10^{-5} \text{ mol dm}^{-3}$, $[DMTU] = 5.6 \times 10^{-2} \text{ mol dm}^{-3}$, $[H^+] = (2.0 - 20.0) \times 10^{-2} \text{ mol dm}^{-3}$, $I = 0.5 \text{ mol dm}^{-3}$, $T = 31 \pm 1 \text{ }^\circ\text{C}$ and $\lambda_{\text{max}} = 660 \text{ nm}$

where for: Ru_2O^{4+} / TU system, intercept = 'a' = $11.95 \times 10^{-4} \text{ dm}^3 \text{ mol}^{-1} \text{ s}^{-1}$ and

$$\text{slope} = \text{'b'} = -0.87 \text{ dm}^6 \text{ mol}^{-2} \text{ s}^{-1}$$

Ru_2O^{4+} / MTU system, intercept = 'a' = $4.09 \times 10^{-2} \text{ dm}^3 \text{ mol}^{-2} \text{ s}^{-1}$ and

$$\text{slope} = \text{'b'} = -2.01 \text{ dm}^6 \text{ mol}^{-2} \text{ s}^{-1}$$

Ru_2O^{4+} / ATU system, intercept = 'a' = $0.28 \text{ dm}^3 \text{ mol}^{-2} \text{ s}^{-1}$ and

$$\text{slope} = \text{'b'} = -1.88 \text{ dm}^6 \text{ mol}^{-2} \text{ s}^{-1}$$

Ru_2O^{4+} / DMTU system, intercept = 'a' = $10.43 \times 10^{-2} \text{ dm}^3 \text{ mol}^{-1} \text{ s}^{-1}$ and

$$\text{slope} = \text{'b'} = -0.46 \text{ dm}^6 \text{ mol}^{-2} \text{ s}^{-1}$$

The overall rate equation for the Ru_2O^{4+} / reductant systems under discussion in this section can be represented by Equation 4.16,

$$-\frac{d}{dt} [\text{Ru}_2\text{O}^{4+}] = (a + b[\text{H}^+]^{-1})[\text{Ru}_2\text{O}^{4+}][\text{TSH}] \quad \text{..... (4.16)}$$

where TSH refers to TU, MTU, ATU and DMTU and the values of 'a' and 'b' have been indicated earlier in the text.

4.4.2 Ru_2O^{4+} reaction with $\text{S}_2\text{O}_3^{2-}$

Within the acid range $2 \times 10^{-2} \leq [\text{H}^+] \leq 20 \times 10^{-2} \text{ mol dm}^{-3}$, the reduction of the ruthenium dimer by $\text{S}_2\text{O}_3^{2-}$, keeping $[\text{Ru}_2\text{O}^{4+}]$, $[\text{S}_2\text{O}_3^{2-}]$, I and T constant, indicated an increase in rate with increase in $[\text{H}^+]$. The effect of increase in $[\text{H}^+]$ on the rate constants for the reaction of Ru_2O^{4+} and $\text{S}_2\text{O}_3^{2-}$ is presented in Table 4.5. Plot of acid-dependent second order rate constants, $k_2(\text{H}^+)$ versus $[\text{H}^+]$ was linear with a slope of $6.90 \text{ dm}^6 \text{ mol}^{-2} \text{ s}^{-1}$ and intercept of $5.14 \times 10^{-3} \text{ dm}^3 \text{ mol}^{-1} \text{ s}^{-1}$ (Figure 4.35). The order of reaction with respect to $[\text{H}^+]$ was obtained by plotting $\log k_{\text{obs}}$ versus $\log [\text{H}^+]$ (Figure 4.36). The plot was linear with a slope of 0.92, suggesting a first order dependence on $[\text{H}^+]$. The overall rate equation for Ru_2O^{4+} / $\text{S}_2\text{O}_3^{2-}$ system can be represented by Equation 4.17.

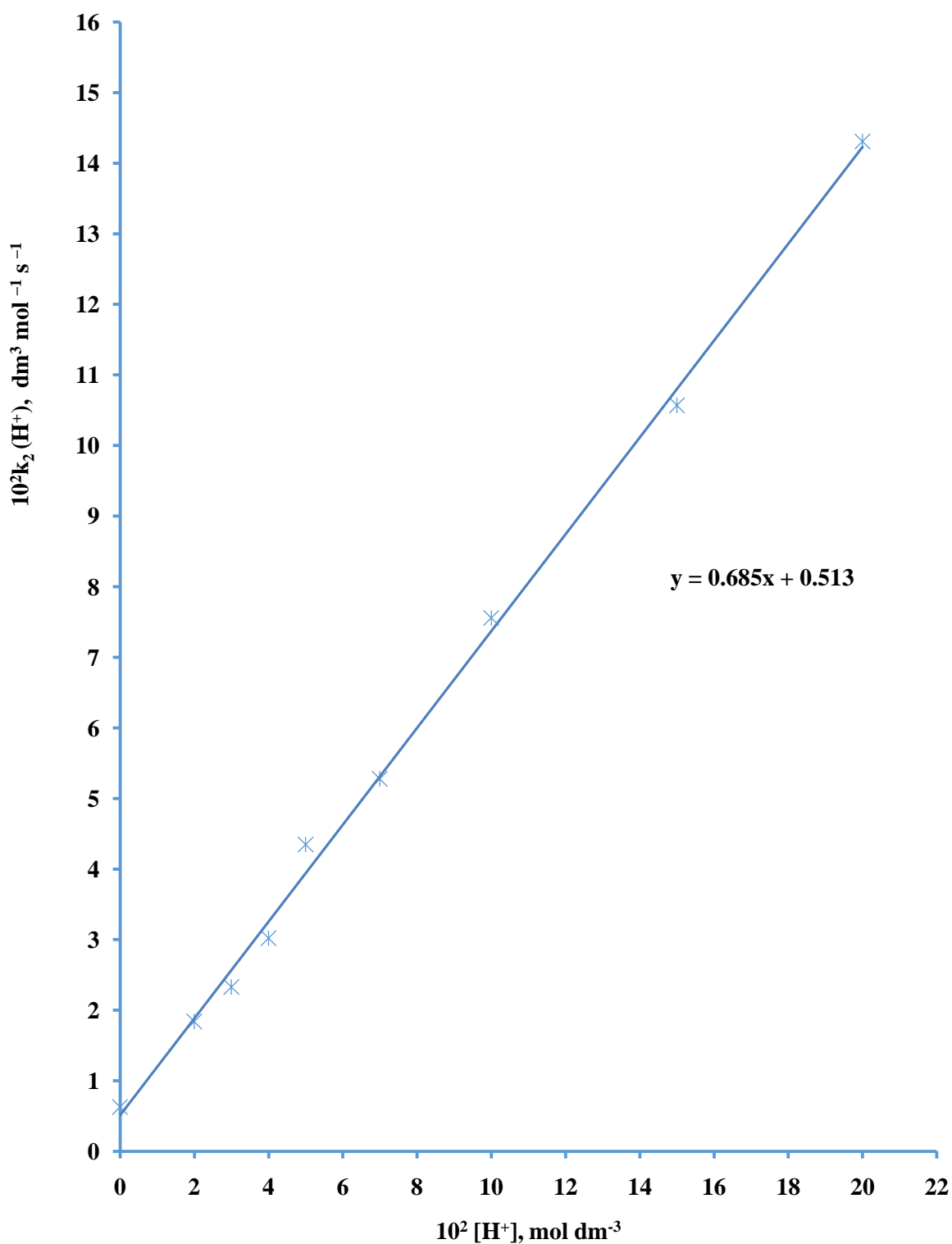


Fig 4.35: Plot of $k_2(H^+)$ against $[H^+]$ for the Reaction of $[(H_2O)_2Ru_2O]^{4+}$ and $S_2O_3^{2-}$ at $[(H_2O)_2Ru_2O^{4+}] = 6.5 \times 10^{-5} \text{ mol dm}^{-3}$, $[S_2O_3^{2-}] = 13.0 \times 10^{-2} \text{ mol dm}^{-3}$, $[H^+] = (2.0 - 20.0) \times 10^{-2} \text{ mol dm}^{-3}$, $I = 0.5 \text{ mol dm}^{-3}$, $T = 321 \text{ K}$ and $\lambda_{\text{max}} = 660 \text{ nm}$

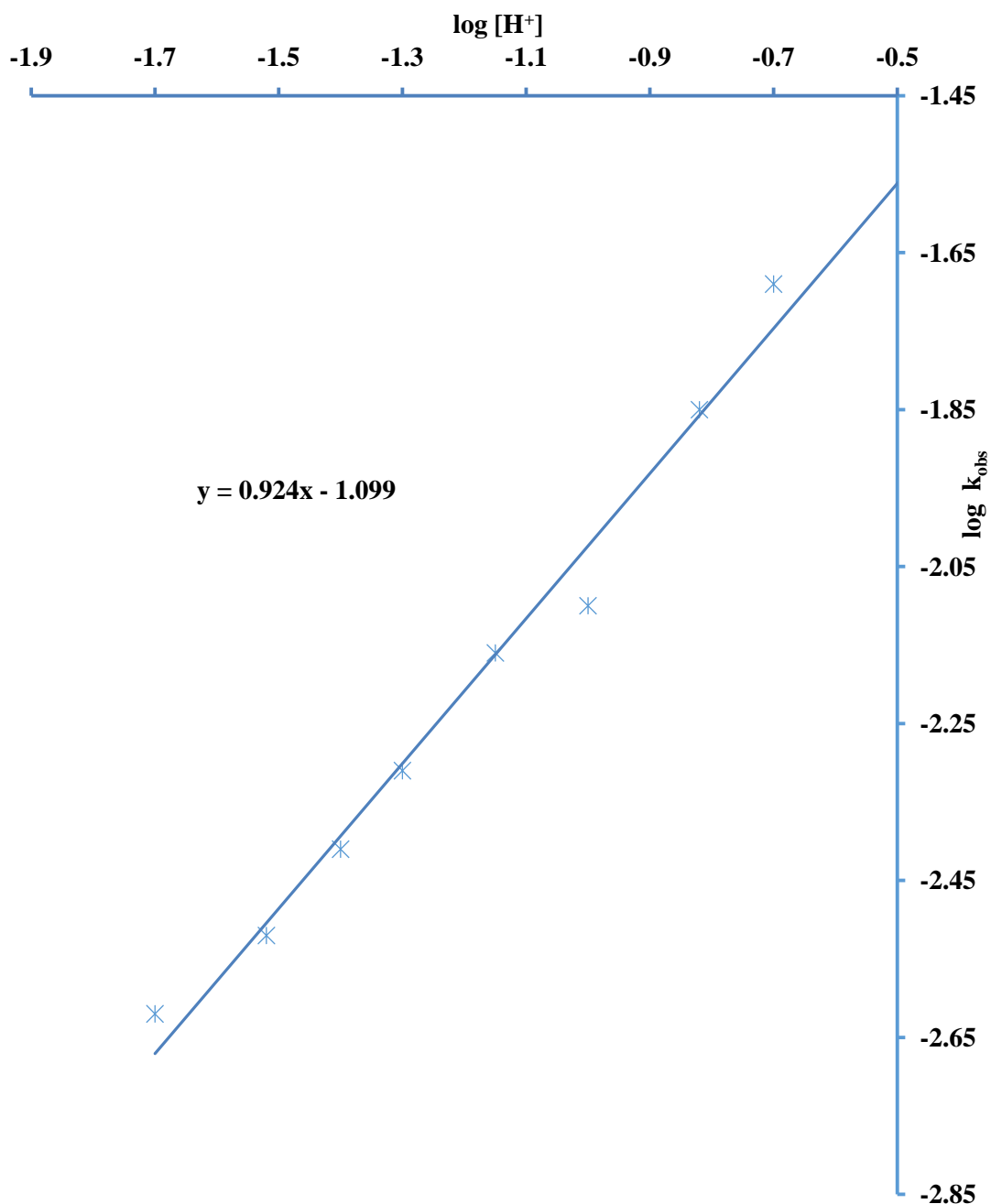


Fig 4.36: Plot of $\log k_{\text{obs}}$ against $\log [H^+]$ for the Reaction of $[(H_2O)_2Ru_2O]^{4+}$ and $S_2O_3^{2-}$ at $[(H_2O)_2Ru_2O^{4+}] = 6.5 \times 10^{-5} \text{ mol dm}^{-3}$, $[S_2O_3^{2-}] = 5.2 \times 10^{-2} \text{ mol dm}^{-3}$, $[H^+] = (2.0 - 20.0) \times 10^{-2} \text{ mol dm}^{-3}$, $I = 0.5 \text{ mol dm}^{-3}$, $T = 31 \pm 1 \text{ C}$ and $\lambda_{\text{max}} = 660 \text{ nm}$

$$-\frac{d}{dt}[\text{Ru}_2\text{O}^{4+}] = (a + b[\text{H}^+])[\text{Ru}_2\text{O}^{4+}][\text{S}_2\text{O}_3^{2-}] \dots\dots (4.17)$$

where values of 'a' and 'b' have been reported earlier.

4.4.3 Ru_2O^{4+} reaction with hypophosphorous acid (H_3PO_2)

For the $\text{Ru}_2\text{O}^{4+}/\text{H}_3\text{PO}_2$ system, the rate constants were not markedly affected by increase in $[\text{H}^+]$ in the acid range $2.0 \times 10^{-2} \leq [\text{H}^+] \leq 20.0 \times 10^{-2} \text{ mol dm}^{-3}$ (Table 4.7).

4.5 Effect of Changes of Ionic Strength of Reaction Medium

4.5.1 Ru_2O^{4+} reaction with thiourea and thiourea derivatives (TU, MTU, ATU

DMTU

Within the range of ionic strength of the media $0.1 \leq I \leq 0.9 \text{ mol dm}^{-3}$ (NaClO_4), effect of changes in I on the reaction rates was investigated for the reaction of Ru_2O^{4+} with thiourea (TU) and some of its derivatives (MTU, ATU and DMTU). At $T = 31 \pm 1^\circ \text{C}$, $[\text{H}^+] = 5 \times 10^{-2} \text{ mol dm}^{-3}$ and maintaining $[\text{Ru}_2\text{O}^{4+}]$ and [reductant] constant, the rate of reaction was not markedly affected by changes in ionic strength. Pseudo-first order, k_{obs} , and second order rate constants, k_2 , remained fairly constant and results are presented in Tables 4.1 – 4.4.

4.5.2 Ru_2O^{4+} reaction with $\text{S}_2\text{O}_3^{2-}$

For the reaction of Ru_2O^{4+} and $\text{S}_2\text{O}_3^{2-}$ studied between the ionic strength 0.2 and 0.8 mol dm^{-3} (NaClO_4), keeping other parameters such as $[\text{H}^+]$, [reductant], [oxidant] and T constant, the rate constants under these conditions were found to decrease as the ionic strength of the medium was increased (Table 4.5). A plot of $\log k_2$ versus \sqrt{I} for this

system was linear with a negative slope of -2.81 , indicating that the product of the charges on the reactants in at least one of the rate determining steps is ≈ 3 (Figure 4.37).

4.5.3 Ru_2O^{4+} reaction with $\text{S}_2\text{O}_4^{2-}$

Within the range of ionic strength $0.2 \leq I \leq 1.1 \text{ mol dm}^{-3}$, the rates of reaction of Ru_2O^{4+} and $\text{S}_2\text{O}_4^{2-}$ was monitored keeping [oxidant], [reductant], I and T constant. Under this condition, it was observed that the rates of reaction remained fairly constant (Table 4.6).

4.5.4 Ru_2O^{4+} reaction with H_3PO_2 , CH_3OH , $\text{C}_2\text{H}_5\text{OH}$ and $\text{C}_3\text{H}_7\text{OH}$

Reactions of Ru_2O^{4+} with H_3PO_2 , CH_3OH , $\text{C}_2\text{H}_5\text{OH}$ and $\text{C}_3\text{H}_7\text{OH}$ were studied in a medium with ionic strength ranging between 0.1 mol dm^{-3} and 1.0 mol dm^{-3} at $T = 31 \pm 1 \text{ }^\circ\text{C}$ and $[\text{H}^+] = 5 \times 10^{-2} \text{ mol dm}^{-3}$ (HClO_4). Maintaining the oxidant and reductant concentrations constant for all the runs, the reaction rate was found to be unaffected by the variation in ionic strength of the medium. Consequently, k_2 remained constant (Tables 4.7 – 4.10).

4.6 Effect of Changes in Dielectric Constant of Reaction Medium on Rate

4.6.1 Ru_2O^{4+} reaction with the thioureas

The effect of changes in the dielectric constant (D) of the reaction medium on the rates of the reactions of Ru_2O^{4+} and the thioureas was investigated at constant [oxidant], [reductant], $[\text{H}^+]$ and I of the medium and T of reaction but varying the dielectric constant of the medium using acetone-water mixture. Decreasing the dielectric constant from $81 - 71$ ($\text{CH}_3\text{COCH}_3/\text{H}_2\text{O}$) had no effect on k_{obs} , and consequently k_2 of the

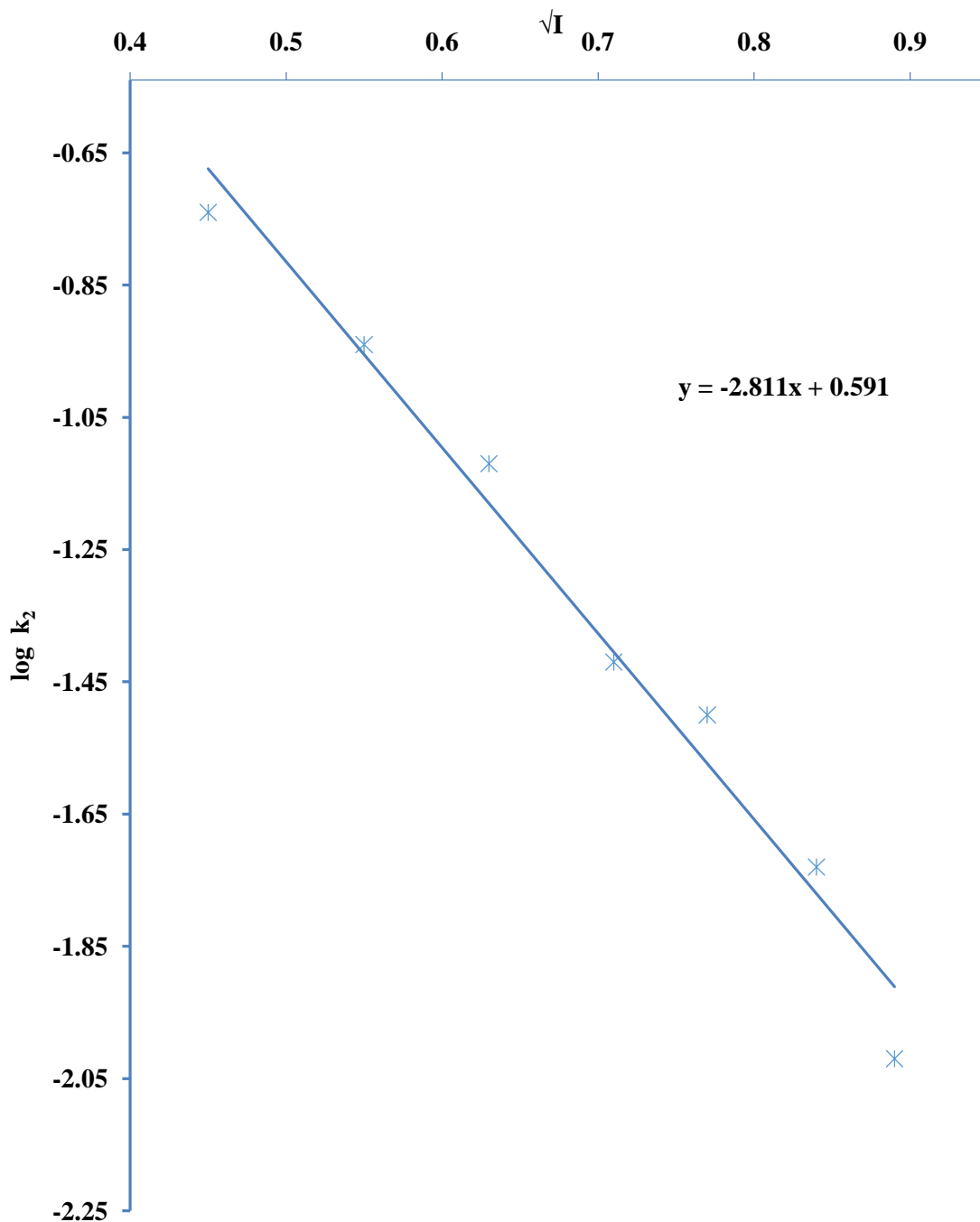


Figure 4.37: Plot of $\log k_2$ versus \sqrt{I} for the Reaction of $[(H_2O)_2Ru_2O]^{4+}$ and $S_2O_3^{2-}$ at $[(H_2O)_2Ru_2O^{4+}] = 6.5 \times 10^{-5} \text{ mol dm}^{-3}$, $[S_2O_3^{2-}] = 13.0 \times 10^{-2} \text{ mol dm}^{-3}$, $[H^+] = 5.0 \times 10^{-2} \text{ mol dm}^{-3}$, $I = (0.2 - 0.8) \times 10^{-3} \text{ mol dm}^{-3}$, $T = 321 \pm 1 \text{ C}$ and $\lambda_{\text{max}} = 660 \text{ nm}$

reactions (Tables 4.11 – 4.14). The effect of dielectric constant (D) on the rate constant, k_2 , for ion-ion interactions is given by Equation 4.18:

$$\ln k_2 = \ln k_0 - \frac{Z_a Z_b e^2 R_{ab}}{2.303 \kappa T D} \quad \dots(4.18)$$

Where k_2 = second order rate constant,

k_0 = specific rate constant at zero ionic strength and infinite dielectric constant,

Z_a and Z_b = valencies of ions 'a' and 'b'.

K = Boltzmann constant,

T = temperature

E = charge on the electron.

R_{ab} = radius of the activated complex.

Equation 4.18 predicts that, at a constant temperature, the logarithm of the rate constant is inversely proportional to the dielectric constant of the medium and that the slope of the plot is proportional to the size of the activated complex (Zaidi, 1991).

4.6.2 Ru_2O^{4+} reaction with $\text{S}_2\text{O}_3^{2-}$

The reduction of Ru_2O^{4+} by $\text{S}_2\text{O}_3^{2-}$ at ionic strength of 0.5 mol dm^{-3} (NaClO_4), $[\text{H}^+] = 5 \times 10^{-2} \text{ mol dm}^{-3}$ and $T = 31 \pm 1^\circ\text{C}$ showed an increase in rate as dielectric constant was reduced from 81.00 to 70.20 ($\text{CH}_3\text{COCH}_3/\text{H}_2\text{O}$). The various k_{obs} and the second order rate constants are displayed in Table (4.15). Plot of $\log k_2$ versus $1/D$ is linear with a positive slope (Figure 4.38).

Table 4.11: Effect of Changes in the Dielectric Constant of Reaction Medium for the Reaction of $[(\text{H}_2\text{O})_2\text{Ru}_2\text{O}]^{4+}$ and Thiourea (TU) at $[(\text{H}_2\text{O})_2\text{Ru}_2\text{O}^{4+}] = 6.0 \times 10^{-5} \text{ mol dm}^{-3}$, $[\text{TU}] = 12.0 \times 10^{-2} \text{ mol dm}^{-3}$, $[\text{H}^+] = 5 \times 10^{-2} \text{ mol dm}^{-3}$, $I = 0.5 \text{ mol dm}^{-3}$ (NaClO_4), $D = (81.0 - 70.2)$, $\lambda_{\text{max}} = 660 \text{ nm}$ and $T = 31 \pm 1^\circ\text{C}$;

D	$10^4 k_{\text{obs}}, \text{s}^{-1}$	$10^3 k_2, \text{dm}^3 \text{mol}^{-1} \text{s}^{-1}$
81.0	8.88	7.40
79.8	8.71	7.26
78.6	8.87	7.39
77.4	8.92	7.43
75.0	8.85	7.38
72.6	8.89	7.41
71.4	8.81	7.34
70.2	8.86	7.38

Table 4.12 : Effect of Changes in the Dielectric Constant of Reaction Medium for the Reaction of $[(\text{H}_2\text{O})_2\text{Ru}_2\text{O}]^{4+}$ and *N*-methylthiourea (MTU) at $[(\text{H}_2\text{O})_2\text{Ru}_2\text{O}^{4+}] = 6.5 \times 10^{-5} \text{ mol dm}^{-3}$, $[\text{S}_2\text{O}_3^{2-}] = 5.2 \times 10^{-2} \text{ mol dm}^{-3}$, $[\text{H}^+] = 5 \times 10^{-2} \text{ mol d}^{-3}$, $I = 0.5 \text{ mol dm}^{-3}$ (NaClO_4), $D = (81.0 - 70.2)$, $T = 31 \pm 1^\circ\text{C}$ and $\lambda_{\text{max}} = 660 \text{ nm}$

D	$10^4 k_{\text{obs}}, \text{ s}^{-1}$	$10^2 k_2, \text{ dm}^3 \text{ mol}^{-1} \text{ s}^{-1}$
81.0	16.30	3.14
79.8	16.43	3.16
78.6	16.07	3.09
77.4	16.38	3.15
75.0	16.28	3.13
72.6	15.86	3.05
71.4	16.29	3.13
70.2	16.36	3.15

Table 4.13: Effect of Changes in the Dielectric Constant of Reaction Medium for the Reaction of $[(\text{H}_2\text{O})_2\text{Ru}_2\text{O}]^{4+}$ and *N*-allylthiourea (ATU) at $[(\text{H}_2\text{O})_2\text{Ru}_2\text{O}^{4+}] = 5.75 \times 10^{-5} \text{ mol dm}^{-3}$, $[\text{ATU}] = 3.45 \times 10^{-2} \text{ mol dm}^{-3}$, $[\text{H}^+] = 5 \times 10^{-2} \text{ mol dm}^{-3}$, $I = 0.5 \text{ mol dm}^{-3}$ (NaClO_4), $D = (81.0 - 70.2)$, $T = 31 \pm 1^\circ\text{C}$ and $\lambda_{\text{max}} = 660 \text{ nm}$

D	$10^3 k_{\text{obs}}, \text{ s}^{-1}$	$k_2, \text{ dm}^3 \text{ mol}^{-1} \text{ s}^{-1}$
81.0	6.14	0.18
79.8	7.25	0.21
78.6	6.54	0.19
77.4	7.60	0.22
75.0	6.97	0.20
72.6	6.62	0.19
71.4	6.78	0.20
70.2	6.94	0.20

Table 4.14: Effect of Changes in the Dielectric Constant of Reaction Medium for the Reaction of $[(\text{H}_2\text{O})_2\text{Ru}_2\text{O}]^{4+}$ and *N, N'*-dimethylthiourea (DMTU) at $[(\text{H}_2\text{O})_2\text{Ru}_2\text{O}^{4+}] = 7.0 \times 10^{-5} \text{ mol dm}^{-3}$, $[\text{DMTU}] = 5.6 \times 10^{-2} \text{ mol dm}^{-3}$, $I = 0.5 \text{ mol dm}^{-3}$ (NaClO_4), $D = (81.0 - 69)$, $T = 31 \pm 1^\circ\text{C}$ and $\lambda_{\text{max}} = 660 \text{ nm}$

D	$10^3 k_{\text{obs}}, \text{ s}^{-1}$	$10^2 k_2, \text{ dm}^3 \text{ mol}^{-1} \text{ s}^{-1}$
81.0	4.54	8.11
79.2	4.55	8.13
78.0	4.52	8.07
76.8	4.55	8.13
75.6	4.54	8.11
74.4	4.53	8.09
72.0	4.54	8.11
69.0	4.55	8.13

Table 4.15: Effect of Changes in the Dielectric Constant of Reaction Medium for the Reaction of $[(\text{H}_2\text{O})_2\text{Ru}_2\text{O}]^{4+}$ and $\text{S}_2\text{O}_3^{2-}$ at $[(\text{H}_2\text{O})_2\text{Ru}_2\text{O}^{4+}] = 6.5 \times 10^{-5} \text{ mol dm}^{-3}$, $[\text{S}_2\text{O}_3^{2-}] = 1.3 \times 10^{-2} \text{ mol dm}^{-3}$, $[\text{H}^+] = 5 \times 10^{-2} \text{ mol dm}^{-3}$, $I = 0.5 \text{ mol dm}^{-3}$ (NaClO_4), $D = (81.0 - 70.2)$, $T = 31 \pm 1^\circ\text{C}$ and $\lambda_{\text{max}} = 660 \text{ nm}$

D	$10^4 k_{\text{obs}}, \text{ s}^{-1}$	$10^2 k_2, \text{ dm}^3 \text{ mol}^{-1} \text{ s}^{-1}$
81.0	4.88	3.75
79.8	5.04	3.88
78.6	5.67	4.36
77.4	5.93	4.56
75.0	6.79	5.22
72.6	8.39	6.45
71.4	9.01	6.93
70.2	9.80	7.54

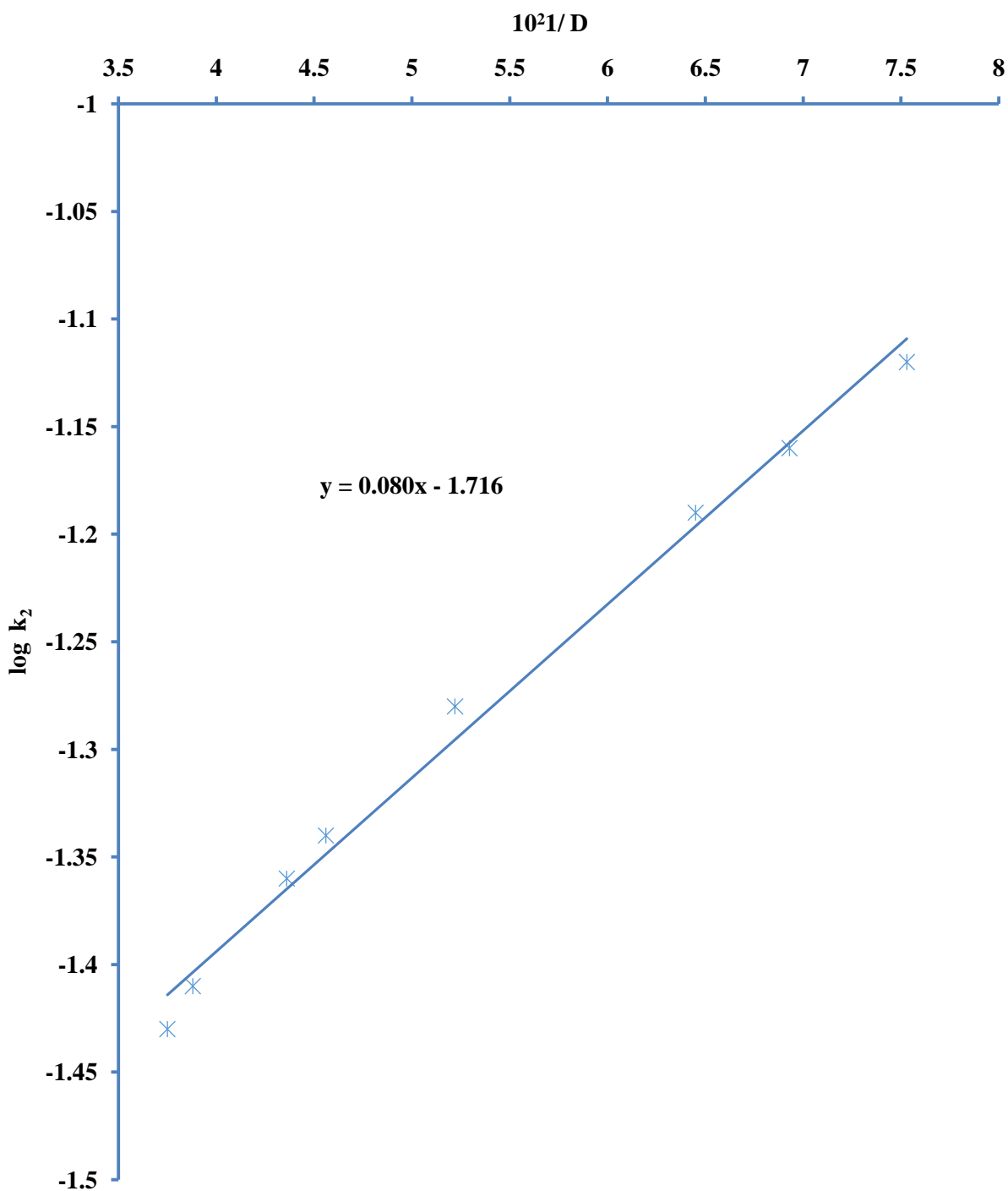


Figure 4.38: Plot of $\log k_2$ against $1/D$ for the Reaction of $[(H_2O)_2Ru_2O]^{4+}$ and $S_2O_3^{2-}$ at $[(H_2O)_2Ru_2O^{4+}] = 6.5 \times 10^{-5} \text{ mol dm}^{-3}$, $[S_2O_3^{2-}] = 13.0 \times 10^{-2} \text{ mol dm}^{-3}$, $[H^+] = 5.0 \times 10^{-2} \text{ mol dm}^{-3}$, $I = 0.5 \text{ mol dm}^{-3}$, $D = (81 - 70.20)$, $T = 31 \pm 1 \text{ C}$ and $\lambda_{\text{max}} = 660 \text{ nm}$

4.6.3 Ru_2O^{4+} reaction with $\text{S}_2\text{O}_4^{2-}$, H_3PO_2 , CH_3OH , $\text{C}_2\text{H}_5\text{OH}$ and $\text{C}_3\text{H}_7\text{OH}$

Varying D between 81 – 7.08 ($\text{CH}_3\text{COCH}_3/\text{H}_2\text{O}$) while maintaining the concentrations of H^+ , Ru_2O^{4+} and the reductants constant and maintaining T at 31 ± 1 °C and I at 0.5 mol dm^{-3} , the reactions between Ru_2O^{4+} and $\text{S}_2\text{O}_4^{2-}$, H_3PO_2 , CH_3OH , $\text{C}_2\text{H}_5\text{OH}$ and $\text{C}_3\text{H}_7\text{OH}$ showed lack of dependence of the rates of reactions on D as shown in Tables 4.16 – 4.20.

4.7 Effect of Added Ions

4.7.1 Ru_2O^{4+} reaction with the thioureas

At constant concentrations of all other reactants, the effect of added ions on the rates of the reaction was investigated by varying the concentrations of X, where X represents either nitrate ion (NO_3^-), acetate ion (CH_3COO^-), magnesium ion (Mg^{2+}) or ammonium ion (NH_4^+). For the reactions of Ru_2O^{4+} and thiourea (TU), *N*-methylthiourea (MTU), *N*-allylthiourea (ATU) and *N,N'*-dimethylthiourea (DMTU) the rate constants were found to be unaffected by the addition of the ions as shown in Tables 4.21 – 4.27.

4.7.2 Ru_2O^{4+} reaction with $\text{S}_2\text{O}_3^{2-}$

Keeping the concentrations of the oxidant, reductants, other reactants and T constant, varying amounts of NO_3^- , CH_3COO^- , Mg^{2+} and NH_4^+ were added. Results showed that for the reaction of Ru_2O^{4+} and $\text{S}_2\text{O}_3^{2-}$ the rates of the reaction decreased with increase in the concentrations of anions added but increased with the concentrations of the cations added (Tables 4.28 and 4.29). The plot of the ion dependent second order rate constant,

Table 4.16: Effect of Change in the Dielectric Constant of Reaction Medium for the Reaction of $[(\text{H}_2\text{O})_2\text{Ru}_2\text{O}]^{4+}$ and $\text{S}_2\text{O}_4^{2-}$ at $[(\text{H}_2\text{O})_2\text{Ru}_2\text{O}^{4+}] = 5.75 \times 10^{-5} \text{ mol dm}^{-3}$, $[\text{S}_2\text{O}_4^{2-}] = 4.31 \times 10^{-2} \text{ mol dm}^{-3}$, $I = 0.5 \text{ mol dm}^{-3}$ (NaClO_4), $D = (81.0 - 70.8)$, $T = 31 \pm 1^\circ\text{C}$ and $\lambda_{\text{max}} = 660 \text{ nm}$

D	$10^3 k_{\text{obs}}, \text{ s}^{-1}$	$10^2 k_2, \text{ dm}^3 \text{ mol}^{-1} \text{ s}^{-1}$
81.0	4.74	11.00
79.2	4.76	11.04
78.0	4.75	11.02
76.8	4.71	10.93
75.6	4.72	10.95
73.2	4.75	11.02
72.0	4.75	11.02
70.8	4.71	10.93

Table 4.17: Effect of Change in the Dielectric Constant of Reaction Medium for the Reaction of $[(\text{H}_2\text{O})_2\text{Ru}_2\text{O}]^{4+}$ and H_3PO_2 at $[(\text{H}_2\text{O})_2\text{Ru}_2\text{O}^{4+}] = 6.0 \times 10^{-5} \text{ mol dm}^{-3}$, $[\text{H}_3\text{PO}_2] = 9.6 \times 10^{-2} \text{ mol dm}^{-3}$, $[\text{H}^+] = 5 \times 10^{-2} \text{ mol dm}^{-3}$, $I = 0.5 \text{ mol dm}^{-3}$ (NaClO_4), $D = (81.0 - 70.8)$, $T = 31 \pm 1^\circ\text{C}$ and $\lambda_{\text{max}} = 660 \text{ nm}$

D	$10^4 k_{\text{obs}}, \text{ s}^{-1}$	$10^3 k_2, \text{ dm}^3 \text{ mol}^{-1} \text{ s}^{-1}$
81.0	6.83	7.12
79.2	6.82	7.10
78.0	6.83	7.12
76.8	6.84	7.13
75.6	6.80	7.08
73.2	6.84	7.13
72.0	6.82	7.10
70.8	6.83	7.12

Table 4.18: Effect of Change in the Dielectric Constant of Reaction Medium for the Reaction of $[(\text{H}_2\text{O})_2\text{Ru}_2\text{O}]^{4+}$ and CH_3OH at $[(\text{H}_2\text{O})_2\text{Ru}_2\text{O}^{4+}] = 5.5 \times 10^{-5} \text{ mol dm}^{-3}$, $[\text{CH}_3\text{OH}] = 16.5 \times 10^{-2} \text{ mol dm}^{-3}$, $I = 0.5 \text{ mol dm}^{-3}$ (NaClO_4), $D = (81.0 - 70.8)$, $T = 31 \pm 1^\circ\text{C}$ and $\lambda_{\text{max}} = 660 \text{ nm}$

D	$10^4 k_{\text{obs}}, \text{ s}^{-1}$	$10^2 k_2, \text{ dm}^3 \text{ mol}^{-1} \text{ s}^{-1}$
81.0	19.73	11.96
79.2	19.93	12.08
78.0	19.87	12.04
76.8	19.87	12.04
75.6	19.83	12.02
73.2	19.88	12.05
72.0	19.77	11.98
70.8	19.82	12.01

Table 4.19: Effect of Change in the Dielectric Constant of Reaction Medium for the Reaction of $[(\text{H}_2\text{O})_2\text{Ru}_2\text{O}]^{4+}$ and $\text{C}_2\text{H}_5\text{OH}$ at $[(\text{H}_2\text{O})_2\text{Ru}_2\text{O}^{4+}] = 6.5 \times 10^{-5} \text{ mol dm}^{-3}$, $[\text{C}_2\text{H}_5\text{OH}] = 13 \times 10^{-2} \text{ mol dm}^{-3}$, $I = 0.5 \text{ mol dm}^{-3}$ (NaClO_4), $D = (81.0 - 70.2)$, $T = 31 \pm 1^\circ\text{C}$ and $\lambda_{\text{max}} = 660 \text{ nm}$

D	$10^4 k_{\text{obs}}, \text{ s}^{-1}$	$10^2 k_2, \text{ dm}^3 \text{ mol}^{-1} \text{ s}^{-1}$
81.0	11.43	8.79
79.8	11.45	8.81
78.6	11.41	8.78
77.4	11.48	8.83
75.0	11.43	8.79
72.6	11.47	8.82
71.4	11.38	8.75
70.2	11.44	8.80

Table 4.20: Effect of Change in the Dielectric Constant of Reaction Medium for the Reaction of $[(\text{H}_2\text{O})_2\text{Ru}_2\text{O}]^{4+}$ and $\text{C}_3\text{H}_7\text{OH}$ at $[(\text{H}_2\text{O})_2\text{Ru}_2\text{O}^{4+}] = 6.0 \times 10^{-5} \text{ mol dm}^{-3}$, $[\text{C}_3\text{H}_7\text{OH}] = 12.0 \times 10^{-2} \text{ mol dm}^{-3}$, $I = 0.5 \text{ mol dm}^{-3}$ (NaClO_4), $D = (81.0 - 70.8)$, $\lambda_{\text{max}} = 660 \text{ nm}$ $T = 31 \pm 1^\circ\text{C}$ and $\lambda_{\text{max}} = 660 \text{ nm}$

D	$10^4 k_{\text{obs}}, \text{ s}^{-1}$	$10^3 k_2, \text{ dm}^3 \text{ mol}^{-1} \text{ s}^{-1}$
81.0	4.25	3.54
79.2	4.20	3.50
78.0	4.16	3.47
76.8	4.24	3.53
75.6	4.19	3.49
73.2	4.22	3.52
72.0	4.22	3.52
70.8	4.19	3.48

Table 4.21: Effect of Added Anions to Reaction Medium for the Reaction of

$[(\text{H}_2\text{O})_2\text{Ru}_2\text{O}]^{4+}$ and Thiourea (TU) at $[(\text{H}_2\text{O})_2\text{Ru}_2\text{O}]^{4+} = 6.0 \times 10^{-5} \text{ mol dm}^{-3}$, $[\text{TU}] = 12.0 \times 10^{-2} \text{ mol dm}^{-3}$, $[\text{H}^+] = 5 \times 10^{-2} \text{ mol dm}^{-3}$, $I = 0.5 \text{ mol dm}^{-3}$, $T = 31 \pm 1 \text{ }^\circ\text{C}$ and $\lambda_{\text{max}} = 660 \text{ nm}$

Ion	$10^3[\text{ion}]$	$10^4 k_{\text{obs}}, \text{ s}^{-1}$	$10^3 k_2, \text{ dm}^3 \text{ mol}^{-1} \text{ s}^{-1}$
	mol dm^{-3}		
NO_3^-	0.00	8.89	7.41
	10.00	8.86	7.38
	20.00	8.91	7.43
	40.00	8.83	7.36
	60.00	8.88	7.40
	100.00	8.87	7.39
	120.00	8.87	7.39
CH_3COO^-	0.00	8.88	7.40
	10.00	8.90	7.42
	20.00	8.87	7.39
	40.00	8.90	7.42
	60.00	8.86	7.38
	100.00	8.88	7.40
	120.00	8.89	7.41

Table 4.22: Effect of Added Anions to Reaction Medium for the Reaction of

$[(\text{H}_2\text{O})_2\text{Ru}_2\text{O}]^{4+}$ and *N*-methylthiourea (MTU) at $[(\text{H}_2\text{O})_2\text{Ru}_2\text{O}]^{4+} = 6.5 \times 10^{-5} \text{ mol dm}^{-3}$, $[\text{MTU}] = 5.2 \times 10^{-2} \text{ mol dm}^{-3}$, $[\text{H}^+] = 5 \times 10^{-2} \text{ mol dm}^{-3}$, $I = 0.5 \text{ mol dm}^{-3}$, $T = 31 \pm 1 \text{ }^\circ\text{C}$ and $\lambda_{\text{max}} = 660 \text{ nm}$

Ion	$10^3[\text{ion}]$	$10^4 k_{\text{obs}}, \text{ s}^{-1}$	$10^2 k_2, \text{ dm}^3 \text{ mol}^{-1} \text{ s}^{-1}$
	mol dm^{-3}		
NO_3^-	0.00	16.54	3.18
	20.00	16.38	3.15
	40.00	16.22	3.12
	60.00	16.22	3.12
	100.00	15.86	3.05
	200.00	16.32	3.14
CH_3COO^-	0.00	16.11	3.10
	10.00	16.38	3.15
	20.00	16.25	3.13
	40.00	16.12	3.12
	60.00	16.12	3.10
	100.00	15.97	3.07
	200.00	16.38	3.15

Table 4.23: Effect of added cation (Mg^{2+}) to Reaction Medium for the Reaction of $[(\text{H}_2\text{O})_2\text{Ru}_2\text{O}]^{4+}$ and *N*-methylthiourea (MTU) at $[(\text{H}_2\text{O})_2\text{Ru}_2\text{O}]^{4+} = 6.5 \times 10^{-5} \text{ mol dm}^{-3}$, $[\text{MTU}] = 5.2 \times 10^{-2} \text{ mol dm}^{-3}$, $[\text{H}^+] = 5 \times 10^{-2} \text{ mol dm}^{-3}$, $I = 0.5 \text{ mol dm}^{-3}$, $T = 31 \pm 1 \text{ }^\circ\text{C}$ and $\lambda_{\text{max}} = 660 \text{ nm}$

$10^3[\text{Mg}^{2+}]$		
mol dm^{-3}	$10^4 k_{\text{obs}}, \text{ s}^{-1}$	$10^2 k_2, \text{ dm}^3 \text{ mol}^{-1} \text{ s}^{-1}$
0.00	16.25	3.13
1.00	16.41	3.16
20.00	16.08	3.09
40.00	16.20	3.12
60.00	16.38	3.15
100.00	16.11	3.10

Table 4.24: Effect of added anions (NO_3^- and CH_3COO^-) to Reaction Medium for the Reaction of $[(\text{H}_2\text{O})_2\text{Ru}_2\text{O}]^{4+}$ and *N*-allylthiourea (ATU) at $[(\text{H}_2\text{O})_2\text{Ru}_2\text{O}]^{4+} = 5.75 \times 10^{-5} \text{ mol dm}^{-3}$, $[\text{ATU}] = 3.45 \times 10^{-2} \text{ mol dm}^{-3}$, $[\text{H}^+] = 5 \times 10^{-2} \text{ mol dm}^{-3}$, $I = 0.5 \text{ mol dm}^{-3}$, $T = 31 \pm 1^\circ\text{C}$ and $\lambda_{\text{max}} = 660 \text{ nm}$

Ion	$10^3[\text{ion}]$	$10^3 k_{\text{obs}}, \text{ s}^{-1}$	$10^2 k_2, \text{ dm}^3 \text{ mol}^{-1} \text{ s}^{-1}$
	mol dm^{-3}		
NO_3^-	0.00	6.22	18.03
	1.00	7.42	21.51
	20.00	6.89	19.97
	40.00	6.75	19.57
	60.00	6.63	19.22
	100.00	7.25	21.01
	200.00	7.18	20.81
CH_3COO^-	0.00	7.12	20.64
	1.00	6.54	18.96
	20.00	7.28	21.10
	40.00	6.88	19.94
	60.00	6.93	20.09
	100.00	7.12	20.64
	200.00	6.56	19.01

Table 4.25: Effect of added cation (Mg^{2+}) to Reaction Medium for the Reaction of $[(\text{H}_2\text{O})_2\text{Ru}_2\text{O}]^{4+}$ and *N*-allylthiourea (ATU) at $[(\text{H}_2\text{O})_2\text{Ru}_2\text{O}]^{4+} = 5.75 \times 10^{-5} \text{ mol dm}^{-3}$, $[\text{ATU}] = 3.45 \times 10^{-2} \text{ mol dm}^{-3}$, $[\text{H}^+] = 5 \times 10^{-2} \text{ mol dm}^{-3}$, $\text{I} = 0.5 \text{ mol dm}^{-3}$, $T = 31 \pm 1 \text{ }^\circ\text{C}$ and $\lambda_{\text{max}} = 660 \text{ nm}$

$10^3[\text{Mg}^{2+}]$		
mol dm^{-3}	$10^3 k_{\text{obs}}, \text{ s}^{-1}$	$10^2 k_2, \text{ dm}^3 \text{ mol}^{-1} \text{ s}^{-1}$
0.00	6.28	18.20
1.00	7.25	21.01
20.00	6.56	19.01
40.00	6.67	19.33
60.00	6.89	19.97
100.00	6.44	18.67

Table 4.26: Effect of Added Anions to Reaction Medium for the Reaction of **$[(\text{H}_2\text{O})_2\text{Ru}_2\text{O}]^{4+}$ and *N,N'*-dimethylthiourea (DMTU) at** $[(\text{H}_2\text{O})_2\text{Ru}_2\text{O}]^{4+} = 7.0 \times 10^{-5} \text{ mol dm}^{-3}$, $[\text{DMTU}] = 5.6 \times 10^{-2} \text{ mol dm}^{-3}$, $[\text{H}^+] = 5 \times 10^{-2} \text{ mol dm}^{-3}$, $I = 0.5 \text{ mol dm}^{-3}$, $T = 31 \pm 1 \text{ }^\circ\text{C}$ and $\lambda_{\text{max}} = 660$

nm

Ion	$10^3[\text{ion}]$ mol dm^{-3}	$10^3k_{\text{obs}}, \text{ s}^{-1}$	$10^2k_2, \text{ dm}^3 \text{ mol}^{-1} \text{ s}^{-1}$
CH_3COO^-	0.00	4.54	8.11
	10.00	4.48	8.00
	20.00	4.55	8.13
	50.00	4.54	8.11
	80.00	4.51	8.05
	100.00	4.53	8.09
	200.00	4.55	8.13
NO_3^-	0.00	4.51	8.05
	10.00	4.54	8.11
	20.00	4.56	8.14
	50.00	4.53	8.09
	80.00	4.47	7.98
	100.00	4.55	8.13
	120.00	4.54	8.11

Table 4.27: Effect of Added Cations to Reaction Medium for the Reaction of
 $[(\text{H}_2\text{O})_2\text{Ru}_2\text{O}]^{4+}$ and *N, N'*-dimethylthiourea (DMTU) at
 $[(\text{H}_2\text{O})_2\text{Ru}_2\text{O}]^{4+} = 7.0 \times 10^{-5} \text{ mol dm}^{-3}$, $[\text{DMTU}] = 5.6 \times 10^{-2} \text{ mol dm}^{-3}$,
 $[\text{H}^+] = 5 \times 10^{-2} \text{ mol dm}^{-3}$, $I = 0.5 \text{ mol dm}^{-3}$, $T = 31 \pm 1 \text{ }^\circ\text{C}$ and $\lambda_{\text{max}} = 660$
 nm

Ion	$10^3[\text{ion}]$ mol dm^{-3}	$10^3k_{\text{obs}}, \text{ s}^{-1}$	$10^2k_2, \text{ dm}^3 \text{ mol}^{-1} \text{ s}^{-1}$
Mg^{2+}	0.00	4.55	8.13
	10.00	4.49	8.02
	20.00	4.54	8.11
	30.00	4.55	8.13
	50.00	4.56	8.14
	70.00	4.54	8.11
	100.00	4.53	8.09
NH_4^+	0.00	4.56	8.14
	10.00	4.54	8.11
	20.00	4.53	8.09
	30.00	4.52	8.07
	50.00	4.56	8.14
	70.00	4.52	8.07
	100.00	4.55	8.13

Table 4.28: Effect of Added Cations to Reaction Medium for the Reaction of

$[(\text{H}_2\text{O})_2\text{Ru}_2\text{O}]^{4+}$ and $\text{S}_2\text{O}_3^{2-}$ at $[(\text{H}_2\text{O})_2\text{Ru}_2\text{O}]^{4+} = 6.5 \times 10^{-5} \text{ mol dm}^{-3}$;
 $[\text{S}_2\text{O}_3^{2-}] = 1.3 \times 10^{-2} \text{ mol dm}^{-3}$, $[\text{H}^+] = 5 \times 10^{-2} \text{ mol dm}^{-3}$, $I = 0.5 \text{ mol dm}^{-3}$,
 $T = 31 \pm 1 \text{ }^\circ\text{C}$ and $\lambda_{\text{max}} = 660 \text{ nm}$

Ion	$10^3[\text{ion}]$	$10^4 k_{\text{obs}}, \text{ s}^{-1}$	$10^2 k_2, \text{ dm}^3 \text{ mol}^{-1} \text{ s}^{-1}$
	mol dm^{-3}		
Mg^{2+}	0.00	4.89	3.77
	10.00	4.63	3.55
	20.00	4.47	3.44
	40.00	4.06	3.12
	60.00	3.33	2.56
	100.00	2.53	1.95
	120.00	1.51	1.16
NH_4^+	0.00	4.87	3.75
	10.00	4.67	3.59
	20.00	4.63	3.56
	40.00	4.06	3.12
	60.00	3.77	2.90
	100.00	3.18	2.44
	120.00	2.71	2.09

Table 4.29: Effect of Added Anions to Reaction Medium for the Reaction of
 $[(\text{H}_2\text{O})_2\text{Ru}_2\text{O}]^{4+}$ and $\text{S}_2\text{O}_3^{2-}$ at $[(\text{H}_2\text{O})_2\text{Ru}_2\text{O}]^{4+} = 6.5 \times 10^{-5} \text{ mol dm}^{-3}$,
 $[\text{S}_2\text{O}_3^{2-}] = 1.3 \times 10^{-2} \text{ mol dm}^{-3}$, $[\text{H}^+] = 5 \times 10^{-2} \text{ mol dm}^{-3}$, $I = 0.5 \text{ mol dm}^{-3}$,
 $T = 31 \pm 1 \text{ }^\circ\text{C}$ and $\lambda_{\text{max}} = 660 \text{ nm}$

Ion	$10^3[\text{ion}]$ mol dm^{-3}	$10^3k_{\text{obs}}, \text{ s}^{-1}$	$10^2k_2, \text{ dm}^3 \text{ mol}^{-1} \text{ s}^{-1}$
CH_3COO^-	0.00	4.93	3.79
	10.00	5.05	3.88
	20.00	5.64	4.34
	40.00	6.05	4.65
	60.00	6.63	5.10
	100.00	7.94	6.11
	120.00	8.26	6.36
NO_3^-	0.00	4.89	3.76
	10.00	5.09	3.92
	20.00	5.40	4.15
	40.00	5.75	4.43
	60.00	6.39	4.91
	100.00	7.28	5.60
	140.00	8.35	6.42

$k_2(X)$, versus concentrations of the ions, $[X]$ are presented as Figures 4.39 – 4.42. The relationship between the ion-dependent second order rate constant, $k_2(X)$, and the concentrations of the ions for the $\text{Ru}_2\text{O}^{4+}/\text{S}_2\text{O}_3^{2-}$ is given by Equations 4.19 and 4.20.

$$k_2(X) = p - q(X) \quad \text{.....(4.19)}$$

where $X = \text{Mg}^{2+}$ and NH_4^+ and

$$k_2(X) = p + q(X) \quad \text{.....(4.20)}$$

where $X = \text{NO}_3^-$ and CH_3COO^- ; p = intercept and q = slope whose values for:

$$\text{Mg}^{2+} \text{ 'p' } = 3.83 \times 10^{-2} \text{ dm}^3 \text{ mol}^{-1} \text{ s}^{-1} \text{ and 'q' } = -2.07 \times 10^{-2} \text{ dm}^6 \text{ mol}^{-2} \text{ s}^{-1}$$

$$\text{NH}_4^+ \text{ 'p' } = 3.73 \times 10^{-2} \text{ dm}^3 \text{ mol}^{-1} \text{ s}^{-1} \text{ and 'q' } = -1.40 \times 10^{-3} \text{ dm}^6 \text{ mol}^{-2} \text{ s}^{-1}$$

$$\text{CH}_3\text{COO}^- \text{ 'p' } = 3.74 \times 10^{-2} \text{ dm}^3 \text{ mol}^{-1} \text{ s}^{-1} \text{ and 'q' } = 2.20 \times 10^{-3} \text{ dm}^6 \text{ mol}^{-2} \text{ s}^{-1}$$

$$\text{NO}_3^- \text{ 'p' } = 3.76 \times 10^{-2} \text{ dm}^3 \text{ mol}^{-1} \text{ s}^{-1} \text{ and 'q' } = 18.71 \times 10^{-2} \text{ dm}^6 \text{ mol}^{-2} \text{ s}^{-1}$$

4.7.3 Ru_2O^{4+} reaction with $\text{S}_2\text{O}_4^{2-}$

At constant concentrations of all the reactants and at a constant T, varying amounts of CH_3COO^- , HCOO^- , Mg^{2+} and NH_4^+ were added. Results showed that for the reaction of Ru_2O^{4+} and $\text{S}_2\text{O}_4^{2-}$, the rates of the reaction increased with increase in the concentrations of anions added but decreased with the concentrations of the anions added (Tables 4.30 and 4.31). The plot of the ion-dependent second order rate constant, xk_2 , versus concentrations of the ions, $[X]$ are presented as Figures 4.43 – 4.46. The relationship between the ion dependent second order rate constant, $k_2(X)$, and the concentrations of the ions for this system is given by Equations 4.21 and 4.22,

$$k_2(X) = p + q(X) \quad \text{.....(4.21)}$$

where $X = \text{CH}_3\text{COO}^-$ and HCOO^- ; p = intercept and q = slope and

$$k_2(X) = p - q(X) \quad \text{.....(4.22)}$$

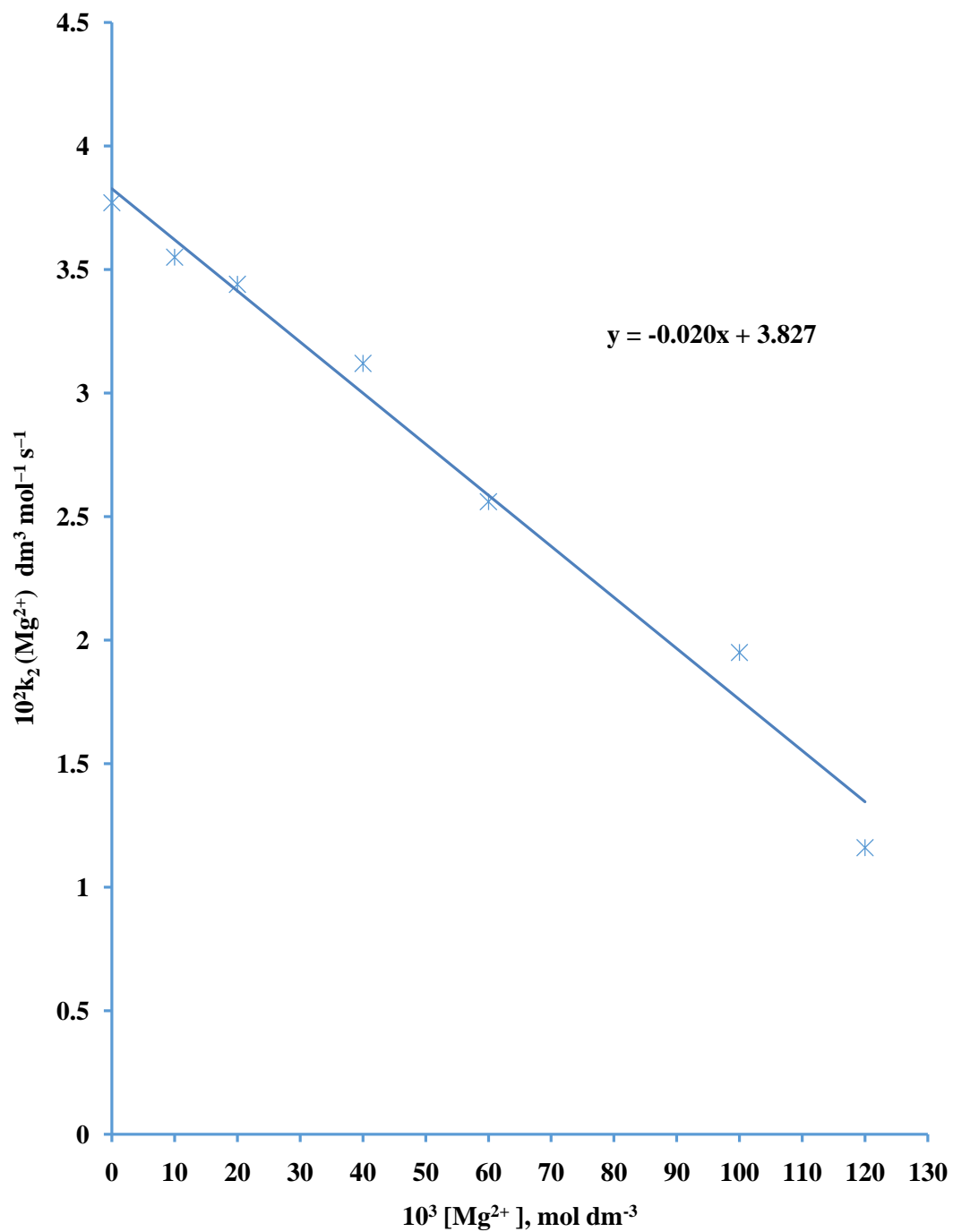


Figure 4.39: Plot of $k_2 (\text{Mg}^{2+})$ versus $[\text{Mg}^{2+}]$ for the Reaction of $[(\text{H}_2\text{O})_2\text{Ru}_2\text{O}]^{4+}$ and $\text{S}_2\text{O}_3^{2-}$ at $[(\text{H}_2\text{O})_2\text{Ru}_2\text{O}^{4+}] = 6.5 \times 10^{-5} \text{ mol dm}^{-3}$, $[\text{S}_2\text{O}_3^{2-}] = 13.0 \times 10^{-2} \text{ mol dm}^{-3}$, $[\text{H}^+] = 5.0 \times 10^{-2} \text{ mol dm}^{-3}$, $[\text{Mg}^{2+}] = (0.0 - 120.0) \times 10^{-3} \text{ mol dm}^{-3}$, $I = 0.5 \text{ mol dm}^{-3}$, $T = 31 \pm 1 \text{ C}$ and $\lambda_{\text{max}} = 660 \text{ nm}$

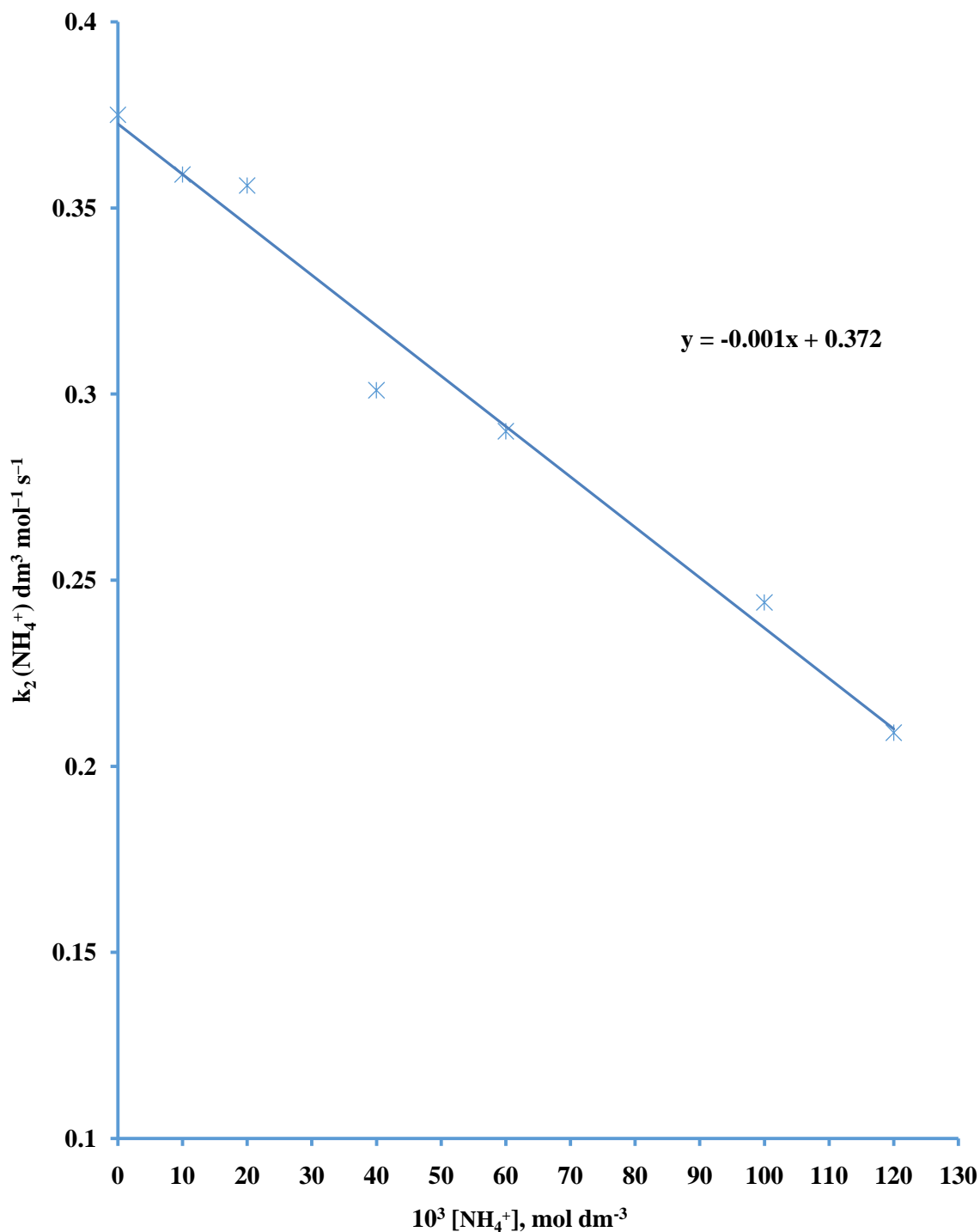


Figure 4.40: Plot of $k_2(\text{NH}_4^+)$ versus $[\text{NH}_4^+]$ for the Reaction of $[(\text{H}_2\text{O})_2\text{Ru}_2\text{O}]^{4+}$ and $\text{S}_2\text{O}_3^{2-}$ at $[(\text{H}_2\text{O})_2\text{Ru}_2\text{O}^{4+}] = 6.5 \times 10^{-5} \text{ mol dm}^{-3}$, $[\text{S}_2\text{O}_3^{2-}] = 1.3 \times 10^{-2} \text{ mol dm}^{-3}$, $[\text{H}^+] = 5.0 \times 10^{-2} \text{ mol dm}^{-3}$, $[\text{NH}_4^+] = (0.0 - 16.0) \times 10^{-2} \text{ mol dm}^{-3}$, $I = 0.5 \text{ mol dm}^{-3}$, $T = 31 \pm 1 \text{ C}$ and $\lambda_{\text{max}} = 660 \text{ nm}$

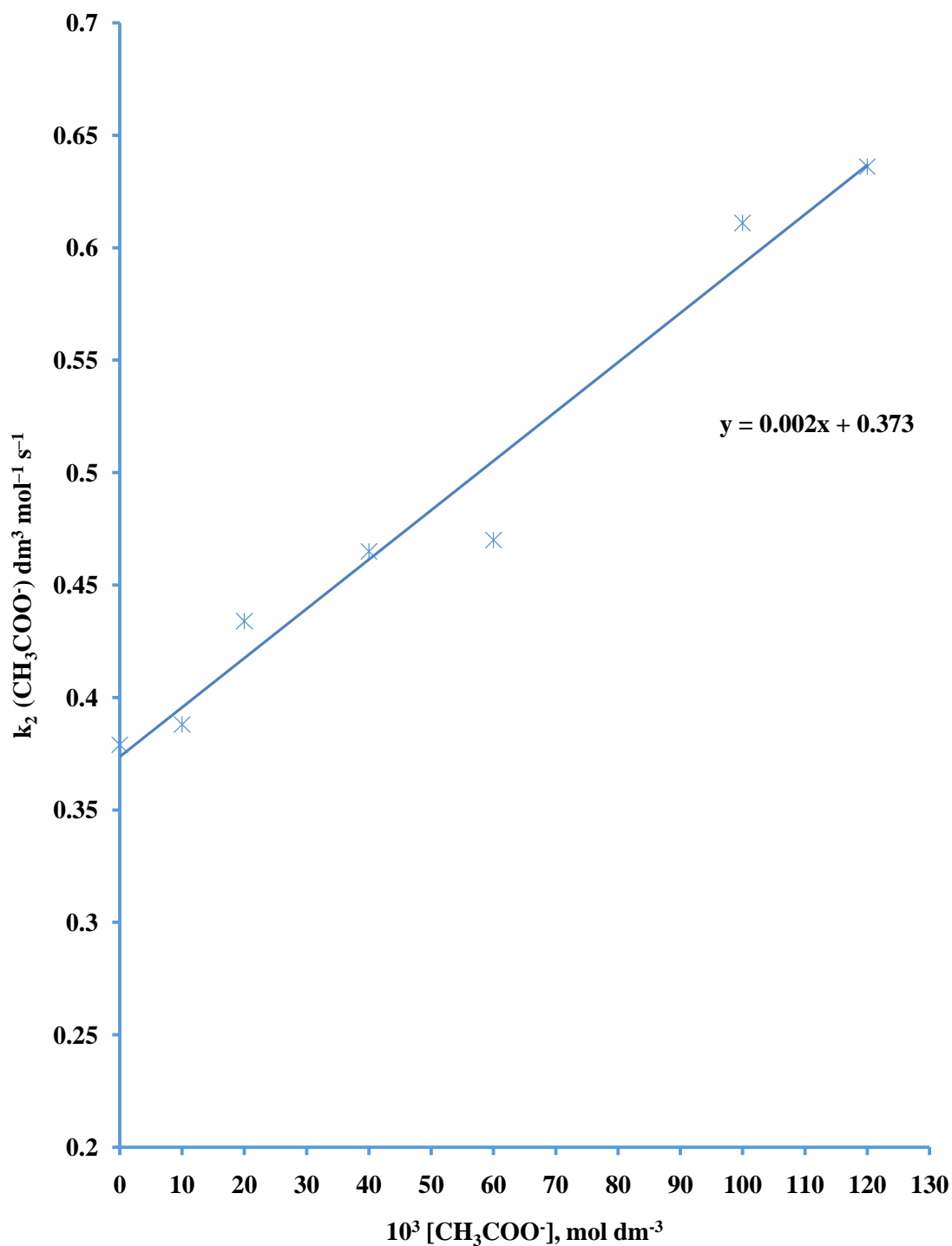


Figure 4.41: Plot of $k_2 (\text{CH}_3\text{COO}^-)$ versus $[\text{CH}_3\text{COO}^-]$ for the Reaction of $[(\text{H}_2\text{O})_2\text{Ru}_2\text{O}]^{4+}$ and $\text{S}_2\text{O}_3^{2-}$ at $[(\text{H}_2\text{O})_2\text{Ru}_2\text{O}^{4+}] = 6.5 \times 10^{-5} \text{ mol dm}^{-3}$, $[\text{S}_2\text{O}_3^{2-}] = 1.3 \times 10^{-2} \text{ mol dm}^{-3}$, $[\text{H}^+] = 5.0 \times 10^{-2} \text{ mol dm}^{-3}$, $[\text{CH}_3\text{COO}^-] = (0.0 - 12.0) \times 10^{-2} \text{ mol dm}^{-3}$, $I = 0.5 \text{ mol dm}^{-3}$, $T = 31 \pm 1 \text{ C}$ and $\lambda_{\text{max}} = 660 \text{ nm}$

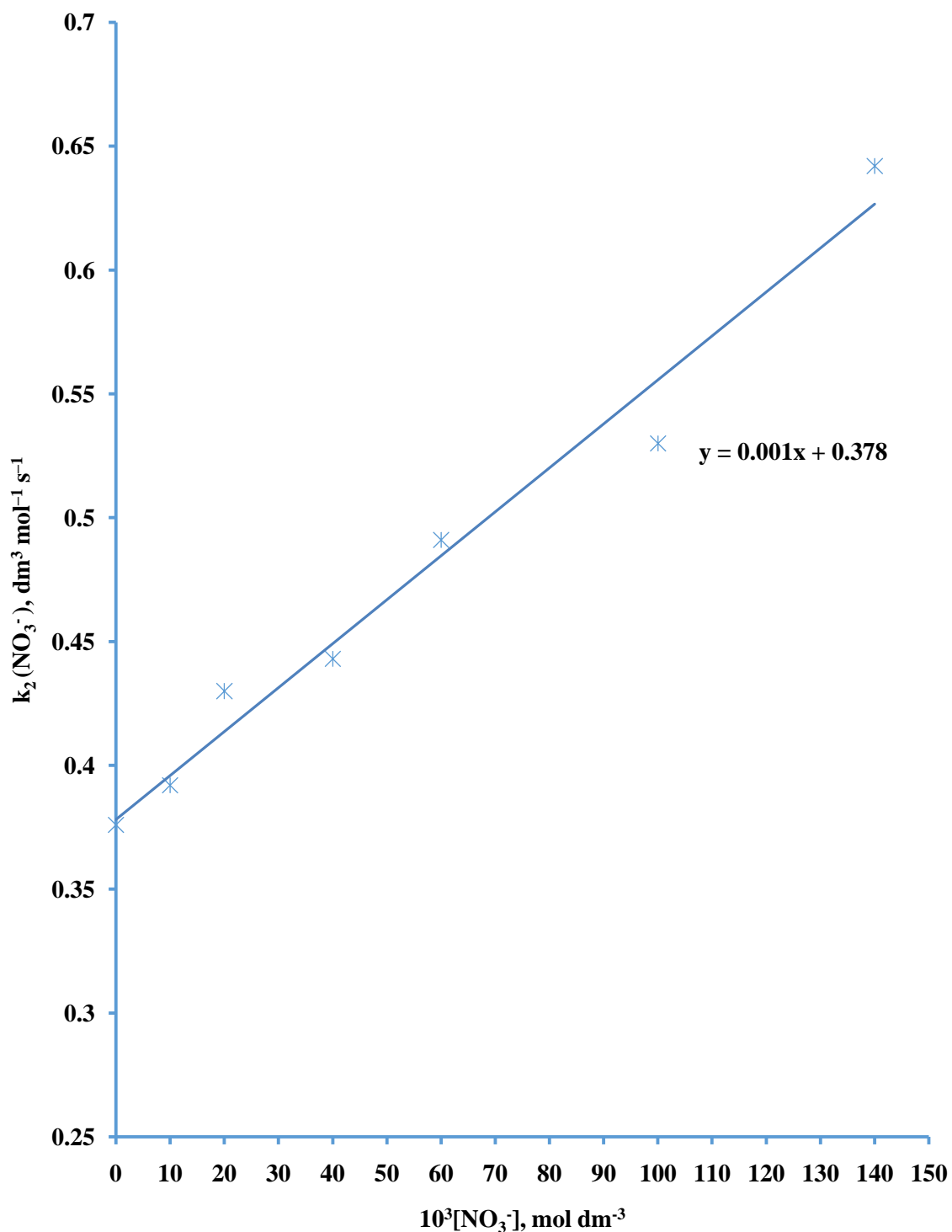


Figure 4.42: Plot of $k_2(\text{NO}_3^-)$ versus $[\text{NO}_3^-]$ for the Reaction of $[(\text{H}_2\text{O})_2\text{Ru}_2\text{O}]^{4+}$ and $\text{S}_2\text{O}_3^{2-}$ at $[(\text{H}_2\text{O})_2\text{Ru}_2\text{O}^{4+}] = 6.5 \times 10^{-5} \text{ mol dm}^{-3}$, $[\text{S}_2\text{O}_3^{2-}] = 1.3 \times 10^{-2} \text{ mol dm}^{-3}$, $[\text{H}^+] = 5.0 \times 10^{-2} \text{ mol dm}^{-3}$, $[\text{NO}_3^-] = (0.0 - 14.0) \times 10^{-2} \text{ mol dm}^{-3}$, $I = 0.5 \text{ mol dm}^{-3}$, $T = 31 \pm 1 \text{ }^\circ\text{C}$ and $\lambda_{\text{max}} = 660 \text{ nm}$

Table 4.30: Effect of Added Anions to Reaction Medium for the Reaction of

**$[(\text{H}_2\text{O})_2\text{Ru}_2\text{O}]^{4+}$ and $\text{S}_2\text{O}_4^{2-}$ at $[(\text{H}_2\text{O})_2\text{Ru}_2\text{O}]^{4+} = 5.75 \times 10^{-5} \text{ mol dm}^{-3}$,
 $[\text{S}_2\text{O}_4^{2-}] = 4.31 \times 10^{-2} \text{ mol dm}^{-3}$, $I = 0.5 \text{ mol dm}^{-3}$, $T = 31 \pm 1 \text{ }^\circ\text{C}$ and
 $\lambda_{\text{max}} = 660 \text{ nm}$**

Ion	$10^3[\text{ion}]$	$10^4 k_{\text{obs}}, \text{ s}^{-1}$	$10^2 k_2, \text{ dm}^3 \text{ mol}^{-1} \text{ s}^{-1}$
	mol dm^{-3}		
CH_3COO^-	0.00	4.72	10.95
	20.00	5.09	11.81
	60.00	5.52	12.81
	120.00	6.56	15.22
	140.00	6.72	15.59
	160.00	7.16	16.61
	240.00	8.37	19.42
HCOO^-	0.00	4.76	11.04
	20.00	5.01	11.62
	60.00	5.68	13.18
	120.00	6.21	14.41
	140.00	6.59	15.29
	160.00	6.81	15.80
	240.00	7.89	18.31

Table 4.31: Effect of Added Cations to Reaction Medium for the Reaction of

$[(\text{H}_2\text{O})_2\text{Ru}_2\text{O}]^{4+}$ and $\text{S}_2\text{O}_4^{2-}$ at $[(\text{H}_2\text{O})_2\text{Ru}_2\text{O}]^{4+} = 5.75 \times 10^{-5} \text{ mol dm}^{-3}$,
 $[\text{S}_2\text{O}_4^{2-}] = 4.31 \times 10^{-2} \text{ mol dm}^{-3}$, $I = 0.5 \text{ mol dm}^{-3}$, $T = 31 \pm 1 \text{ }^\circ\text{C}$ and λ_{max}
 $= 660 \text{ nm}$

Ion	$10^3[\text{ion}]$ mol dm^{-3}	$10^3k_{\text{obs}}, \text{ s}^{-1}$	$10^2k_2, \text{ dm}^3 \text{ mol}^{-1} \text{ s}^{-1}$
Mg^{2+}	0.00	4.92	10.95
	10.00	4.56	10.59
	20.00	4.48	10.40
	40.00	4.06	9.42
	60.00	3.84	8.91
	100.00	3.19	7.40
	120.00	3.10	7.19
NH_4^+	0.00	4.74	11.00
	20.00	4.66	10.81
	60.00	3.96	9.19
	120.00	3.37	7.82
	140.00	2.94	6.82
	160.00	2.84	6.59
	240.00	2.03	4.71

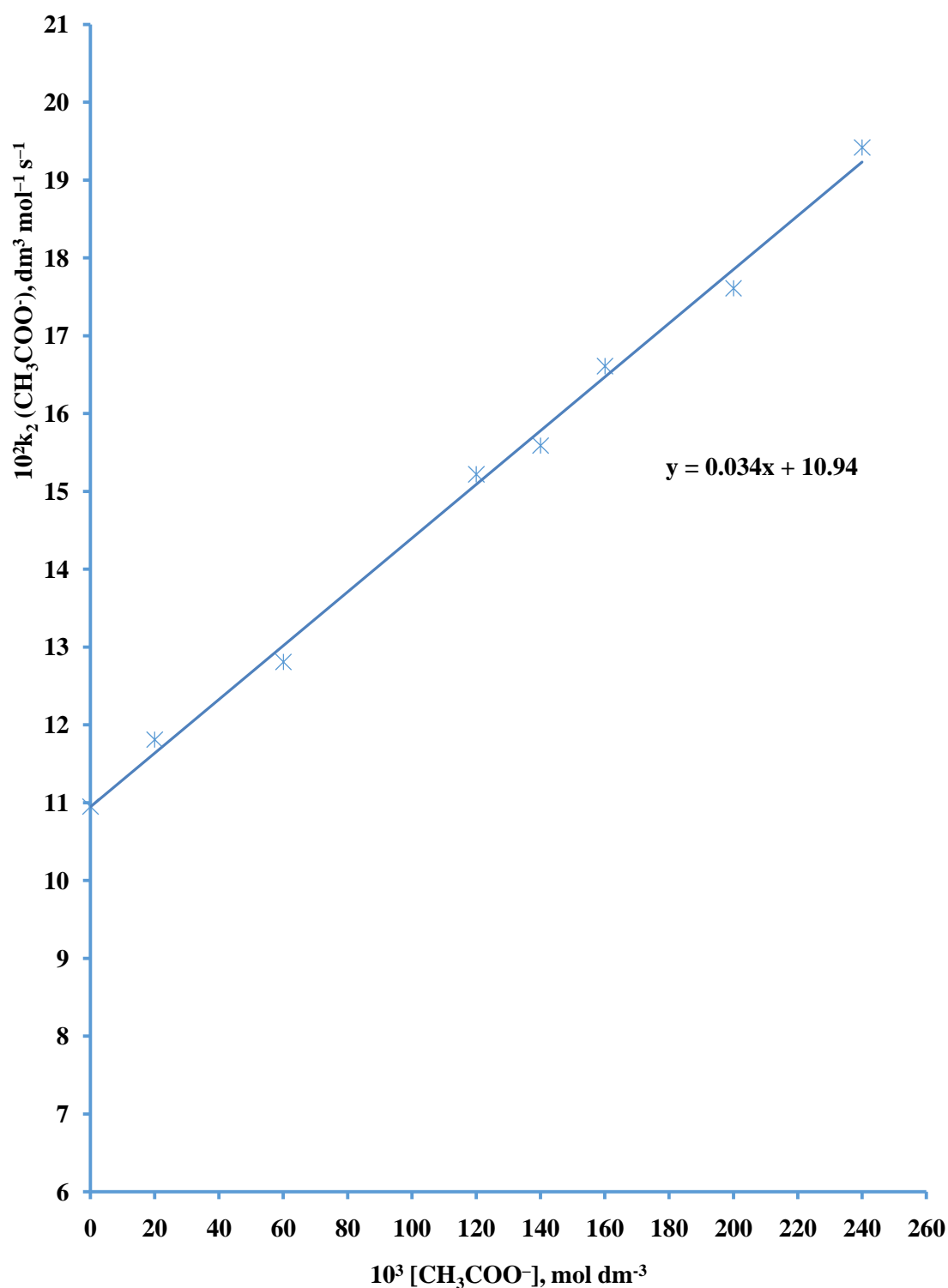


Figure 4.43: Plot of $k_2(\text{CH}_3\text{COO}^-)$ versus $[\text{CH}_3\text{COO}^-]$ for the Reaction of $(\text{H}_2\text{O})_2\text{Ru}_2\text{O}^{4+}$ and $\text{S}_2\text{O}_4^{2-}$ at $[(\text{H}_2\text{O})_2\text{Ru}_2\text{O}^{4+}] = 5.75 \times 10^{-5} \text{ mol dm}^{-3}$, $[\text{S}_2\text{O}_4^{2-}] = 4.31 \times 10^{-2} \text{ mol dm}^{-3}$, $[\text{CH}_3\text{COO}^-] = (0.0 - 24.0) \times 10^{-2} \text{ mol dm}^{-3}$, $I = 0.5 \text{ mol dm}^{-3}$, $T = 32 \pm 1 \text{ C}$ and $\lambda_{\text{max}} = 660 \text{ nm}$

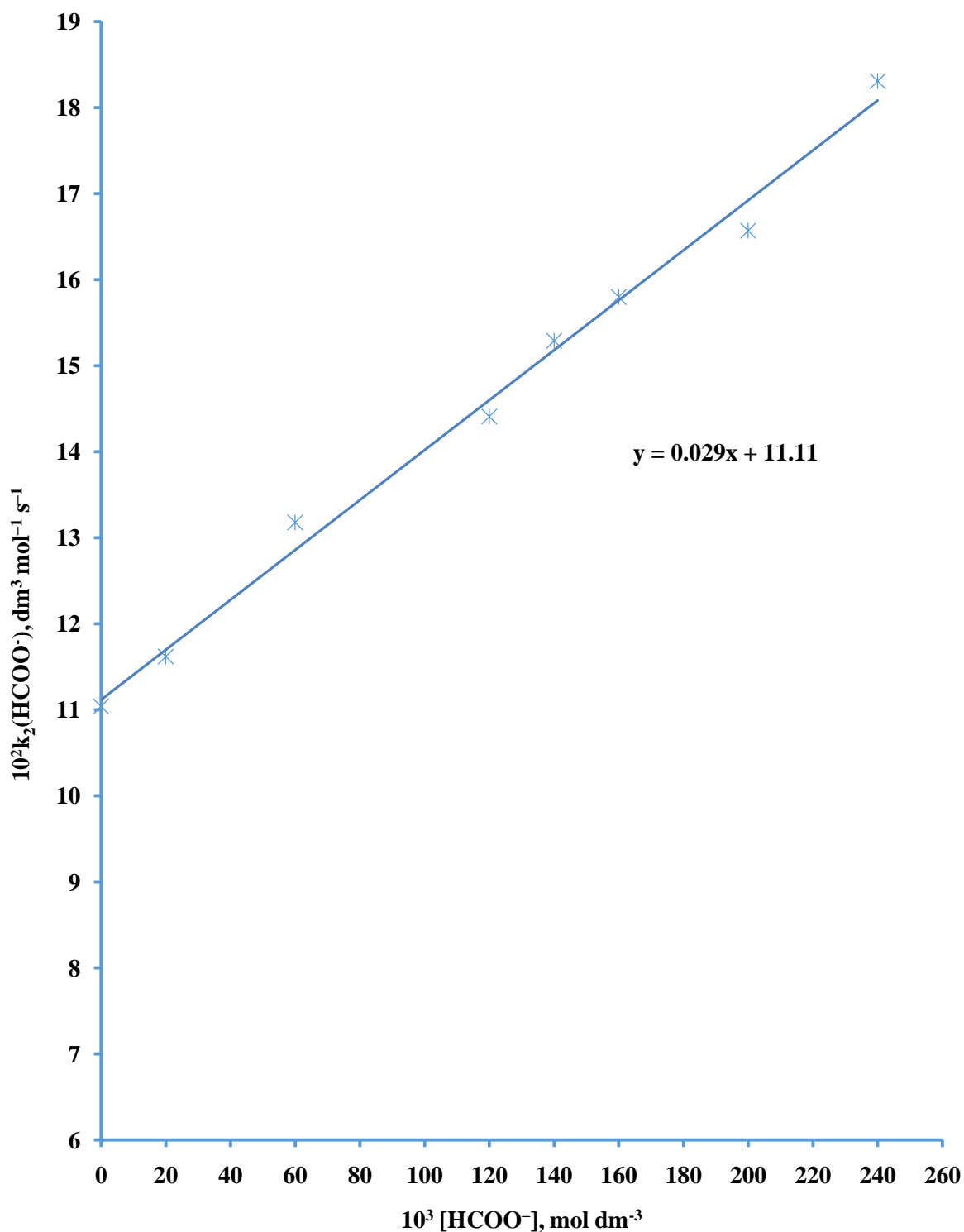


Figure 4.44: Plot of $k_2(\text{HCOO}^-)$ versus $[\text{HCOO}^-]$ for the Reaction of $[(\text{H}_2\text{O})_2\text{Ru}_2\text{O}]^{4+}$ and $\text{S}_2\text{O}_4^{2-}$ at $[(\text{H}_2\text{O})_2\text{Ru}_2\text{O}^{4+}] = 5.75 \times 10^{-5} \text{ mol dm}^{-3}$, $[\text{S}_2\text{O}_4^{2-}] = 4.31 \times 10^{-2} \text{ mol dm}^{-3}$, $[\text{HCOO}^-] = (0.0 - 24.0) \times 10^{-2} \text{ mol dm}^{-3}$, $I = 0.5 \text{ mol dm}^{-3}$, $T = 31 \text{ } ^\circ\text{C}$ and $\lambda_{\text{max}} = 660 \text{ nm}$

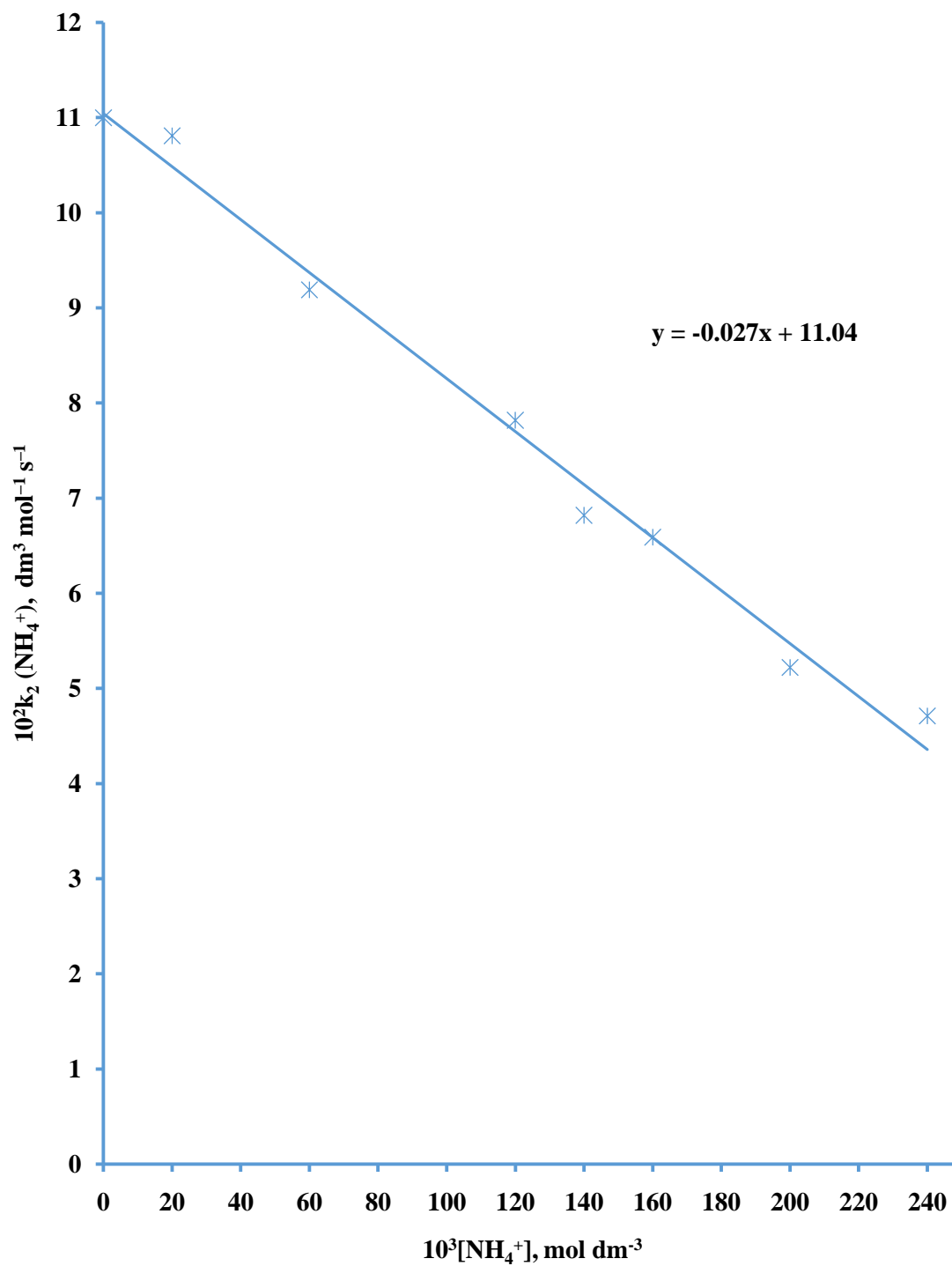


Figure 4.45: Plot of $k_2 (\text{NH}_4^+)$ versus $[\text{NH}_4^+]$ for the Reaction of $[(\text{H}_2\text{O})_2\text{Ru}_2\text{O}]^{4+}$ and $\text{S}_2\text{O}_4^{2-}$ at $[(\text{H}_2\text{O})_2\text{Ru}_2\text{O}^{4+}] = 5.75 \times 10^{-5} \text{ mol dm}^{-3}$, $[\text{S}_2\text{O}_4^{2-}] = 4.31 \times 10^{-2} \text{ mol dm}^{-3}$, $[\text{NH}_4^+] = (0.0 - 24.0) \times 10^{-2} \text{ mol dm}^{-3}$, $I = 0.5 \text{ mol dm}^{-3}$, $T = 31 \text{ } ^\circ\text{C}$ and $\lambda_{\text{max}} = 660 \text{ nm}$

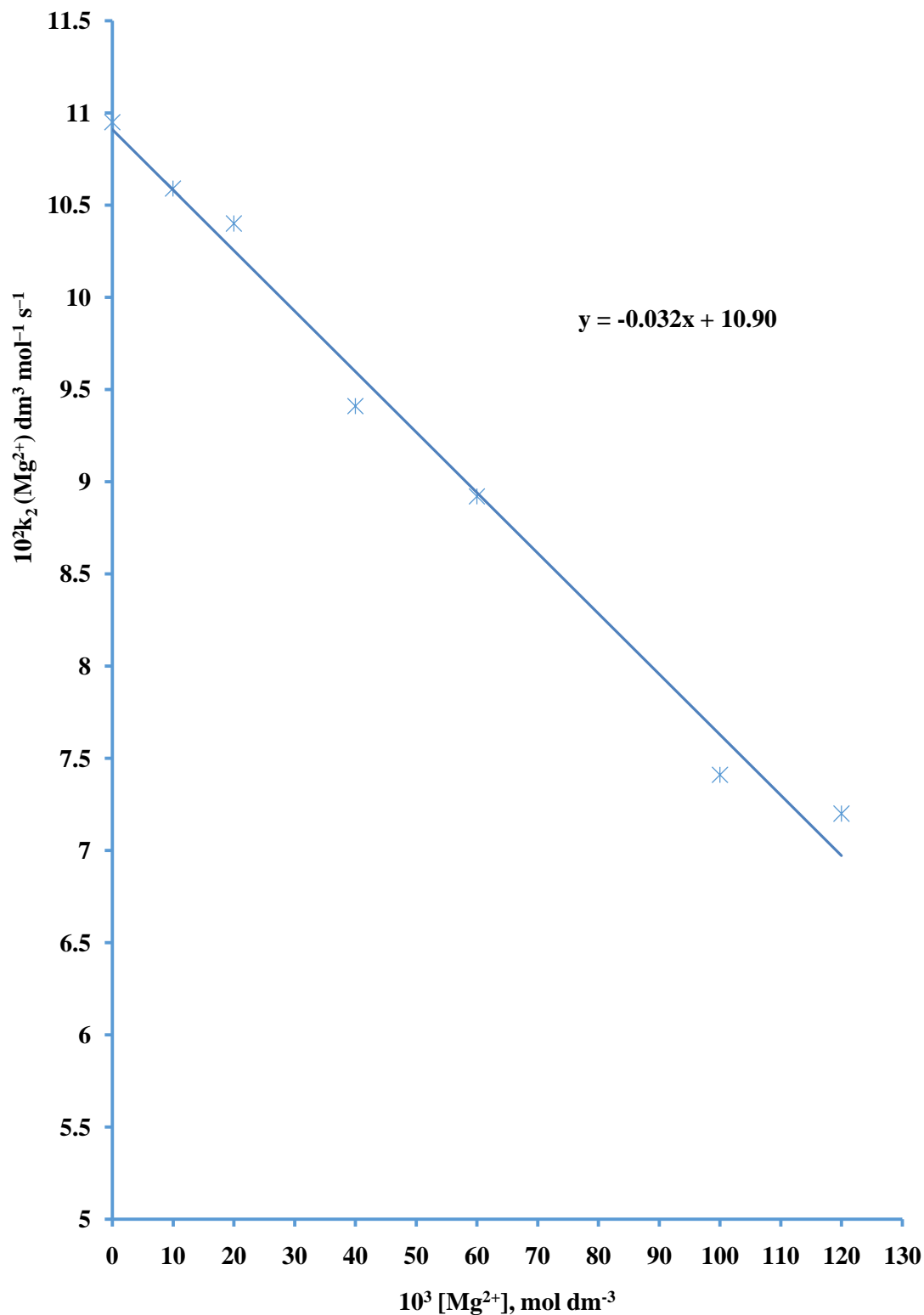


Figure 4.46: Plot of $k_2 (\text{Mg}^{2+})$ versus $[\text{Mg}^{2+}]$ for the Reaction of $[(\text{H}_2\text{O})_2\text{Ru}_2\text{O}]^{4+}$ and $\text{S}_2\text{O}_4^{2-}$ at $[(\text{H}_2\text{O})_2\text{Ru}_2\text{O}^{4+}] = 5.75 \times 10^{-5} \text{ mol dm}^{-3}$, $[\text{S}_2\text{O}_4^{2-}] = 4.31 \times 10^{-2} \text{ mol dm}^{-3}$, $[\text{Mg}^{2+}] = (0.0 - 12.0) \times 10^{-2} \text{ mol dm}^{-3}$, $I = 0.5 \text{ mol dm}^{-3}$, $T = 31 \pm 1 \text{ }^\circ\text{C}$ and $\lambda_{\text{max}} = 660 \text{ nm}$

where $X = \text{Mg}^{2+}$ and NH_4^+ ; p = intercept and q = slope.

Results obtained showed that for :

$$\text{CH}_3\text{COO}^- \quad 'p' = 10.95 \times 10^{-2} \text{ dm}^3 \text{ mol}^{-1} \text{ s}^{-1} \text{ and } 'q' = 3.50 \times 10^{-2} \text{ dm}^6 \text{ mol}^{-2} \text{ s}^{-1}$$

$$\text{HCOO}^- \quad 'p' = 11.12 \times 10^{-2} \text{ dm}^3 \text{ mol}^{-1} \text{ s}^{-1} \text{ and } 'q' = 2.90 \times 10^{-2} \text{ dm}^6 \text{ mol}^{-2} \text{ s}^{-1}$$

$$\text{NH}_4^+ \quad 'p' = 11.04 \times 10^{-2} \text{ dm}^3 \text{ mol}^{-1} \text{ s}^{-1} \text{ and } 'q' = 2.80 \times 10^{-2} \text{ dm}^6 \text{ mol}^{-2} \text{ s}^{-1}$$

$$\text{Mg}^{2+} \quad 'p' = 10.97 \times 10^{-2} \text{ dm}^3 \text{ mol}^{-1} \text{ s}^{-1} \text{ and } 'q' = 33.85 \times 10^{-2} \text{ dm}^6 \text{ mol}^{-2} \text{ s}^{-1}$$

4.7.4 Ru_2O^{4+} reaction with H_3PO_2

At constant concentrations of all other reactants and reacting conditions, the effect of added ions on the rates of reaction was investigated by varying the concentrations of the ions (CH_3COO^- , HCOO^- , NH_4^+ , and Mg^{2+}) from $(0 - 160) \times 10^{-3} \text{ mol dm}^{-3}$ for CH_3COO^- , HCOO^- , NH_4^+ and $(0 - 120) \times 10^{-3} \text{ mol dm}^{-3}$ for Mg^{2+} . The studies showed that the rate constants for Ru_2O^{4+} reaction with H_3PO_2 was unaffected by the presence of the ions (Tables 4.32 and 4.33).

4.7.5 Ru_2O^{4+} reaction with the alcohols (CH_3OH , $\text{C}_2\text{H}_5\text{OH}$, $\text{C}_3\text{H}_7\text{OH}$)

For the reactions of Ru_2O^{4+} reaction with CH_3OH , $\text{C}_2\text{H}_5\text{OH}$ and $\text{C}_3\text{H}_7\text{OH}$, concentrations of the added ions was varied from $(0 - 120.0) \times 10^{-3} \text{ mol dm}^{-3}$ (Mg^{2+} , NH_4^+ , CH_3COO^- , NO_3^- and HCOO^-), keeping the other reactants and reacting conditions constant. It was found that the rate constants decreased with increase in the concentrations of added ions (Table 4.34 – 4.36). The plot of the ion-dependent second order rate constant, $k_2(X)$, versus concentrations of the ions, $[X]$ are presented as Figures 4.47 – 4.52. The relationship between the ion dependent second order rate constant, $k_2(X)$, and the concentrations of the ions for this system is given by Equation 4.23.

Table 4.32: Effect of Added Anions to Reaction Medium for the Reaction of

$[(\text{H}_2\text{O})_2\text{Ru}_2\text{O}]^{4+}$ and H_3PO_2 at $[(\text{H}_2\text{O})_2\text{Ru}_2\text{O}]^{4+} = 6.0 \times 10^{-5} \text{ mol dm}^{-3}$,
 $[\text{H}_3\text{PO}_2] = 9.6 \times 10^{-2} \text{ mol dm}^{-3}$, $[\text{H}^+] = 5.0 \times 10^{-2} \text{ mol dm}^{-3}$, $I = 0.5 \text{ mol dm}^{-3}$, $T = 31 \pm 1 \text{ }^\circ\text{C}$ and $\lambda_{\text{max}} = 660 \text{ nm}$

Ion	$10^3[\text{ion}]$	$10^4 k_{\text{obs}}, \text{ s}^{-1}$	$10^2 k_2, \text{ dm}^3 \text{ mol}^{-1} \text{ s}^{-1}$
	mol dm^{-3}		
CH_3COO^-	0.00	6.82	7.10
	20.00	6.80	7.08
	40.00	6.84	7.13
	60.00	6.83	7.12
	100.00	6.83	7.12
	120.00	6.84	7.13
	160.00	6.82	7.10
HCOO^-	0.00	6.82	7.10
	20.00	6.84	7.13
	40.00	6.80	7.08
	60.00	6.84	7.13
	100.00	6.83	7.12
	120.00	6.83	7.12
	160.00	6.82	7.10

Table 4.33: Effect of Added Cations to Reaction Medium for the Reaction of

$[(\text{H}_2\text{O})_2\text{Ru}_2\text{O}]^{4+}$ and H_3PO_2 at $[(\text{H}_2\text{O})_2\text{Ru}_2\text{O}]^{4+} = 6.0 \times 10^{-5} \text{ mol dm}^{-3}$,
 $[\text{H}_3\text{PO}_2] = 9.6 \times 10^{-2} \text{ mol dm}^{-3}$, $[\text{H}^+] = 5.0 \times 10^{-2} \text{ mol dm}^{-3}$, $I = 0.5 \text{ mol dm}^{-3}$, $T = 31 \pm 1 \text{ }^\circ\text{C}$ and $\lambda_{\text{max}} = 660 \text{ nm}$

Ion	$10^3[\text{ion}]$ mol dm^{-3}	$10^4 k_{\text{obs}}, \text{ s}^{-1}$	$10^3 k_2, \text{ dm}^3 \text{ mol}^{-1} \text{ s}^{-1}$
NH_4^+	0.00	6.84	7.13
	10.00	6.80	7.08
	20.00	6.84	7.13
	40.00	6.83	7.12
	60.00	6.83	7.12
	100.00	6.82	7.10
	160.00	6.82	7.10
Mg^{2+}	0.00	6.82	7.10
	10.00	6.84	7.13
	20.00	6.82	7.10
	40.00	6.80	7.08
	60.00	6.84	7.13
	100.00	6.85	7.14
	120.00	6.83	7.12

Table 4.34: Effect of Added Cations to Reaction Medium for the Reaction of
 $[(\text{H}_2\text{O})_2\text{Ru}_2\text{O}]^{4+}$ and CH_3OH at $[(\text{H}_2\text{O})_2\text{Ru}_2\text{O}]^{4+} = 5.5 \times 10^{-5} \text{ mol dm}^{-3}$,
 $[\text{CH}_3\text{OH}] = 16.5 \times 10^{-2} \text{ mol dm}^{-3}$, $I = 0.5 \text{ mol dm}^{-3}$, $T = 31 \pm 1 \text{ }^\circ\text{C}$ and
 $\lambda_{\text{max}} = 660 \text{ nm}$

Ion	$10^3[\text{ion}]$ mol dm^{-3}	$10^4 k_{\text{obs}}, \text{ s}^{-1}$	$10^3 k_2, \text{ dm}^3 \text{ mol}^{-1} \text{ s}^{-1}$
Mg^{2+}	0.00	19.72	11.95
	10.00	19.14	11.60
	20.00	18.18	11.02
	40.00	17.16	10.40
	60.00	15.38	9.32
	100.00	12.99	7.87
	120.00	11.22	6.80
NH_4^+	0.00	19.81	12.01
	20.00	19.16	11.61
	60.00	18.81	11.40
	120.00	17.84	10.81
	140.00	16.70	10.12
	160.00	15.08	9.14
	240.00	13.53	8.20

Table 4.35: Effect of Added Cations to Reaction Medium for the Reaction of

$[(\text{H}_2\text{O})_2\text{Ru}_2\text{O}]^{4+}$ and $\text{C}_2\text{H}_5\text{OH}$ at $[(\text{H}_2\text{O})_2\text{Ru}_2\text{O}]^{4+} = 6.5 \times 10^{-5} \text{ mol dm}^{-3}$,
 $[\text{C}_2\text{H}_5\text{OH}] = 13.0 \times 10^{-2} \text{ mol dm}^{-3}$, $I = 0.5 \text{ mol dm}^{-3}$, $T = 31 \pm 1 \text{ }^\circ\text{C}$ and
 $\lambda_{\text{max}} = 660 \text{ nm}$

Ion	$10^3[\text{ion}]$ mol dm^{-3}	$10^4 k_{\text{obs}}, \text{ s}^{-1}$	$10^3 k_2, \text{ dm}^3 \text{ mol}^{-1} \text{ s}^{-1}$
Mg^{2+}	0.00	11.45	8.81
	10.00	10.78	8.29
	20.00	10.15	7.81
	40.00	9.39	7.22
	60.00	8.13	6.25
	100.00	6.12	4.71
	120.00	4.84	3.72
NH_4^+	0.00	11.43	8.79
	10.00	11.05	8.50
	20.00	10.80	8.31
	40.00	10.04	7.72
	60.00	9.13	7.02
	100.00	7.74	5.95
	120.00	6.81	5.24

Table 4.36: Effect of Added Anions to Reaction Medium for the Reaction of

$[(\text{H}_2\text{O})_2\text{Ru}_2\text{O}]^{4+}$ and $\text{C}_3\text{H}_7\text{OH}$ at $[(\text{H}_2\text{O})_2\text{Ru}_2\text{O}]^{4+} = 5.5 \times 10^{-5} \text{ mol dm}^{-3}$,
 $[\text{C}_3\text{H}_7\text{OH}] = 16.5 \times 10^{-2} \text{ mol dm}^{-3}$, $I = 0.5 \text{ mol dm}^{-3}$, $T = 31 \pm 1 \text{ }^\circ\text{C}$ and
 $\lambda_{\text{max}} = 660 \text{ nm}$

Ion	$10^3[\text{ion}]$	$10^4 k_{\text{obs}}, \text{ s}^{-1}$	$10^3 k_2, \text{ dm}^3 \text{ mol}^{-1} \text{ s}^{-1}$
	mol dm^{-3}		
CH_3COO^-	0.00	4.18	3.48
	10.00	3.97	3.31
	20.00	3.54	2.95
	40.00	3.18	2.65
	60.00	2.71	2.26
	120.00	1.15	0.96
	160.00	0.50	0.42
HCOO^-	0.00	4.21	3.51
	10.00	4.02	3.35
	20.00	3.84	3.20
	40.00	3.37	2.81
	60.00	2.94	2.45
	100.00	2.15	1.79
	120.00	0.98	0.82

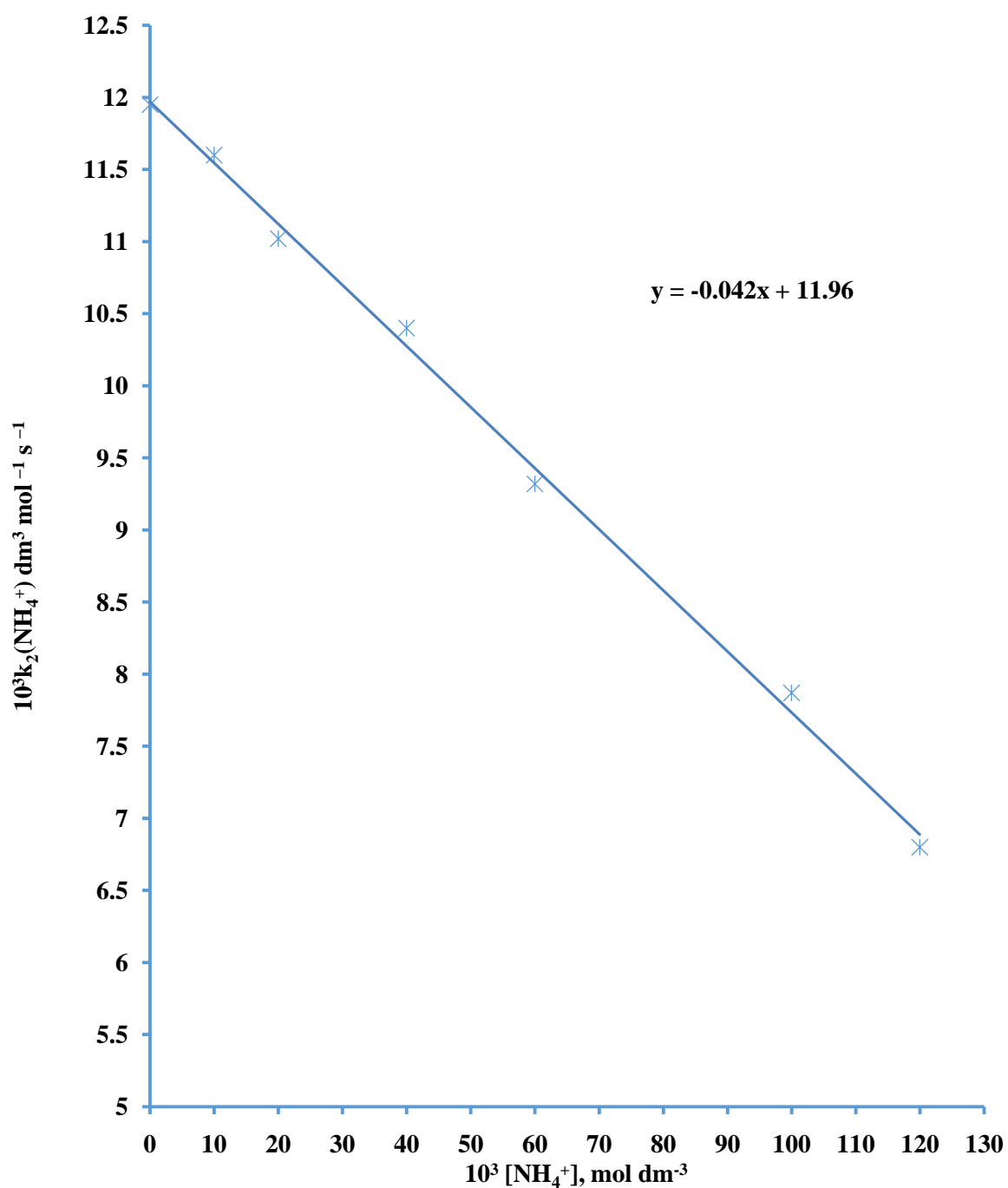


Figure 4.47: Plot of $k_2(\text{NH}_4^+)$ versus $[\text{NH}_4^+]$ for the Reaction of $[(\text{H}_2\text{O})_2\text{Ru}_2\text{O}]^{4+}$ and CH_3OH at $[(\text{H}_2\text{O})_2\text{Ru}_2\text{O}^{4+}] = 5.5 \times 10^{-5} \text{ mol dm}^{-3}$, $[\text{CH}_3\text{OH}] = 16.5 \times 10^{-2} \text{ mol dm}^{-3}$, $[\text{NH}_4^+] = (0.0 - 120.0) \times 10^{-3} \text{ mol dm}^{-3}$, $I = 0.5 \text{ mol dm}^{-3}$, $T = 321 \text{ K}$ and $\lambda_{\text{max}} = 660 \text{ nm}$

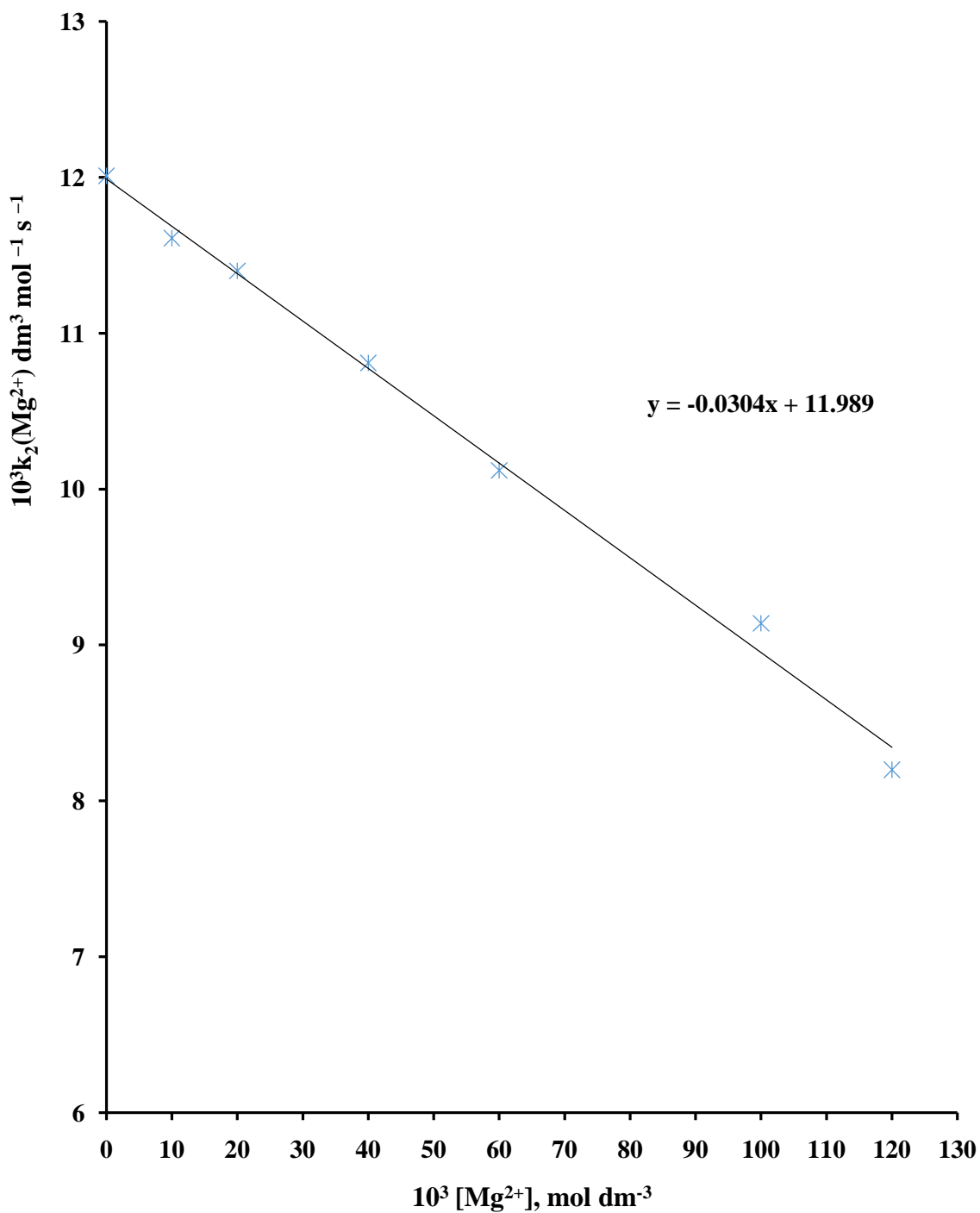


Figure 4.48: Plot of $k_2(\text{Mg}^{2+})$ versus $[\text{Mg}^{2+}]$ for the Reaction of $[(\text{H}_2\text{O})_2\text{Ru}_2\text{O}]^{4+}$ and CH_3OH at $[(\text{H}_2\text{O})_2\text{Ru}_2\text{O}^{4+}] = 5.5 \times 10^{-5} \text{ mol dm}^{-3}$, $[\text{CH}_3\text{OH}] = 16.5 \times 10^{-2} \text{ mol dm}^{-3}$, $[\text{Mg}^{2+}] = (0.0 - 120.0) \times 10^{-3} \text{ mol dm}^{-3}$, $I = 0.5 \text{ mol dm}^{-3}$, $T = 31 \pm 1 \text{ }^\circ\text{C}$ and $\lambda_{\text{max}} = 660 \text{ nm}$

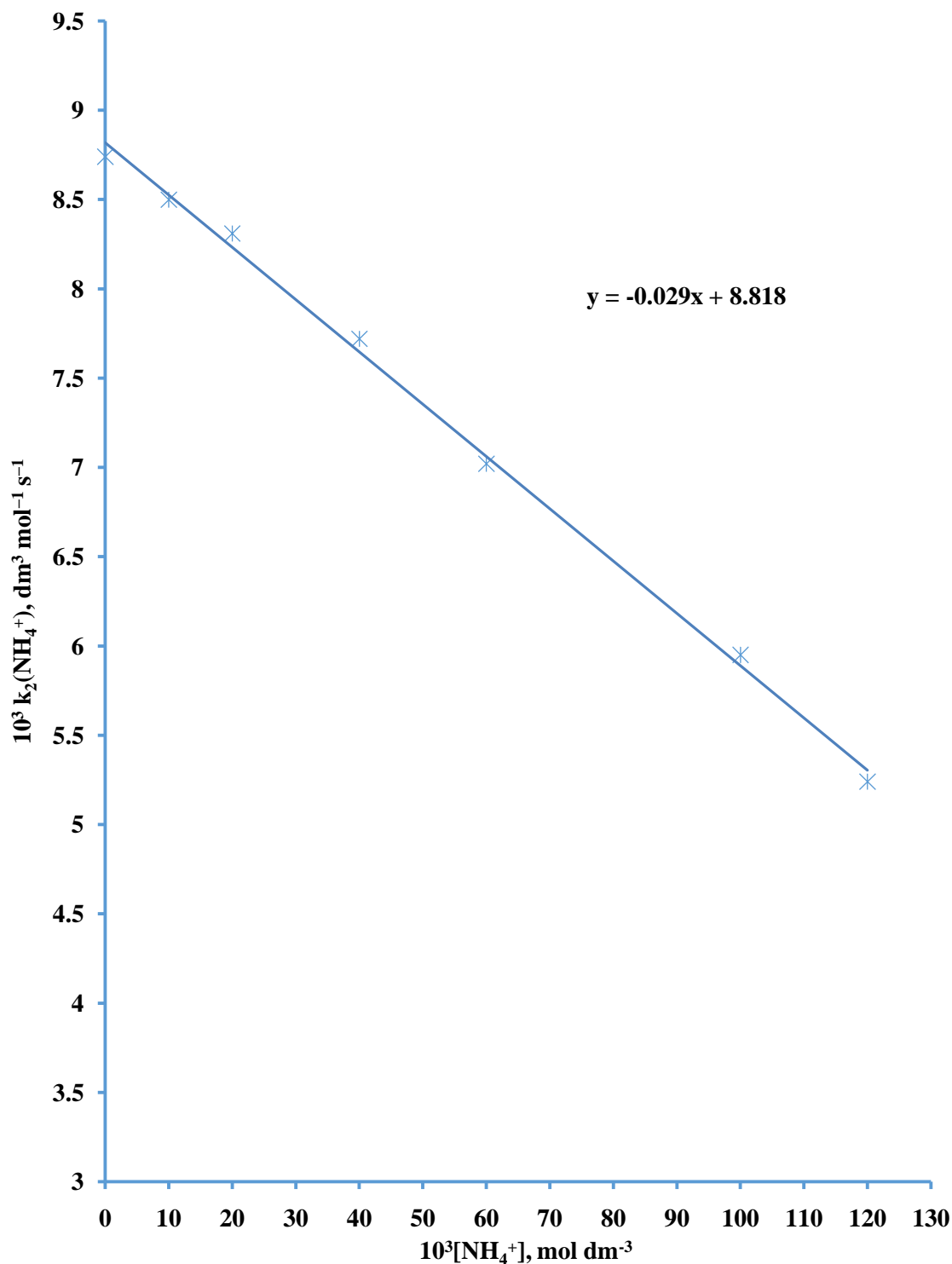


Figure 4.49: Plot of $k_2(\text{NH}_4^+)$ versus $[\text{NH}_4^+]$ for the Reaction of $[(\text{H}_2\text{O})_2\text{Ru}_2\text{O}]^{4+}$ and $\text{C}_2\text{H}_5\text{OH}$ at $[(\text{H}_2\text{O})_2\text{Ru}_2\text{O}^{4+}] = 6.5 \times 10^{-5} \text{ mol dm}^{-3}$, $[\text{C}_2\text{H}_5\text{OH}] = 13.00 \times 10^{-2} \text{ mol dm}^{-3}$, $[\text{NH}_4^+] = (0.0 - 120.0) \times 10^{-3} \text{ mol dm}^{-3}$, $I = 0.5 \text{ mol dm}^{-3}$, $T = 32 \pm 1 \text{ C}$ and $\lambda_{\text{max}} = 660 \text{ nm}$

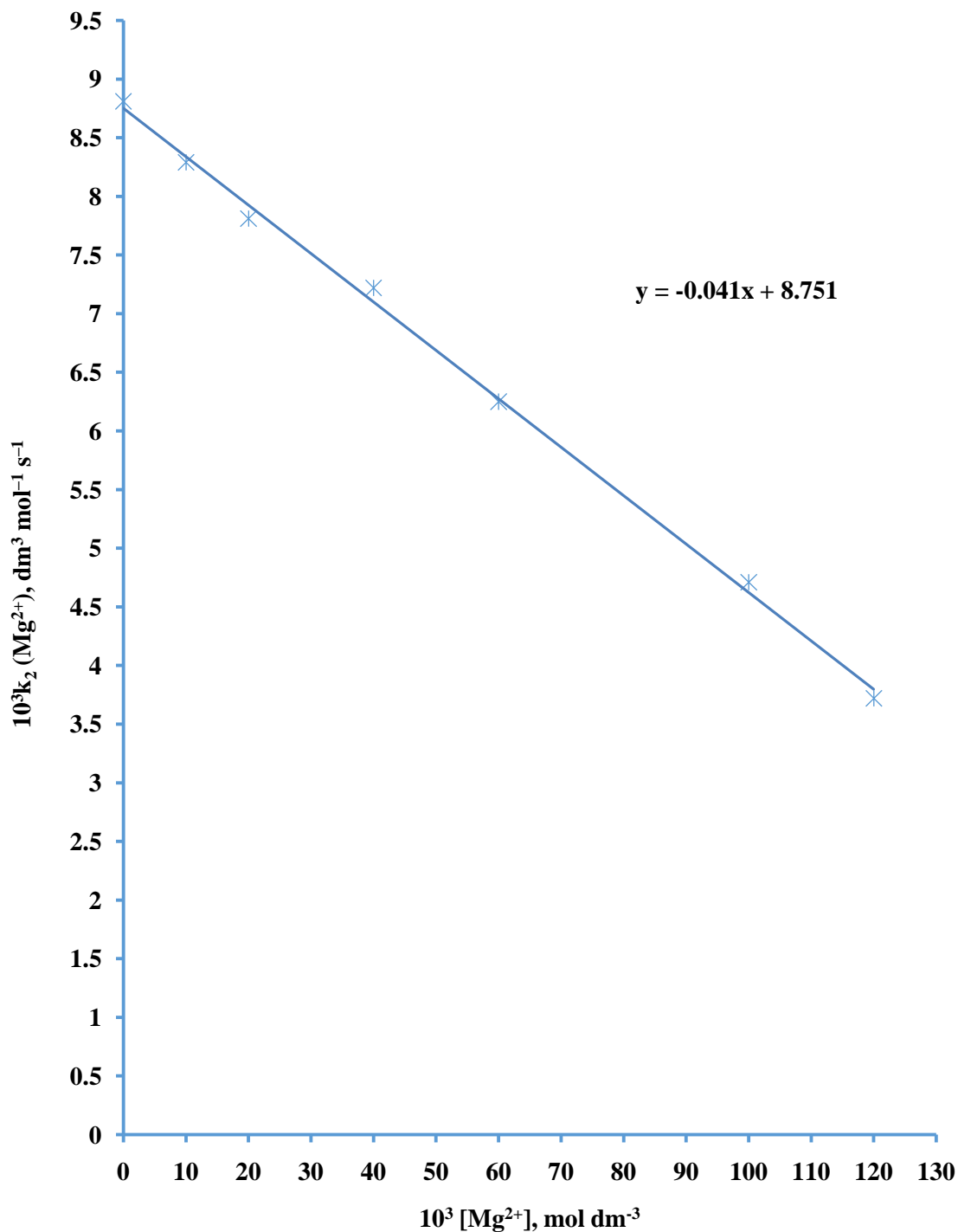


Figure 4.50: Plot of $k_2 (\text{Mg}^{2+})$ versus $[\text{Mg}^{2+}]$ for the Reaction of $[(\text{H}_2\text{O})_2\text{Ru}_2\text{O}]^{4+}$ and $\text{C}_2\text{H}_5\text{OH}$ at $[(\text{H}_2\text{O})_2\text{Ru}_2\text{O}^{4+}] = 6.5 \times 10^{-5} \text{ mol dm}^{-3}$, $[\text{C}_2\text{H}_5\text{OH}] = 13.00 \times 10^{-2} \text{ mol dm}^{-3}$, $[\text{Mg}^{2+}] = (0.0 - 120.0) \times 10^{-3} \text{ mol dm}^{-3}$, $I = 0.5 \text{ mol dm}^{-3}$, $T = 31 \text{ } ^\circ\text{C}$ and $\lambda_{\text{max}} = 660 \text{ nm}$

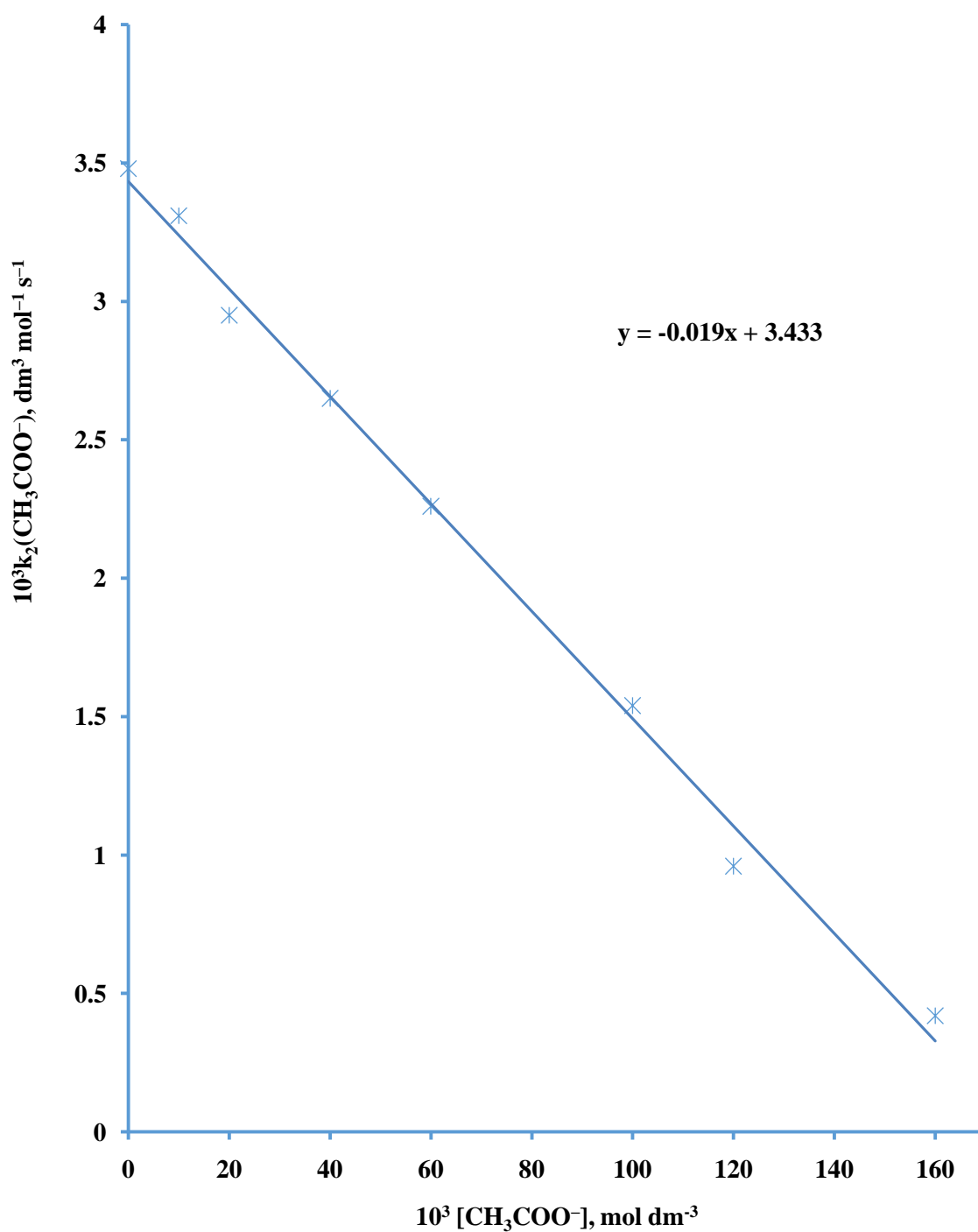


Figure 4.51: Plot of $k_2(\text{CH}_3\text{COO}^-)$ versus $[\text{CH}_3\text{COO}^-]$ for the Reaction of $[(\text{H}_2\text{O})_2\text{Ru}_2\text{O}]^{4+}$ and $\text{C}_3\text{H}_7\text{OH}$ at $[(\text{H}_2\text{O})_2\text{Ru}_2\text{O}^{4+}] = 6.0 \times 10^{-5} \text{ mol dm}^{-3}$, $[\text{C}_3\text{H}_7\text{OH}] = 12.0 \times 10^{-2} \text{ mol dm}^{-3}$, $[\text{CH}_3\text{COO}^-] = (0.0 - 160.0) \times 10^{-3} \text{ mol dm}^{-3}$, $I = 0.5 \text{ mol dm}^{-3}$, $T = 31 \pm 1 \text{ }^\circ\text{C}$ and $\lambda_{\text{max}} = 660 \text{ nm}$

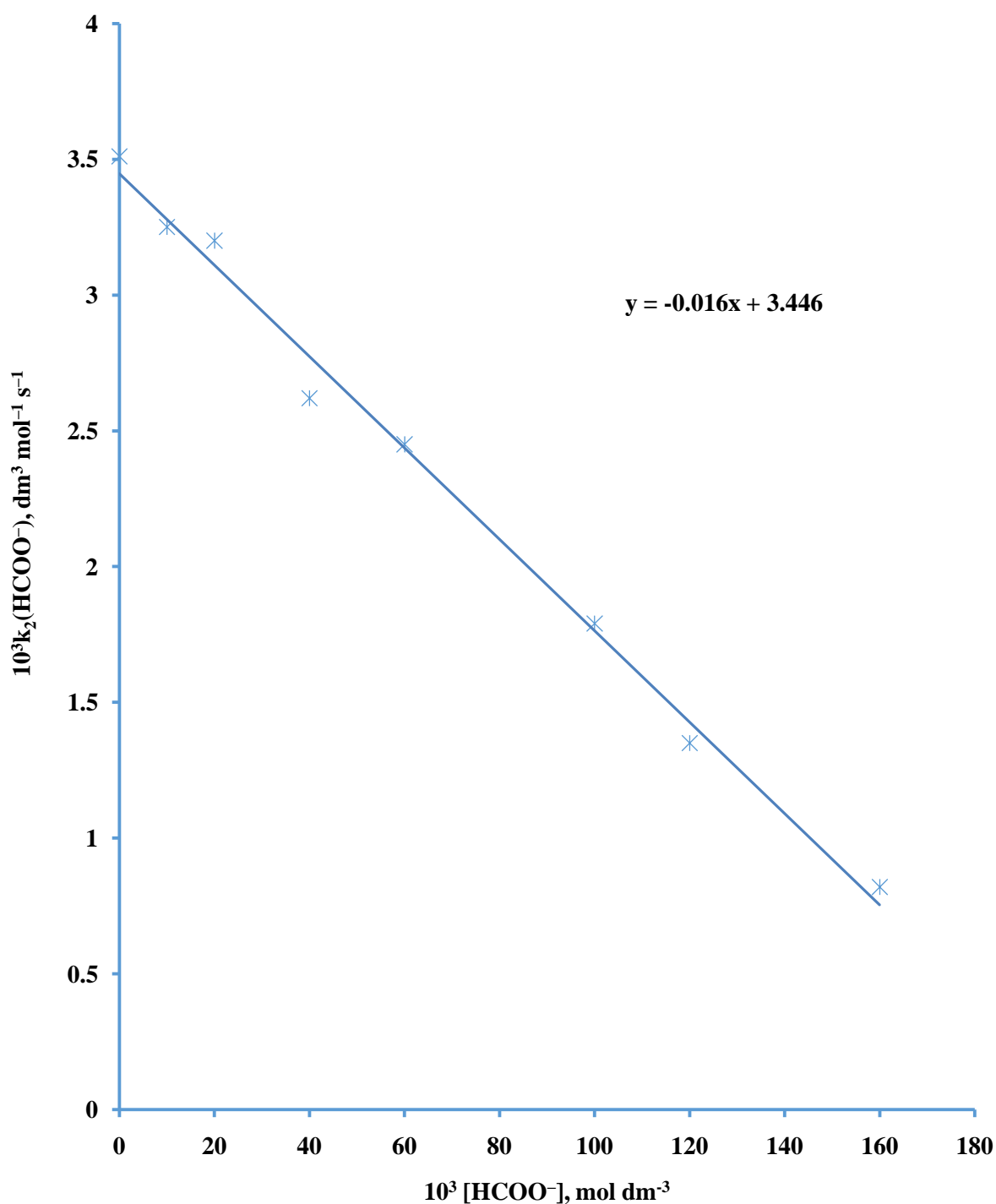


Figure 4.52: Plot of $k_2(\text{HCOO}^-)$ versus $[\text{HCOO}^-]$ for the Reaction of $[(\text{H}_2\text{O})_2\text{Ru}_2\text{O}]^{4+}$ and $\text{C}_3\text{H}_7\text{OH}$ at $[(\text{H}_2\text{O})_2\text{Ru}_2\text{O}^{4+}] = 6.0 \times 10^{-5} \text{ mol dm}^{-3}$, $[\text{C}_3\text{H}_7\text{OH}] = 12.0 \times 10^{-2} \text{ mol dm}^{-3}$, $[\text{HCOO}^-] = (0.0 - 160.0) \times 10^{-3} \text{ mol dm}^{-3}$, $I = 0.5 \text{ mol dm}^{-3}$, $T = 31 \text{ } ^\circ\text{C}$ and $\lambda_{\text{max}} = 660 \text{ nm}$

$$k_2(X) = p - q[X] \dots\dots\dots(4.23)$$

where $X = \text{Mg}^{2+}$ and NH_4^+ ; p = intercept and q = slope.

Results obtained showed that for:

Ru_2O^{4+} - CH_3OH system,

$$\text{NH}_4^+ \text{ 'p' } = 11.97 \times 10^{-3} \text{ dm}^3 \text{ mol}^{-1} \text{ s}^{-1} \text{ and 'q' } = -2.90 \times 10^{-2} \text{ dm}^6 \text{ mol}^{-2} \text{ s}^{-1}$$

$$\text{Mg}^{2+} \text{ , 'p' } = 11.99 \times 10^{-3} \text{ dm}^3 \text{ mol}^{-1} \text{ s}^{-1} \text{ and 'q' } = -3.04 \times 10^{-2} \text{ dm}^6 \text{ mol}^{-2} \text{ s}^{-1}$$

Ru_2O^{4+} - $\text{C}_2\text{H}_5\text{OH}$ system,

$$\text{Mg}^{2+} \text{ , 'p' } = 8.75 \times 10^{-3} \text{ dm}^3 \text{ mol}^{-1} \text{ s}^{-1} \text{ and 'q' } = -4.13 \times 10^{-2} \text{ dm}^6 \text{ mol}^{-2} \text{ s}^{-1}$$

$$\text{NH}_4^+ \text{ , 'p' } = 8.82 \times 10^{-3} \text{ dm}^3 \text{ mol}^{-1} \text{ s}^{-1} \text{ and 'q' } = -2.9-3 \times 10^{-2} \text{ dm}^6 \text{ mol}^{-2} \text{ s}^{-1}$$

Ru_2O^{4+} - $\text{C}_3\text{H}_7\text{OH}$ system,

$$\text{CH}_3\text{COO}^- \text{ , 'p' } = 3.43 \times 10^{-3} \text{ dm}^3 \text{ mol}^{-1} \text{ s}^{-1} \text{ and 'q' } = -1.94 \times 10^{-2} \text{ dm}^6 \text{ mol}^{-2} \text{ s}^{-1}$$

$$\text{HCOO}^- \text{ , 'p' } = 3.44 \times 10^{-2} \text{ dm}^3 \text{ mol}^{-1} \text{ s}^{-1} \text{ and 'q' } = -1.68 \times 10^{-2} \text{ dm}^6 \text{ mol}^{-2} \text{ s}^{-1} .$$

4.8 Test for the Formation of Intermediate Complex

4.8.1 Spectroscopic test

Spectroscopic tests were carried out to ascertain whether any spectroscopically determinable intermediate complex was formed from the reaction of the oxidant and the reductants. The electronic spectra of reacting mixtures were run between 400 – 800nm for the Ru_2O^{4+} - reductant systems at intervals of one, three or six minutes of reaction. These studies showed that for all the systems under study, there was no enhancement of absorption, neither was there any shift in λ_{max} .

4.8.2 Michaelis-Menten Plots

Least square plots of $1/k_{\text{obs}}$ versus $1/[\text{reductant}]$ for the Ru_2O^{4+} -reductant systems gave straight lines with negligible intercepts. These plots are presented in Figures 4.53 – 4.62.

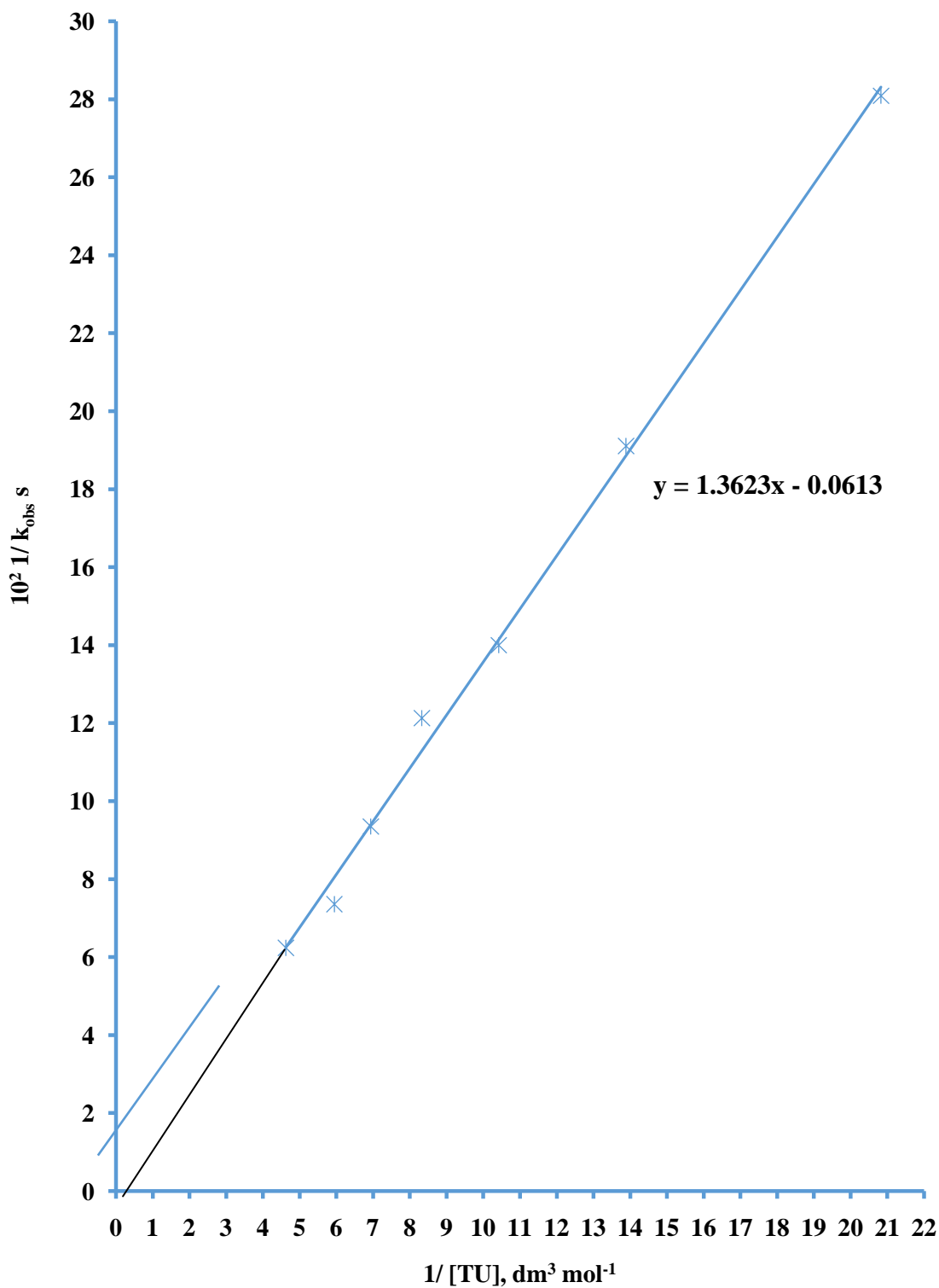


Figure 4.53: Plot of $1/k_{\text{obs}}$ versus $1/[TU]$ for the Reaction of $[(\text{H}_2\text{O})_2\text{Ru}_2\text{O}^{4+}]$ and Thiourea [TU] at $[(\text{H}_2\text{O})_2\text{Ru}_2\text{O}^{4+}] = 6.0 \times 10^{-5} \text{ mol dm}^{-3}$, $[TU] = (4.8 - 21.60) \times 10^{-2} \text{ mol dm}^{-2}$, $[\text{H}^+] = 5.0 \times 10^{-2} \text{ mol dm}^{-3}$, $I = 0.5 \text{ mol dm}^{-3}$, $T = 31 \text{ } ^\circ\text{C}$ and $\lambda_{\text{max}} = 660 \text{ nm}$

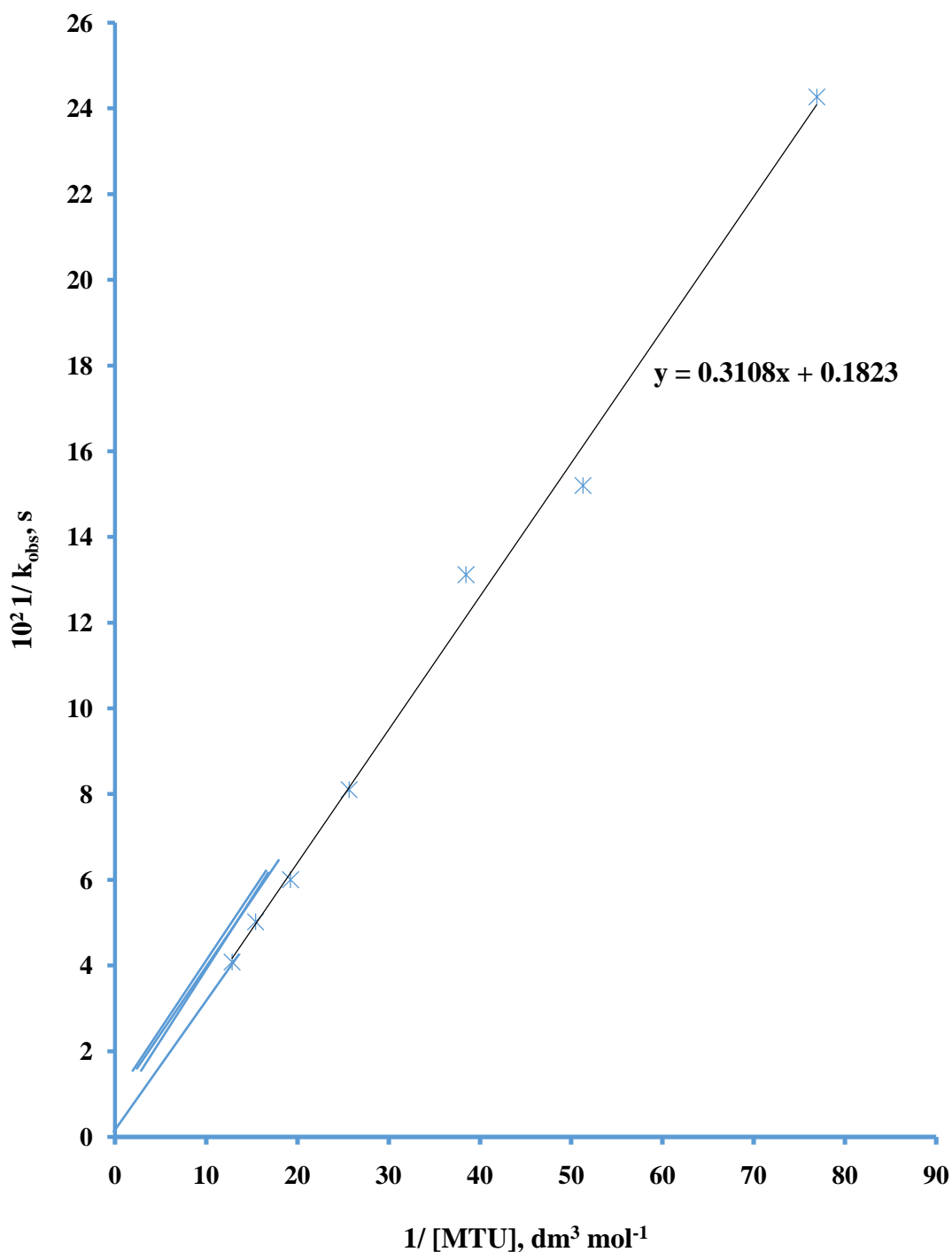


Figure 4.54: Plot of $1/k_{\text{obs}}$ versus $1/[\text{MTU}]$ for the Reaction of $(\text{H}_2\text{O})_2\text{Ru}_2\text{O}^{4+}$ and *N*-methylthiourea (MTU) at $[(\text{H}_2\text{O})_2\text{Ru}_2\text{O}^{4+}] = 6.5 \times 10^{-5} \text{ mol dm}^{-3}$, $[\text{MTU}] = (1.3\text{-}7.80) \times 10^{-2} \text{ mol dm}^{-3}$, $[\text{H}^+] = 5.0 \times 10^{-2} \text{ mol dm}^{-3}$, $I = 0.5 \text{ mol dm}^{-3}$, $T = 31 \pm 1 \text{ }^\circ\text{C}$ and $\lambda_{\text{max}} = 660 \text{ nm}$

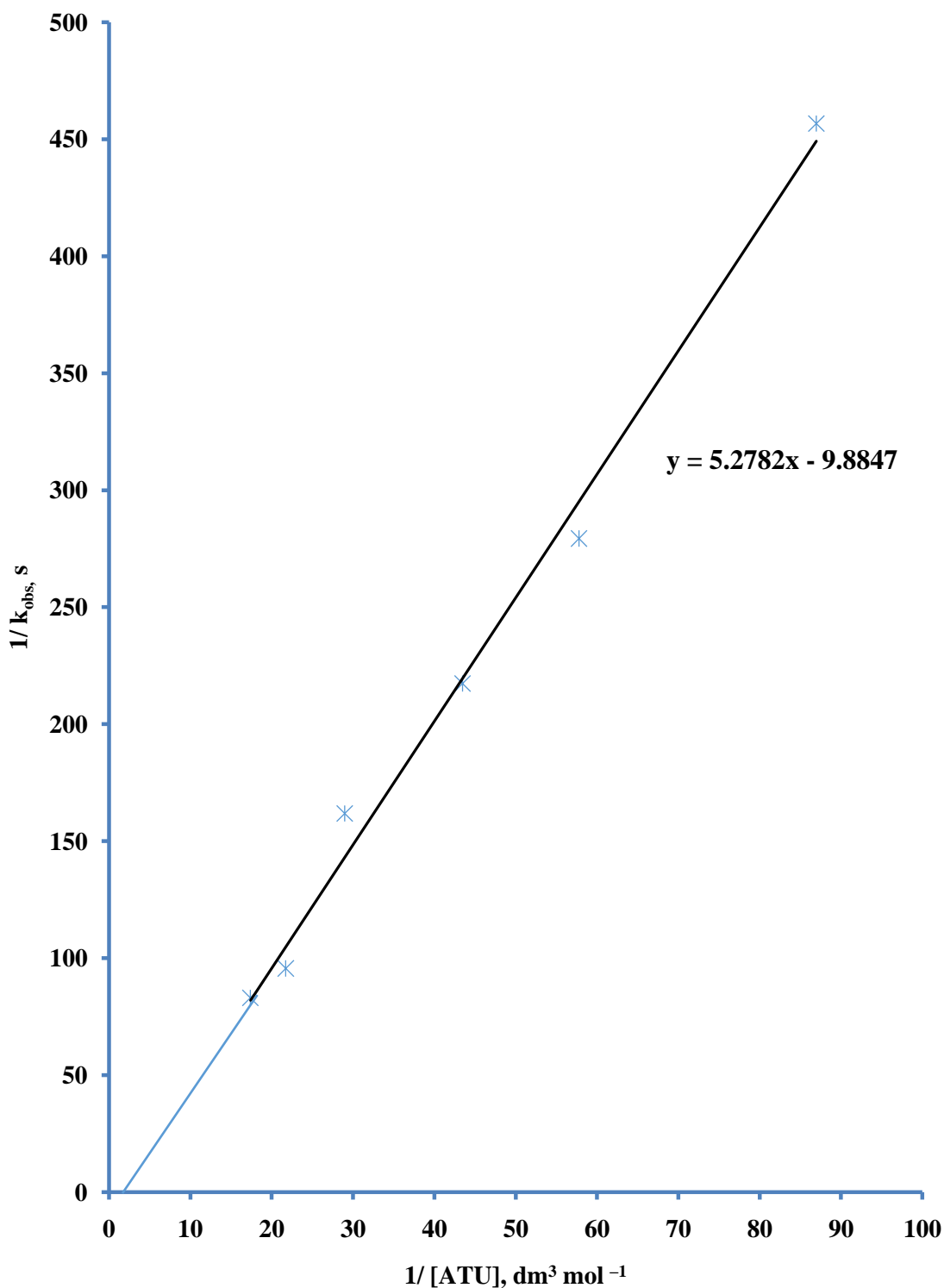


Figure 4.55 : Plot of $1/k_{\text{obs}}$ versus $1/[ATU]$ for the Reaction of $[(\text{H}_2\text{O})_2\text{Ru}_2\text{O}]^{4+}$ and *N*-allylthiourea (ATU) at $[(\text{H}_2\text{O})_2\text{Ru}_2\text{O}^{4+}] = 5.75 \times 10^{-5} \text{ mol dm}^{-3}$, $[\text{ATU}] = (1.15-5.75) \times 10^{-2} \text{ mol dm}^{-3}$, $[\text{H}^+] = 5.0 \times 10^{-2} \text{ mol dm}^{-3}$, $I = 0.5 \text{ mol dm}^{-3}$, $T = 31 \pm 1 \text{ }^\circ\text{C}$ and $\lambda_{\text{max}} = 660 \text{ nm}$

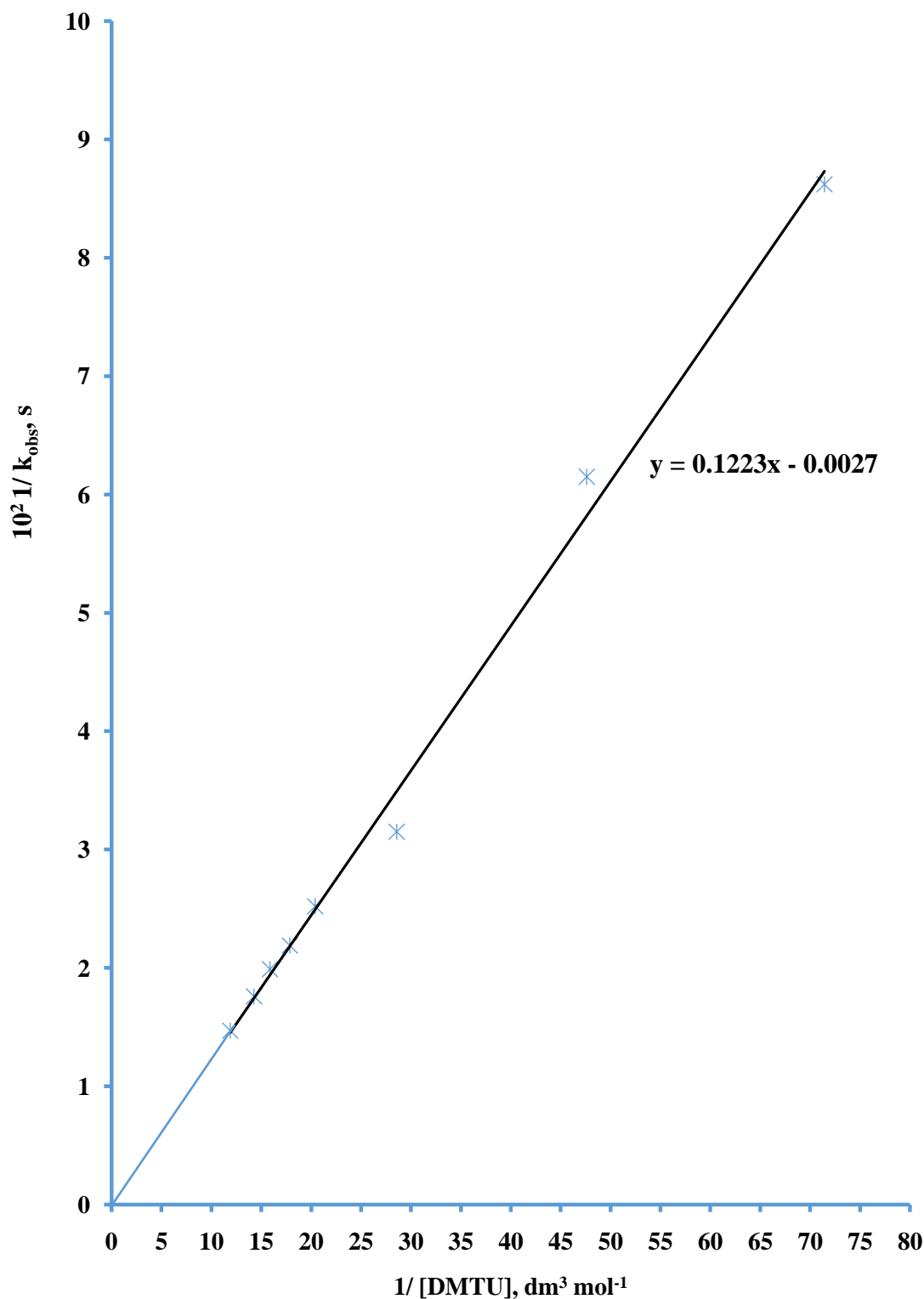


Figure 4.56: Plot of $1/k_{\text{obs}}$ versus $1/[\text{DMTU}]$ for the Reaction of $[(\text{H}_2\text{O})_2\text{Ru}_2\text{O}]^{4+}$ and N,N' -dimethylthiourea (DMTU) at $[(\text{H}_2\text{O})_2\text{Ru}_2\text{O}^{4+}] = 7.0 \times 10^{-5} \text{ mol dm}^{-3}$, $[\text{DMTU}] = (1.4 - 8.4) \times 10^{-2} \text{ mol dm}^{-3}$, $[\text{H}^+] = 5.0 \times 10^{-2} \text{ mol dm}^{-3}$, $I = 0.5 \text{ mol dm}^{-3}$, $T = 31 \text{ } ^\circ\text{C}$ and $\lambda_{\text{max}} = 660 \text{ nm}$

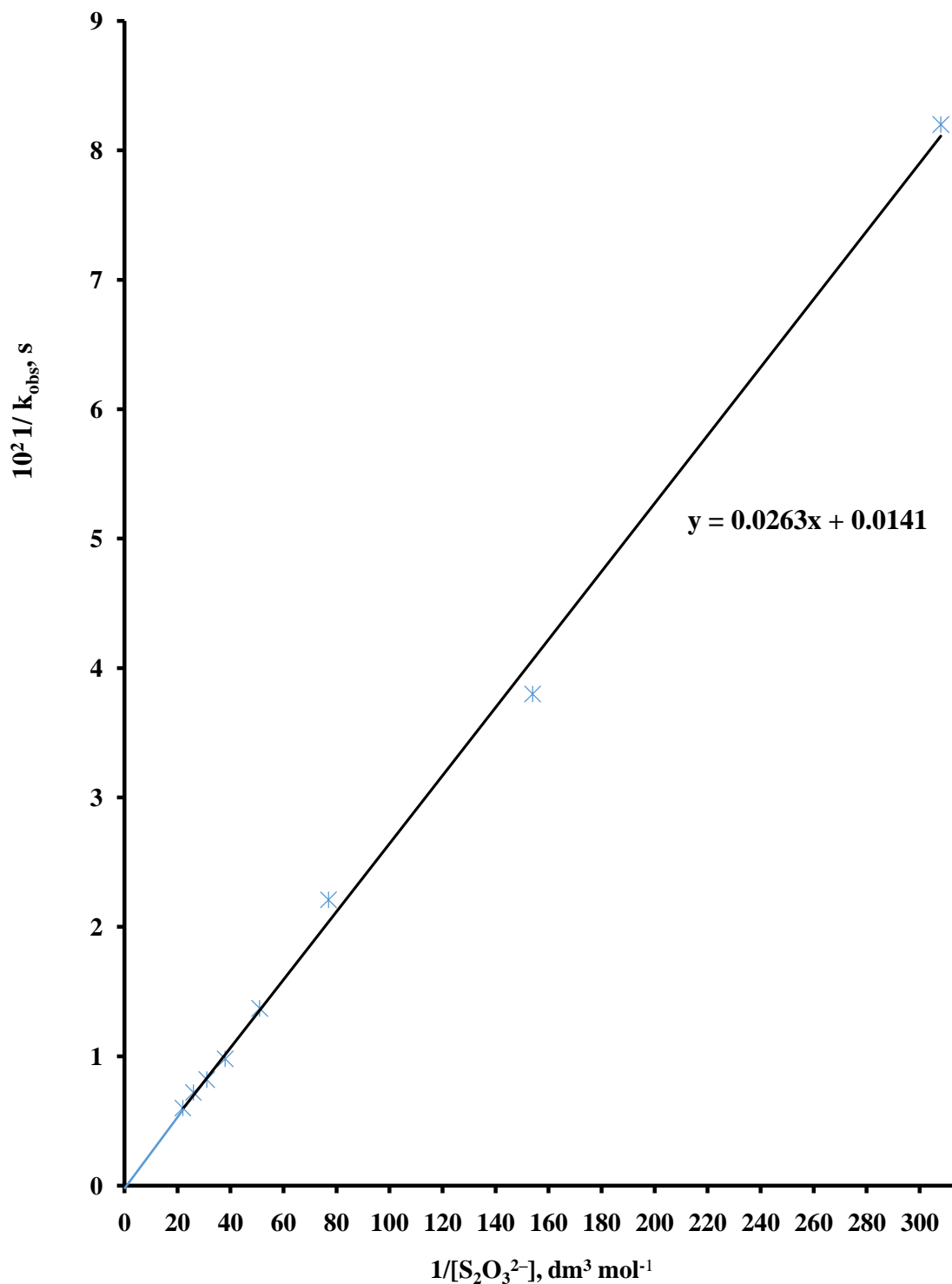


Figure 4.57: Plot of $1/k_{\text{obs}}$ versus $1/[S_2O_3^{2-}]$ for the Reaction of $[(H_2O)_2Ru_2O]^{4+}$ and Thiosulphate ($S_2O_3^{2-}$) at $[(H_2O)_2Ru_2O^{4+}] = 6.5 \times 10^{-5} \text{ mol dm}^{-3}$, $[S_2O_3^{2-}] = (3.25 - 45.50) \times 10^{-3} \text{ mol dm}^{-3}$, $[H^+] = 5.0 \times 10^{-2} \text{ mol dm}^{-3}$, $I = 0.5 \text{ mol dm}^{-3}$, $T = 31 \text{ } ^\circ\text{C}$ and $\lambda_{\text{max}} = 660 \text{ nm}$

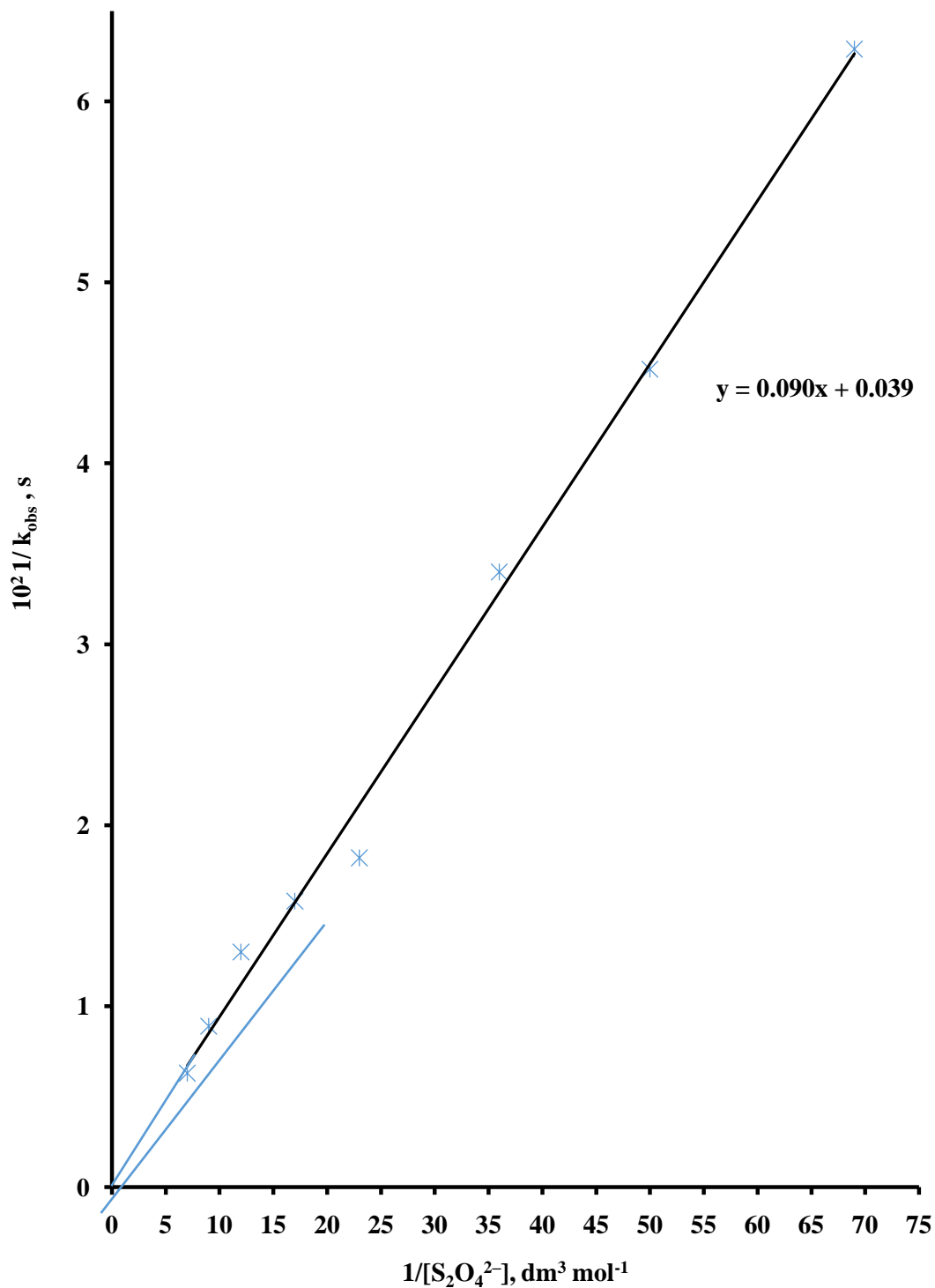


Figure 4.58: Plot of $1/k_{\text{obs}}$ versus $1/[S_2O_4^{2-}]$ for the Reaction of $[(H_2O)_2Ru_2O]^{4+}$ and Dithionite ($S_2O_4^{2-}$) at $[(H_2O)_2Ru_2]O^{4+} = 5.75 \times 10^{-5} \text{ mol dm}^{-3}$, $[S_2O_4^{2-}] = (1.44-14.38) \times 10^{-2} \text{ mol dm}^{-3}$, $[H^+] = 5.0 \times 10^{-2} \text{ mol dm}^{-3}$; $I = 0.5 \text{ mol dm}^{-3}$; $T = 31 \pm 1 \text{ } ^\circ\text{C}$ and $\lambda_{\text{max}} = 660 \text{ nm}$

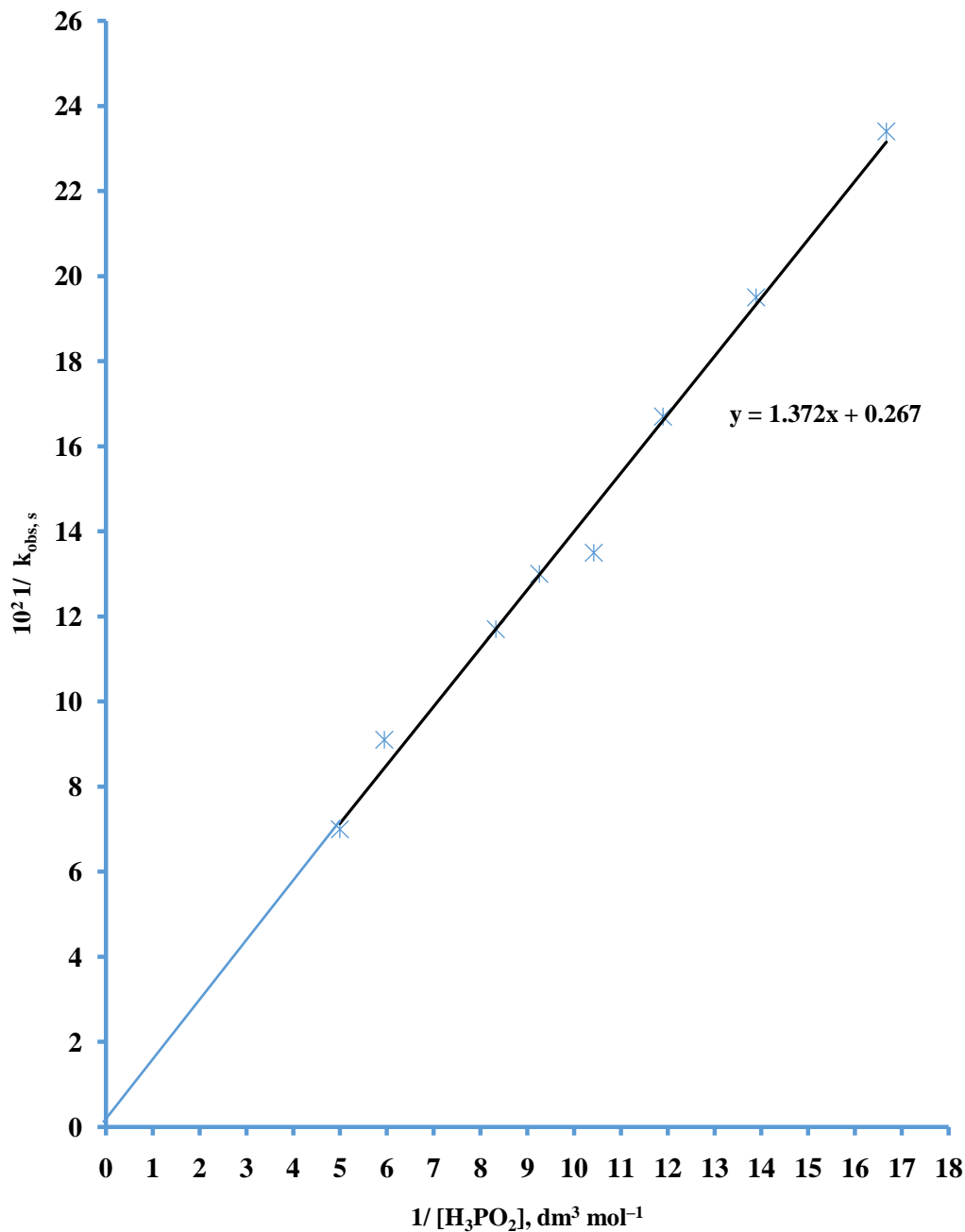


Figure 4.59: Plot of $1/k_{\text{obs}}$ versus $1/[H_3PO_2]$ for the Reaction of $[(H_2O)_2Ru_2O]^{4+}$ and Hypophosphorus acid (H_3PO_2) at $[(H_2O)_2Ru_2O^{4+}] = 6.0 \times 10^{-5} \text{ mol dm}^{-3}$, $[H_3PO_2] = (6.0 - 20.0) \times 10^{-2} \text{ mol dm}^{-3}$, $[H^+] = 5.0 \times 10^{-2} \text{ mol dm}^{-3}$, $I = 0.5 \text{ mol dm}^{-3}$, $T = 31 \pm 1 \text{ } ^\circ\text{C}$ and $\lambda_{\text{max}} = 660 \text{ nm}$

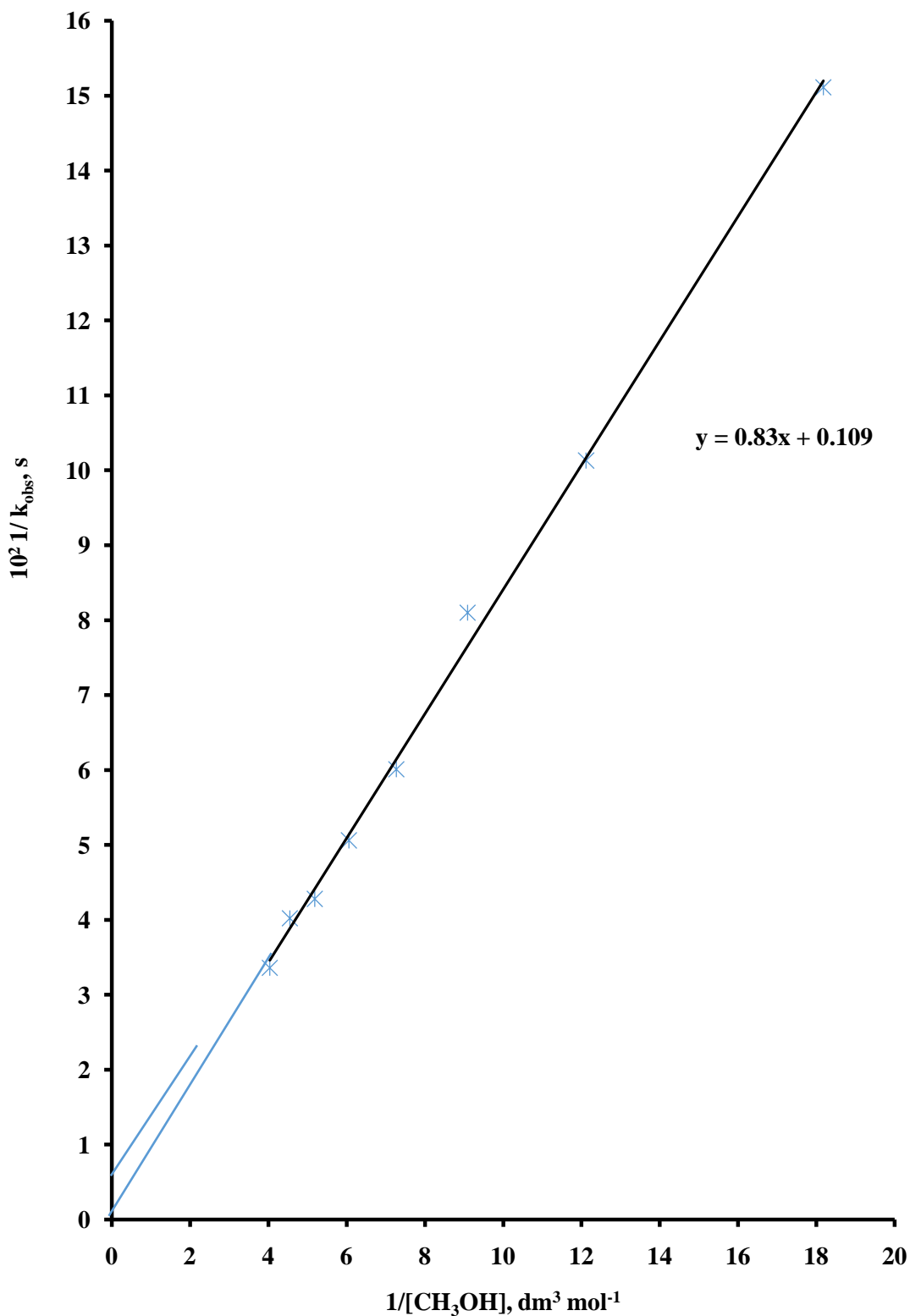


Figure 4.60: Plot of $1/k_{\text{obs}}$ versus $1/[\text{CH}_3\text{OH}]$ for the Reaction of $[(\text{H}_2\text{O})_2\text{Ru}_2\text{O}]^{4+}$ and Methanol (CH_3OH) at $[(\text{H}_2\text{O})_2\text{Ru}_2\text{O}^{4+}] = 5.5 \times 10^{-5} \text{ mol dm}^{-3}$, $[\text{CH}_3\text{OH}] = (5.50 - 24.75) \times 10^{-2} \text{ mol dm}^{-3}$, $I = 0.5 \text{ mol dm}^{-3}$, $T = 31 \text{ } ^\circ\text{C}$ and $\lambda_{\text{max}} = 660 \text{ nm}$

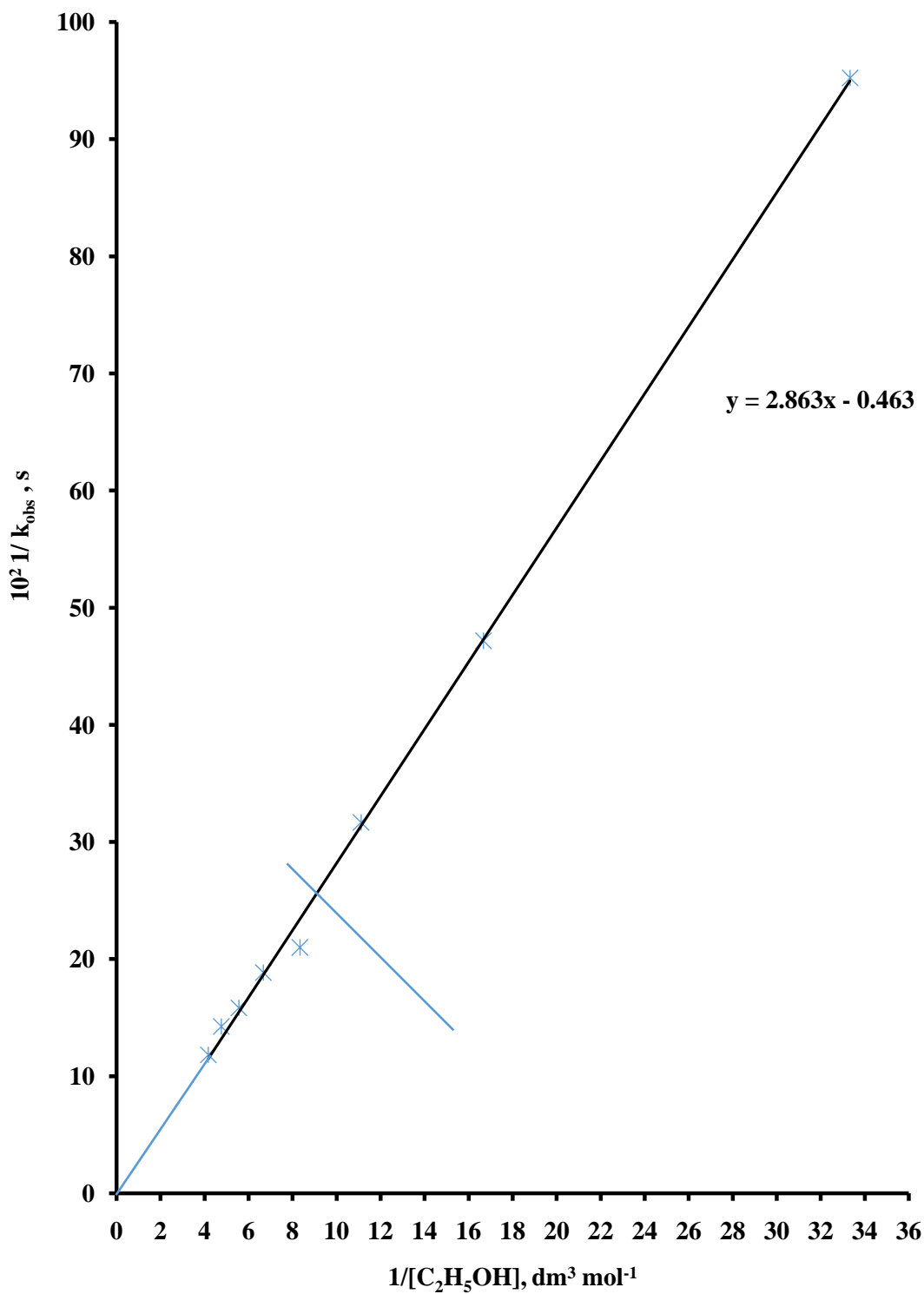


Figure 4.61: Plot of $1/k_{\text{obs}}$ versus $1/[C_2H_5OH]$ for the reaction of $[(H_2O)_2Ru_2O]^{4+}$ and Ethanol (C_2H_5OH) at $[(H_2O)_2Ru_2O^{4+}] = 6.5 \times 10^{-5} \text{ mol dm}^{-3}$, $[C_2H_5OH] = (3.25 - 0.00) \times 10^{-2} \text{ mol dm}^{-3}$, $I = 0.5 \text{ mol dm}^{-3}$, $T = 31 \text{ } ^\circ\text{C}$ and $\lambda_{\text{max}} = 660 \text{ nm}$

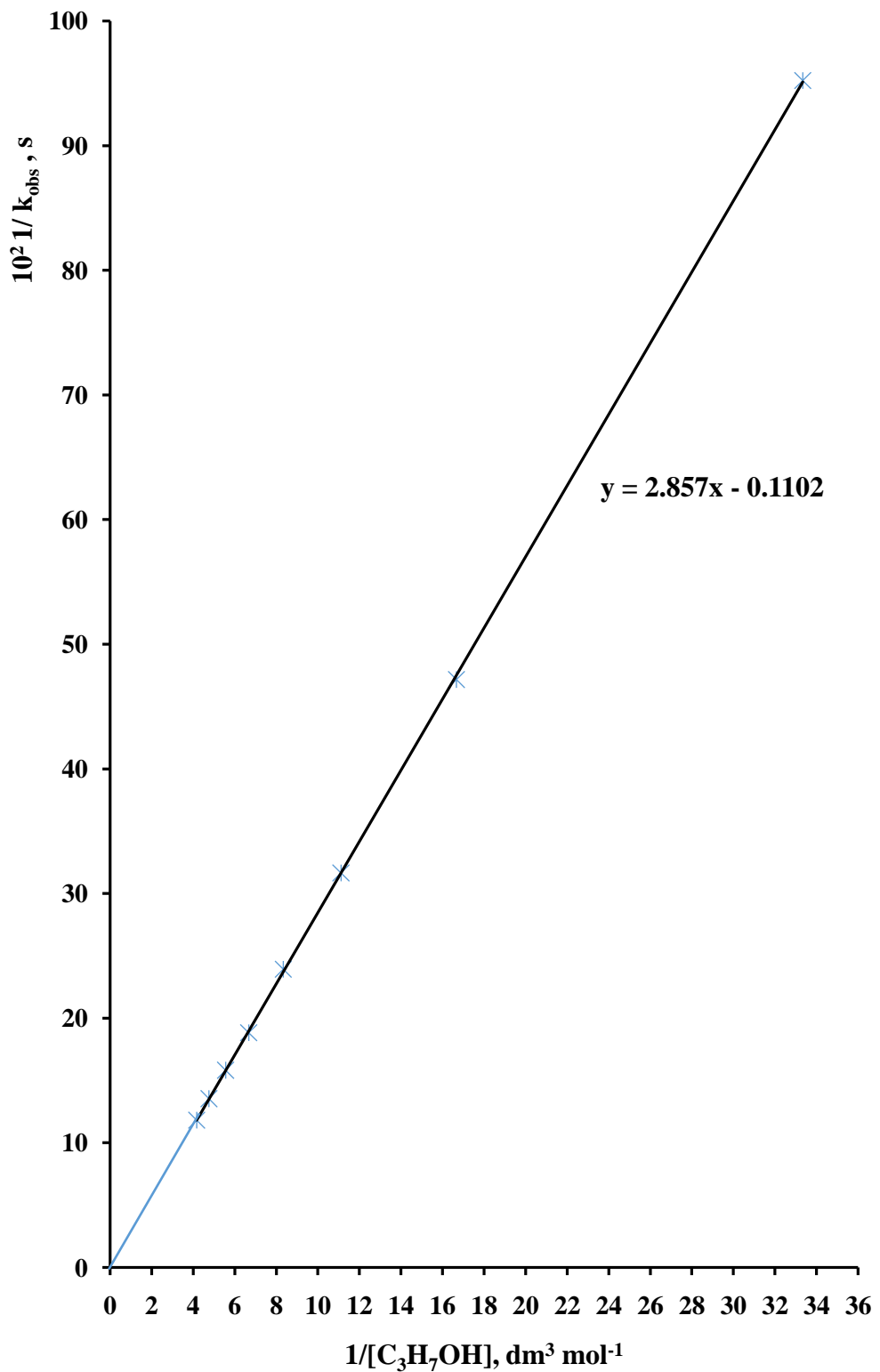


Figure 4.62: Plot of $1/k_{\text{obs}}$ versus $1/[C_3H_7OH]$ for the reaction of $[(H_2O)_2Ru_2O]^{4+}$ and Propanol (C_3H_7OH) at $[(H_2O)_2Ru_2O^{4+}] = 6.0 \times 10^{-5} \text{ mol dm}^{-3}$, $[C_3H_7OH] = (3.0 - 24.0) \times 10^{-2} \text{ mol dm}^{-3}$, $I = 0.5 \text{ mol dm}^{-3}$, $T = 31 \text{ } ^\circ\text{C}$ and $\lambda_{\text{max}} = 660 \text{ nm}$

4.9 Free Radical Test

For the reactions of Ru_2O^{4+} and the thioureas, H_3PO_2 and the alcohols, the addition of acrylamide to partially reacted mixture of Ru_2O^{4+} and the reductants followed by excess methanol showed gel formation. However, for the reaction of Ru_2O^{4+} and $\text{S}_2\text{O}_4^{2-}$ and $\text{S}_2\text{O}_4^{2-}$, the same procedure resulted in no gel formation.

4.10 Product Analysis

Isolation and characterization of the products of a reaction could give hints or suggestions about the possible pathway for the redox reaction under study.

For all the systems under study, $[\text{Ru}(\text{bipy})_2(\text{H}_2\text{O})_2]^{2+}$ was identified by taking the uv-visible spectrum of the product solution (Appendix 2). The products had a λ_{max} of 485 nm, characteristic of the Ru^{2+} complex (Davies and Mullins, 1967)

4.10.1 Ru_2O^{4+} reaction with thiourea and its derivatives

The formation of disulphides as the only organic products in the four reactions was confirmed using the method of McAuley and Gomwalk (1968 and 1969). In this aspect, the thiourea and its derivatives are behaving as thiols, where disulphide has been identified as the predominant products in their oxidation due the possession of the $-\text{SH}$ group (Ayoko and Olatunji, 1983, Petri et al., 1975; McAuley and Gomwalk, 1968, 1969).

4.10.2 Ru_2O^{4+} reaction with hypophosphorous acid

The presence of phosphorous acid as the oxidation product of hypophosphorous acid was confirmed by the addition of saturated ammonium molybdate solution to the

reaction mixture. Phosphate ion presence was ruled out on the basis of the absence of any precipitate of ammonium phosphomolybdate (Yusuf et al., 2004).

4.10.3 Ru_2O^{4+} reaction with the alcohols (CH_3OH , $\text{C}_2\text{H}_5\text{OH}$ $\text{C}_3\text{H}_7\text{OH}$)

The identification of aldehydes as the oxidation product of alcohols was confirmed by employing the Fehling's test. A mixture of equal amounts of Fehling's A solution and Fehling's B solution was made. To 2 cm³ of this mixture in a test tube, 3 drops of the solution to be tested was added. The test tube is then placed in a water-bath that is maintained at 60°C. Appearance of brick-red precipitate confirms the presence of aldehydes (Vogel, 1958).

CHAPTER FIVE

DISCUSSION

5.1 Ru₂O⁴⁺ Reaction with Thiourea and its Derivatives

Stoichiometric studies by using the mole ratio method showed that plots of A_∞ (absorbance at infinity) versus mole ratio (Ru₂O₄²⁺/ TSH) (where TSH represents TU, MTU, ATU and DMTU) had sharp breaks at ratio 1:2 (Figures 4.1 – 4.4). This is suggestive of 2 moles of TSH being oxidised by 1 mole of Ru₂O⁴⁺ as presented in Equation 5.1.



(where TSH = TU, MTU, ATU and DMTU)

Equation 5.1 is similar to Equations 4.1 – 4.4.

A similar stoichiometry has been reported for the reaction of the oxo-bridged ruthenium dimer with L-cysteine (Iyun *et al.*, 1996) and glutathione (Ayoko *et al.*, 1993b). However, a stoichiometry of 1:1 was found for the reaction of Ru₂O⁴⁺ with iodide (Iyun *et al.*, 1992c), sulphite (Iyun *et al.*, 1992d), mercaptoethanol and mercaptoethylamine (Iyun *et al.*, 1995b). Also a stoichiometry of 2:1 (Ru₂O⁴⁺/ reductant) was found for the reaction of Ru₂O⁴⁺ and ascorbic acid (Iyun *et al.*, 1995a) and 1:5 (Ru₂O⁴⁺ / reductant) for the reaction of Ru₂O⁴⁺ and bromate (Iyun *et al.*, 1992b). Comparably, a stoichiometry of 1:2 (Ru₂O⁴⁺ / reductant) has been reported in the reaction of Fe₂O⁴⁺ with mercaptoacetic acid, mercaptoethanol, and mercaptoethylamine (Ukoha and Iyun, 2001). A summary of the stoichiometries of similar systems is reported in Table 5.1.

Table 5.1: A Summary of the Stoichiometries of Similar Systems Studied

elsewhere

Systems	Report	Stoichiometry
Fe_2O^{4+} / mercaptoacetic acid	Ukoha, 1999	1:2
Fe_2O^{4+} / mercaptoethanol	Ukoha and Iyun, 2001	1:2
Fe_2O^{4+} / mercaptoethylamine	„	1:2
Fe_2O^{4+} / ascorbic acid	Ukoha and Iyun, 2002	1:1
Ru_2O^{4+} / glutathione	Ayoko <i>et al.</i> , 1993b	1:2
Ru_2O^{4+} / l-cysteine	Iyun <i>et al.</i> , 1996	1:2
Ru_2O^{4+} / ascorbic acid	Iyun <i>et al.</i> , 1995a	2:1
Ru_2O^{4+} / sulphite	Iyun <i>et al.</i> , 1992d	1:1
Ru_2O^{4+} / bromate	Iyun <i>et al.</i> , 1992b	1:5
Ru_2O^{4+} / iodide	Iyun <i>et al.</i> , 1992c	1:1
Ru_2O^{4+} / mercaptoethanol	Iyun <i>et al.</i> , 1995b	1:1
Ru_2O^{4+} / mercaptoethylamine	Iyun <i>et al.</i> , 1995b	1:1

The 1:2 stoichiometry observed in the reactions of Ru_2O^{4+} and the thioureas (TU, MTU, ATU, DMTU) confirms that the thiourea and its derivative, under study, are two electron reductants. The formation of disulphides as the only organic products in the four reactions was confirmed by using the method of McAuley and Gomwalk (1968 and 1969) as earlier reported. In the oxidation of glutathione by Ru_2O^{4+} , disulphide formation had been documented (Ayoko *et al.*, 1993b), where the oxo-bridged dimer was reduced to Ru^{2+} . Disulphide has, similarly, been identified as the predominant product in the oxidation of thiols possessing the $-\text{SH}$ group (Ayoko and Olatunji, 1983; Petri and Baldea, 1975; McAuley and Gomwalk, 1968 and 1969). U-V spectrum of the completely reacted mixtures of the four reactions indicated that the mixtures absorbed maximally at 485nm, which is the characteristic λ_{max} of $[\text{Ru}(\text{bipy})_2(\text{H}_2\text{O})_2]^{2+}$ (Davies and Mullins, 1967). As reported earlier for the oxo-bridged chloro dimer, $[(\text{bipy})_2\text{ClRuORuCl}(\text{bipy})_2]^{4+}$ (Iyun and Adegite, 1990), reduction of the aqua dimer by one electron initially occurs to give a compound which may formally be a $\text{Ru}^{\text{III}}\text{-O-Ru}^{\text{II}}$ dimer (however, the odd electron may be delocalised between the two ruthenium ions). This initial product, being unstable, undergoes a slow bridge cleavage upon further reduction (Davies and Mullins, 1967) to give two equivalents of $[\text{Ru}(\text{bipy})_2(\text{H}_2\text{O})_2]^{2+}$.

Pseudo-first order plots of $\log(A_t - A_\infty)$ versus time were linear to > 90% of reactions (Figures 4.11 – 4.14), indicating first order with respect to $[\text{Ru}_2\text{O}^{4+}]$. Plots of $\log k_{\text{obs}}$ versus $\log [\text{TSH}]$ were linear with slopes approximately equal to unity, suggesting that the reactions were approximately first order in reductant concentrations. The kinetic studies of the oxidation of TU, MTU, ATU and DMTU by Ru_2O^{4+} , therefore, indicated a second order overall.

Similar second order kinetics have been reported for other reactions of Ru_2O^{4+} with benzenediol (Iyun *et al.*, 1992a), bromate (Iyun *et al.*, 1992b), iodide (Iyun *et al.*, 1992c), sulphite (Iyun *et al.*, 1992d), glutathione (Ayoko *et al.*, 1993b) and L – cysteine (Iyun *et al.*, 1996).

Thus, these reactions fit into equation (5.2)

$$-\frac{d}{dt} [\text{Ru}_2\text{O}^{4+}] = k_{\text{obs}}[\text{Ru}_2\text{O}^{4+}] = k_2 [\text{Ru}_2\text{O}^{4+}][\text{TSH}] \quad \dots(5.2)$$

The values of k_2 for the four systems at $[\text{H}^+] = 5.0 \times 10^{-3} \text{ mol dm}^{-3}$; $\text{I} = 0.5 \text{ mol dm}^{-3}$; $\text{T} = 31 \pm 1 \text{ }^\circ\text{C}$ and $\lambda_{\text{max}} = 660\text{nm}$ are as follows:

$\text{Ru}_2\text{O}^{4+} - \text{TU}$ system = $(7.39 \pm 0.05) \times 10^{-3} \text{ dm}^3 \text{ mol}^{-1} \text{ s}^{-1}$ with $[\text{Ru}_2\text{O}^{4+}] = 6.0 \times 10^{-5} \text{ mol dm}^{-3}$.

$\text{Ru}_2\text{O}^{4+} - \text{MTU}$ system = $(3.14 \pm 0.05) \times 10^{-2} \text{ dm}^3 \text{ mol}^{-1} \text{ s}^{-1}$ with $[\text{Ru}_2\text{O}^{4+}] = 6.5 \times 10^{-5} \text{ mol dm}^{-3}$.

$\text{Ru}_2\text{O}^{4+} - \text{ATU}$ system = $(20.08 \pm 0.10) \times 10^{-2} \text{ dm}^3 \text{ mol}^{-1} \text{ s}^{-1}$ with $[\text{Ru}_2\text{O}^{4+}] = 5.75 \times 10^{-5} \text{ mol dm}^{-3}$.

$\text{Ru}_2\text{O}^{4+} - \text{DMTU}$ system = $(8.12 \pm 0.04) \times 10^{-2} \text{ dm}^3 \text{ mol}^{-1} \text{ s}^{-1}$ with $[\text{Ru}_2\text{O}^{4+}] = 7.0 \times 10^{-5} \text{ mol dm}^{-3}$.

Within the acid $[\text{H}^+]$ range of 2.0×10^{-2} to $20.0 \times 10^{-2} \text{ mol dm}^{-3}$, the reaction rate decreased as $[\text{H}^+]$ increases for all the four systems as shown in Tables (4.1 – 4.4). The plots of the acid dependent second order rate constant, $k_2(\text{H}^+)$ versus $[\text{H}^+]$ for the four systems are given in Figures 4.31 – 4.34 and the relationship fits equation (5.3).

$$k_2(\text{H}^+) = a + b[\text{H}^+]^{-1} \quad \dots(5.3)$$

where $k_2(\text{H}^+)$ = acid dependent second order rate constant, 'a' = intercept and 'b' = slope.

This suggests that this reaction occurs by two parallel pathways, one of the pathways is inverse acid dependent and the other acid independent. The values of 'a' and 'b' for the various systems are:

Ru_2O^{4+} – TU system 'a' = $11.95 \times 10^{-4} \text{ dm}^3 \text{ mol}^{-1} \text{ s}^{-1}$ and 'b' = $-0.88 \text{ dm}^6 \text{ mol}^{-2} \text{ s}^{-1}$

Ru_2O^{4+} – MTU system 'a' = $4.09 \times 10^{-2} \text{ dm}^3 \text{ mol}^{-1} \text{ s}^{-1}$ and 'b' = $-2.01 \text{ dm}^6 \text{ mol}^{-2} \text{ s}^{-1}$

Ru_2O^{4+} – ATU system 'a' = $27.61 \times 10^{-2} \text{ dm}^3 \text{ mol}^{-1} \text{ s}^{-1}$ and 'b' = $-1.78 \text{ dm}^6 \text{ mol}^{-2} \text{ s}^{-1}$

Ru_2O^{4+} – DMTU system 'a' = $10.43 \times 10^{-2} \text{ dm}^3 \text{ mol}^{-1} \text{ s}^{-1}$ and 'b' = $-0.46 \text{ dm}^6 \text{ mol}^{-2} \text{ s}^{-1}$

These results fit equation (5.4)

$$-\frac{d}{dt}\text{Ru}_2\text{O}^{4+} = (a + b[\text{H}^+])^{-1}[\text{Ru}_2\text{O}^{4+}] [\text{TSH}] \dots\dots(5.4)$$

Similar inverse acid dependence was reported in the reduction of Ru_2O^{4+} by bromate (Iyun *et al.*, 1992b), sulphite (Iyun *et al.*, 1992d), glutathione (Ayoko, *et al.*, 1993b), mercaptoethylamine (Iyun *et al.*, 1995b) and L-cysteine (Iyun *et al.*, 1996) have been reported. However, the oxidation of Γ^- by Ru_2O^{4+} displayed direct H^+ dependence (Iyun *et al.*, 1992c). Decrease in rate of reaction with increase in $[\text{H}^+]$ is attributable to the deprotonation of the thiourea and its derivatives under study. Although the deprotonation of $(\text{bipy})_2(\text{H}_2\text{O})\text{RuORu}(\text{H}_2\text{O})(\text{bipy})_2]^{4+}$ to give $[(\text{bipy})_2(\text{OH})\text{Ru}^{\text{III}}\text{ORu}^{\text{II}}(\text{H}_2\text{O})(\text{bipy})_2]^{3+}$ and $[[(\text{bipy})_2(\text{OH})\text{Ru}^{\text{III}}\text{ORu}^{\text{II}}(\text{OH})(\text{bipy})_2]^{2+}$ can not be ruled out under the acid conditions of this reaction (Davies and Mullin, 1967). On the basis of our observed products it seems more plausible to attribute the present inverse acid dependence to the deprotonation of TSH. In this respect, therefore, TSH is

behaving as a thiol, in which there is the deprotonation of its sulphydryl (–SH) groups prior to electron transfer (McAuley and Gomwalk, 1969; Zueva *et al.*, 1990).

Varying the ionic strength of the reaction medium between 0.1 – 0.9 mol dm⁻³ (NaClO₄), had minimal effect on the rates of reaction as shown in Tables 4.1 – 4.4. For reactions of ions in aqueous media, according to Atkins (1979), the rate of reaction is directly dependent on the square root of the ionic strength of the reaction medium according to equation 5.5.

$$\log k_2 = \log k_1 + 2 Z_A Z_B I^{1/2} \quad \dots(5.5)$$

Where k_2 = second order rate constant for the reaction

k_1 = hypothetical rate constant in a medium of infinite dielectric constant.

Z_A and Z_B = Charges on reactants A and B respectively

I = ionic strength of the medium

β = 0.5 at 25 °C

If ionic strength is varied, the various values of the second order rate constants, k_2 , obtained can be plotted as $\log k_2$ against \sqrt{I} . The magnitude of the slope of the plot gives an idea of the product of the charges on the species' reacting in the rate determining step (Bronsted, 1922). Non-dependence of rate of reaction on ionic strength will likely be due to no charge on one or both of the reactants. Since ion-pair complex does not possess a formal charge, the rate of reaction would also not be affected by changes in ionic strength if ion-pairs are involved in reactions with outersphere character (Iyun *et al.*, 1992a, 1995b).

By using water-acetone mixture at various proportions, the dielectric constant of the reaction medium was varied between 81 – 72.60. Our studies showed that changes in D had no effect on the reaction rates. (Tables 4.11 – 4.14). This suggests that the reaction occurred between cation and neutral molecule or free radical. This is also consistent with a reaction involving ion-pairs with outersphere character (Iyun *et al.*, 1992a,1995b).

Added anions did not affect the reaction rates in the reactions between Ru_2O^{4+} and TSH (Tables 4.21 – 4.27). Absence of ion catalysis is in line with the formation of ion – pairs in the reaction prior to electron transfer. Since the ion – pair complex does not have a formal charge, interaction with added ions will not be possible suggesting that the reaction might have proceeded via the outersphere pathway. Iyun *et al* (1995b) have reported formation of ion-pair intermediates in the reaction of Ru_2O^{4+} with 2-mercaptoethanol and 2-mercaptoethylamine.

On addition of acrylamide to the reaction mixtures for the four reactions followed by excess methanol, a gelatinous precipitate was formed, suggesting that polymerisation has occurred. This confirms the participation of free radicals during the reactions.

In ascertaining the presence or absence of the formation of intermediate complexes in the course of the reactions of the oxo-bridged ruthenium dimer and the thioureas, Michaelis-Menten plots of $1/k_{\text{obs}}$ versus $1/[\text{reductant}]$ were made, as applied by Kumar *et al* (1991). All the plots were linear with negligible intercepts, indicating that the intermediates participating in these reactions have no appreciable equilibrium constants thereby ruling out the formation of intermediate complexes in the reactions.

For an enzymatic action, under certain assumptions, such as the enzyme concentration being much less than the substrate concentration, the rate of product formation is given by Equation 5.6.

$$\frac{d[\text{Product}]}{dt} = k_{\text{obs}}[E_0] \quad (5.6)$$

$$\text{with } k_{\text{obs}} = \frac{V_{\text{max}}[S]}{k_m + [S]} \quad \dots(5.7)$$

where k_{obs} is the rate constant for the overall reaction,

E_0 is total enzyme concentration,

V_{max} represents the rate constant for the break-up of an active intermediate into products

k_m is the Michaelis-Menten rate constant representing the substrate concentration at which the reaction rate is half of V_{max} .

Leonor Michaelis and Maud Menten in 1913 (Johnson and Goody, 2011) observed that by taking the reciprocal of Equation 5.7 and rearranging it, it becomes Equation 5.8.

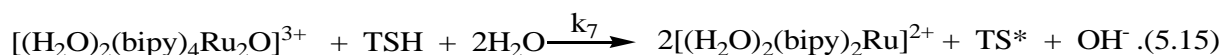
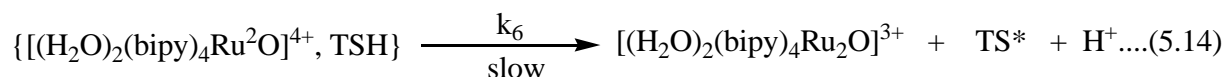
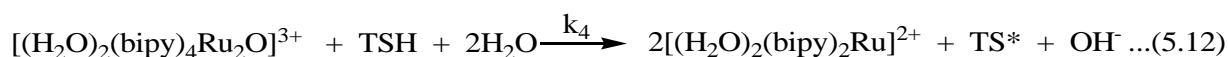
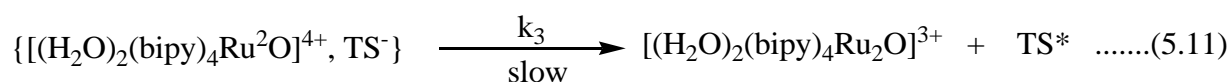
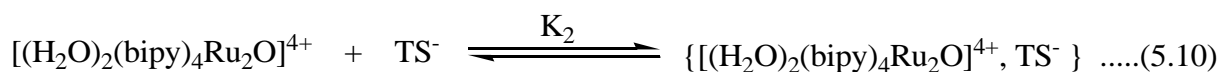
$$\frac{1}{k_{\text{obs}}} = \frac{1}{V_{\text{max}}} + \left(\frac{k_m}{V_{\text{max}}}\right) [S]^{-1} \quad \dots\dots(5.8)$$

where, for a normal redox reaction, S represents the reductant.

According to Equation 5.8, a plot of $1/k_{\text{obs}}$ versus $1/[S]$ gives $1/V_{\text{max}}$ as intercept. If, however, a linear plot which passes through the origin is obtained, it shows that the intercept is zero and $1/V_{\text{max}}$ is zero. This means that V_{max} or the equilibrium constant for the active intermediates is zero (Ukoha, 1999).

Furthermore, spectrophotometric studies showed no shift in λ_{\max} in the spectrum of the reaction mixtures taken 1, 2, and 3 minutes after commencement of reactions, suggesting the absence of any stable precursor complexes but formation of ion-pairs. These ion pairs could be formed via the N or S atoms of the thioureas (Iyun *et al.*, 1995b).

Based on the above findings and discussions, it is proposed that the oxidation of thiourea and its derivatives (*N*-methylthiourea, *N*-allylthiourea and *N,N*-dimethylthiourea) by Ru_2O^{4+} most probably occur by the outersphere mechanism and the following mechanistic scheme is proposed for the reactions.





With Equations 5.11 and 5.14 as the rate determining steps,

$$\text{Rate} = k_3\{[(H_2O)_2(bipy)_4Ru_2O]^{4+}, TS^-\} + k_6\{[(H_2O)_2(bipy)_4Ru_2O]^{4+}, TSH\} \dots(5.18)$$

But from equation 5.14:

$$\{[(H_2O)_2(bipy)_4Ru_2O]^{4+}, TS^-\} = K_2[(H_2O)_2(bipy)_4Ru_2O^{4+}] [TS^-] \dots(5.19)$$

Putting Equation 5.19 into 5.18 we have:

$$\text{Rate} = k_3K_2\{[(H_2O)_2(bipy)_4Ru_2O^{4+}] [TS^-]\} + k_6\{[(H_2O)_2(bipy)_4Ru_2O]^{4+}, TSH\} \dots(5.20)$$

Also from Equation 5.9:

$$TS^- = K_1 \frac{[TSH]}{[H^+]} \quad (5.21)$$

Substituting Equation 5.21 into Equation 5.20, we have Equation 5.22:

$$\text{Rate} = k_3K_1K_2\{[(H_2O)_2(bipy)_4Ru_2O^{4+}] \frac{[TSH]}{[H^+}]\} + k_6\{[(H_2O)_2(bipy)_4Ru_2O]^{4+}, TSH\} \dots(5.22)$$

From Equation 5.17,

$$\{[(H_2O)_2(bipy)_4Ru_2O]^{4+}, TSH\} = K_5[(H_2O)_2(bipy)_4Ru_2O^{4+}] [TSH] \dots(5.23)$$

Substituting Equation 5.23 into Equation 5.22 we have Equation 5.24:

$$\text{Rate} = k_3K_1K_2\{[(H_2O)_2(bipy)_4Ru_2O^{4+}] \frac{[TSH]}{[H^+}]\} + k_6K_5[(H_2O)_2(bipy)_4Ru_2O^{4+}][TSH] \quad (5.24)$$

$$= (k_6K_5 + k_3K_1K_2 \frac{1}{[H^+]})[(H_2O)_2(bipy)_4Ru_2O^{4+}][TSH] \dots(5.25)$$

Equation 5.2 is similar to Equation 4.16, where $k_6K_5 = 'a'$ and $k_3K_1K_2 = 'b'$ and the values of 'a' and 'b' for the various systems under study have been reported earlier.

The inverse acid dependence is consistent with the deprotonation of the thioureas (TSH) in Equation 5.9, while the positive polymerisation test is rationalized by the participation of free radicals in Equations 5.11, 5.12, 5.14 and 5.16..

Formamidine disulphide is obtained as the product of the oxidation of the thioureas in these reactions. Similar products have been obtained in the oxidation of thioureas by copper(II) perchlorate in acetonitrile (Zatko and Kratochvil., 1968). An outersphere oxidant, IrCl_6^{2-} , was used to oxidise thiourea to formamidine disulphide (Henry *et al.*, 1979). Other thiourea derivatives such as *N,N'*-dimethylthiourea also afforded corresponding disulphide derivatives as oxidation products. Henry *et al* (1979) used hexacyanoferrate(III) to oxidise thiourea and *N*-substituted thiourea under acidic condition. The reaction proceeds by an outersphere mechanism to yield formamidine disulphide.

5.2 Ru_2O^{4+} Reaction with $\text{S}_2\text{O}_3^{2-}$

Spectrophotometric titration following the mole ratio method indicated that the plot of absorbance at infinity (A_∞) against mole ratio had a sharp break at 1:2 (Figure 4.5), suggesting that one mole of Ru_2O^{4+} was reduced by two moles of $\text{S}_2\text{O}_3^{2-}$. This is consistent with the stoichiometric Equation 4.5.

A similar stoichiometry had been observed in the oxidation of thiosulphates by chlorine dioxide (Pan and Stanbury, 2014), copper ions (Byerley *et al.*, 1973) and chromate

(Balden and Niac, 1970). However, a stoichiometry of 1:2 ($\text{S}_2\text{O}_3^{2-} / \text{ClO}_2^-$) was reported for the reaction of $\text{S}_2\text{O}_3^{2-}$ and ClO_2^- (Nagypal and Epstein, 2004)

From kinetic studies, the reaction between Ru_2O^{4+} and $\text{S}_2\text{O}_3^{2-}$ has been shown to have first order dependence on $[\text{Ru}_2\text{O}^{4+}]$. This is a consequence of the linearity of the pseudo-first order plots of $\log (A_t - A_\infty)$ versus time for 85% extent of reaction. Also, the slope the plot of $\log k_{\text{obs}}$ versus $\log [\text{S}_2\text{O}_3^{2-}]$ gave a slope of 0.93, suggesting a first order dependence in $[\text{S}_2\text{O}_3^{2-}]$. Similar first order dependence with respect to $[\text{S}_2\text{O}_3^{2-}]$ was reported in its reaction with ferrate ions (Johnson and Read, 1996), chlorine dioxide (Pan and Stanbury, 2014), copper ions (Byerley *et al.*, 1973), chlorite (Nagypal and Epstein, 2004) and chromate (Balden and Niac, 1970). However, in its reaction with octacyanotungstate(V) the reaction was zero order with respect to $[\text{W}(\text{CN})_8^{3-}]$ and second order with respect to $[\text{S}_2\text{O}_3^{2-}]$ (Dennis *et al.*, 1985). The overall rate law for the reaction, therefore, can be presented by Equation 5.26

$$-\frac{d}{dt} [\text{Ru}_2\text{O}^{4+}] = k_{\text{obs}}[\text{Ru}_2\text{O}^{4+}] = k_2[\text{Ru}_2\text{O}^{4+}][\text{S}_2\text{O}_3^{2-}] \quad \text{..(5.26)}$$

At $[\text{Ru}_2\text{O}^{4+}] = 6.5 \times 10^{-5} \text{ mol dm}^{-3}$, $[\text{H}^+] = 5 \times 10^{-2} \text{ mol dm}^{-3}$, $I = 0.5 \text{ mol dm}^{-3}$ (NaClO_4), $T = 31.0 \pm 1.0 \text{ }^\circ\text{C}$, k_2 was found to be $(3.75 \pm .05) \times 10^{-2} \text{ dm}^3 \text{ mol}^{-1} \text{ s}^{-1}$.

Within the acid concentration range of $2.0 \times 10^{-2} - 20.0 \times 10^{-2} \text{ mol dm}^{-3}$, the rate of reaction increased with increase in $[\text{H}^+]$ (Table 4.5). Relationship between the acid dependent rate constant, $k_2(\text{H}^+)$ and $[\text{H}^+]$ is determined by plotting $k_2(\text{H}^+)$ against $[\text{H}^+]$. The plot (Figure 4.35) was found to be linear and represented by Equation 5.27.

$$k_2[\text{H}^+] = a + b[\text{H}^+] \quad \dots(5.27)$$

where 'a' = intercept = $6.33 \times 10^{-2} \text{ dm}^3 \text{ mol}^{-1} \text{ s}^{-1}$ and 'b' = slope = $6.75 \text{ dm}^6 \text{ mol}^{-2} \text{ s}^{-1}$.

To determine the order of reaction with respect to $[\text{H}^+]$, a plot of $\log k_{\text{obs}}$ was plotted against $\log [\text{H}^+]$. This plot (Figure 4.36) was linear with a slope of 1.08, suggesting a first order dependence with respect to $[\text{H}^+]$. The overall rate law as a function of $[\text{H}^+]$ is given by Equation 5.28.

$$-\frac{d}{dt} [\text{Ru}_2\text{O}^{4+}] = (a + b[\text{H}^+])[\text{Ru}_2\text{O}^{4+}][\text{S}_2\text{O}_3^{2-}] \quad \dots(5.28)$$

Similar acid dependence has been reported for the reaction of super-reduced cobalamin and cobinamide and thiosulphates (Dereven'kov *et al.*, 2013). This acid dependence is attributed to the protonation of the $\text{S}_2\text{O}_3^{2-}$ to its reactive species, HS_2O_3^- (Dereven'kov *et al.*, 2013).

Variation of ionic strength from 0.2 to 0.8 mol dm^{-3} using NaClO_4 led to the decrease in the rate of reaction as the ionic strength increased (Table 4.5). Least square plots of $\log k_2$ versus \sqrt{I} was linear with a slope of -2.81 (Figure 4.37). This suggests that the products of the charges on the reactants in the rate-determining step is -2.81 , the negative charge suggesting that the interaction is between unlike charges. By varying the dielectric constant, D , of the reaction medium from 81 – 70.2 using $(\text{CH}_3)_2\text{CO}-\text{H}_2\text{O}$ mixture, it was observed that the reaction rate increased with a decrease in D (Table 4.15). This suggests that unlike charges were reacting in the rate-determining step,

confirming the suggestion made earlier on the observation of the effect of change of ionic strength of reaction medium on rate. Conformity of the result of the variation of ionic strength with that due to effect of varying D could suggest one route for the reaction (Gupta and Gupta, 1981 and Iyun *et al.*, 1995a).

Increase in reaction rates by added NO_3^- and CH_3COO^- , represented by 'X' was observed and the result is depicted in Table 4.29. Least square plots of $k_2(\text{X})$ versus $[\text{X}]$ (Figures) were linear and represented by Equation 5.29.

$$k_2(\text{X}) = p + q[\text{X}] \quad \dots(5.29)$$

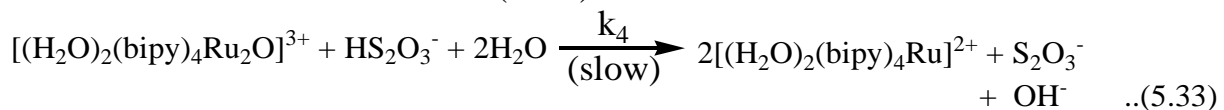
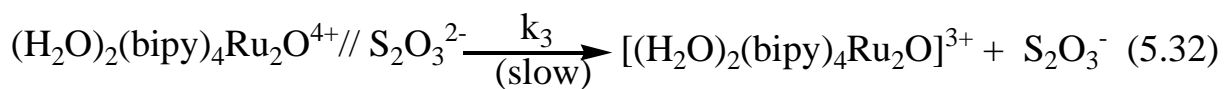
where $p(\text{NO}_3^-) = 3.78 \times 10^{-2} \text{ dm}^3 \text{ mol}^{-1} \text{ s}^{-1}$ and $q(\text{NO}_3^-) = 1.80 \times 10^{-3} \text{ dm}^6 \text{ mol}^{-2} \text{ s}^{-1}$ and $p(\text{CH}_3\text{COO}^-) = 3.73 \times 10^{-2} \text{ dm}^3 \text{ mol}^{-1} \text{ s}^{-1}$ and $q(\text{CH}_3\text{COO}^-) = 2.23 \text{ dm}^6 \text{ mol}^{-1} \text{ s}^{-1}$.

Similar anion catalysis has been reported for the reaction of $\text{S}_2\text{O}_3^{2-}$ and hexacyanoferrate(III) (Howelett and Wedzicha, 1976). Ion catalysis has been associated with outersphere electron transfer process (Pryztas and Sutin, 1973).

Polymerisation test to determine the active participation of free radicals in the reaction was negative as no gel was formed on the addition of acrylamide to partially reacted reaction mixture in excess methanol.

Running the U-v spectrum of the partially reacted reaction mixture revealed a consistency of the wavelength of maximum absorption of 660 nm. This lack of shift in λ_{max} suggests that spectroscopically identifiable intermediate complex was not formed in the course of the reaction. Furthermore, the Michaelis-Menten plot of $1/k_{\text{obs}}$ versus $1/$

$[S_2O_3^{2-}]$ was linear with no appreciable intercept (Figure 4.58), implying the absence of any stable intermediates with a large enough formation constant. These facts support the postulation of an outersphere redox pathway operating for the oxidation of $S_2O_3^{2-}$ by Ru_2O^{4+} . On the basis of the results and observations made, the following is proposed.



Assuming Equations 5.32 and 5.33 to represent the rate determining steps, it follows that:

$$\text{Rate} = k_3[(H_2O)_2(bipy)_4Ru_2O^{4+} // S_2O_3^{2-}] + k_4[(H_2O)_2(bipy)_4Ru_2O^{3+}][HS_2O_3^-] \quad \dots (5.36)$$

From Equation (5.31),

$$[(H_2O)_2(bipy)_4Ru_2O^{4+} // S_2O_3^{2-}] = K_2[(H_2O)_2(bipy)_4Ru_2O^{4+}][S_2O_3^{2-}] \quad \dots (5.37)$$

and from Equation 5.30,

$$[HS_2O_3^-] = K_1[S_2O_3^{2-}][H^+] \quad \dots (5.38)$$

Substituting Equations 5.37 and 5.38 into Equation 5.36 gives Equation 5.39:

$$\text{Rate} = k_3K_2[(\text{H}_2\text{O})_2(\text{bipy})_4\text{Ru}_2\text{O}^{4+}][\text{S}_2\text{O}_3^{2-}] = k_4K_1[(\text{H}_2\text{O})_2(\text{bipy})_4\text{Ru}_2\text{O}^{3+}][\text{S}_2\text{O}_3^{2-}][\text{H}^+] \quad \dots(5.39)$$

But from Equation 5.32 and 5.33, we have Equation 5.40.

$$[(\text{H}_2\text{O})_2(\text{bipy})_4\text{Ru}_2\text{O}^{3+}] = k_3K_2[(\text{H}_2\text{O})_2(\text{bipy})_4\text{Ru}_2\text{O}^{4+}][\text{S}_2\text{O}_3^{2-}] \quad \dots(5.40)$$

Substitution of Equation 5.40 into Equation 5.39 gives Equation 5.41.

$$\text{Rate} = k_3K_2[(\text{H}_2\text{O})_2(\text{bipy})_4\text{Ru}_2\text{O}^{4+}][\text{S}_2\text{O}_3^{2-}] + k_4k_3K_1K_2[(\text{H}_2\text{O})_2(\text{bipy})_4\text{Ru}_2\text{O}^{4+}][\text{S}_2\text{O}_3^{2-}][\text{H}^+] \quad \dots(5.41)$$

$$= (k_3K_2 + k_4k_3K_1K_2[\text{H}^+])[(\text{H}_2\text{O})_2(\text{bipy})_4\text{Ru}_2\text{O}^{4+}][\text{S}_2\text{O}_3^{2-}] \quad (5.42)$$

Equation 5.42 is the same as Equation 5.28, where $k_3K_2 = 'a' = 6.33 \times 10^{-2} \text{ dm}^3 \text{ mol}^{-1} \text{ s}^{-1}$ and $K_4k_3K_2K_1 = 'b' = 6.75 \text{ dm}^6 \text{ mol}^{-2} \text{ s}^{-1}$.

The acid dependence is rationalised on the protonation of $\text{S}_2\text{O}_3^{2-}$ to give the active species, HS_2O_3^- in equation (5.30). Derevenikov *et al.* (2013) also reported that the reactive form of $\text{S}_2\text{O}_3^{2-}$ in the reaction of thiosulphates and super-reduced cobalamin and cobinamide species is HS_2O_3^- .

The cation inhibition and anion catalysis observed suggests that the reaction proceeded through the outersphere pathway, as innersphere mechanisms are rarely accompanied by ion catalysis or inhibition (Pryztas and Sutin, 1973 and Adegite *et al.*, 1977).

5.3 Ru_2O^{4+} Reaction with $\text{S}_2\text{O}_4^{2-}$

Plot of absorbance against mole ratio showed a sharp break at the ratio 1:1. This suggests that 1 mole of Ru_2O^{4+} was consumed by 1 mole of $\text{S}_2\text{O}_4^{2-}$ (Figure 4.6). This assertion is represented by Equation 4.6. Similar stoichiometry was reported for the

reaction of dithionite and malachite green (Idris *et al.*, 2015), dicyanoporphyrinato ferrate(III) complex (Worthington and Hambright, 1980), p-phenylazobenzene sulphonic acid (Wasmuth *et al.*, 2008), toluidine blue (Hamza *et al.*, 2012, Babatunde and Ajayi, 2013) and potassium ferrate (Read *et al.*, 2001).

Pseudo-first order plots of $\log (A_t - A_\infty)$ versus time was linear to over 85% extent of reaction. This suggests a first order dependence on $[\text{Ru}_2\text{O}^{4+}]$. Also a plot of $\log k_{\text{obs}}$ versus $\log [\text{S}_2\text{O}_4^{2-}]$ was linear with a slope of 0.98, suggesting a first with respect to $[\text{S}_2\text{O}_4^{2-}]$. In the reactions of dithionite with malachite green (Idris *et al.*, 2015) and toluidine blue (Hamza, *et al.*, 2012) a first order dependence on $[\text{S}_2\text{O}_4^{2-}]$ was reported. However, in the reduction of p-phenylazobenzene sulphonic acid by $\text{S}_2\text{O}_4^{2-}$ (Wasmuth *et al.*, 2008) and in the reduction of some azo-dyes by $\text{S}_2\text{O}_4^{2-}$ (Gameay, 2002) half-order dependence on $[\text{S}_2\text{O}_4^{2-}]$ was reported.

The overall rate equation for the oxidation of dithionite by Ru_2O^{4+} can, therefore, be written as Equation 5.43.

$$-\frac{d}{dt}[\text{Ru}_2\text{O}^{4+}] = k_{\text{obs}}[\text{Ru}_2\text{O}^{4+}] = k_2[\text{Ru}_2\text{O}^{4+}][\text{S}_2\text{O}_4^{2-}] \quad \dots(5.43)$$

At $[\text{Ru}_2\text{O}^{4+}] = 5.75 \times 10^{-5} \text{ mol dm}^{-3}$; $I = 0.5 \text{ mol dm}^{-3}$ (NaClO_4) and $T = 31 \pm 1 \text{ }^\circ\text{C}$, k_2 was found to be $(10.99 \pm .04) \times 10^{-2} \text{ dm}^3 \text{ mol}^{-1} \text{ s}^{-1}$

Dithionite was only studied at high pH because it undergoes hydrolysis at $\text{pH} < 10$ (Read *et al.*, 2001). This means that at the hydrogen ion concentration of $5 \times 10^{-2} \text{ mol dm}^{-3}$ ($\text{pH} = 1.3$) the dithionite would be decomposed. Therefore, the study was carried out in the absence of acid.

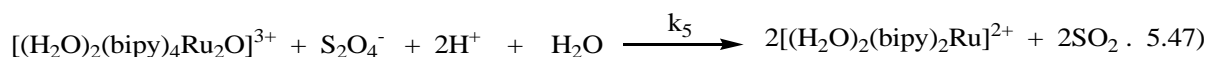
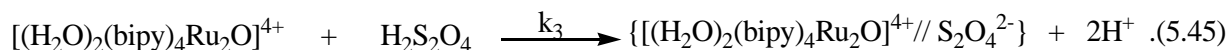
Varying the ionic strength of the medium from 0.2 – 1.1 mol dm⁻³ (NaClO₄) had no effect on the rate constants of the reaction (Table 4.6). This suggests that charged ions are with a neutral species in the rate determining step. This is supported by the effect of changes in the dielectric constant, D, from 81 - 70.8 on the rates of the reaction. It was observed that the rate constants remained constant for all the values of D.

Added anions (CH₃COO⁻ and HCOO⁻) led to increase in rates of reaction (Table 4.30) while added cations led to decrease in rates (Table 4.31). The relationship between the anion-dependent second order rate constants, k₂(X) and [X] was captured in the least square plots of k₂[X] versus [X] (Figures 4.43 – 4.46), which were linear with intercepts and slopes as reported earlier and the results are represented by Equations 4.21 and 4.22. The anion catalysis and cation inhibition observed has been associated with outersphere electron transfer process (Pryztas and Sutin, 1973).

Polymerisation was not induced on addition of acrylamide to the reaction mixture followed by excess methanol 1 minute, 2 minutes and 3 minutes after onset of reaction. This suggests that free radicals were not produced in the reaction of Ru₂O⁴⁺ and S₂O₄²⁻. This agrees with the lack of free radical participation in the reaction of malachite green and dithionite (Idris *et al.*, 2015). However, in the reaction of dithionite and toluidine blue, free radicals were detected (Hamza *et al.*, 2012), while Derven'ikov *et al* (2013) reported that in the reaction of dithionite and super-reduced cobalamin and cobinamide the reactive species was SO₂⁻. The electrochemical behaviour of sodium dithionite at a gold electrode in alkaline solution shows that dithionite is oxidised with SO₂⁻ as intermediate (Westbroek *et al.*, 2001).

Scanning the reaction mixture spectrophotometrically as the reaction progressed did not show any shift in λ_{\max} , thereby ruling out the formation of an intermediate complex prior to electron transfer. Also, Michaelis-Menten plot of $1/k_{\text{obs}}$ versus $1/[\text{S}_2\text{O}_4^{2-}]$ was linear without any appreciable intercept (Figure 4.58). This confirms the absence of stable intermediates with large enough formation constants. The above facts support the suggestion of an outersphere mechanism operating in the oxidation of $\text{S}_2\text{O}_4^{2-}$ by Ru_2O^{4+} .

Based on the results and observations therefrom, a mechanism for reaction is hereby proposed.



If Equation 5.46 is the rate determining step, then:

$$\text{Rate} = [[(\text{H}_2\text{O})_2(\text{bipy})_4\text{Ru}_2\text{O}]^{4+} // \text{S}_2\text{O}_4^{2-}] \quad \dots (5.48)$$

From Equations 5.45 and 5.44 we get Equation 5.49.

$$[[(\text{H}_2\text{O})_2(\text{bipy})_4\text{Ru}_2\text{O}]^{4+} // \text{S}_2\text{O}_4^{2-}] = k_3 K_1 [(\text{H}_2\text{O})_2(\text{bipy})_4\text{Ru}_2\text{O}^{4+}] [\text{S}_2\text{O}_4^{2-}] \quad (5.49)$$

Substituting Equation 5.49 into Equation 5.48 we have Equation 5.50:

$$\text{Rate} = k_4 k_3 K_1 [(\text{H}_2\text{O})_2(\text{bipy})_4\text{Ru}_2\text{O}^{4+}] [\text{S}_2\text{O}_4^{2-}] \quad (5.50)$$

Equation 5.50 agrees with Equation 5.43, where $k_4 k_3 K_1 = k_2 = (10.99 \pm .04) \times 10^{-2} \text{ dm}^3 \text{ mol}^{-1} \text{ s}^{-1}$.

In the reaction under study, the oxidation product of $\text{S}_2\text{O}_4^{2-}$ is SO_2 , while in the reaction of dithionite with potassium ferrate, the product has been reported to be sulphite (Read, *et al.*, 2001). However, in the oxidation of sodium dithionite at a platinum electrode in alkaline solution, the final product of $\text{S}_2\text{O}_4^{2-}$ oxidation is sulphate.

5.4 Ru_2O^{4+} Reaction with H_3PO_2

Mole ratio determination showed that for every mole of Ru_2O^{4+} reduced, one mole of H_3PO_2 was oxidised because a plot of absorbance at infinity (A_∞) versus mole ratio ($\text{Ru}_2\text{O}^{4+}/\text{H}_3\text{PO}_2$) had a sharp break at 1. This mole ratio is consistent with the stoichiometric Equation 4.7. Similar stoichiometry has been reported for the oxidation of hypophosphorous acid by peroxomonosulphate (Dubey *et al.*, 2002), Au(III) (Sengupta *et al.*, 1983), MnO_4^- (Zahonyi-Budo and Simandi, 1991), Cr(VI) (Sengupta *et al.*, 1973) and ferrate(VI) (Hightower, 2012). However, in the oxidation of hypophosphorous acid by poly(pyridine)iron(III) complexes, the stoichiometry was reported to be 2:1, 2 moles of $\text{Fe}(\text{LL})_3^{3+}$ being reduced by 1 mole of H_3PO_2 (Yusuf *et al.*, 2004). The stoichiometry of 1:1 and the formation of phosphorous acid is rationalised on the Ru_2O^{4+} being a two-electron oxidant.

The linearity of the pseudo-first order plots of $\log (A_t - A_\infty)$ versus time for greater than 85% extent of reaction suggests that the reaction is first order with respect to $[\text{Ru}_2\text{O}^{4+}]$. First order dependence with respect to $[\text{H}_3\text{PO}_2]$ obtained is rationalised by the plot of $\log k_{\text{obs}}$ versus $\log [\text{H}_3\text{PO}_2]$ having a slope of 1.02. Most redox reactions of H_3PO_2 have

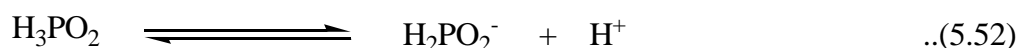
been documented to show first order dependence with respect to the reductant concentration (Dubey *et al.*, 2002, Sengupta *et al.*, 1973, Sengupta *et al.*, 1983, Zahonyi – Budo and Simandi, 1991, Yusuf *et al.*, 2004).

The rate law for the reaction is given as Equation 5.51.

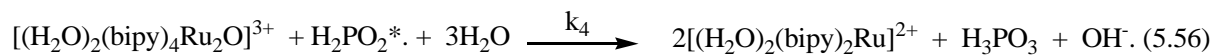
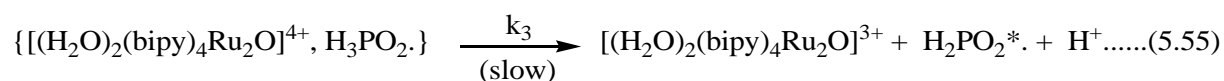
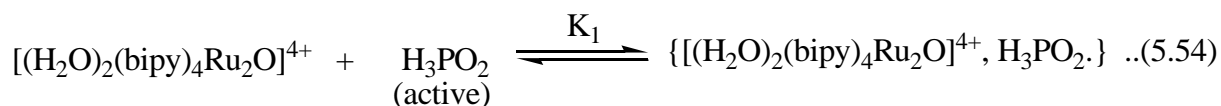
$$-\frac{d}{dt}[\text{Ru}_2\text{O}^{4+}] = k_{\text{obs}}[\text{Ru}_2\text{O}^{4+}] = k_2[\text{H}_3\text{PO}_2][\text{Ru}_2\text{O}^{4+}] \quad \dots(5.51)$$

Second order rate constant, k_2 , as evaluated from $k_{\text{obs}}/[\text{H}_3\text{PO}_2]$ for this reaction has been found to be $(7.12 \pm .04) \times 10^{-3} \text{ dm}^3 \text{ mol}^{-1} \text{ s}^{-1}$ at $[\text{Ru}_2\text{O}^{4+}] = 6.0 \times 10^{-5} \text{ mol dm}^{-3}$, $[\text{H}^+] = 5 \times 10^{-2} \text{ mol dm}^{-3}$, $I = 0.5 \text{ mol dm}^{-3}$ (NaClO_4) and $T = 31 \pm 1^\circ\text{C}$.

The second order rate constants for the oxidation of hypophosphorous acid was independent of acid and ionic strength in the range $0.1 - 1.0 \text{ mol dm}^{-3}$ (NaClO_4) (Table 4.7) and dielectric constant (Table 4.17). This suggests that none of the reactants is significantly protonated under our reaction condition and that the reaction is either between charged and uncharged reactants. The constancy of the electronic spectra of the reactants in the acid concentration range of $2.0 \times 10^{-2} - 20.0 \times 10^{-2} \text{ mole dm}^{-3}$ further suggests non-protonation. Hypophosphorous acid has a dissociation constant of $8.9 \times 10^{-2} \text{ mol dm}^{-3}$ at 25°C and ionises according to the equilibrium as represented by Equation 5.52.



The acid exists in the unionised form in a fairly strong acid medium. There are reports of the existence of the oxyacid in two tautomeric forms in aqueous solution, an



If Equation 5.55 is the rate determining step, then:

$$\text{Rate} = k_3 \{[(\text{H}_2\text{O})_2(\text{bipy})_4\text{Ru}_2\text{O}]^{4+}, \text{H}_3\text{PO}_2\} \dots(5.58)$$

From Equation 5.54, we have:

$$\{[(\text{H}_2\text{O})_2(\text{bipy})_4\text{Ru}_2\text{O}]^{4+}, \text{H}_3\text{PO}_2\} = K_1 [(\text{H}_2\text{O})_2(\text{bipy})_4\text{Ru}_2\text{O}]^{4+} [\text{H}_3\text{PO}_2] \dots(5.59)$$

Substituting Equation 5.59 into Equation 5.58 gives Equation 5.60.

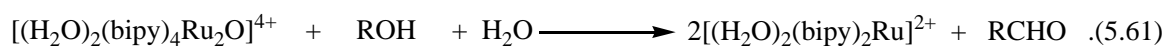
$$\text{Rate} = k_3 K_1 [(\text{H}_2\text{O})_2(\text{bipy})_4\text{Ru}_2\text{O}]^{4+} [\text{H}_3\text{PO}_2] \dots(5.60)$$

$$\text{where } k_3 K_1 = k_2 = (7.12 \pm .04) \times 10^{-3} \text{ dm}^3 \text{ mol}^{-1} \text{ s}^{-1}$$

The absence of catalysis or inhibition on addition of CH_3COO^- , HCOO^- , NH_4^+ and Mg^{2+} is rationalised on the basis of ion-pair formation as shown in Equation 5.54. Since the decay of the ion-pair (Equation 5.55) is a rate determining step in the reaction, it rules out any available site for attack by the ions, hence lack of ion catalysis or inhibition. The oxidation product of hypophosphorous acid in this reaction has been confirmed to be phosphorous acid. This agrees with the product obtained in the oxidation of hypophosphorous acid by ferrate(VI) (Hightower *et al.*, 2012), Au(III) (Sengupta *et al.*, 1973,1983) and permanganate ions (Zahonyi-Budo and Simandi, 1991).

5.5 Ru₂O⁴⁺ reaction with alcohols (CH₃OH, C₂H₅OH, C₃H₇OH)

Stoichiometric studies of the oxidation of the alcohols (ROH) by Ru₂O⁴⁺ indicated that for every mole of ROH oxidised, one mole of Ru₂O⁴⁺ was consumed. This stoichiometry is represented by Equation 5.61.



Similar stoichiometry has been reported for most reactions of aliphatic alcohols with other oxidising agents such as quinolinium bromochromate (Saraswat, *et al.*, 2003) ruthenate and perruthenate (Lee and Congson, 1990), pyridinium dichromate (Harit *et al.*, 2015) and sodium *N*-chloroethylcarbamate (Mittal *et al.*, 2004). The oxidation of benzyl alcohol by dichromate (Lee and Spitzer, 1975; Bijudas, 2014; Sengupta *et al.*, 1986), quinolinium fluorochromate (Dhage, *et al.*, 2013) and benzimidazolium fluorochromate (Dharmaraja *et al.*, 2008) also gave the same stoichiometry of 1:1. Even oxidation of substituted benzyl alcohols by sodium *N*-chlorobenzenesulphonamide (Mukherjee and Banerji, 1980) and sodium *N*-bromobenzenesulphonamide (Kothari and Banerji, 2011) had the same stoichiometry. The oxidation of chloramphenicol by 1-chlorobenzotriazole in acidic medium also had same stoichiometry (Hiremath *et al.*, 2005)

From kinetic studies, the reactions between Ru₂O⁴⁺ and ROH have been shown to have a first order dependence with respect to the oxidant concentrations, [Ru₂O⁴⁺]. Evidence of this assertion is based on the linearity of the pseudo-first order plots of log (A_t - A_∞) versus time for greater than 85% extent of reaction. Also, plots of log k_{obs} versus log [H⁺] for the three alcohols under study, were linear with slopes = 0.98 for the CH₃OH

system, 1.03 for the C₂H₅OH system and 0.91 for the C₃H₇OH system, suggesting first order dependence with respect to [ROH] for the three alcohols. Similar first order dependence with respect to [ROH] has been reported for the oxidation of aliphatic alcohols by quinolinium bromochromate (Saraswat *et al.*, 2003), ruthenate and perruthenate (Lee and Congson, 1990), Cerium(IV) catalysed by chromium (III)(Nimbalkar and Chavan, 1998), chromium(VI) (Sengupta *et al.*, 1986), and pyridinium dichromate (Harit *et al.*, 2015). Also, similar first order dependence with respect to alcohol concentration was reported for the oxidation of benzyl alcohol by sodium dichromate (Lee and Spitzer, 1975; Bijudas, 2014; and Sengupta *et al.*, 1986), quinolinium fluorochromate (Dhage *et al.*, 2013) and benzimidazolium fluorochromate (Dharmaraja *et al.*, 2008). The oxidation of substituted benzyl alcohols by sodium *N*, chlorobenzenesulphonate (Mukherjee and Banerji, 1980) and sodium *N*, bromobenzenesulphonate (Kothari and Banerji, 2011) also had first order dependence with respect to [ROH].

The overall rate law for the reaction, therefore, can be written as Equation 5.62.

$$-\frac{d}{dt}[\text{Ru}_2\text{O}^{4+}] = k_{\text{obs}}[\text{Ru}_2\text{O}^{4+}] = k_2[\text{Ru}_2\text{O}^{4+}][\text{ROH}] \quad \dots(5.62)$$

(where R = CH₃, C₂H₅, C₃H₇)

The values for the second order rate constants, k_2 , at $I = 0.5 \text{ mol dm}^{-3}$ and $T = 31 \pm 1 \text{ C}^\circ$ for the three systems have been reported elsewhere and reproduced below: $(12.01 \pm .03) \times 10^{-3} \text{ dm}^3 \text{ mol}^{-1} \text{ s}^{-1}$ for Ru₂O⁴⁺/ CH₃OH system; $(8.79 \pm .02) \times 10^{-3} \text{ dm}^3 \text{ mol}^{-1} \text{ s}^{-1}$ for Ru₂O⁴⁺/ C₂H₅OH system and $(3.51 \pm .02) \times 10^{-3} \text{ dm}^3 \text{ mol}^{-1} \text{ s}^{-1}$ for Ru₂O⁴⁺/ C₃H₇OH system.

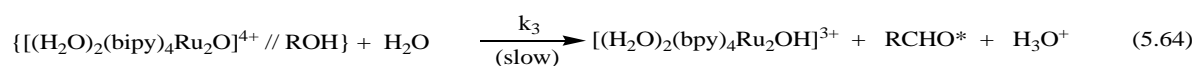
Addition of acid to the reaction mixture leads to the cessation of the reaction. Possibly, due to the protonation of the alcohol to form ROH^+ which undergoes electrostatic repulsion in the vicinity of the highly positively charged Ru_2O^{4+} . However, the reaction proceeded in the absence of acid and was subsequently monitored. This is in contrast to the H^+ catalysis reported for the oxidation of aliphatic alcohols by chromium(VI) (Sengupta *et al.*, 1986), ruthenate and perruthenate (Lee and Congson, 1990), chromium(III) (Nimbalkar and Chavan, 1998), quinolinium bromochromate (Saraswat *et al.*, 2003), sodium N-chloroethylcarbamate (Mittal *et al.*, 2004) and pyridium dichromate (Harit *et al.*, 2015). Similar H^+ was reported for the oxidation of benzyl alcohols by acidified dichromate (Lee and Spitzer, 1975; Sengupta *et al.*, 1986 and Bijudas, 2014), benzimidazolium fluorochromate (Dharmaraja, 2008) and quinolinium fluorochromate (Dhage *et al.*, 2013), while oxidation of substituted benzyl alcohols with sodium-N-chlorobenzenesulphonamide (Mukherjee and Banerji, 1980) and sodium-N-bromobenzenesulphonamide (Kothari and Banerji, 2011) was also catalysed by H^+ . The H^+ catalysis in all the above reactions was rationalised on the basis of the protonation of the oxidant prior to electron transfer.

Rates of reaction of Ru_2O^{4+} and ROH were unaffected by variation of the ionic strength and reduction in the dielectric constant of the reaction medium. This could mean that in the rate determining step one of the reactants is a neutral species or the reaction involved an ion – pair or adduct (Atkins, 1979). The lack of dependence of rate of reaction on variation in I is seen in the oxidation of chloramphenicol by 1 – chlorobenzotriazole (Hiremath *et al.*, 2005). However, in the oxidation of primary alcohols by pyridium dichromate (Harit *et al.*, 2015) and benzyl alcohol by benzimidazolium fluorochromate (Dharmaraja *et al.*, 2008) the reaction rate increased with increase in I and with decrease in D.

Added ions inhibited the rates of the reactions. This points to an outersphere electron transfer process in operation. This assertion is supported by the lack of spectrophotometric evidence for the formation of precursor complexes prior to electron transfer. When the reaction mixture was scanned as reaction progressed, λ_{max} remained at 660 nm, an indication that the reaction proceeded without the formation of intermediate complexes. This view was further reinforced by lack of intercept obtained from the Michaelis-Menten (Figures 4.53 – 4.62) plot of $1/k_{\text{obs}}$ versus $1/[\text{ROH}]$. These observations denote that the formation constants for such intermediates are negligible.

On addition of acrylamide to reaction mixture followed by excess methanol, polymerisation was induced. This is inferred from the formation of a gel, suggesting that free radicals are participating in the reaction.

On the basis of the above results and conclusions inferred from the results, the possibility of the oxidation of ROH by Ru_2O^{4+} occurring via the outersphere pathway is very high. A concerted mechanism involving the transfer of hydride ion from the C–H bond of the alcohol to the oxidant and removal of a proton from the O–H group is proposed for the reaction and is depicted in Equations 5.63 – 5.65.



Assuming Equation 5.64 to be the rate determining step, then the rate law is represented by Equation 5.66.

$$\text{Rate} = k_3 [[(\text{H}_2\text{O})_2(\text{bipy})_4\text{Ru}_2\text{O}]^{4+} // \text{ROH}] \quad (5.66)$$

From Equation 5.62,

$$[[(\text{H}_2\text{O})_2(\text{bipy})_4\text{Ru}_2\text{O}]^{4+} // \text{ROH}] = K_1 [(\text{H}_2\text{O})_2(\text{bipy})_4\text{Ru}_2\text{O}^{4+}] [\text{ROH}] \quad (5.67)$$

Substitution of Equation 5.67 into Equation 5.66 gives Equation 5.68.

$$\text{Rate} = k_3 K_1 [[(\text{H}_2\text{O})_2(\text{bipy})_4\text{Ru}_2\text{O}^{4+}] [\text{ROH}]] \quad (5.68)$$

Equation 5.68 resembles Equation 4.14

The mechanism is rationalised on the formation of an alcohol/ Ru_2O^{4+} adduct in a rapid equilibrium step (Equation 5.63) followed by rate limiting decomposition of the adduct to give the products (Equation 5.64).

5.6 Comparison of the Redox Reactions of Ru_2O^{4+} and the Various Reductants

Under study

All the reactions involving thiourea and its derivatives (TSH) had a stoichiometry of 1:2 (Ru_2O^{4+} / TSH), confirming that the thiourea and its derivatives under study are two-electron reductants. All the reactions progressed with inverse acid dependence, which is rationalised on the basis of the deprotonation of the thioureas prior to electron transfer. Here, the thioureas are mimicking thiols. The rate constants of the reactions increased in the order : ATU > DMTU > MTU > TU. This is in agreement with the study by Shaun *et al* (2011) who reported that the reactivity of some thioureas to oxidation is in the order : *N*-allylthiourea > *N*-phenylthiourea > *N*-methylthiourea > thiourea > *N*-tolylthiourea (Sahu *et al.*, 2011). Varying I and D had no effect on the reactions, this being attributable to the formation of ion-pairs. For all the ten systems under study,

$[(\text{H}_2\text{O})_2(\text{bipy})_2\text{Ru}]^{2+}$ was identified in the products, while in the reaction with the thioureas, disulphides were identified in the products of the four reactions. Free radicals played a role in all the reactions with the thioureas.

Comparably, while the stoichiometry of the reaction with $\text{S}_2\text{O}_3^{2-}$ was 1:2, that with $\text{S}_2\text{O}_4^{2-}$ was 1:1. Also, while the reaction with $\text{S}_2\text{O}_3^{2-}$ progressed with an acid dependence, that with $\text{S}_2\text{O}_4^{2-}$ had occurred in the absence of acid because of the likelihood of $\text{S}_2\text{O}_4^{2-}$ to be hydrolysed at a $\text{pH} < 10$. The reactivity of $\text{S}_2\text{O}_4^{2-}$ and that of $\text{S}_2\text{O}_3^{2-}$ in the reduction of Ru_2O^{4+} is of the order: $\text{S}_2\text{O}_4^{2-} > \text{S}_2\text{O}_3^{2-}$, suggesting that $\text{S}_2\text{O}_4^{2-}$ is a better reducing agent than $\text{S}_2\text{O}_3^{2-}$. Increase in I led to decrease in rate in the reaction with $\text{S}_2\text{O}_3^{2-}$ while varying I and D had no effect on the rate of reaction with $\text{S}_2\text{O}_4^{2-}$. In the two reactions, ion catalysis and inhibition were observed, but polymerization was not induced in the two reactions, suggesting that free radicals did not participate in the two reactions.

In the reduction of the oxo-bridged ruthenium dimer by the alcohols (CH_3OH , $\text{C}_2\text{H}_5\text{OH}$ and $\text{C}_3\text{H}_7\text{OH}$), the stoichiometries of the three reactions was consistently 1:1. The second order rate constants increased in the order: $\text{CH}_3\text{OH} > \text{C}_2\text{H}_5\text{OH} > \text{C}_3\text{H}_7\text{OH}$. This is consistent with the findings of Rao *et al* (1989), who reported the order of reactivity of the alcohols to be: benzyl alcohol $>$ methanol $>$ ethanol $>$ *n*-propanol $>$ *n*-butanol $>$ isopropanol. This order is expected taking into consideration the increase in chain length and branching at the α -carbon, which decreased the rate probably due to increase in electron density at this carbon. This, invariably, renders it difficult to part with the hydrogen, suggesting the cleavage of α -CH proton in the transition state analogous to cleavage of α -CH proton in acids (Jerry, 1977).

CHAPTER SIX

SUMMARY CONCLUSION AND RECOMMENDATION

6.1 Summary

The redox kinetics and mechanisms of the oxidation of thiourea (TU), *N*-methylthiourea (MTU), *N*-Allylthiourea (ATU), *N,N'*-dimethylthiourea (DMTU), thiosulphates ($\text{S}_2\text{O}_3^{2-}$) ion, dithionite ($\text{S}_2\text{O}_4^{2-}$) ion, hypophosphorous acid (H_3PO_2), methanol (CH_3OH), ethanol ($\text{C}_2\text{H}_5\text{OH}$) and propanol ($\text{C}_3\text{H}_7\text{OH}$) by Ru_2O^{4+} by diaquotetrakis(2, 2'-bipyridine)- μ -oxo-diruthenium(III) ions was studied. For the reactions with thiourea and its derivatives and $\text{S}_2\text{O}_3^{2-}$, the stoichiometries were determined to be 1:2 (oxidant/ reductant), while for the reactions with $\text{S}_2\text{O}_4^{2-}$, H_3PO_2 and the alcohols, a mole

ratio of 1:1 was found. All the reactions showed a second order dependence with respect to both oxidant and reductant concentrations. The reactions with the thioureas showed an inverse acid dependence, while that with $\text{S}_2\text{O}_3^{2-}$ showed direct acid dependence and that with H_3PO_2 was not affected by acid. In the reaction with alcohols, it was observed in preliminary tests that addition of acid seems to halt the reaction from taking place and with $\text{S}_2\text{O}_4^{2-}$, literature has confirmed that in the pH of this investigation the reductant undergoes hydrolysis. Based on the aforementioned reasons, the reactions with alcohols and $\text{S}_2\text{O}_4^{2-}$ were allowed to proceed in the absence of acid. The rates of all of the reactions, apart from the one with $\text{S}_2\text{O}_3^{2-}$, were unaffected by changes in I and D. The rate of reaction with $\text{S}_2\text{O}_3^{2-}$, however, decreased with increase in I and increased with decrease in D. Added ion catalysis and inhibition was observed for the reaction with $\text{S}_2\text{O}_3^{2-}$, $\text{S}_2\text{O}_4^{2-}$ and the alcohols, whereas for the reactions the thioureas, and H_3PO_2 , addition of ions had no effect on the reaction rates, this being attributable to the formation of ion-pairs. For the Ru_2O^{4+} / thioureas, Ru_2O^{4+} / H_3PO_2 and the Ru_2O^{4+} / alcohols reactions, polymerization was induced on addition of acrylamide, suggesting the participation of free radicals in the reactions, whereas the free radical test was negative for the $\text{Ru}_2\text{O}^{4+}/\text{S}_2\text{O}_3^{2-}$ and $\text{Ru}_2\text{O}^{4+}/\text{S}_2\text{O}_4^{2-}$ reactions.

6.2 Conclusion

Based on the stoichiometries, order of reactions, rate constants, effect of changes of H^+ concentrations, effect of changes in ionic strength and dielectric constant of the reaction medium, effect of addition of ions to the reaction medium, polymerization test as well as the absence of kinetic and spectroscopic evidence for intermediate complex formation prior to electron transfer, the outersphere mechanism has been postulated for all of the reactions.

6.3 Recommendation

- i. It is recommended that more work should be carried out on this versatile dimer, diaquotetrakis(2, 2'-bipyridine)- μ -oxo-diruthenium(III) ions so as to improve on its utilization.
- ii. Where equipment is available temperature dependent studies should be carried out to determine thermodynamic parameters for the reactions of the dimer.
- iii. Similar studies should be carried out on the ruthenium monomers for broader knowledge of the kinetics and mechanisms of the complex and for comparison with the redox behaviour of the ruthenium dimer.

REFERENCES

- Adegite, A., Iyun J.F. and Ojo, J.F. (1977). Kinetics and Mechanisms of Electron Transfer Reactions Between Uranium (III) and Some Ruthenium(III) Ammine Complexes. *Journal Chemical Society. Dalton Transactions*, 115 – 120.
- Adman, E.T. (1979). A Comparison of the Structures of Electron Transfer Proteins. *Biochimica et Biophysica Acta*, 549, 107-144.
- Alamgir, M. and Epstein, I.R. (1985). Complex Dynamical Behaviour in a New Chemical Oscillator. The Chlorite–Thiourea Reaction in A CSTR. *International Journal of Chemical Kinetics*, 17: 429 – 439 .
- Alessio, E., Mestronis, G., Bergamo, A. and Sava, G. (2004). Metal Ions and Their Complexes in Medication. *Cancer Diagnosis and Therapy*, 42-52
- Aparna, P., Kothari, S. and Baneji, K.K. (1995). Kinetics and Mechanism of the Oxidation of Primary Aliphatic Alcohols by Pyridinium Bromochromate. *Proceedings of Indian Academy of Sciences (Chemical Science.)*.107(3): 213 – 220.

- Arifoglu, M.A., Marmer, W.N. and Dudley, R.L. (1992). Reaction of Thiourea with Hydrogen Peroxide: ^{13}C NMR Studies of an Oxidative/ Reductive Bleaching Process. *Textile Research Journal*, 62: 94-100.
- Atkins, P.W. (1979). *Physical Chemistry*. English Language Book Society and Oxford University Press. Oxford, pp. 914–917.
- Aviram, I. and Sharabani, M. (1986). Kinetic Studies of the Reduction of Neutrophil Cytochrome B – 558 by Dithionite. *Biochemistry Journal* 237(2): 567 – 572.
- Ayoko, G.A. (1981). Reactions of 12 – Tungstocobaltate(III) Ion with Some Organic and Inorganic Ligands in Aqueous Solution. M. Sc Thesis, Ahmadu Bello University, Zaria – Nigeria and The References Therein.
- Ayoko, G.A. (1990). Oxidation of Hypophosphorous and Arsenious Acids by 12 – Tungstocobaltate(III) Ion in Aqueous Solution. *Transition Metal Chemistry* 15: 421 – 431.
- Ayoko, G.A. and Olatunji, M.A. (1983). Oxidation of L-Cysteine, Mercaptoacetic Acid and β -Mercaptoethylamine by 12-Tungstocobaltate(III). *Polyhedron*, 7: 577 – 579.
- Ayoko, G.A., Iyun, J.F. and Mamman, S. (1993a). Kinetics and Mechanism Of Oxidation of Nitrilotriacetate by Poly(Pyridyl) Iron(II) Complexes and Dodecatungstocobaltate(III) Ion. A Comparative Study. *Indian Journal of Chemistry*, 32A: 1089-1091.
- Ayoko, G. A., Iyun, J.F. and Ekubo, A. T. (1993b). Oxidation of Glutathione by Diaquotetrakis (2, 2'-Bipyridine)- μ -oxodiruthenium(III) Ion in Aqueous Acidic Solution. *Transition Metal Chemistry*, 18 (1): 6 – 8.
- Ayres, J.A. (1970). *Decontamination of Nuclear Reactors and Equipment* 2nd Ed. Ronald Press Co. New York, pp. 177.
- Babatunde, O.A. and Iyun, J.F. (2004). Kinetics of the Reduction of Di- μ -Oxo-Tetrakis (1, 10 - Phenanthroline) – Dimanganese (III, IV) Perchlorate by Thiosulphate Ions in Acid Medium. *Chemclass Journal*, 1-5.
- Babatunde, O.A. and Ajayi, J.O. (2013). Kinetic Approach to the Reduction of Toluidine Blue by Dithionite Ion in Aqueous Acidic Medium. *Global Journal Of Science Frontier Research Chemistry*, 13(8): 234 – 244.
- Babcock, G.T., Barry, B.A., Debus, R.J., Hoganson, C.W., Atamian, M., McIntosh, L., Sithole, I. and Yocum, C.F. (1989). Water Oxidation in Photosynthesis in Photosystem II: From the Radical Chemistry to Multielectron Chemistry. *Biochemistry*, 28: 9557.
- Babcock, G.T. and Wikstrom, M. (1992). Oxygen Activation and the Conservation of Energy In Cell Respiration. *Nature*, 356: 301-313

- Balden, I. and Niac, G. (1970). Reaction Between Chromate and Thiosulphates. II. Kinetics of Tetrathionate Formation. *Inorganic Chemistry*, 9(1): 110-119
- Balzani, V., Juris, A., Ventura, M., Campagna, S. and Serroni, S. (1996). Luminescent and Redox-Active Polynuclear Transition Metal Complexes. *Chemical Reviews*, 96: 759.
- Barigelletti, F. and Flamigni, L. (2000). Photoactive Molecular Wires Based on Metal Complexes. *Chemical Society Reviews*, 29: 1 – 14.
- Ben – Zvi, E. (1967). Oxidation of Hypophosphorous Acid by Peroxydisulphate. Kinetics Mechanism. *Inorganic Chemistry*. 6(6): 1143 – 1147.
- Bennet, L.E. (1972). Metalloprotein Redox Reactions. *Progress in Inorganic Chemistry* 18: 1-8
- Bijudas, K (2014). Kinetics and Mechanisms of the Selective Oxidation of Benzyl alcohols by Acidified Dichromate in Aqueous Acetic Acid. *Oriental Journal of Chemistry*, 30(3): 45 – 49.
- Binstead, R.A., Chronister, C.W., Ni, J.F., Hartshorn, C.M. and Meyer, T.J. (2000). Mechanism of Water Oxidation by the μ -Oxo Dimer $[(bpy)_2(H_2O)Ru^{III}ORu^{III}(OH_2)(bpy)_2]^{4+}$. *Journal of American Chemical Society* 122: 8464-8472
- Brønsted, J.M (1922). Activities of Ions in Solution. *Zeitschrift fur Physikalische Chemie*, 102: 60-63
- Burlamacchi, L', Casini, G., Fagioli, O. and Teizi, E. (1967). Electron Spin Resonance Study of the Dissociation of the Dithionite Ion ($S_2O_4^{2-}$). *Ric Science*. 37: 97-115
- Byerley, J.J., Fouda, S.A., Rempel, G.L. (1973). Kinetics and Mechanism of the oxidation of Thiosulphates Ions by Copper Ions in Aqueous Ammonia Solution. *Journal of Chemical Society, Dalton Transactions*. 8: 889 – 893.
- Caldin, J.P., Halpern, J. and Trimm, D.T. (1964). Kinetics of the Reduction of Some Cobalt(III) Complexes by Chromium(II), Vanadium(II) and Europium(III). *Journal of American Chemical Society*, 86: 1019-1021.
- Caldin, E.F. (1974). *Fast Reactions in Solution*. 3rd ed. Blackwell, Oxford. pp. 87-94
- Callaghan, R.W., Brown, G.H. and Meyer, T.J. (1975). Effects of Weak Metal-Metal Interactions in Ligand Bridged Complexes of Ruthenium Dimeric Complexes Containing Ruthenium Ions in Different Coordination Environments. *Inorganic Chemistry*, 14: 1441-1445
- Camacho, F., Paez, M.P., Jimenez, M.C. and Fernandez, M. (1997). Application of the

- Dithionite Oxidation to Measure Oxygen Transfer Parameters. *Chemical Engineering Science* 52(8): 1387 – 1391.
- Campion, R.J., Deck, C.F., King, P. and Wahl, A.C. (1967). Kinetics of Electron Exchange Between Hexacyanoferrate(II) and –(III) Ions. *Inorganic Chemistry*, 6: 672-676
- Carrol, R.L. and Thomas, L.B. (1966). Kinetics and Mechanism of Oxidation of Hypophosphorous Acid by Cerium (IV) in Perchloric Acid Solution. *Journal of American Chemical Society* 88(7): 1376 – 1381.
- Catalano, V. J., Heck, R. A., Ohman, A. and Hill, M.G. (2000). Synthesis, Characterization and Electrocatalytic Oxidation of Benzyl Alcohol by a Pair of Geometric Isomers of $[\text{Ru}(\text{trpy})(4, 4' - \text{Me}_2\text{dppi}(\text{OH}_2))^{2+}$ where 4,4' - Dppi is 3,6-Di-(4-Methylpyrid-2-Yl)Pyridazine. *Polyhedron* 19: 1049-1055.
- Chao, H., Mei, W.H., Huang, Q.W. and Ji, L.N. (2002). DNA Binding Studies of Ruthenium(II) Complexes Containing Asymmetric Tridentate. *Journal of Inorganic Biochemistry*, 92: 165-170.
- Che, C.M. and Yam, V.W.W. (1992). Spectroscopy and X – Ray Crystal Structure of Luminescent bis – [bis (Diphenylphosphino) Methane] Tetracyanodiplatinum. *Inorganic Chemistry*, 39: 233-237
- Chigwada, T.R., Chikwana, E., Ruwona, T., Olagunju, O. and Simoyi, R.H. (2007). Non – Linear Kinetics in the Oxidation of Trimethylthiourea by Acidic Bromate. *Journal of Physical Chemistry A* 111(43): 11552 – 11561.
- Corsaro, A. and Pistara, V. (1998). Conversion of the Thiocarbonyl Group into the Carbonyl Group. *Tetrahedron* 54(50): 15027 – 15062.
- Davidson, B., Soodak, M., Strout, H.V., Neary, J.T., Nakamura, C. and Maloof, F. (1979). Thiourea and Cyanamide as Inhibitors of Thyroid Peroxidase. The Role of Iodide. *Endocrinology*, 104(4): 919 – 924.
- Davies, D.M. and Lawther, J.M. (1989). Kinetics and Mechanism of Electron Transfer from Dithionite to Microsomal Cytochrome b_5 and to Form the Protein Associated with Charged and Neutral Vesicles. *Biochemistry Journal*, 258: 375 – 380.
- Davies, N.R. and Mullins, T.L. (1967). Substitution Reactions of Some Bis (2, 2'-Bipyridine) and Mixed 2,2'- Bipyridine, 2,2', 2'-Terpyridine Complexes of Ruthenium (II). *Australian Journal of Chemistry*, 20(4): 657 – 658.
- De Agazio, M. and Zacchini, M. (2001). Dimethylthiourea, a Hydrogen Peroxide Trap Partially Prevents Stress Effects and Ascorbate Peroxidase Increase in Spermidine – Treated Maize Roots. *Plant, Cell and Environment*, 24(2), 237 – 244.
- Deck, C.F. and Wahl, A.C (1954). Rate of the Ferrocyanide - Ferricyanide Exchange

- Reaction. *Journal of American Chemical Society*, 76, 4054 – 4059.
- Dennis, C.R., Leipoldt, J.G., Basson, S.S. and Lamprecht, G.J. (1985). The Oxidation of Thiosulphates Ions by Octacyanotungstate (V) in Weak Acidic Medium. *Polyhedron*, 4(9): 1621 – 1624.
- Dereven' kov, I.A., Salnikov, D.S., Makarov, S.V., Boss, G.R., and Koifman, O.I. (2013). Kinetics and Mechanism of Oxidation of Super – reduced Cobalamin and Cobinamide species by Thiosulphates, Sulphite and Dithionite. *Journal of Chemical Society, Dalton Transactions*, 42(43): 15307 – 15316.
- Dhage, S.D., Patwari, S.B. and Mukhedkar, S. (2013). Kinetics and Mechanisms of Oxidation of Benzyl Alcohol and Cyclohexanol by Quinolinium Fluorochromate. *Journal of Chemical and Pharmaceutical Research* 5(5): 41 – 45.
- Dharmaraja, J., Krishnasamy, K. and Shanmugam, M. (2008). Kinetics and Mechanism of Oxidation of Benzyl Alcohol by Benzimidazolium Fluorochromate. *E – Journal of Chemistry*, 5(4): 754 – 760.
- Dodd, A.N. (2002). Perspectives in Experimental Botany. *Journal Of Experimental Botany*, 54 (383): 609 - 622.
- Dong, Y., Venkatachalam, T.K., Sudbeck, E.A. and Uckun, F.M. (2000). Antioxidant Function of Phenethyl – 5 – Bromopyridyl Thiourea Compounds with Potent Anti – HIV Activity. *Bioorganic and Medicinal. Chemistry Letters*, 10(1): 87 – 90.
- Dubey, S., Hemkar, S., Khandelwal, C.L. and Sharma, P.D. (2002). Kinetics and Mechanisms of the Oxidation of Hypophosphorous Acid by Peroxomonosulphate in Aqueous Acid Medium. *Inorganic Chemistry Communications*, 5(10): 903 – 908.
- Edwards, J.O. (1954). Rates of Substitution Reactions in Oxyanions. *Journal of Chemical Education*, 31: 270.
- Eigen, M. and De Maeyer, L. (1963). *Technique of Organic Chemistry*. 3rd Ed. Interscience. New York. pp. 895-902.
- El-Ghayoury, A., Harriman, A., Khaytr, A. and Ziesel, R. (2000). Controlling Electronic Communication In Ethynylated-Polypyridine Metal Complexes. *Angewandte Chemie International Edition in English*, 39: 185-188
- El – Wassimy, M.T.M., Jorgensen, K.A. and Lawesson, S.O (1983). The Reaction of t – Butylhypochlorite with Thiocarbonyl Compound – A Convenient Method for the transformation *Tetrahedron* 39: 1729 – 1734.
- Endicott, J.F. and Taube, H. (1964). Kinetics of Some Outersphere Electron Transfer Reactions. *Journal of American Chemical Society*, 86: 1986 – 1987.

- Espenson, J.H (1965). Kinetics of The Reaction of Vanadium(III) and Chromium(II) Ions in Acid Solution. Evidence for a Binuclear Reaction Intermediate. *Inorganic Chemistry*, 4(7): 1025-1029
- Espenson, J.H. (1967). Innersphere Reduction of an Azidocobalt(III) Complex by Vanadium(II). Kinetics of Formation and Decomposition of the Metastable Monoazido-Vanadium (III) Ion. *Journal Of American Chemical Society*, 89: 127-132
- Fox, R.B. (1984). Prevention of Granulocyte – Mediated Oxidant Lung Injury in Rats by a Hydroxyl Radical Scavenger Dimethylthiourea. *Journal of Clinical Investigation*, 74(4): 1456 – 1464.
- Freemantle, M. (1998). Mimicking Natural Photosynthesis. *Chemical Engineering News*, 76: 37- 46.
- Gameay, A.H. (2002). Kinetics and Mechanism of the Reduction of Some Azo-dyes by Inorganic Oxysulphur Compounds. *Dye and Pigments* 54(3): 201 – 212.
- Gasana, E., Westbroek, P., De Wael, K., Temmerman, E., De Clerck, K. and Kieken, P. (2002). Kinetics and Mechanism of the Oxidation of Sodium Dithionite at a Platinum Electrode in Alkaline Solution. *Journal of Electroanalytical Chemistry*, 353: 35 – 42.
- Gaswick, D.C. and Krueger J.H. (1969). Kinetics and Mechanism of the Chromium (VI) – Iodide Reaction. *Journal of American Chemical Society*, 91: 2240.
- Geneste, F. and Moinet, C. (2004). Electrocatalytic Activity of Polypyridyl Ruthenium Oxo Complex Covalently Attached to a Graphite Felt Electrode. *New Journal of Chemistry*, 28: 722-726.
- Gersten, S. W., Samuels, G. J. and Meyer, T. J. (1982). Catalytic Oxidation of Water by an Oxobridged Ruthenium Dimer. *Journal of American Chemical Society*, 104: 4029-4030.
- Geselowitz, D. and Meyer, T.J. (1990). Water oxidation by μ -Oxobis[bis(bipyridine) Oxoruthenium(V)]⁴⁺. An Oxygen-labelling Study. *Inorganic Chemistry*, 29: 3894-3896.
- Ghosh, M.C., Reed, J.W. and Gould, E.S. (1994). Electron Transfer. 118. Proton Coupled Reductions of a Dinuclear Dimanganese (III, IV) Model for the Reactive Centre in Photosystem II. *Inorganic Chemistry*, 33: 73.
- Gilbert, J. A., Eggleston, D. S., Murphy, W. R., Geselowitz, D. A., Gersten, S. W., Hodgson, D. J. and Meyer, T. J. (1985). Structure and Redox Properties of the Water-Oxidation Catalyst [(bipy)₂(OH₂)RuORu(OH₂)(bpy)₂]⁴⁺. *Journal of American Chemical Society*, 107: 3855-3866.
- Greenwood, N.N. and Earnshaw, A. (1997). *Chemistry of the Elements* 2nd Ed. Butterworth. Heinemann. pp. 143 – 158.

- Griffiths, W.P (1970). Transition Metal Oxo – Complexes. *Coordination Chemistry Reviews*, 5: 459 – 517.
- Goyal, B, Solanki, S, Arora, S, Prakash, A and Mehotra, R.N (1995). Kinetics and Mechanism of the Oxidation of Thiosulphates by Hexachloroiridate (IV). *Journal of Chemical Society, Dalton Transactions*, 3109 – 3112.
- Grossman, B. and Haim, A. (1970). The Reduction Reaction between Hexachloroiridate (IV) and Pentacyanocobaltate (II). Evidence for the Binuclear Intermediate - μ - Chloro-Pentacyanocobaltate(III) and Pentachloroiridate(III). *Journal of American Chemical Society*, 92: 4835-4838
- Gupta, K.S. and Gupta, Y. K. (1970). Kinetics and Mechanism of the Reduction of Thallium(III) by Hypophosphite. *Journal of Chemical Society (A)*, 256 – 262.
- Haim, A. (1970). Some Comments on the Mechanisms of Substitution Reactions of Cobalt(III) Complexes of the Pentaamine Class. *Inorganic Chemistry*, 9: 426-431
- Haim, A. (1983). Electron Transfer Reactions: The Bridged Activated Complex. *Progress in Inorganic Chemistry*, 30: 273-357.
- Haim, A. and Sutin, N. (1966). Innersphere Mechanisms for the Reduction of Cobalt (III) Complexes by Iron (III). *Journal of American Chemical Society*, 88: 5343-5349.
- Hammerstrom, L., Sun, L.C., Akermark, B. and Styring, S. (2000). Mimicking Photosystem II Reactions in Artificial Photosynthesis. *Catalysis Today*, 58: 51-59.
- Hamza, S.A., Iyun, J.F. and Idris S.O. (2012). Kinetics and Mechanisms of Toluidine blue Reduction by Dithionite Ion in Aqueous Acidic Medium. *Journal of Chemical and Pharmaceutical Research*, 4(1): 6 – 13.
- Harit, H., Hiran, B. L. and Joshi, S.N. (2015). Kinetics and Mechanism of Oxidation of Primary Alcohols by Pyridinium Dichromate. *Chemical Science Transactions*, 4(1): 49 – 58.
- Henry, N.P.O., Harutyuneram, K.Y. and Byrd, J.E. (1979). Oxidation of Thiourea and *N,N*- Dialkylthioureas by Hexachloroiridate(IV) Ions. *Inorganic Chemistry*, 18(1):197 – 201.
- Hightower, S.M., Lorenz, B.B., Bernard, J.G. and Johnson, M.D. (2012). Oxidation of Phosphorus Centres by Ferrate(VI): Spectral Observation of an Intermediate. *Inorganic Chemistry*, 51(12): 6626 – 6632.
- Hintz, M.J. and Peterson J.A. (1980). Kinetics and Investigation of the Reduction of Cytochrome p-450 cam by Sodium Dithionite. *Micromes, Drug Oxidations and Chemical Carcinogenesis*, 1: 339 – 342

- Hiremath, R.C., Jagadeesh, R.V., Puttaswamy, C and Mayana, S. (2005). Kinetics and Mechanisms of Oxidation of Chloramphenicol by 1-Chlorobenzotriazole in Acidic Medium. *Journal of Chemical Society*, 117(4): 333–336.
- Hoffman, M. and Edwards, J.O. (1977). Kinetics and Mechanism of the Oxidation of Thiourea and *N,N'*- Dialkylthioureas by Hydrogen Peroxide. *Inorganic Chemistry*, 16(12): 3333 – 3338.
- Holze, A.C.G., Broekhuisen, M.E.T., Velders, A.H., Vanderschilden, K., Hassnoot, J.G. and Reedijk, J. (2002). Unusual Coordination of the Rare Neutral Imine Tautomer of 9-Methylaminechelating in The *N6, N7* – Mode to Ruthenium(II) Complexes. *European Journal of Inorganic Chemistry*, 369-376.
- Howelett, K.E. and Wedzicha, B.I. (1970). Kinetics of the Reaction Between Hexacyanoferrate(III) and Thiosulphate Ions, the Initial Reaction. *Inorganica Chimica Acta*, 18: 133 – 138.
- Hubbard, C.D., Gerhard, A. and van Eldik, R. (1991). Oxidation of Dihydroxy Aromatic Substrates by Hexachloroiridate (IV). Mechanistic Information from Volume of Activation. *Inorganic Chemistry*, 30: 5023-5027
- Hurst, J.K. (2005). Water Oxidation Catalysed by Dimeric μ -Oxo Bridged Ruthenium Diimine Complexes. *Coordination Chemistry Reviews*, 249: 313-328.
- Hurst, J.K., Zhou, J.Z., Lei, Y.B. (1992). Pathways for Water Oxidation Catalysed by the μ -Oxobis[Aquabis(Bipyridine)Ruthenium]⁴⁺ Ion. *Inorganic Chemistry*, 31: 1010-1017.
- Idris, S.O., Tanimu, A., Iyun, J.F. and Mohammed, Y. (2015). Kinetics and Mechanism of the Reaction of Malachite Green and Dithionite Ion. *International Research Journal of Pure and Applied Chemistry*. 5(2): 177 – 184.
- Indrayan A.K., Mishra, S.K. and Gupta, Y. (1981). Kinetics and Mechanism of Oxidation of Hypophosphorous Acid with Ag(II) in aqueous Perchloric Acid Solution. *Inorganic Chemistry*, 20(2): 450 – 454.
- Islam, A., Sughara, H. and Arakawa, H. (2003). Molecular Design of Ruthenium(II) Polypyridyl Photosensitizers for Efficient Nanocrystalline TiO₂ Solar Cells. *Journal of Photochemistry and Photobiology. A-Chemistry*, 158: 131-138.
- Iyun, J.F (1982). *The Kinetics and Mechanisms of the Oxidation-Reduction and Substitution Reactions of some Metal Ion Complexes in Acid Solutions*. Ph.D Thesis, Ahmadu Bello University, Zaria, Nigeria.
- Iyun, J.F. and Adegite, A. (1990). Kinetics and Mechanism of the Reduction of Dichlorotetrakis(2, 2'-Bipyridine)- μ -oxodiruthenium ion by Ti(III)-EDTA in Aqueous Acidic Medium. *Bulletin of Chemical Society of Ethiopia*, 4:27-31
- Iyun, J. F., Ayoko, G. A. and Lawal, H.M. (1992a). The Stoichiometry and Kinetics of

- Oxidation of 1,4-Benzenediol by Diaquotetrakis(2, 2'-Bipyridine)- μ -oxodiruthenium(III) Cation in Perchloric Media. *Indian Journal of Chemistry*, 31(A): 943 – 947.
- Iyun, J. F., Ayoko, G. A. and Lohdip, Y. N. (1992b). The Kinetics and Mechanism of the Oxidation of Diaquotetrakis(2, 2'-Bipyridine)- μ -oxodiruthenium(III) by Bromate in Aqueous Perchloric Acid. *Polyhedron*, 11(18): 2277-2433.
- Iyun, J. F., Ayoko, G. A. and Lawal, H.M. (1992c). Kinetics and Mechanism of the Oxidation of Iodide by Diaquotetrakis(2,2¹-Bipyridine)- μ -oxodiruthenium(III) Ion in Acid Medium. *Transition Metal Chemistry*, 17(1): 63 – 65.
- Iyun, J. F., Ayoko., G. A. and Lohdip, Y. N. (1992d). The Oxidation of Sulphite by Diaquotetrakis(2, 2'-Bipyridine)- μ -oxodiruthenium(III) Ion in Perchloric Acid. *Bulletin of Chemical Society of Ethiopia*, 6(1): 1–9.
- Iyun, J. F., Ayoko, G. A. and Lawal, H.M. (1995a). The Kinetics and Mechanism of the Reduction of Diaquotetrakis(2, 2'-Bipyridine)- μ -oxodiruthenium(III) by Ascorbic Acid. *Transition Metal Chemistry*, 20(1): 30 – 33.
- Iyun, J. F., Musa, K.Y. and Ayoko, G.A. (1995b). Oxidation of 2 – mercaptoethanol and 2 – mercaptoethylamine by [(bpy)₂H₂O]Ru^{III}]₂O⁴⁺ in Aqueous Media. *Indian Journal of Chemistry*, 34(A): 635 – 638.
- Iyun, J. F, Ayoko, G.A and Lawal, H.M. (1996). Kinetics of the Reduction of μ -oxobis [aquobis(2, 2' - bipyridine)] Ruthenium(III) by l-cysteine in Aqueous Solution. *Indian Journal of Chemistry*, 35(A): 210 – 213.
- Iyun, J.F. and Shehu, A.R. (2004). Kinetics and Mechanism of the Oxidation of Ethanol and Propanol by Chromium(VI) in Acidic Medium. *ChemClass Journal*, 55 – 58.
- Iyun, J. F. and Ukoha, P.U. (1999). Kinetics and Mechanism of Oxidation of 1,3 Dihydroxybenzene by Trioxiodate (V) ion in Aqueous Perchloric Acid. *Indian Journal of Chemistry*, 38: 180 – 187.
- Jerry, M. (1977). *Advanced Organic Chemistry*. 3rd Ed. McGraw-Hill Book Company, London. pp. 530 – 536.
- Jiang, C.W., Chao, H., Hong, X.L., Li, H., Mei, W.J. and Ji, L.N. (2003). Enantiopreferential DNA-binding of a novel Dinuclear Complex [(bpy)₂Ru(bdptb)Ru(bpy)₂]⁴⁺. *Inorganic Chemistry, Communications*, 6: 773-775.
- Johnson, K.A. and Goody, R.S. (2011). The Original Michaelis-Menten Constant: Translation of the 1913 Michaelis-Menten Paper. *Biochemistry*, 50(39): 8264 – 8269.
- Johnson, M.D. and Balahura, R.J. (1998). Kinetics and Mechanism of the Oxidation of

- Coordinated Thiosulphates by Peroxymonosulphate. *Inorganic Chemistry*, 27(18): 3104 – 3107.
- Johnson, M.D. and Read, J.F. (1996). Kinetics and Mechanism of the Ferrate Oxidation of Thiosulphates and Other Sulphur – containing Species. *Inorganic Chemistry*, 35(23): 6795 – 6799.
- Jordan, J. and Catherino, H.A. (1963). Divalent Thallium. *Journal of Physical Chemistry*, 67:2241 – 2249.
- Juris, A., Balzani, V., Barigelleti, F., Campagna, S., Belser, P. and Vonzelewsky, A. (1998). Ru(II) Polypyridine Complexes: Photophysics, Photochemistry, Electrochemistry and Chemiluminescence. *Coordination Chemistry Reviews*, 84: 85-89
- Kagan, H.B., Roman, B. (1992). Transition- Metal Coordination Chemistry of Sulphoxides. *Reviews on Heteroatom Chemistry*, 7: 92-116.
- Kalyanasundaram, K. and Gratzel, M. (1998). Applications of Functionalised Transition Metal Complexes in Photonic and Optoelectronic Devices. *Coordination Chemistry Review*, 177: 347-414.
- Kalyanasundaram, K (1982). Photophysics, Photochemistry and Solar Energy Conversion with Tris(Bipyridyl) Ruthenium(II) and its Analogues. *Coordination Chemistry Review*, 46: 159.
- Keene, F.R (1999). Metal-Ion Promotion of the Oxidative Dehydrogenation of Coordinated Amines and Alcohols. *Coordination Chemistry Review*, 187: 121 – 149.
- Kothari, A., Kothari, S. and Banerji, K.K. (2005). Kinetics and Mechanism of the Oxidation of Alcohols by Butyltriphenylphosphonium Dichromate. *Indian Journal of Chemistry*, 44A: 2039 – 2043.
- Kothari, S. and Banerji, K.K. (2011). Kinetics and Mechanism of the Oxidation of Substituted Benzyl Alcohols by Sodium *N*-bromobenzenesulphonamide. *Canadian Journal of Chemistry*, 63(10): 2726 – 2729.
- Kotowski, M. and van Eldik, R. (1989). Applications of High Pressure Kinetic Techniques to Mechanistic studies in Coordination Chemistry. *Coordination Chemistry Reviews*, 93: 19-23
- Kumar, C.C., Chandaraiah, U., Siddiqui, M.A.A. and Kordlikars, S. (1991). Kinetics and Mechanism of the Oxidation of Amino Acids of the Type NH₂CH(R)COOH with Hexachloroiridate(IV). *Indian Journal of Chemistry* 30(A): 714 – 715.
- Lagford, C.H. (1979). Mechanisms in Electron Transfer Reactions. *Inorganic Chemistry*, 18: 3288-3294
- Larsen, D.W. and Wahl, A.C. (1965). Electron Rates for Unsubstituted and

- Disubstituted tris(1,10-phenanthroline)iron-(II) and -(III) Ions from N.M.R Studies. *Journal of Chemical Physics*, 43: 3765-3768
- Lebeau, E.L. and Meyer, T.J. (1999). Oxidation of Benzyl Alcohol by a Dioxo Complex of Ruthenium(VI). *Inorganic Chemistry*. 38: 2174-2181.
- Lee, D.G. and Spitzer, U.A. (1975). Kinetics and Mechanisms of the Oxidation of Benzyl Alcohol and Benzaldehyde by Aqueous Sodium Dichromate. *Canadian Journal of Chemistry*, 53: 3709-3712
- Lee, D.G. and Congson, L.N. (1990). Kinetics and Mechanisms of the Oxidation of Alcohols by Ruthenate and Perruthenate. *Canadian Journal of Chemistry* 68 (1): 1774 – 1779.
- Lei, Y.B. and Hurst, J.K. (1994a). Dynamical Investigations of the Catalytic Mechanism of Water Oxidation by the $[(bpy)_2Ru(OH_2)]_2O^{4+}$ Ion. *Inorganica Chimica Acta* 226: 179-185.
- Lei, Y.B. and Hurst, J.K. (1994b). Structural Investigations of the Catalytic Mechanisms of Water Oxidation by the $[(bpy)_2Ru(OH_2)]_2O^{4+}$ Ion. *Inorganic Chemistry*, 33: 4460-4467.
- Lohdip, Y.N. and Iyun, J.F. (1998). Kinetics of the Reduction of Di- μ -oxo-tetrakis (1, 10-Phenanthroline) Dimanganese(III, IV) Perchlorate by D, L–Methionine in Acid Solution. *Bulletin of Chemical Society of Ethiopia* 12 (2): 1-7.
- Lohdip, Y.N. and Iyun, J.F. (2003). Kinetics And Mechanism of the Oxidation Of Thiocyanate Ion by Di- μ -Oxo-Tetrakis (1,10 - Phenanthroline) Dimanganese (III, IV) Ion in Acid Medium. *Global Journal Of Pure And Applied Sciences*, 9 (1): 105-112.
- Lohdip, Y.N. and Ogara, J.I. (2004). Kinetics and Mechanism of the Reduction of Di- μ -Oxo-Tetrakis (1,10-Phenanthroline) Dimanganese (III,IV) Perchlorate by Ascorbic Acid in Acid Medium. *Journal of Chemical Society of Nigeria*, 29 (2): 78.
- Lohdip, Y.N. and Shamle, N.J. (2004). Kinetics and Mechanism of the Oxidation of Hypophosphorous Acid by Di- μ -Oxo-Tetrakis (2, 2'-Bipyridyl) Dimanganese (III, IV) Perchlorate by Ascorbic Acid in Acid Medium. *Chemclass Journal*, 95-98.
- Lohdip, Y.N., Davies, A.K. and Iyun, J.F. (1998). Kinetics and Mechanism of the Oxidation of Formaldehyde by Permanganate Ion in Aqueous Perchloric Acid. *Nigerian Journal of Textile Education*, 15(2): 57- 64.
- Malmstrom, B.G. (1993). Vectorial Chemistry in Bioenergetics: Cytochrome c Oxidase as a Redox – linked Proton Group. *Accounts in Chemical Research*, 26: 332-338.
- Mathur, D., Sharma, P.K. and Banerji, K.K. (1993). Kinetics and Mechanism of the

Oxidation of Primary Alcohols by Pyridinium Hydrobromide Perbromide. *Journal Chemical Society, Perkins Transactions*, 2: 205 – 208.

- Matsumoto, K., Aizawa, H., Koto, H., Fukuyama, S. and Hara, N. (2000). Effect of Dimethylthiourea, a Hydroxyl Radical Scavenger, on Cigarette Smoke-Induced Bronchoconstriction in Guinea Pigs. *European Journal of Pharmacology*, 403: 157 – 161.
- Mayhew S.G. (1978). The Redox Potential of Dithionite and Sulphonyl Radical from Equilibrium Reactions with Flavodoxins, Methyl Viologen and Hydrogen plus Hydrogenase. *European Journal of Biochemistry*, 85: 535 – 547.
- Mayhew, S.G. and Massey, V. (1973). Studies on the Kinetics and Mechanism of Reduction of Flavodoxin from *peptostreptococcus Elsdonii* by Sodium Dithionite. *Biochimica et Biophysica Acta*, 315: 181 – 186.
- McAuley, A. and Gomwalk, U.D. (1968). Metal Ion Oxidations in Solution. Part V. Cerium (IV) Oxidation of Thiourea and its N – Substituted Derivatives. *Journal of Chemical Society*, 2948 – 2951.
- McAuley, A. and Gomwalk, U.D. (1969). Metal Ion Oxidations in Solution. Part VI. Oxidation of Thiourea and its N–Substituted Derivatives by Cobalt (III). *Journal of Chemical Society (A)*, 977 – 2951.
- Mehrotra, R.N. (2013). Three Oxyacids of Phosphorus: Tautomerism and Oxidation Mechanism. *European Chemical Bulletin*, 2(10): 758 – 776.
- Melvin, W.S. and Haim, A. (1977). Reductions of hexabromoiridate(IV) by chromium (II) and by pentacyanocobaltate(II). Evidence for Bromo-bridged Binuclear Intermediates. *Inorganic Chemistry*, 16(8): 2016-2022
- Meyer, T. J. (1984). Electron Transfers in Chemistry and Biology. *Journal Electrochemical Society*, 131: 221c.
- Meyer, T. J. (1989). Chemical Approaches to Artificial Photosynthesis. *Account of Chemical Research*, 22: 163-167
- Meyer, T. J. (1990). Intramolecular Control of Excited State Electron and Energy Electron Transfer. *Pure and Applied Chemistry*, 62: 10-16
- Meyer, T.J. and Huynh, M.H.V. (2003). The Remarkable Reactivity of High Oxidation State of Ruthenium and Osmium Polypyridyl Complexes. *Inorganic Chemistry*, 42: 8140-8160.
- Meyer, T.J. and Taube, H. (1987). Electron Transfer Reactions. In: Wilkinson, G. (Ed) *Comprehensive Coordination Chemistry* Vol. 1 Pergamon Press. U.K 1. pp 331-338.
- Meyer, T.J. and Miller, F.J. (1971). Reaction between Azide ion and $[\text{Ru}(\text{bipy})_2(\text{NO})\text{Cl}]^{2+}$. *Journal of American Chemical Society*, 93: 1294 – 1299.

- Miller, A.E, Bischoff, J.J. and Pane, K. (1988). Chemistry of Aminoiminomethanesulphinic and –Sulphonic Acids Related to Toxicity of Thioureas. *Chemical Research in Toxicology*, 1: 169 – 174.
- Mishra, L., Yadaw, A.K. and Govil, G. (2003). Tailored ruthenium polypyridyl complexes as molecular electronic materials. *Indian Journal of Chemistry, Section A*. 42, 1797-1814.
- Mishra, S.K. and Gupta, Y.K. (1967). Kinetics and Mechanism of Oxidation of Hypophosphite by Ce (IV) in Sulphuric Acid Solution. *Journal Inorganic and Nuclear Chemistry*, 29: 1643 – 1656.
- Mittal, S, Sharma, V. and Banerji, K.K. (2004). Kinetics and Mechanism of the Oxidation of Primary Alcohols by Sodium N – Chloroethylcarbamate. *International Journal of Chemical Kinetics*. 18(6): 689 – 699.
- Morgan, J.E. and Wikstrom, M. (1991). Steady-State Redox Behaviour of Cytochrome C, Cytochrome A, and of Cytochrome C Oxidase in Intact Rat Liver Mitochondria. *Biochemistry*, 30: 948-952
- Movius, W.G. and Kaus, R.G. (1970). Studies on the Rate of Reduction of Ruthenium(III) Complexes by Chromium(III) and Vanadium(II). *Journal of American Chemical Society*, 92: 2677.
- Mukherjee, J. and Banerji, K.K. (1980). Kinetics and Mechanism of the Oxidation of Substituted Benzyl Alcohols by Sodium N–Chlorobenzenesulfonamide. *Journal of Chemical Society, Perkin Transactions*, 1324-1327
- Nagoshi, K., Yagi, M. and Kaneko, M. (2000). Analysis of Water Oxidation Catalysts by Dinuclear Ruthenium Complex $[(\text{NH}_3)_5\text{Ru}-\text{O}-\text{Ru}(\text{NH}_3)_5]^{4+}$ Incorporated in a Nafion Membrane. *Bulletin of Chemical Society of Japan* 73: 2193-2199
- Nagoshi, K, Yamashita, S, Yagi, M and Kaneko, M. (1999). Catalytic activity of $[(\text{bpy})_2(\text{H}_2\text{O})\text{Ru} - \text{O} - \text{Ru}(\text{H}_2\text{O})(\text{bpy})_2]^{4+}$ for Four-electron Water Oxidation. *Journal of Molecular Catalysis A, Chemical*, 144: 71-81
- Nagypal, I. and Epstein, I.R. (2004). Kinetics and Mechanism of the Reaction between Thiosulphates and Chlorite Ions at 90°C. *International Journal of Chemical Kinetics*, 18(3): 345 – 353.
- Nazeeruddin, M.K., Rotzinger, F.P., Comte, P. and Gratzel, M.J. (1988). Spontaneous Oxidation of Water to Oxygen by the Mixed-Valence μ - Oxo Ruthenium Dimer. *Journal of Chemical Society, Chemical Communications*, 872-883
- Newkome, G.R., Cho, T.J., Moorefield, C.N., Mohapatra, P.P. and Grodzinez, L.A. (2004). Towards Ordered Architectures: Self-Assembly and Stepwise Procedures to the Hexameric Metallomacrocycles $[\text{Arylbis}(\text{Terpyridinyl})_6 \text{Fe}^{\text{II}}_{-N-} \text{Ru}^{\text{II}}_{-n}]$. (N=0, 2, 3, 5). *Chemistry – A European Journal*, 10: 1493-1500.

- Nickless, G. (1968). *Inorganic Sulphur Chemistry*, Elsevier, Amsterdam, 3rd Ed. pp. 199-207.
- Nimbalkar, L.V. and Chavan, A.M. (1998). Kinetics and Mechanism of Cerium (III) oxidation of Primary Alcohols by Chromium (III). *Journal of Physical Organic Chemistry*, 11(10): 697 – 700.
- Okamura, M.Y And Feher, G (1992). Proton Transfer On Reaction Centres From Photosynthetic Bacteria. *Annual. Review in Biochemistry*, 61: 861-875
- Ossipov, D., Gohil, S. and Chattopadhyaya, J. (2002). Synthesis of DNA-[Ru(tpy)(dppz)(CH₃CN)]²⁺ Conjugates and Their Photo Cross Linking Studies with the Complementary DNA Strand. *Journal of American Chemical Society*, 124: 13416-13433
- Pal, B. and Gupta, K.K.S. (2012). Kinetics and Mechanism of the Innersphere Reduction of Hexachloroplatinate(IV) by Dithionite in Acetate Buffer. *Transition Metal Chemistry*, 37(7): 671 – 678
- Pan, C. and Stanbury, D.M. (2014). Kinetics and Initial Steps in the Aqueous Oxidation of Thiosulphates by Chlorine Dioxide. *Journal of Physical Chemistry A*, 118(34): 6827- 6831.
- Petach, H.H, Elliot, O.M (1992). Characterization and catalytic activity of covalently linked bipyridyl ruthenium oxodimers. *Journal of Electrochemical Society* 139: 221-227.
- Petri, A. and Baldea, I. (1975). Oxidation of Methionine by Chromates. *Studia Universitatis Babes–Bolyai, Seria Chemia* 20: 76 [C.A. 84:44629a]
- Price, H.J. and Taube, H. (1968). The Reduction of α – carbonylcarboxylic Acid Complexes of Pentaamminecobalt(III) by Chromous, Vanadous And Hexaammine Ruthenium(II) Ions. *Inorganic Chemistry*. 7: 1114 - 1119
- Prince, R.C. and George, G.N. (1990). Tryptophan Radicals. *Trends in Biochemical Sciences*. 15: 170-172.
- Pryztas, T.J. and Sutin, N. (1973). Kinetic Studies of Anion – assisted Outersphere Electron Transfer Reactions. *Journal of American Chemical Society*, 95:5545.
- Rabai, G and Beck, M.T (1985). Oxidation of Thiourea by Iodate: A New Type of Oligo – Oscillatory Reaction. *Journal of the Chemical Society* 107(6): 1669 – 1672
- Rabai, G, Wang, R.T and Kustin, K. (1993). Kinetics and Mechanism of the Oxidation of Thiourea by Chlorine Dioxide. *International Journal of Chemical Kinetics* 25: 53 – 62
- Ramaraj, R, Kira, A , and Kaneko, M (1986). O₂ - generation by Oxidation of Water

with Di – and Trinuclear Ruthenium Complexes as Homogenous and Heterogenous Catalysts. *Angewandte Chemie International Edition in English*, 25, 1009-1013

- Ramaraj, R, Kira, A , and Kaneko, M (1986). Heterogenous Water Oxidation by an Amide-Bridged Dinuclear Ruthenium Complex Adsorbed on Ion-Exchange Resins. *Journal of Chemical Society, Communications*.1707-1709
- Ramaraj, R, Kira, A , and Kaneko, M (1987). Mononuclear ruthenium-ammine complexes as catalysts for water oxidation. *Journal of Chemical Society, Communication*, 227-228
- Ramaraj, R.J, Kaneko, M and Kira, A (1991). Hexaammineruthenium complex as two-electron catalyst for oxygen evolution by homogenous and heterogenous water oxidation. *Bulletin of Chemical Society of Japan* 64: 1028-1034
- Rao, P.M, Sethuram, B. and Rao N.T. (1989). Kinetics and Mechanism of Rh(III) Catalysed Oxidation of Alcohols by Periodate. *Proceedings of Indian Science Academy* 55A(6): 858 – 863.
- Read, J.F, John, J, Macpherson, J, Schaubel, C and Therian, H.A (2001). Kinetics and Mechanism of the Oxidation of Inorganic Oxysulphur Compounds by Potassium Ferrate: Part I. Sulphite, Thiosulphates and Dithionite. *Inorganica Chimica Acta*, 315(1): 96 – 106.
- Robin, M. B. and Day, P. (1967). Mixed Valence Chemistry: A Survey and Classification. *Advances in Inorganic Chemistry and Radiochemistry*, 10: 247-422.
- Rodriguez, M, Romero, I and Llobet, A (2001). Synthesis, Structure and Redox and Catalytic Properties of a New Family of Ruthenium Complexes Containing the Tridentate bpea Ligand. *Inorganic Chemistry*, 49: 4150-4156.
- Rosseinsky, D. R (1972). Aqueous Electron – Transfer Reactions. Vanadium (IV) as a Reductant Compound with Iron(II). *Chemical Reviews*, 72: 215-221
- Rossenheim, L, Speiser, D and Laim, A (1974). Reduction Of Ethylenediaminetetra Acetatocobalt(III) Complexes by Hexacyanoferrate(III). *Inorganic Chemistry*, 11: 1571 – 1583.
- Rotzinger, F. P., Munavalli, Comte, P., Hurst, J. K., Gratzel, M., Pern, F. J. and Frank, A. J. (1987). A Molecular Water Oxidation Catalyst Derived from Ruthenium Diaquo bis (2, 2'-Bipyridyl-5,5'-Dicarboxylic Acid). *Journal of American Chemical Society*, 109: 661-672
- Sahu, S., Sahoo, P.R., Patel, S. and Mishra, B.R. (2011). Oxidation of Thiourea and Substituted Thioureas: A Review. *Journal of Sulphur Chemistry*, 32(2): 171 – 197.
- Saraswat, S, Sharma, V, and Banerji, K.K. (2003). Kinetics and Mechanism of

- Oxidation of Aliphatic Alcohol by Quinolinium Bromochromate. *Proceedings of Indian Academy of Sciences (Chemical. Science)*. 115(1): 654 – 663.
- Schoonover, R.J, Ni, J.F, Roeker, L, Whiter, P.S. and Meyer, T.J. (1996). Structural and Resonance Raman Studies of an Oxygen-Evolving Catalyst Crystal Structure of [(bpy)₂(H₂O)Ru^{III}ORu^{IV}(OH₂)(bpy)₂](ClO₄)₄. *Inorganic Chemistry*, 35:5885-5892.
- Sengupta, K.K., Pal, B, B and Mukherjee, D.C. (1970). Kinetics of the Oxidation of Hypophosphite ion by V(III) in Hydrochloric Acid Medium. *Zeitschrift fur Physikalische Chemie (Muenchen)*, 72: 230-237
- Sengupta, K.K, Chakladar, J.K and Chatterjee, A.K. (1973).). Kinetics and Mechanisms of the Oxidation of Hypophosphorous and Phosphorous Acids by Chromium(IV). *Journal of Inorganic and Nuclear Chemistry*, 35(3): 901 – 908.
- Sengupta, K.K, Basu, B., Sengupta, S and Nandi, S (1983). Kinetics of the Oxidation of Hypophosphite ion by Au(III) in Hydrochloric Acid Medium. *Polyhedron*, 2(10) : 983 – 986.
- Sengupta, K.K, Samanta, T. and Basu, S.N. (1986). Kinetics and Mechanism of Oxidation of Ethanol, Isopropanol and Benzyl Alcohol by Chromium(VI) in Perchloric Acid Medium. *Tetrahedron*, 42(2): 681 – 685.
- Sengupta, K.K, and De, P.C (1975). Kinetics of the Oxidation of Hypophosphite ion in Acid Medium. *Indian Chemical Society Journal*, 52, 252-261
- Shea, H and Haim, A (1973). Adjacent attack in redox reaction between pentammine cobalt(IV). *Inorganic Chemistry*, 12: 3013-3018.
- Shubha, J.P. and Puttaswamy, J. (2009). Oxidative Conversion of Thiourea and N-substituted Thioureas into Formamidine Disulphides with Acidified Chloramine-T: A Kinetic and Mechanistic Approach. *Journal of Sulphur Chemistry*. 30 : 490 – 499.
- Simonsen, R.P. and Tollin, G (1980).Structure-functions Relations in Flavodoxins. *Molecular Cellular Biochemistry*, 33: 13-24.
- Simoyi, R.H. (1986). New Bromate Oscillator: The Bromate – Thiourea Reaction in a CTCR. *Journal of Physical Chemistry*, 90: 2802 – 2804.
- Simoyi, R.H. and Epstein, I.R. (1987). Systematic Design of Chemical Oscillators. 40. Oxidation of Thiourea by Aqueous Bromine: Autocatalysis by Bromide. *Journal of Physical Chemistry*, 91(19): 5124 – 5128.
- Simoyi, R.H., Epstein, I.R. and Kustin, K. (1994). Kinetics and Mechanism of the Oxidation of Thiourea by Bromate in Acidic Solution. *Journal of Physical Chemistry*, 98: 551 – 557.
- Smith, A.L. (1997). *Oxford Dictionary of Biochemistry and Molecular Biology*.

Oxford [Oxfordshire]. Oxford University Press. 508 ISBN 0-19-854768-4

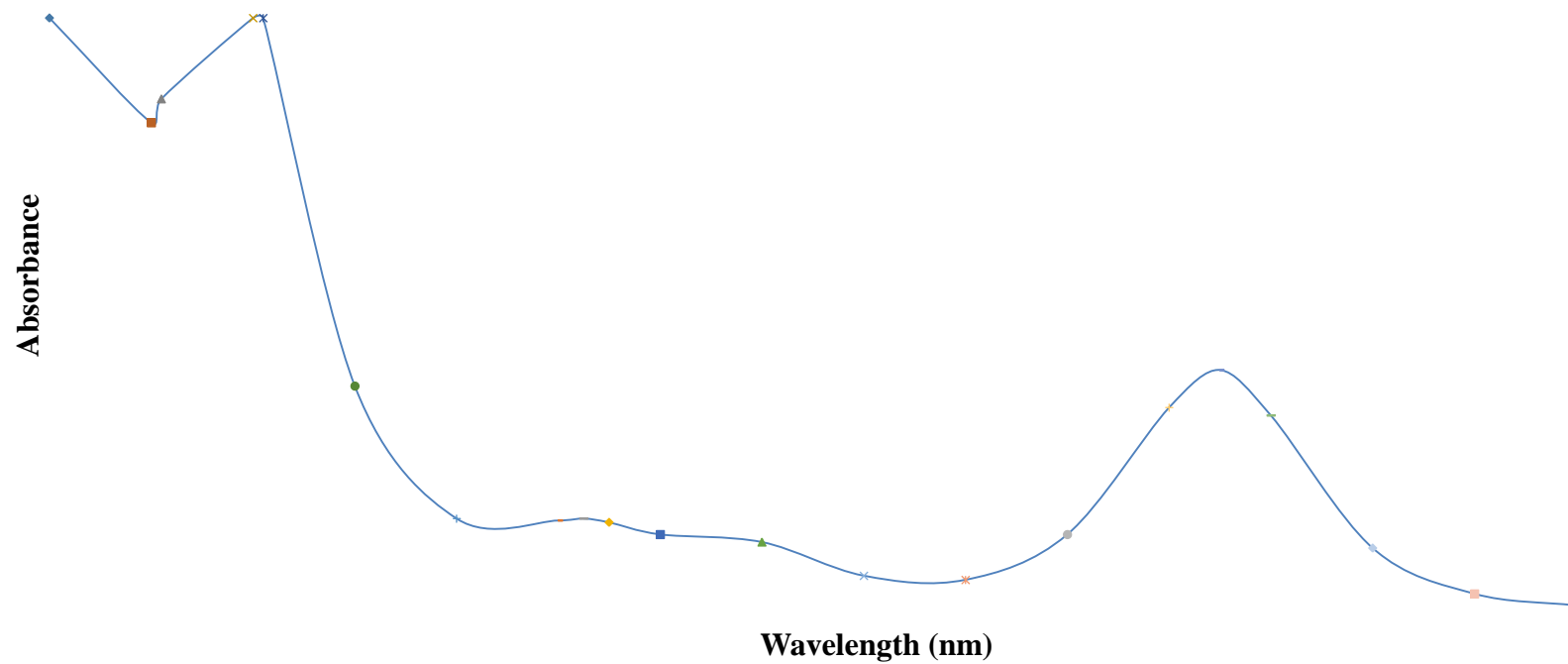
- Snell, F.D. (1978). *Photometric and Fluorometric Methods of Analysis*. Parts I and II. Wiley; New York, pp 271 – 283.
- Sprong, R.C., Arsman, C.J.M, van Oirschot, J.F.L.M. and van Asbeck, B.S. (1997). Dimethylthiourea Protects Rats Against Gram – Negative Sepsis and Decreases Tumour Necrosis Factor and Nuclear Factor IB Activity. *Journal of Laboratory and Clinical Medicine*, 129: 470 – 481.
- Stranks, D.R. (1960). Mechanism of Some Electron Exchange Reactions. *Discussions of the Faraday Society*, 13: 270 and 29: 73.
- Stranks, D.R. (1974). The Elucidation Of Inorganic Reaction Mechanisms by High Pressure Studies. *Pure and Applied Chemistry*, 38: 303-323.
- Sutin, N. (1966). Electron Exchange Reactions in Solution. *Energy Communication BNL 9191 Chemical Abstract*, 62: 14.
- Sykes, A.G. (1966). *Kinetics of Inorganic Reactions*. Pergamon Press, Oxford, 98-119
- Sykes, A.G. (1967). Further Advances in The Study of Mechanisms of Redox Reactions. *Advances in Inorganic Chemistry and Radiochemistry*, 10: 153-161
- Sykes, P. (1963). *A Guidebook to Mechanism in Organic Chemistry*. 5th Ed. Longman. 215 – 228.
- Taube, H. (1959). Bridging and Non – Bridging Ligand Effect on Redox Reaction of Metal Ions. *Canadian Journal of Chemistry*, 37: 129-134
- Taube, H, Meyers, H And Rich, R.L (1953). Observations on the Mechanism of Electron Transfer in Solution. *Journal of American Chemical Society*, 75: 4118-4129
- Tennakone, K, Kumara, G.R.R.A, Koltegodu, I.R.M, Wijayantha, K.G.U and Perera, V.P.S. (1998). A Solid State Photovoltaic Cell Sensitized with a Ruthenium Bipyridyl Complex. *Journal of Physics D: Applied Physics*, 31: 1492-1501
- Thakuria, B.J and Gupta, Y.K. (1975). Kinetics and Mechanisms of Electron – Transfer Reactions of Aqueous and Coordinated Thallium(III). Reduction of Hexaquotheallium(III) by hydrazine. *Journal of Chemical Society, Dalton*, 23:2541-2548
- Thanasekaran, P., Rajendran, T., Rajagopal, S., , C., Ramaraj, R., Ramamurthy, P. and Venkatachalapathy, B. (1997). Marcus Inverted Region In the Photoinduced Electron Transfer Reaction of Ruthenium(II)-Polypyridine Complexes with Phenolate Ions. *Journal of Physical Chemistry A*. 101(44): 8195-8199.
- Thomas, A., Maxcy, G., Willhite, P., Green, D.W. and James, K.B. (1998). A Kinetic

- Study of the Reduction of Chromium(VI) to Chromium(III) by Thiourea. *Journal of Petroleum Science and Engineering*, 19: 253 – 263.
- Turro, C., Chang, C.K., Leroi, G.E., Cukier, R.I. and Nocera, D.G. (1992). Photoinduced Electron Transfer Mediated by a Hydrogen-Bonded Interface. *Journal of American Chemical Society*, 114: 4013-4019..
- Ukoha, P.O. (1999). Kinetics and Mechanisms of Some Redox Reactions of μ -Oxo – Bridged Iron(III) Complex Ion $[(\text{Fehedta})_2\text{O}]^{2-}$ and Some Oxyanions and Thiols. Ph.D Thesis, Ahmadu Bello University, Zaria, Nigeria and The References therein.
- Ukoha, P.O. and Ibrahim, E. (2004). Mechanism of the Oxidation of β -Mercaptoacetic Acid by Trioxiodate(V) in Aqueous Acid Medium. *Chemclass Journal*, 138-141.
- Ukoha, P.O. and Iyun, J.F. (2001). Kinetics of Reduction of an Iron (III) Complex Ion by Mercaptoethanol and Mercaptoethylamine in Perchloric Acid Medium. *Journal of the Chemical Society of Nigeria*, 26(2): 163-168.
- Ukoha, P.O. and Iyun, J.F. (2002). Oxidation of l-ascorbic Acid by $\text{enH}_2[(\text{FeHEDTA})_2\text{O}].6\text{H}_2\text{O}$ in Aqueous Medium. *Journal of Chemical Society of Nigeria*, 27 (2): 119 – 122.
- Vaidya, V.K., Pitlia, R.L., Kabra, B.V., Mali, S.L. and Ameta, S.C. (1991). Dye – Sensitized Photo-oxidation of Thiourea by Singlet Oxygen. *Journal of Photochemistry and Photobiology A* 60(1): 47 – 50.
- van Eldik, R., Asano, T., le Noble, W.J. (1989). Activation and Reaction Volumes In Solution 2. *Chemical Review.*, 89: 549 – 688.
- van Eldik, R. and Merbach, A.E. (1992). High Pressure Kinetics. A Decisive Dimension in Mechanistic Studies of Inorganic Reactions. *Comment Inorganic Chemistry*, 12: 341- 378.
- Vogel, A.I. (1958). *Qualitative Organic Analysis*. 2nd Ed. Logman, London p117.
- Vogel, A.I. (1978). *Vogels's Textbook of Quantitative Inorganic Analysis: Including Elementary Instrumental Analysis*. ELBS and Longman, London. pp 125 – 247.
- Wasmuth, C.R., Donnel, R.L., Harding, C.E. and Hankle, G.E. (2008). Kinetics of the Reduction of *p*-Phenylazobenzene Sulphonic Acid by Sodium Dithionite in Alkaline Solution. *Review of Progress in Coloration and Related Topics*, 81(9): 403 – 405.
- Warnqvist, B. and Dodson, R.W. (1971). Induction of the Thallium (I) – Thallium (III) Exchange by Iron (II). *Inorganic Chemistry*, 10: 2624.
- Weaver, T.R., Meyer, T.J., Adeyemi, S.A., Brown, G.M., Ecberg, R.P., Hatfield, W.E.,

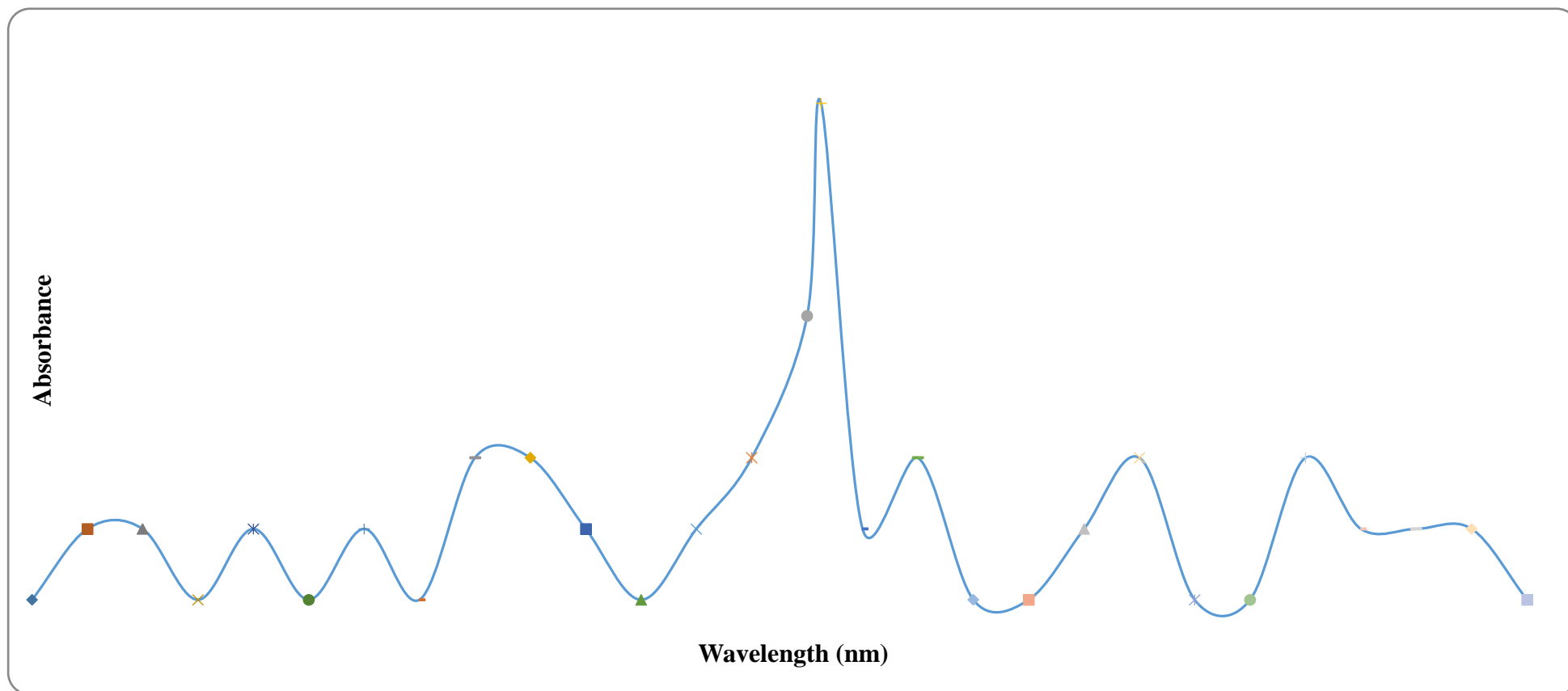
- Johnson, E.C., Murray, R.W. and Untereker, D. (1975). Chemically Significant Interactions Between Ruthenium Ions in Oxo-Bridged Complexes of Ruthenium(III). *Journal of American Chemical Society*, 97: 3039-3047.
- Westbroek, P., De Strycker, J., Van Uytvanghe, K. and Temmerman, E. (2001). Electrochemical Behaviour of Sodium Dithionite and Sulphite at Gold Electrode in Alkaline Solution. *Journal of Electroanalytical Chemistry*, 516(1-2): 83 – 88.
- Wikstrom, M. (1989). Identification of the Electron Transfers in Cytochrome Oxidase that are Coupled To Proton-Pumping. *Nature* 338: 776.
- Wilkins, G.R. (1974). *The Study of Kinetics and Mechanisms of Cobalt(III)- EDTA Type Complexes*. Allyn and Bacon, Inc. Boston. 231-239.
- Worthington, P. and Hambright, P. (1980). Kinetics of Oxidation of Dithionite by Dicyanoporphyryratoferrate(III) Complexes. *Journal of Inorganic and Nuclear Chemistry* 42(11): 1651 – 1654.
- Yagi, M., Tokita, S., Nagoshi, K., Ogino, I. and Kaneko, M. (1996). Activity Analysis of a Water Oxidation Catalyst Immobilized in a Polymer Membrane. *Journal of Chemical Society, Faraday Transactions*, 92: 2457-2461.
- Yagi, M., Nagoshi, K. and Kaneko, M. (1997). Cooperative Catalysis and Critical Decomposition Distances Between Molecular Water Oxidation Catalysts Incorporated in a Polymer Membrane. *Journal of Physical Chemistry B* 101: 5143-5146.
- Yagi, M., Osawa, Y., Sukegawa, N. and Kaneko, M. (1999). Catalytic Activity of Tri (μ -Chloro)- Bridged Dinuclear Ruthenium Complex Confined in a Polymer Membrane as an Artificial Model of Photosynthetic Oxygen Evolving Centre. *Langmuir* 15: 7406-7408.
- Yagi, M., Sukegawa, N., Kasamastu, M. and Kaneko, M. (1999). Cooperative Catalysis and Critical Decomposition Distances in Water Oxidation by the Mononuclear Ammineruthenium(III) Complex in a Nafion Membrane. *Journal of Physical Chemistry B*: 2143-2151.
- Yagi, M., Kasamastu, M. and Kaneko, M. (2000a). Cooperative Catalysis and Critical Decomposition Distances in Water Oxidation by Tris (Ethylenediammine) Ruthenium(III) Complex Confined in a Nafion Membrane. *Journal of Molecular Catalysis A: Chemical*, 151, 29-35.
- Yagi, M., Kasamastu, M. and Kaneko, M. (2000b). Analysis of Catalytic Water Oxidation by *Cis*-Tetraamminedichlororuthenium(III) Complex Incorporated in a Polymer Membrane. *Journal of Physical Chemistry B*, 104: 4111-4114.
- Yagi, M. and Kaneko, M. (2001). Molecular Catalysts for Water Oxidation. *Chemical Reviews*, 101: 21-35.
- Yamada, H, Koike, T. and Hurst, J. K. (2001). Water Exchange Rates in the

- Diruthenium μ - Oxo Dion *Cis, Cis-* [(Bpy)₂Ru(OH₂)]₂O⁴⁺. *Journal of American Chemical Society*, 123: 12775-12780.
- Yamada, H., Siems, W.F., Koike, T. and Hurst, J.K. (2004). Mechanisms of Water Oxidation Catalysed by the *Cis, Cis-*[(Bpy)₂Ru(OH₂)]₂O⁴⁺. *Journal of American Chemical Society*, 126: 9786 – 9792.
- Yusuf, U.F., Iyun, J.F. and Ayoko, G.A. (2004). Oxidation of Hypophosphorous Acid by Poly(pyridine)iron(III) Complexes. *ChemClass Journal*, 118 – 122.
- Zahonyi-Budo, E. and Simandi, L.T. (1991). Oxidation of Hypophosphorous Acid by Permanganate Ion. *Inorganica Chimica Acta*. 149 – 151.
- Zaidi, S.A.H. (1991). The Influence of Dielectric Constant Variations on the Kinetics of Reaction Between Bromate and Tellurite Ions in Aqueous Ethanol Mixed Solvents. *Journal of Chemical Society of Pakistan* 13(2): 67-70
- Zatko, D.A. and Kratochvil, B. (1968). Copper (II) Oxidation of Thioureas in Acetonitrile. *Analytical Chemistry* 40(14): 2120 – 2123.
- Zueva, T.S, Protopopov, E.V. and Ivanov, I.A. (1990) Role of Thiols (Cysteine and Thiourea) in the Mechanism of the Periodic Decomposition Reaction of Hydrogen Peroxide by Potassium Iodate in an Acid Medium. *TERCAXA* 26:51 – 56

**APPENDIX I:UV VISIBLE SPECTRUM FOR AN AQUEOUS SOLUTION OF DIAQUOTETRAKIS(2,2'-BIPYRIDINE)-
 μ -OXODIRUTHENIUM(III) ION at $[(\text{H}_2\text{O})_2(\text{bpy})_4\text{Ru}_2\text{O}^{4+}] = 6 \times 10^{-5} \text{ mol dm}^{-3}$**



APPENDIX II: UV VISIBLE SPECTRUM FOR THE REDUCTION PRODUCT OF DIAQUOTETRAKIS (2, 2'-BIPYRIDINE)- μ -OXODIRUTHENIUM(III) ION



224